Immunogenicity of Novel CHO- and HEK293- Produced Variants of the Atheroprotective chP3R99 mAb in Distinct Animal Models

by

Gala P. Araujo

A thesis submitted in partial fulfillment of the requirements for the degree of

Master of Science

in

Nutrition and Metabolism

Department of Agricultural, Food and Nutritional Science
University of Alberta

© Gala P. Araujo, 2024

ABSTRACT

Cardiovascular diseases (CVDs) are the leading cause of death globally and exert a significant burden on healthcare systems and public governmental institutions. Atherosclerosis is a predominant form of CVD characterized by the accumulation of cholesterol-rich lipoproteins within the innermost wall of the artery, known as the tunica intima. This lipoprotein accumulation ultimately leads to fibrous-rich plaque formation, which reduces blood flow and causes major cardiovascular events, including myocardial infarctions, strokes, and disabling peripheral artery disease. Atherosclerosis is theorized to be linked to specialized sugar side chains, known as Glycosaminoglycans (GAGs), in the tunica intima that can specifically bind cholesterol-rich lipoproteins. Two main forms of cholesterol can interact with these GAGs (i) namely Low-Density Lipoprotein (LDL) (or ‘bad’) cholesterol and (ii) 'Remnant' cholesterol. Despite the prevalence of atherosclerosis, therapeutic approaches for the treatment of atherosclerosis have been primarily limited to the management of atherosclerotic risk factors (e.g. lipid-lowering) rather than disease prevention per se. In this thesis, we introduce the development of a new class of monoclonal antibody (mAb) (called chP3R99) that has been demonstrated to compete with lipoprotein binding to GAGs within the extracellular matrix of the tunica intima. ChP3R99 is a novel human-murine chimeric mAb capable of binding specifically to proatherogenic GAGs with high specificity and has been shown to inhibit lipid retention and reduce atherosclerosis progression in a number of small animal models. Previous studies of chP3R99 have attributed these atheroprotective features to be associated with the induction of secondary (Ab2) and tertiary antibodies (Ab3) generated in the host due to the unique immunogenic idiotype of the P3R99.

However, inefficiencies with the production of P3R99 via the murine myeloma, NS0, cell line has led to the development of two new P3R99 variants produced from more productive cell lines: the

Chinese Hamster Ovary, CHO-P3R99, and Human Embryonic Kidney, HEK-P3R99. Despite the maintenance of the P3R99 structure postproduction and recognition of chondroitin sulfate, the CHO-P3R99 and HEK-P3R99 variants are yet to be tested for the conservation of the original NS0-P3R99 (chP3R99) immunogenic function.

Thus, this thesis aimed to assess the immunogenicity and idiotypic strength of the variant P3R99s in distinct animal models compared to the original NS0-P3R99 and a negative isotype-matched control hR3. Immunogenicity was assessed through the induction of host-derived Ab2 and Ab3 antibodies.

Heterozygous lean JCR:LA-cp rats, homozygous obese-insulin resistant JCR:LA-cp rats, and white-landrace piglets were used as models for immunogenicity assessment. Rodents received 6 doses of 200 μg (400 μg/mL) and underwent 5 blood draws during treatment, while piglets received 5 doses of 1.0mg (0.33 μg/mL) and underwent 4 blood draws. Sera taken during blood sampling was separated via differential centrifugation and used for Enzyme-linked Immunosorbent Assay (ELISA) Ab2 and Ab3 antibody detection. Results in lean JCR:LA-cp rats and white-landrace piglets confirmed the immunogenicity of the CHO-P3R99, NS0-P3R99, and HEK-P3R99 variants, following a minimum of 4 and 5 doses, respectively. Furthermore, results in obese insulin-resistant JCR:LA-cp rats confirmed the immunogenicity of the CHO-P3R99 and NS0-P3R99 variants following a minimum of four doses. Additionally, both rodent studies confirmed the conserved immunogenic strength of the NS0-P3R99 in the HEK-P3R99 and CHO-P3R99 variants. Similarly, piglet studies demonstrated the conserved immunogenic strength of the NS0-P3R99 in the two variants in regard to Ab3 antibody induction. Although this was independent of the Ab2 response for the HEK-P3R99.

In conclusion, we demonstrate for the first time that the new P3R99 variants are not inferior in their capacity of inducing anti-CS anti-atherogenic Ab3 antibodies in rodents and swine, but due to some inconsistencies between animal models used for their anti-atherogenic properties, further testing will be required.

PREFACE

This thesis is an original work by Gala Araujo, with contributions listed below.

Chapter 1 is an adapted manuscript in preparation that will be submitted to Frontiers in Cell and Developmental Biology as "Gala Araujo, Agata Martin-Ozimek, Leidy Valencia, Yosdel Soto, Spencer Proctor. A narrative review of monoclonal antibody immunotherapies for atherosclerosis management: special focus on the novel chP3R99 mAb."

Some of the research conducted for this thesis forms part of an international research collaboration led by Dr. Yosdel Soto at the Centre for Molecular Immunology (CIM) in Havana, Cuba. Staff at the CIM and Leidy Valencia produced the original chP3R99 (NS0-P3R99), HEK-P3R99 and CHO-P3R99 variants. Students and staff at the CIM also assisted in experimental procedures and data analysis. Chapter 2, Figure 2.2 P3R99 variants *in-vitro* recognition to chondroitin sulfate via ELISA was completed by the CIM staff, Dr. Yosdel Soto, and Leidy Valencia.

Lab members and staff from the Metabolic and Cardiovascular Diseases (MCVD) laboratory and Swine Research and Technology Centre (SRTC) at the Department of Agriculture, Food and Nutritional Science also assisted in experimental procedures and animal treatments for Chapters 3 and 4 and Chapter 5, respectively. Sharon Sokolik, Kun Wang, Agata Martin-Ozemik, and SRTC staff assisted in animal housing, surgeries, and/or sample collections along with myself and Dr. Yosdel Soto.

Enzyme-linked Immunosorbent Assay protocols used in Chapters 3,4 and 5 were designed by staff at the CIM and adapted by myself, Dr. Yosdel Soto and Kun Wang as necessary. The data analysis in Chapters 3,4, and 5 are my original work, as well as the literature review in Chapter 1. Dr. Yosdel Soto and Dr. Spencer Proctor assisted with the data collection and contributed to manuscript edits. Dr. Spencer Proctor was the supervisory author and was involved with concept formation and manuscript composition.

The research experiments containing the JCR:LA-cp rats described in this thesis were approved by the University of Alberta Animal Care and Use Committee for Livestock (ACUC) and the Canadian Council of Animal Care (CACC), Project Name: "Pharmacological treatment of insulin

resistance, obesity and atherosclerosis in a rat model of chronic disease." Study ID: AUP00004174.

The research experiments containing the white-landrace piglets described in this thesis were approved by the University of Alberta Animal Care and Use Committee for Livestock (ACUC) and the Canadian Council of Animal Care (CACC), Project Name: "Idiotypic antibody response in pigs." Study ID: AUP002321.

Under the supervision of:

Dr. Spencer D. Proctor,

Department of Agricultural, Food and Nutritional Science,

4-002J Li Ka Shing Centre for Health Research Innovation

University of Alberta, Edmonton, Alberta, Canada T6G 2E1

Email: spencer.proctor@ualberta.ca

Dr. Yosdel Soto,

Department of Immunobiology,

Street and 216 Street, Siboney, Playa, La Habana, Cuba. A.P 16040

Centre for Molecular Immunology, Havana, Cuba.

Email: yosdel@cim.sld.cu

Dedication

To my wonderful family and partner John.

~ In loving memory of Gail Wilkinson ~

ACKNOWLEDGEMENTS

I would be remiss if I did not mention the countless hours and support given to me by the students and staff at the University of Alberta who were involved in this project. I would specifically like to thank my supervisors, Dr. Spencer Proctor, Dr. Yosdel Soto, and Dr. Rabban Mangat, for their guidance, encouragement, advice, and never-ending support throughout my academic journey. Thank you all for being incredible mentors and continuing to inspire me during my master's program and beyond.

Furthermore, I would like to acknowledge the work of Mrs. Sharon Sokolik, Mr. Kun Wang, Mrs. Leidy Valencia, Mrs. Agata Martin-Ozemik, Mr. Yongbo She, Mrs. Niusha Taheri, Mrs. Xiaoying Wu, and Mr. Alexander Makarowski. Thank you for all of your assistance, both inside and outside the lab.

Additionally, I need to thank my parents, my sister Maria, my best friend Taiye, and my two cats for their endless support, love, and comfort during stressful moments.

I'd also like to thank my partner John and his parents, Craig and Gail Wilkinson, for being a second family to me these last four years. Although Gail is no longer with us, I am forever appreciative of her, and I know she would be proud of my accomplishments. I would not be here without all of their constant and unwavering belief in me and my potential.

Lastly, thank you to the animals that gave up their lives for the sake of our research. This could not have happened without their sacrifice.

TABLE OF CONTENTS

LIST OF TABLES

LIST OF FIGURES

LIST OF ABBREVIATIONS

Ab2	Anti-idiotypic antibodies
Ab3	Anti-anti-idiotypic antibodies
ACE	Angiotensin-Converting Enzyme
ACUC	Animal Care and Use Committee
APCs	Antigen Presenting Cells
Apo(A)(B)(C)(E)	Apolipoproteins
ApoE-/-	ApoE knock out
ANOVA	Analysis Of Variance
ARISE	Alberta Research Information Services
ASCVD	Atherosclerotic Cardiovascular Disease
ATP	Adenosine Triphosphate (ATP)
ATP	Alberta Tomorrow Project
BHB	Ketone Metabolite β-Hydroxybutyrate
BSA	Bovine Serum Albumin
CACC	Canadian Council of Animal Care
CAD	Coronary Artery Disease
CANTOS	Canakinumab Anti-inflammatory Thrombosis Outcomes Study
CIM	Center for Molecular Immunology
CHO-K1	Chinese Hamster Ovary
chP3R99	Chimeric P3R99
COLCOT	Colchicine Cardiovascular Outcomes Trial
CP	Corpulent
CS	Chondroitin Sulfate
CSF	Colony Stimulating Factor
CSPG	Chondroitin Sulfate Proteoglycans
CTLA	Cytotoxic T-Lymphocyte-Associated Protein
CVD	Cardiovascular Disease
CXCL1	Chemokine (C-X-C motif) Ligand 1

DC	Dendritic Cells
DLS	Dynamic Light Scattering
E3L	APOE 3-Leiden
ECM	Extracellular Matrix
ECHO	Echocardiogram
EDTA	Ethylenediaminetetraacetic Acid
ELISA	Enzyme-linked Immunosorbent Assays
EtOH	Ethanol
FBS	Fetal Bovine Serum
FDA	Federal Drug Agency
FITC	Fluorescein Isothiocyanate
GAG	Glycosaminoglycans
GCSF	Granulocyte Colony Stimulating Factor
GLAGOV	Global Assessment of Plaque Regression with a PCSK9 Antibody as Measured by Intravascular Ultrasound
GM-CSF	Granulocyte-Macrophage Colony-Stimulating Factor
HBS	Hepes Buffer Saline
HCDR3	Heavy Chain Complementarity Determining Region 3
HDL	High-Density Lipoproteins
HEK-293	Human Embryonic Kidney 293
HMG-COA	β-Hydroxy β-methylglutaryl-CoA
HOMA-IR	Homeostatic Model Assessment for Insulin Resistance
HPLC	High Performance Liquid Chromatography
hR3	Humanized R3
hsCRP	high-sensitivity C-Reactive Protein
IL	Interleukins
ICI	Immune Checkpoint Inhibitor
IDL	Intermediate-Density Lipoproteins
IFN-γ	Interferon gamma

IGFBP	Insulin-like Growth Factor Binding Proteins
IGF	Insulin-like Growth Factor
IHC	Immunohistochemistry
IRF	Interferon-Regulatory Factors
JAK/STAT	Janus Kinase/Signal Transducers and Activators of Transcription
JMJD3	Jumonji Domain-containing protein-3
JNK	Jun N-terminal Kinase
LDL	Low-Density-Lipoprotein
LDL-r	Low-Density-Lipoprotein receptor
LDLr−/−	Low-Density-Lipoprotein receptor knock out
LLT	Lipid-lowering therapies
LoDoCo	Low-Dose Colchicine
LV	Left Ventricle
mAb	Monoclonal Antibody
MACE	Major Adverse Cardiovascular Events
MAPK	Mitogen-Activated Protein Kinases
MCP-1	Monocyte Chemoattractant Protein-1
MCVDL	Metabolic Cardiovascular Disease Laboratory
MHC	Major Histocompatibility Complex
MI	Myocardial Infarction
MMP	Matrix Metalloproteinase
MPO	Myeloperoxidase
MR	Mendelian Randomization
(99)mTC	Technetium-99m
NCD	Non-Communicable Disease
NF-kB	Nuclear Factor Kappa-B
NK	Natural Killer cells
NLR	Nod-Like Receptors
NLRP3	NLR Family Pyrin Domain Containing 3
NS0	Murine Myeloma

OD	Optical Density
ODYSSEY	Evaluation of Cardiovascular Outcomes After an Acute Coronary Syndrome During Treatment With Alirocumab
OR	Odds Ratio
ox-LDL	Oxidized Low-Density-Lipoprotein
PAMPs	Pathogen-Associated Molecular Patterns
PBS	Phosphate Buffer Saline
PCR	Polymerase Chain Reaction
PCSK9	Proprotein Convertase Subtilisin/Kexin type 9
PD-1	Programmed Cell Death Protein 1
PD-L	Programmed Death-Ligand
PGs	Proteoglycans
PGE2	Prostaglandin E2
PI3K	Phosphatidylinositol-3-kinase
PPAR	Peroxisome Proliferator Activated Receptor
PRRs	Pattern-Recognition Receptors
PTM	Post Translational Modifications
RC	Remnant Cholesterol
RM	Remnant lipoproteins
ROS	Reactive Oxygen Species
S.C	Subcutaneous
SD	Standard Deviation
SDS-PAGE	Sodium Dodecyl-Sulfate Polyacrylamide Gel Electrophoresis
SEM	Standard Error of the Mean
SHP2	Src Homology region 2-containing Protein tyrosine phosphatase 2 (SHP-2)
SNP	Single Nucleotide Polymorphism
SPR	Surface Plasmon Resonance
SRTC	Swine Research and Technology Center
STAT	Signal Transducer and Activator of Transcription

T2D	Type 2 Diabetes
TC	Total Cholesterol
TGs	Triglycerides
TGF-β	Transforming Growth Factor-beta
Th	T helper
TLR	Toll Like Receptors
TMB	3,3′,5,5′-Tetramethylbenzidine
TNF-α	Tumor Necrosis Factor-alpha
Treg	T regulatory
VLDL	Very Low-Density Lipoproteins
VSMC	Vascular Smooth Muscle Cells
WHO	World Health Organization

CHAPTER 1: LITERATURE REVIEW

1.1 Background and introduction

Cardiovascular diseases (CVD) have a profound global impact, consistently occupying a position among the top 10 leading causes of death worldwide (World Health Organization, 2022)(Roth et al., 2020). Atherosclerosis, the predominant form of CVD found globally, is a low-grade chronic inflammatory disorder (Roth et al., 2020). Atherosclerosis' hallmark features include the retention of lipids, the development of arterial lesions, and eventual plaque formation, culminating in compromised blood flow and subsequent complications (Libby et al., 2019)(Makover et al., 2022). The intricate development of atherosclerosis, subject to the influence of both systemic and non-systemic factors such as diet, genetics, and physical activity, increases the complexity of its pathophysiology and highlights the challenge of managing atherosclerosis throughout an individual's lifespan (ARUP consult, 2024). The response-to-retention hypothesis of atherosclerosis suggests that atherogenesis is triggered when apoB-lipoproteins bind to the arterial wall via Proteoglycans (PG) of the Extracellular Matrix (ECM), thereby initiating inflammatory changes that promote lipid retention and plaque formation (Yurdagul et al.,2016)(Williams & Tabas, 1995). Lipoproteins bind to arterial PGs through Chondroitin Sulfate (CS) Glycosaminoglycan (GAG) branches (Yurdagul et al., 2016)(Fogelstrand & Borén, 2012)(Brito et al., 2012)(Khalil, 2004). The subsequent inflammatory response encourages further lipid retention, accumulation, and oxidation, resulting in the activation of macrophages, clearance of oxidized lipids, and the formation of foam cells that make up atherosclerotic plaques (Shapiro & Fazio, 2016)(Fogelstrand & Borén, 2012)(Andersson, 2010). This lipoprotein – GAG interaction provides a key focal point for preventive therapies that, to date, remains largely unexplored (Shapiro & Fazio, 2016)(Andersson, 2010).

Current CVD therapies primarily focus on managing risk factors, such as hypertension, circulating lipoproteins, inflammation, and oxidative stress (Libby, 2005)(Makover et al., 2022). However, due to the multifactorial pathophysiology of atherosclerosis, there is a continued risk of cardiovascular events during ongoing treatment (Libby, 2005)(Makover et al., 2022)(Akyea et al., 2019). Lipid-Lowering Therapies (LLT), notably statins, have proven effective in lowering Low-Density-Lipoprotein (LDL) levels and reducing some CVD risk; however, two-thirds of cardiovascular events occur in individuals undergoing statin treatment (Makover et al.,

2022)(Akyea et al., 2019)(Abdul-Rahman, et al., 2022). This residual risk occurs due to several factors, including untreated inflammation, statin intolerance, unequal access to therapy, and the inability of at-risk populations to achieve on-treatment LDL targets (Libby, 2005)(Akyea et al., 2019)(Sirtori, 2014). In response, therapies are being developed that can address this residual risk through secondary lipid-lowering therapies that target cholesterol synthesis pathways alongside other therapies, including vasodilators, antihypertensives, and anti-inflammatories, which each address different aspects of atherosclerosis (Hetherington & Totary-Jain, 2022)(Libby et al., 2019)(Kim et al., 2022). However, while these multiple approaches to atherosclerosis management have shown efficacy over time, on-treatment cardiovascular events persist, underscoring the need for new treatment targets (Libby et al., 2019)(Makover et al., 2022). Monoclonal antibodies (mAbs) are of specific interest due to their high specificity, adaptability, rapid development, low cost, and history of therapeutic success. The Canakinumab Anti-inflammatory Thrombosis Outcomes Study (CANTOS) study was a landmark clinical trial that used a canakinumab mAb to reduce the concentration of Interleukin-1-beta (IL-1β), a critical pro-inflammatory cytokine in atherosclerosis (Makover et al., 2022)(Sirtori, 2014)(Rikhi & Shapiro, 2022)(Shapiro & Fazio, 2016). Lipid-lowering mAbs function by targeting cholesterol synthesis mediators and LDL directly. However, similar to anti-inflammatory agents, they have encountered challenges in reducing all cardiovascular event incidences across patients (Bermúdez et al., 2018).

MAbs targeting ECM proteins have recently been recognized for their vast potential due to the role of the ECM in the early stages of atherogenesis (Kim et al., 2022)(Ait-Oufella et al., 2020). The chP3R99 is a novel mAb which can bind to proteoglycan side chains and directly interfere with lipoprotein binding. Through competitive inhibition, the chP3R99 mAb inhibits lipid retention and the subsequent formation of an atherosclerotic plaque, thus acting as a potential new preventative therapy for atherosclerosis (Soto et al., 2012).

Despite strong pre-clinical evidence supporting the efficacy of chP3R99 mAb in atherosclerosis management, information about its structural characteristics, functional basis, challenges, and prospects is still under development.

Thus, the aim of the literature review section of my thesis is threefold:

1) To document a comprehensive background on the etiology of atherosclerosis, including the complex role of inflammation and the associated modes of action.

2) To provide a summary of mAbs and other immunotherapies used for atherosclerosis treatment, focusing on anti-inflammatory and lipid-lowering therapies.
3) To review data on the structural characteristics, theory, and therapeutic effect of the chP3R99 mAb that will provide relevant context for my thesis and objectives.

1.1.1 Cardiovascular disease epidemiology

Cardiovascular diseases (CVDs) are a consistent major clinical problem in healthcare. CVDs are extremely widespread and pose a significant cost to patients and public institutions worldwide (Roth et al., 2020)(Hennekens, 1998). Yearly CVD costs in Canada alone are estimated to be worth 22 billion dollars (CAD) (Government of Canada, 2009). CVDs are a major cause of morbidity and mortality (Figure 1.1) and include a broad range of diseases that affect the heart and blood vessels, including coronary artery disease, heart failure, hypertension, stroke, and peripheral artery disease, among others.

The World Health Organization (WHO) statistics from 2023 reported that Non-Communicable Diseases (NCDs) have the highest disease incidence worldwide (World Health Organization, 2023). The number one NCD over the past decade has consistently been CVDs, affecting 22.9 million people in 2023, more than cancer, chronic respiratory diseases and diabetes combined, which respectively occupy the positions 2nd, 3rd, and 4th top NCDs (World Health Organization, 2023). Additionally, NCDs increased by 28% from 2019 to 2023, in large part due to rising cases of CVDs (World Health Organization, 2023). Generally, nearly one-third of all fatalities in low and middle-income countries are linked to CVDs and over four-fifths of CVD-related deaths worldwide currently occur within these low and middle-income countries (World Health Organization, 2023).

This epidemic of CVDs is linked to a rapid epidemiological transition associated with significant lifestyle and demographic changes (Minelli et al., 2020). Industrialization, urbanization, and globalization have facilitated the adoption of high-risk habits such as physical inactivity, tobacco and alcohol use, and consumption of highly processed diets (Institute of Medicine, 2010). These changes promote the onset of CVDs by increasing circulating lipids, blood pressure, inflammation, and oxidative stress. Circulating lipids and inflammation specifically are significant contributors to Atherosclerotic Cardiovascular Disease (ASCVD), the predominant type of CVD. Atherosclerosis is a type of vascular disease that involves lipid deposition in the inner arterial wall.

Atherosclerosis can lead to various high-risk outcomes, including left ventricular dysfunction, which consists of the loss of function of the left ventricle that supplies blood to the rest of the body (Chahine & Alvey, 2023). Both vascular diseases are promoted by imbalances in lipid metabolism, known as dyslipidemia.

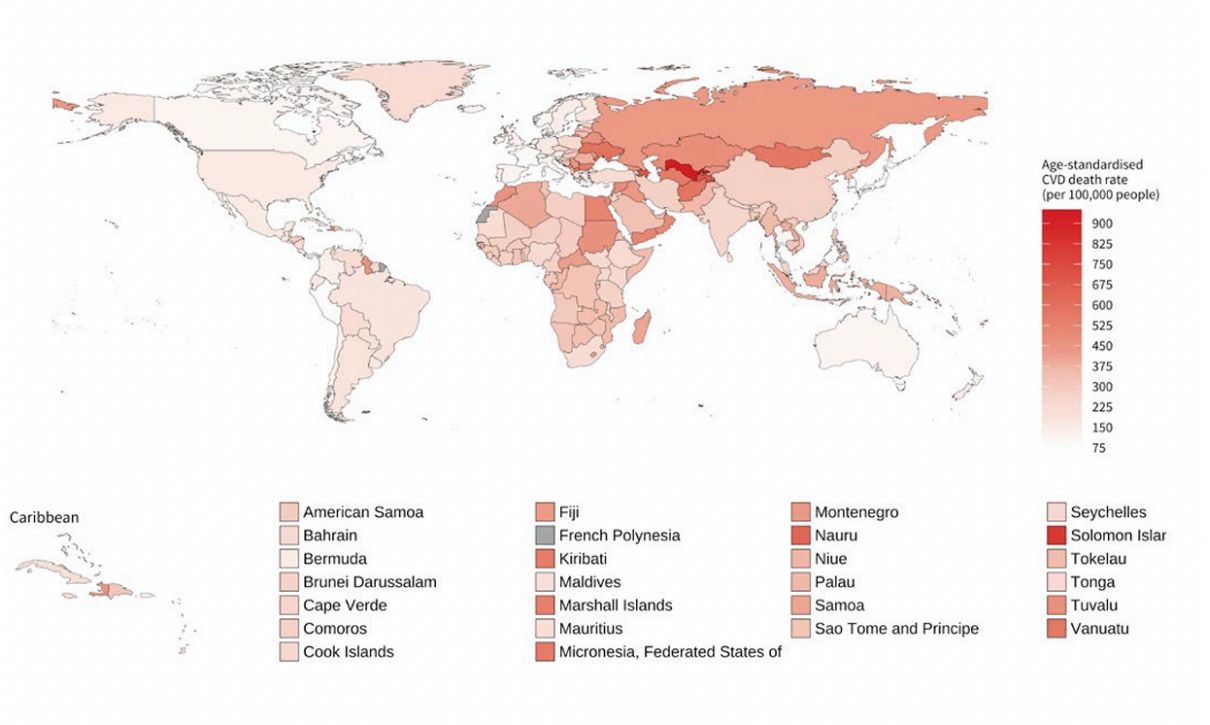

Figure 1.1 Global Cardiovascular Disease (CVD) death rate per 100,000 people in 2019 (male and female, all ages). World Heart Federation (2023). World Heart Report 2023. Available at: https://world-heart-federation.org/resource/world-heart-report-2023/.

1.1.2 Lipid metabolism

Lipoprotein metabolism involves a set of processes that includes the synthesis, storage, transport, and degradation of dietary and liver-derived lipids (Schoeler & Caesar, 2019). The small intestine absorbs and breaks down dietary lipids for delivery to the liver and tissues via blood circulation. This process begins through fat solubilization via gastric lipases in the stomach (Dash et al., 2015). Next, the solubilized fat becomes emulsified in the small intestine via bile acids from the gallbladder. Pancreatic lipase is then released to the small intestine to hydrolyze the emulsified fat, forming amphipathic micelles (Dash et al., 2015). Enterocytes then absorb micelles via passive or active diffusion. Fatty acids taken from the micelles are then rearranged to form triglycerides

(TGs), which are packaged into chylomicrons (Cianflone et al., 2008). Chylomicrons are a type of transport protein for lipids known as lipoproteins, which travel to the lymphatic system to enter the bloodstream through the thoracic duct (Dash et al., 2015). In the bloodstream, chylomicrons transport lipids to various tissues for storage or beta-oxidation for Adenosine Triphosphate (ATP) generation. Chylomicrons then return to the liver for breakdown. Lipoproteins can be divided into four sets: chylomicrons, very low-density lipoproteins (VLDL), low-density lipoproteins (LDL), and high-density lipoproteins (HDL) (Eisenberg & Levy, 1975)(Feingold et al., 2000). Like chylomicrons, VLDL is involved in transporting TGs to various tissues. However, VLDL is synthesized in the liver rather than from dietary sources (Eisenberg & Levy, 1975). The TGs in circulating VLDL are hydrolyzed by lipoprotein lipase, releasing free fatty acids and converting VLDL to intermediate-density lipoproteins (IDL) (Lent-Schochet & Jialal 2023)(Feingold et al., 2000). The remaining VLDL returns to the liver for breakdown, while IDL loses TGs and increases cholesterol content, converting to LDL. Colloquially known as 'bad cholesterol,' LDL continues circulating in the blood, binding to LDL receptors found on various tissues for cholesterol uptake. However, due to their cholesterol-rich nature, increases in circulating LDL levels, known as hyperlipidemia, can cause LDL deposition in artery walls, leading to atherosclerosis. LDL receptors in the liver can clear circulating LDL through receptor-mediated endocytosis. Once inside the liver, LDL can be broken down for storage or cholesterol repackaging. Conversely, HDL, referred to as 'good cholesterol,' has low cholesterol and TG content and is involved in reverse cholesterol transport (Tall, 1998). HDL transports cholesterol from tissues to the liver for breakdown, thereby reducing excess cholesterol (Figure 1.2)(Marques et al., 2018).

Lipoproteins generally comprise a water-insoluble lipid core and a water-soluble outer layer of phospholipids, cholesterol, and apolipoproteins (Lent-Schochet & Jialal 2023)(Feingold et al., 2000). Apolipoproteins are present in all lipoproteins and contribute to the stability, function, and activation of lipoproteins (Feingold et al., 2000). Apolipoproteins can be divided into four types: ApoA, ApoB, ApoC, and ApoE (Eisenberg & Levy, 1975). To briefly summarize, ApoA apolipoproteins are predominately involved in the function of HDL, ApoBs are critical in the formation of VLDL and LDL from the liver and cholesterol transport, ApoCs regulate Lipoprotein Lipase (LPL) activity that hydrolyzes TGs from VLDL and chylomicrons, and ApoEs facilitate the uptake of lipoproteins through cell surface receptors (Eisenberg & Levy, 1975).

Lastly, an often-ignored critical class of lipids is Remnant Cholesterol (RC). Remnant cholesterol includes the cholesterol contained within remnant lipoproteins. These remnant lipoproteins are products from the larger precursor triglyceride-rich lipoproteins such as VLDL, VLDL remnants and chylomicrons (Zilversmit, 1979)(Proctor & Mamo, 1998). Similar to LDL, RC has been linked as a significant risk factor for CVD and, specifically, the onset of atherosclerosis (Proctor & Mamo, 1998).

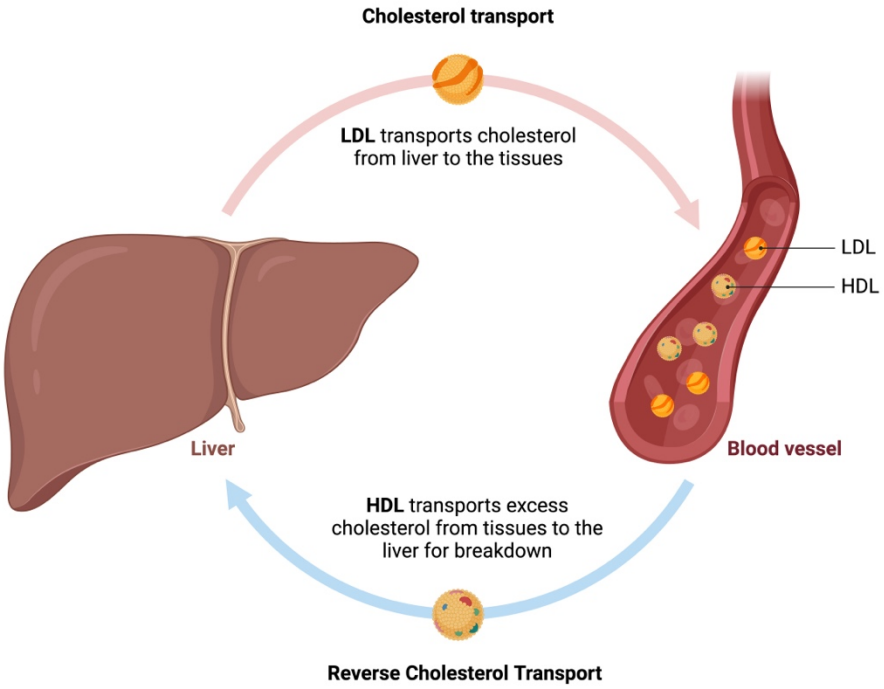

Figure 1.2 Illustration of cholesterol transport and reverse cholesterol transport. Adapted from: BioRender (2022). Available at: https://app.biorender.com/biorender-templates/figures/all/t-63693700c4d9addfeb935791-liver-and-cholesterol. Created with BioRender.

1.1.3 Residual risk and atherogenic lipoproteins

Fasting LDL levels are commonly measured in patients to determine their overall risk of CVD and prevent the onset of CVDs. Interestingly, however, many patients continue to experience Major Adverse Cardiovascular Events (MACE) despite reductions in LDL, known as residual risk. Additionally, non-fasting lipid levels have been proven to be an equal indicator of CVD risk

compared to fasting lipid levels (Varbo et al., 2013)(Nordestgaard et al., 2016). Non-fasting measurements are also more representative of a patient's lipid composition as most of the day is spent in the non-fasting state compared to the fasting state (Nordestgaard et al., 2016) (Zilzersmit, 1979)(Langsted & Nordestgaard, 2019)(Proctor & Mamo, 1998). Due to the limitations regarding fasting LDL as both a target and assessment tool for CVD, research has shifted towards adopting more overarching approaches for CVD treatment. Recent advancements in our understanding of atherosclerosis have highlighted the critical role of RC in combination with LDL (Varbo et al., 2013)(Weaver et al., 2023)(Weaver et al., 2023). During the early stages of atherogenesis, both RC and LDL infiltrate the inner tunica intima of the arterial wall, where they are digested by phagocytes, becoming foam cells and ultimately leading to plaque formation (Proctor & Mamo, 1998).

Three extensive Copenhagen cohort studies previously established the link between non-fasting RC and CVD risk (Aguib & Suwaidi, 2015)(Varbo et al., 2013) Although, interestingly the Copenhagen cohort studies also discovered an occasional link between LDL and CVD risk (Varbo et al., 2013)(Weaver et al., 2023). Similarly, the Alberta Tomorrow Project (ATP) was a Canadian longitudinal cohort study that collected blood samples and health-related data. An analysis by Weaver et al. in 2023 using ATP data determined whether non-fasting RC could serve as a suitable indicator of CVD and future CV events, particularly in individuals with underlying health conditions like diabetes mellitus (Weaver et al., 2023). The group reported that non-fasting RC levels were significantly increased in individuals with CVD compared to the control group. However, this trend was not observed for the group with diabetes + CVD. (Weaver et al., 2023). The diabetes + CVD group and the diabetes alone group had similar LDL levels. Furthermore, in 2023, a comprehensive large-scale investigation conducted by Navarese et al. used Mendelian Randomization (MR) analysis techniques to determine the relationship between RC and the development of atherosclerosis-related CVDs, specifically Coronary Artery Disease (CAD), Myocardial Infarction (MI), and stroke (Navarese et al., 2023). The study used Single Nucleotide Polymorphism (SNPs) associated with RC and LDL found on publicly available genome databases as representative variables for RC and LDL. The group additionally used data from various databases to create a participant pool of 958,434 people (Navarese et al., 2023). Using the SNPs for RC, the study found evidence of a strong relationship between RC levels and CVD risk. Each RC Standard Deviation (SD) increase was assigned a corresponding risk level as an

Odds Ratio (OR). For CAD, the group found that one SD increase in RC resulted in an OD of 1.51; for MI, one SD increase in RC resulted in an OD of 1.57; and for stroke, one SD increase in RC resulted in an OD of 1.23 (Navarese et al., 2023). Notably, this relationship between RC and CAD, MI, and stroke was independent of LDL levels.

1.1.4 Common therapies for atherosclerosis

Popular therapies for atherosclerosis involve a wide range of targets and effects (Figure 1.3). Although these therapies differ in their underlying mode of action, they all work to slow the progression of atherosclerosis, manage risk factors, and improve overall cardiovascular function. Apart from lifestyle changes like increased physical activity, adopting whole food dietary habits, reducing tobacco and alcohol intake, and reducing stress, medications for atherosclerosis are a significant part of atherosclerosis treatment (Lechner et al., 2020)(Lewis, 2009). The most commonly prescribed treatment for atherosclerosis are statins, which, similar to other cholesterol-lowering medications like PCSK9 inhibitors and omega-3 fatty acids, work to reduce circulating lipid levels, which can contribute to the pathogenesis of atherosclerosis (Gupta et al., 2019). Other medications include anti-hypertensive therapies, which function by lowering blood pressure and range from diuretics to Angiotensin-Converting Enzyme (ACE) inhibitors, beta-androgenic signalling blockers, calcium channel blockers, and vasodilators (National Heart Lung and Blood Institute, 2022)(Palmas et al., 2007). Additionally, vasodilation therapies can be both compound and surgically delivered, such as through nitroglycerin administration or angioplasty and stent procedures. Other treatments for atherosclerosis include anti-platelet or anti-clotting agents, which reduce the risk of blood clot formation, such as aspirin and warfarin, respectively (National Heart, Lung and Blood Institute, 2022). Moreover, some medications treat comorbidities of atherosclerosis, like diabetes mellitus-related high blood sugar, which can cause inflammation and oxidative stress, among other pro-atherogenic effects (National Heart, Lung and Blood Institute, 2022).

However, despite this extensive and comprehensive range of therapies for atherosclerosis, the incidence of severe CVD events due to atherosclerosis continues to increase globally. This occurrence is in part associated with these pharmacotherapies targeting risk factors of atherosclerosis rather than disease progression per se, indicating an urgent need for new and specifically preventative therapies for atherosclerosis.

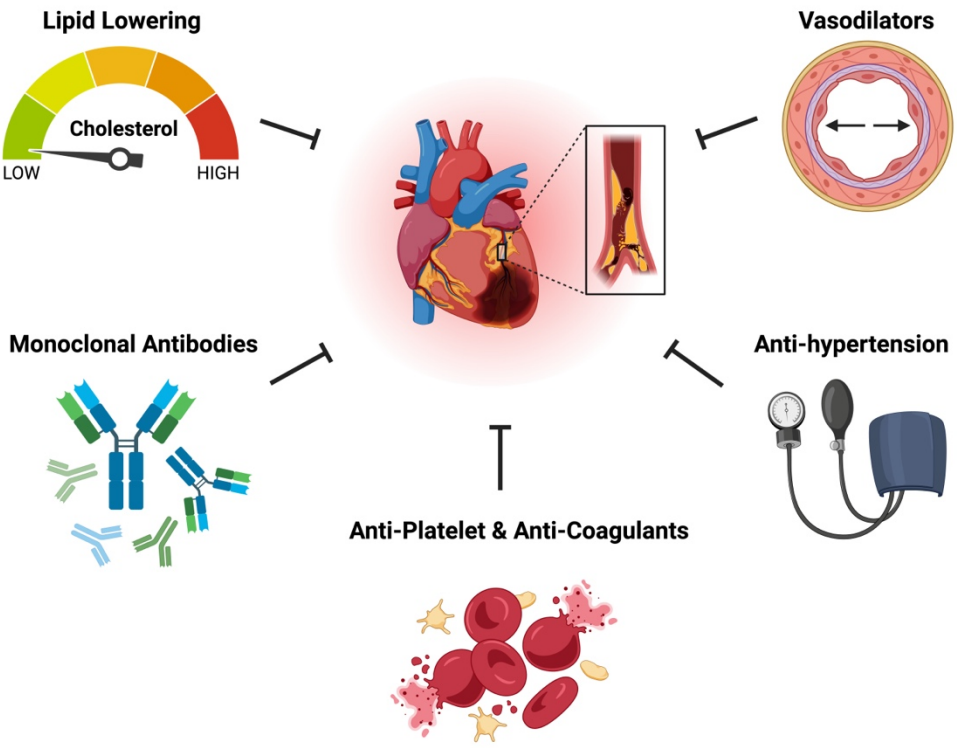

Figure 1.3 Depiction of common therapies for atherosclerosis. Figure includes lipid-lowering therapies, monoclonal antibodies, anti-platelet and anti-coagulants, anti-hypertension, and vasodilators. Created with BioRender.

1.1.5 Pathogenesis and evolution of atherosclerosis

Atherosclerosis is the predominant form of CVD globally (Herrington et al., 2016a)(Herrington et al., 2016b). Risk factors for atherosclerosis begin in adolescence and continue throughout the life cycle, reaching their peak in the mid to late thirties (Insull, 2009). Individuals over the age of 40 have a 50% chance of developing atherosclerosis (Song et al., 2020), and this number is steadily increasing due to rapid cultural changes and globalization. Economic development and urbanization have promoted atherosclerosis by facilitating dangerous lifestyle choices, such as diets rich in saturated fat or reduced physical activity (Shah et al., 2015).

Despite considerable research on modifiable factors' role in atherosclerosis onset and progression, discrepancies continue in the scientific community regarding atherosclerosis initiation. Historically, atherosclerosis was commonly described through two hypotheses: A) The response

to injury hypothesis that proposed atherosclerosis resulted from endothelial damage caused by higher shear stress at arterial bends and bifurcations. B) The lipid hypothesis which suggested that atherosclerosis occurs due to high levels of circulating lipoproteins (Williams & Tabas, 1995)(Paszkowiak & Dardik, 2003)(Shah et al., 2015). While endothelial damage and lipoprotein levels have been proven to be considerable risk factors for atherosclerosis progression, inconsistent evidence supports these events as initiating factors. Notably, the lack of atherosclerotic remodelling in areas of endothelial damage and the presence of remodelling in areas void of endothelial damage challenges the response to injury hypothesis. Meanwhile, the occurrence of variations in the severity of atherosclerosis among individuals with similar lipid levels undermines the consistency of the lipid hypothesis (Paszkowiak & Dardik, 2003).

Due to these observations, the last two decades of atherosclerosis research has since adopted the theoretical basis of the 'response-to-retention' hypothesis, which provides a more active role for the ECM in atherosclerosis initiation (Williams & Tabas, 1995). Specifically, that the retention of lipoproteins LDL and RC is caused by strong ionic interactions between the positively charged amino acid residues of the apolipoproteins present on the surface of cholesterol-rich lipoproteins like LDL and RC and the negatively charged proteoglycan Glycosaminoglycan (GAG) branches in the ECM of the tunica intima (Figure 1.4)(Figure 1.5) (Tannock & King, 2008)(Gisterå & Hansson, 2017)(Nakashima et al., 2008). Collagen fibres allow proteoglycan attachment and interact and trap LDL and RC within this matrix. The progression of atherosclerosis thus occurs in three key steps: 1). lipoprotein deposition, 2). a subsequent inflammatory response (a result of oxidation), and 3). smooth muscle cell cap formation (Insull, 2009)(Williams & Tabas, 1995). Endothelial cells, which form the outermost layer of the tunica intima, are exposed to the circulating lipoproteins from the bloodstream (Paszkowiak & Dardik, 2003)(Rafieian-Kopaei et al., 2014). Following lipoprotein infiltration and accumulation within the tunica intima, LDL undergoes oxidation, creating the pro-inflammatory signal ox-LDL (Rafieian-Kopaei et al., 2014)(Hansson, 2001). Ox-LDL then stimulates endothelial cells for adhesion molecule mobilization to the injury site. Simultaneously, smooth muscle cells secrete chemoattractants and chemokines, attracting monocytes for phagocytosis (Miteva et al., 2018)(Insull, 2009). Interestingly, RC stimulates an immune response similar to ox-LDL following infiltration of the tunica intima; however, this occurs without oxidative modification. Upon entry of the tunica intima, monocytes transform into macrophages, digest ox-LDL and RC in a process known as

phagocytosis and ultimately become foam cells (Miteva et al., 2018). Plaque formation is further promoted and stabilized by a smooth muscle cell fibrous cap, which occurs once smooth muscle cells proliferate and simultaneously secrete proteoglycans, collagen, and elastic fibres (Insull, 2009)(Doran et al., 2008)(Tannock & King, 2008). Lipoprotein oxidation and the subsequent inflammatory response can be reversed up to this stage. The formation of multiple layers of individual foam cells only contributes to microscopic arterial changes (Insull, 2009). However, atherosclerosis becomes challenging to treat in the advanced stage, when lipid accumulation appears and the smooth muscle cell fibrous cap is fully formed, thus stabilizing the plaque (Doran et al., 2008).

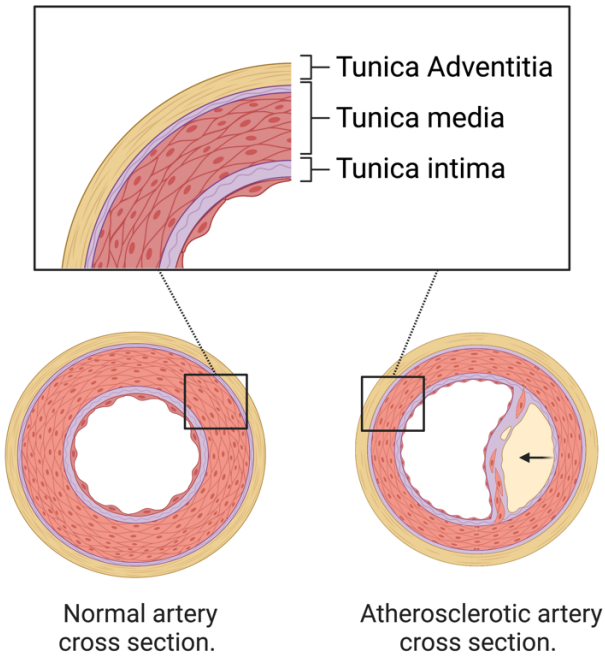

Figure 1.4 Cross section of the arterial wall under both normal and atherosclerotic conditions. The tunica adventitia represents the outermost layer of the arterial wall, predominantly consisting of connective tissue containing collagen and elastic fibres. The tunica media is the middle layer, composed mainly of ECM proteins, including smooth muscle cells, collagen, elastin, and proteoglycans. The tunica intima constitutes the innermost layer of the arterial wall, which is in direct contact with the bloodstream and primarily comprises a thin layer of endothelial cells and some ECM proteins, including proteoglycans. Created with BioRender.

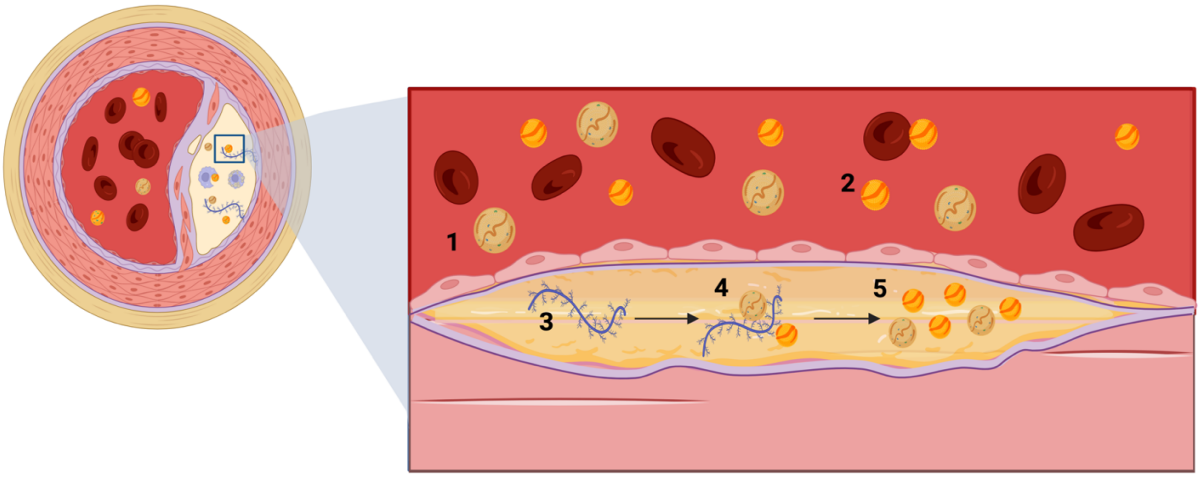

Figure 1.5 Cross-section of the artery wall during atherosclerosis. As per the response-to-retention hypothesis, atherosclerosis is initiated by apolipoprotein B-containing lipoproteins binding to proteoglycans in the extracellular matrix of the artery wall. 1) Circulating remnant cholesterol 2) Circulating Low-Density Lipoprotein 3) Proteoglycans in the ECM of the tunica intima 4) Remnant cholesterol and LDL bind to glycosaminoglycan side chains on proteoglycans 5) Lipoproteins accumulate in the inner tunica intima. Created with BioRender.

1.2 General pathogen recognition

The immune system is a set of biological processes and agents collaborating to protect against infection (Figure 1.6). The immune system comprises two subtypes: the innate and adaptive immune systems (Delves & Roitt, 2000). The innate immune system exists in all multicellular organisms, reacting rapidly to various stimuli as a first line of defence (Delves & Roitt, 2000). In contrast, the adaptive immune system functions as a slower second defence with pathogen specificity, capable of developing immunological memory.

Although it was initially believed that these defences evolved independently from one another, research has since shown that the innate immune system regulates aspects of the adaptive immune system (Iwasaki & Medzhitov, 2015).

1.2.1 Innate immune system pathogen response

The innate immune response is stimulated by Pattern-Recognition Receptors (PRRs) found on macrophages, mast cells, and Dendritic Cells (DCs). These receptors rely on Pathogen-Associated Molecular Patterns (PAMPs) to assess a variety of stimuli (Iwasaki & Medzhitov, 2015)(Schenten

& Medzhitov, 2011)(Alberts et al., 2002). Different types of PRRs undertake different roles, including but not limited to intracellular signalling, opsonization, chemotaxis, and endocytosis (Schenten & Medzhitov, 2011)(Dempsey et al., 2003). PRRs, like Toll-Like Receptors (TLRs) can monitor the extracellular space, while NOD-Like Receptors (NLRs) monitor the intracellular space (Dempsey et al., 2003)(Schenten & Medzhitov, 2011). Stimulation of PRRs through pathogen recognition activates the innate immune system, triggering an immediate inflammatory cascade termed the acute phase response (Schenten & Medzhitov, 2011)(Zhang & An, 2007)(Beutler, 2004). Monocytes are among the first immune cells to arrive at the injury site, differentiating into macrophages and DCs. Both macrophages and DCs can undergo the digestion of pathogens, known as phagocytosis (Witztum & Lichtman, 2014)(Schenten & Medzhitov, 2011)(Alberts et al., 2002)(Beutler, 2004). Additionally, macrophages and DCs can secrete pro-inflammatory cytokines and chemokines, notably Tumor Necrosis Factor-alpha (TNF-α), Interleukin-1-beta (IL-1β), and interleukin-6 (IL-6) (Miteva et al., 2018)(Witztum & Lichtman, 2014)(Schenten & Medzhitov, 2011). Studies using the IL-1β and Interleukin-1 Receptor Antagonist (IL-1rα) have demonstrated strong evidence of the critical role of Il-1β in the acute phase response through mediation of the vasodilation signal Prostaglandin E2 (PGE2) (Zhang & An, 2007). IL-1β activity has also been linked to activating downstream signalling cascades, notably the Janus Kinase/Signal Transducers and Activators of Transcription (JAK/STAT), Mitogen-Activated Protein Kinase (MAPK), and PI3K/Akt (Phosphatidylinositol-3-Kinase) pathways.

These pathways are necessary for the transcription of genes involved in the proliferation, survival, differentiation, and migration of immune cells. Similarly, TNF-α and IL-1β act as signals for the activation of the Nuclear Factor Kappa-B (NF-kB) pathways, which regulate inflammation, survival, and programmed cell death known as apoptosis (Zhang & An, 2007).

Additionally, TNF-α and IL-1β stimulate phagocytic cells, specifically macrophages, DCs and, in some cases, neutrophils, for cell digestion (Miteva et al., 2018). Interleukin-12 (IL-12) and Interleukin-18 (IL-18) similarly recruit Natural Killer (NK) cells for apoptosis and targeted cell removal (Alberts et al., 2002). This process of targeting cells for digestion and removal without the use of antibodies, exhibited by both NK cells and phagocytes, is known as cell-mediated immunity. The classic symptoms of inflammation, specifically redness, pain, swelling, and heat, occur due to these cytokine and phagocyte-mediated effects (Dempsey et al., 2003) (Zhang & An, 2007).

1.2.2 Adaptive immune system pathogen response

Beyond their phagocytic capabilities, DCs are an essential link between the innate and adaptive immune systems by activating T-cells. DCs convert pathogen segments into antigens for specialized DCs known as Antigen-Presenting Cells (APC)(Janeway et al., 2001)(Marshall et al., 2018). These APCs express the processed antigens on their surface, presenting them using Major Histocompatibility Complexes (MHC) to the T- and B-cells in the lymph nodes, known as antigen presentation (Anaya et al., 2013)(Alberts et al., 2002)(Marshall et al., 2018). T-cells are designed to recognize and react against particular epitopes (Anaya et al., 2013). After activation through antigen presentation and co-stimulation, T-cells multiply rapidly, targeting infected cells through cell-mediated immunity without the use of antibodies. T-cell activation triggers the formation of cytotoxic CD8+ T-cells (Anaya et al., 2013). These CD8+ T-cells secrete perforins and granzymes, which can cause apoptosis or death of infected cells.

Additionally, T-cells can differentiate into helper T (Th) cells and regulatory T (Treg) cells (Schenten & Medzhitov, 2011)(Bonilla & Oettgen, 2010)(Marshall et al., 2018). Treg cells can inhibit inflammation through downstream regulation of pro-inflammatory cytokines.

In contrast, Th cells increase cytokine secretion to stimulate phagocytes to mobilize to the injury site and mediate phagocytosis (Bonilla & Oettgen, 2010)(Marshall et al., 2018). These Th-generated cytokines additionally recruit B-cells to the injury site for antibody-mediated apoptosis of target cells. B-cell activation triggers the multiplication and transformation of B-cells into plasma cells, capable of antibody secretion (Janeway et al., 2001). This process is known as the humoral immune response (Schenten & Medzhitov, 2011)(Bonilla & Oettgen, 2010)(Anaya et al., 2013). As the pathogen levels drop, the immune system undergoes a 'death' or contraction phase (Lau et al., 2005), wherein most immune cells are depleted, except for a select few T- and B-cells that remain for immunological memory. This allows the immune system to maintain B-cell-derived antibodies specific to that pathogen for future defence.

Lastly, coinhibitory receptors found on APCs and T-cells regulate the immune response and prevent overstimulation of the immune system (Banday & Abdalla, 2020). The role of coinhibitory receptors in managing an immune response's regulation, inhibition, severity, and length has been well documented (Cai et al., 2021). As mentioned, T-cells become activated through interactions with APCs. (Yousif et al., 2022). However, in addition to antigen presentation, a second signal is needed for T-cell activation. This second signal can occur through the co-stimulation of receptors

on T-cells and stimulatory molecules on APCs (Yousif et al., 2022), such as the CD28 receptor on T-cells binding to CD80/86 on APCs. This signal is necessary for signalling pathways, specifically the PI3K/Akt pathway (Chen and Flies, 2013)(Yousif et al., 2022). Activating the PI3K/Akt pathway stimulates T-cells' differentiation, proliferation and survival. Moreover, Cytotoxic T-Lymphocyte Antigen (CTLA)-4 inhibits this co-stimulation, providing another avenue for immune regulation (Chen and Flies, 2013)(Cai et al., 2021)(Banday & Abdalla, 2020).

Conversely, the interaction between Programmed cell Death protein 1 (PD-1) on T-cells and the Programmed Death Ligands 1 and 2 (PD-L1)(PD-L2) on blood cells and phagocytes, respectively, acts as a significant immune checkpoint that reduces T-cell activity (Yousif et al., 2022)(Cai et al., 2021). This process occurs through Src Homology region 2-containing Protein tyrosine phosphatase 2 (SHP-2) mediated dephosphorylation and subsequent inhibition of the PI3K-Akt pathway (Yousif et al., 2022).

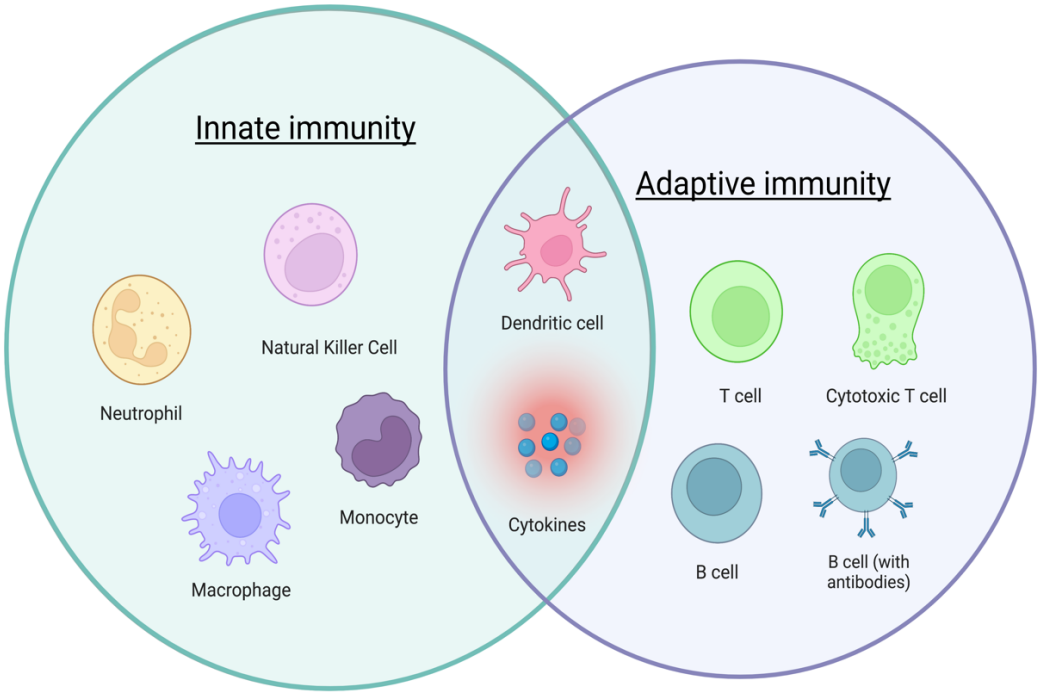

Figure 1.6 Venn diagram illustrating the overlap of innate and adaptive immune cell mediators. The diagram highlights the shared and distinct classifications of macrophages, monocytes,

dendritic cells, cytokines, neutrophils, natural killer cells, T-cells, cytotoxic CD8+ T-cells, B-cells, and B-cells with antibodies. Created with BioRender.

1.3 Innate and adaptive immunity during atherosclerosis

The immune system has been heavily implicated in atherosclerosis due to its pathophysiology of low-grade chronic inflammation (Wolf & Ley, 2019). The severity and duration of the immune response is a major determinant of atherosclerosis outcomes (Skaggs et al., 2012). Various immune cells and immune system derivatives, including macrophages, DCs, lymphocytes (T- and B-cells) and inflammatory cytokines, are found in significant levels in atherosclerotic lesions (Galkina & Ley, 2009). While, immunomodulatory cells like NK cells and neutrophils play critical roles in the initiation and recruitment of the aforementioned immune components (Figure 1.7).

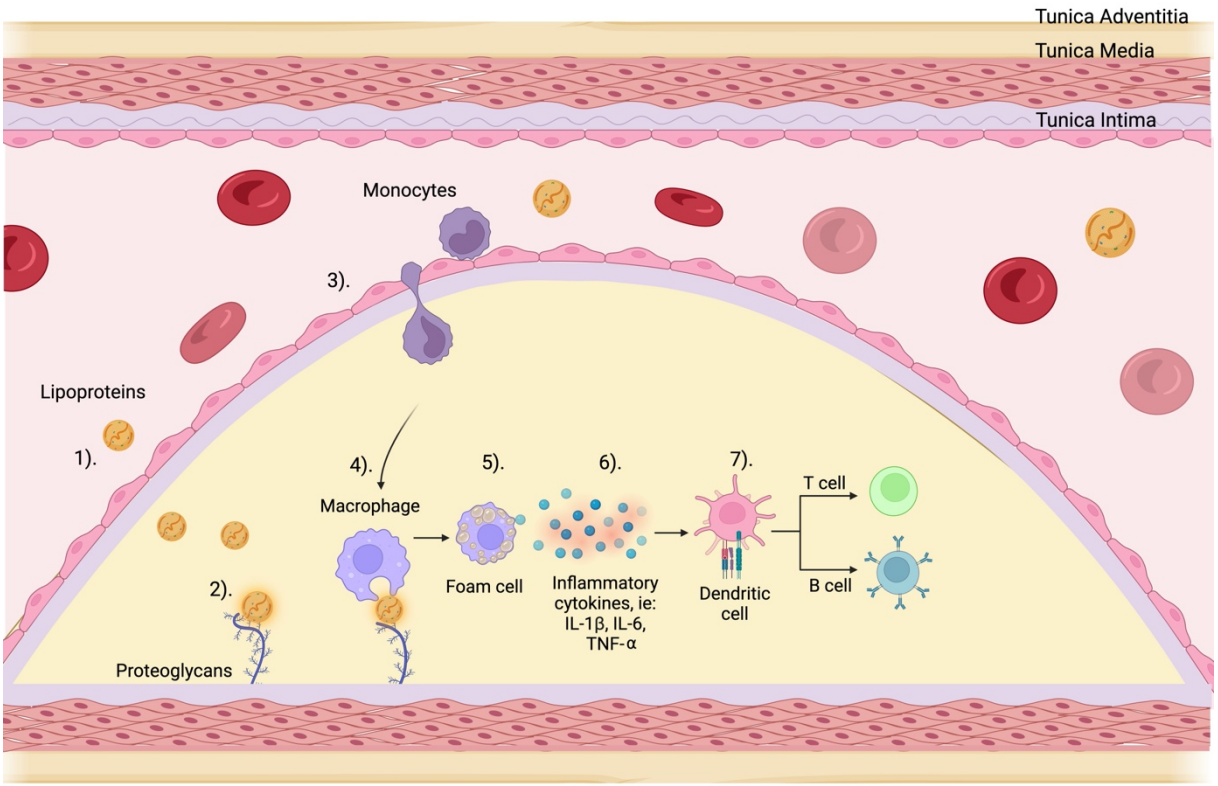

Figure 1.7 Simplified model of the critical immune events (innate and adaptive responses) in the development of atherosclerosis. 1) Lipoprotein infiltration of the ECM of the tunica intima. 2) Lipoprotein-proteoglycan binding. 3) Recruitment of circulating monocytes by adhesion molecules on the endothelium 4) Infiltration of monocytes and their differentiation into

macrophages. 5) Macrophages engulf lipoproteins, forming foam cells. 6) Foam cells release pro-inflammatory cytokines IL-1β, IL-6, and TNF-α 7) Pro-inflammatory cytokines activate DCs. DCs migrate to the draining lymph nodes and use APCs to activate T and B cells, which are then free to enter the tunica intima from the bloodstream. Created with BioRender.

1.3.1 Role of neutrophils in early stage atherogenesis

When infection or tissue damage occurs, neutrophils are among the first immune cells to respond by migrating to the injury site and releasing pro-inflammatory cytokines to neutralize the pathogen (Miteva et al., 2018). However, when neutrophils remain activated for prolonged periods during chronic inflammation, they become pathogenic. For example, prolonged activation of neutrophils can degrade the ECM of the tunica intima through the excessive release of neutrophil enzymes tryptase and chymase. This can weaken the arterial wall and contribute to the formation of an atherosclerotic plaque. Additionally, neutrophils release granules filled with pro-oxidative proteins like Myeloperoxidase (MPO), further promoting chronic inflammation. (Miteva et al., 2018). In a study conducted in 2008 by (van Leeuwen et al., 2008), LDL Receptor knockout (LDLr−/−) mice fed a high-fat diet to induce atherosclerosis had higher levels of neutrophils in both early and late-stage atherosclerotic lesions compared to controls (van Leeuwen et al., 2008)(Soehnlein, 2012).

Furthermore, research has established a connection between the migration of neutrophils and hypercholesterolemia, a significant risk factor in the onset and progression of atherosclerosis (Soehnlein, 2012). Hypercholesterolemia increases levels of chemokine (C-X-C motif) ligand-1 (CXCL1), which acts as a chemoattractant and stimulates the neutrophil surface CXC chemokine receptor 2 (Miteva et al., 2018), causing neutrophil migration and accumulation. Similarly, it has been demonstrated that hypercholesterolemia can trigger the production of Granulocyte Colony-Stimulating Factor *in-vivo* (GCSF), which upregulates neutrophil adhesion molecules (Soehnlein, 2012).

Moreover, neutrophils can enhance the attachment of monocytes and macrophages to the endothelium, leading to their infiltration of the tunica intima (Miteva et al., 2018)(Soehnlein, 2012). Various studies have found that overall increased levels of neutrophils in the bloodstream positively affected the incidence of cardiovascular events (Soehnlein, 2012). Ultimately, increased neutrophil migration, retention, and activation can cause plaque growth and instability, promoting atherogenesis.

1.3.2 Role of natural killer (NK) cells in early stage atherogenesis

There is mounting evidence that NK cells function as biomarkers for the development or degeneration of atherosclerosis (Miteva et al., 2018). However, while the accumulation of NK cells has been associated with chronic inflammation, there are inconsistent results regarding the pathophysiological role of NK cells in atherosclerosis. A study published in 1990 by Paigen et al. established the use of a beige mouse model with a mutation on the gene *Lyst*, causing loss of function of lysosomal transport and subsequently reducing levels of NK cells. The group found that when fed a high-fat diet to induce atherosclerosis, the beige mice demonstrated decreased survival compared to healthy controls provided the same diet (Paigen et al., 1990)(Bonaccorsi et al., 2015). However, they found no significant difference in atherosclerotic lesion size between the treatment groups.

Furthermore, a study conducted in 2002 by Schiller et al. using LDLr−/− beige mice fed a high-fat diet reported significantly increased atherosclerosis compared to the control LDLr−/− mice (Schiller et al., 2002)(Bonaccorsi et al., 2015). However, the group also reported that in LDLr−/− perforin-deficient mouse models, atherosclerotic lesion sizes and levels were similar to those of the control mice. This indicates that impaired NK cell cytotoxic activity was not significant in atherosclerosis progression, suggesting that cytokine production may be the primary mechanism of the atherosclerotic effect of NK cells (Bonaccorsi et al., 2015). Furthermore, several chemokines found in atherosclerotic lesions have been directly linked to the recruitment of NK cells. High Monocyte Chemoattractant Protein-1 (MCP-1) levels have been reported in atherosclerotic lesions and have been shown to function as an attractant for NK cells (Bonaccorsi et al., 2015). Additionally, Interferon-gamma (IFN-γ) is a vital cytokine produced by NK cells, which acts as a pro-atherogenic signal that can induce smooth muscle cell apoptosis, leading to plaque destabilization (Bonaccorsi et al., 2015).

1.3.3 Role of monocytes and macrophages in early stage atherogenesis

Monocytes and macrophages have been vastly implicated in the development of atherosclerosis. During the initiation of atherosclerosis, monocytes travel through the bloodstream to the 'injury site' in the tunica intima, where they differentiate into macrophages and DCs (Ilhan, 2015)(Hansson et al., 2002). High levels of monocytes are an independent predictor of cardiovascular event incidence. Monocytes CD14++CD16+ produce high levels of Reactive

Oxygen Species (ROS), which promote LDL oxidation and activate pro-inflammatory cytokines TNF-α, IL-1β, and IL-6 (Miteva et al., 2018). CD14++CD16+ are also involved in angiogenesis, phagocytosis, and antigen presentation (Miteva et al., 2018).

Additionally, mice deficient in macrophage colony-stimulating factor, which triggers monocyte differentiation to macrophages, have markedly reduced levels of atherosclerosis, evidence that the conversion of monocytes into macrophages plays a significant role in atherogenesis (Smith et al., 1995)(Ilhan, 2015). Monocyte-derived macrophages promote atherogenesis through various mechanisms, including foam cell formation, endothelial dysfunction, and pro-inflammatory cytokine activation.

M1 macrophages release high levels of interleukin cytokines IL-12 and IL-23, which generate ROS, which can contribute to oxidative stress and tissue damage (Miteva et al., 2018). M1 macrophages similarly produce Il-1β, which induces the expression of cytokines IL-6, IL-1α, and TNF-α, which mediate inflammation, cell proliferation, cell differentiation, and cell survival (Miteva et al., 2018)(Moore et al., 2013)(Barrett, 2020). The expression of M1 macrophages has been shown to be regulated by key transcription factors: NF-kB, Signal Transducer and Activator of Transcription (STAT1, STAT5), and Interferon-Regulatory Factors (IRF3, IRF5) (Yao et al., 2019). *In-vitro* studies of M1 macrophages also reported plaque rupture through degradation of the ECM. Additionally, M1 macrophages transform into foam cells when they phagocytose ox-LDL and RC, which play a significant role in fatty streak formation and subsequent plaque formation (Figure 1.8)(Moore et al., 2013)(Barrett, 2020). Macrophages use scavenger receptors expressed on their cell surface, such as CD36, to recognize and bind ox-LDL and RC. Once attached, the macrophages use receptor-mediated endocytosis to engulf the lipoproteins. The accumulated lipoproteins are then broken down in the macrophages, releasing cholesterol. The cholesterol is removed from macrophages through cholesterol efflux (Barrett, 2020); however, if this process is dysfunctional, the macrophage retains excess lipids, creating foam cells (Mohmmad-Rezaei et al., 2021). The critical role of foam cell formation in atherosclerosis is well described (Moore et al., 2013).

However, it is essential to note that some macrophages have been reported to have athero-protective effects. M2 macrophages are considered functionally anti-inflammatory (Barrett, 2020), and M2 gene expression is regulated by STAT6, IRF4, Jumonji Domain-containing protein-3 (JMJD3), and Peroxisome Proliferator Activated Receptor -delta and -gamma (PPARδ, PPARγ)

transcription factors (Yao et al., 2019). M2 macrophages can also be further divided into M2a, M2b, M2c, and M2d subtypes. M2a and M2C macrophages produce high levels of anti-inflammatory cytokines IL-10 and Transforming Growth Factor-beta (TGF-β), encouraging tissue repair, plaque stabilization, clearing cellular debris, and downregulating pro-inflammatory cytokines, which ultimately protect against atherosclerosis (Miteva et al., 2018)(Bobryshev et al., 2016). Additionally, M2c macrophages release IL-1rα, which prevents IL-1β activation through competitive inhibition of the IL-1 receptors (Figure 1.8).

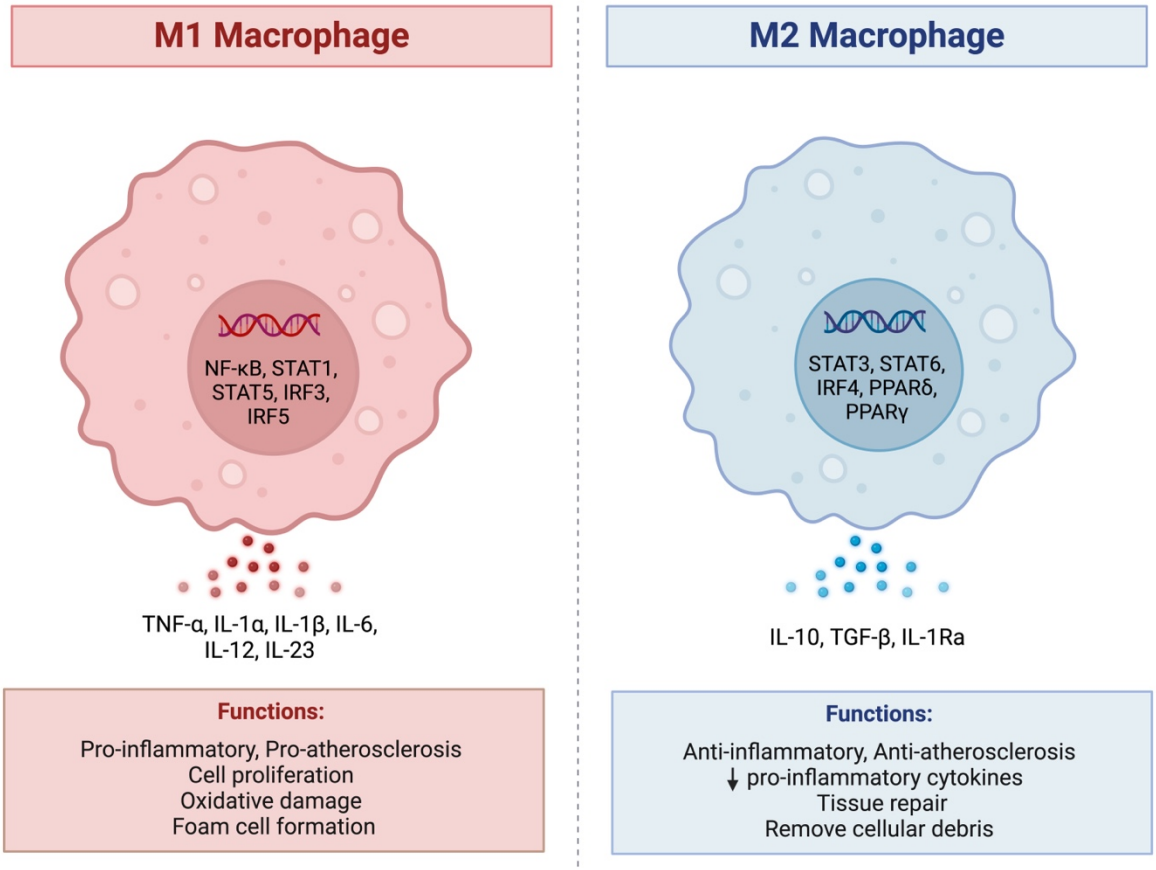

Figure 1.8 Comparison of the main features and atherosclerotic functions of M1 and M2 macrophages. Adapted from: Kim, S. (2022). Macrophage Polarization: M1 and M2 Subtypes. https://app.biorender.com/biorender-templates/figures/all/t-62cc6cda90428ea200a5dfb6-macrophage-polarization-m1-and-m2-subtypes. Created with BioRender.

1.3.4 Role of dendritic cells (DCs) in early stage atherogenesis

DCs play a unique role in atherosclerosis by serving as a link between the innate and adaptive immune systems. A 2009 study conducted using murine models reported an anti-atherosclerotic effect of a diphtheria toxin which reduced intimal DCs by >98% (Mohmmad-Rezaei et al., 2021)(Paulson et al., 2010). Moreover, the detection of DCs in mouse and human atherosclerotic lesions and vasculature has prompted rapid developments in our understanding of the role of DCs in atherogenesis (Subramanian & Tabas, 2014)(Roy et al., 2022). DCs undergo maturation when they encounter an antigen; they can then differentiate into APCs, activating T-cells of the adaptive immune system. DC maturation downregulates various pathways associated with pathogen capture, such as phagocytosis. Additionally, DC maturation has been linked to the secretion of various pro-atherogenic inflammatory cytokines such as IL-1β, IL-6 and TNF-α. Mature dendritic cells can also secrete Matrix Metalloproteinases (MMPs), enzymes that can cause ECM and collagen destruction and reduce the strength of the fibrous cap (Ilhan, 2015). DC maturation also upregulates T-cell stimulatory molecules CD80 and CD86, which have been shown to have pro-atherogenic effects in CD80 and CD86 knockout murine models (Subramanian & Tabas, 2014). This suggests that antigen presentation and subsequent T-cell activation and differentiation also play a significant role in the pro-atherosclerotic effect of DCs.

Th1 T-cells recruit pro-inflammatory cytokines like TNF-α, which have been reported to exacerbate inflammation in atherosclerosis. Moreover, Th1 T-cells recruit IFN-γ, promoting monocyte differentiation into macrophages and consequently increasing foam cell formation. Additionally, T-cell activation and the cytokines released create a feedback loop that further promotes T-cell activation, proliferation, and survival. High levels of T-cell interactions have been linked to advanced atherosclerotic plaques that are prone to rupture (Ilhan, 2015).

Lastly, DCs can play a direct role in foam cell formation through lipoprotein phagocytosis (Subramanian & Tabas, 2014). Like macrophage-derived monocytes, DCs have been shown to take up ox-LDL and RC through CD36 receptors, causing foam cell formation. However, DCs can also form foam cells when they take up immune complexes of lipoproteins, immune cells, and cellular debris.

1.3.5 Role of pro-inflammatory cytokines in intermediate stage atherogenesis

Cytokines are divided into six different categories, which include Interleukins (IL), Tumour Necrosis Factors (TNF), Interferons (IFN), Colony-Stimulating Factors (CSF), Transforming Growth Factors (TGF), and chemokines (Tedgui & Mallat, 2006). Cytokines are reported to play a significant role in atherogenesis by mediating the inflammatory signalling cascades of the innate and adaptive immune systems.

The NLR family pyrin domain containing 3 (NLRP3) inflammasome is a pro-inflammatory immune complex activated by various stimuli, including cholesterol crystals, mechanical stress, modified lipoproteins, immune cells, and ROS (Karasawa & Takahashi, 2017)(Silvis et al., 2021). Once active, the NLRP3 inflammasome mediates the activation of the enzyme caspase 1. Caspase-1 then cleaves and activates the pro-forms of IL-1β and IL-18 (Schenten & Medzhitov, 2011)(Silvis et al., 2021)(Baldrighi et al., 2017). IL-1β and IL-18 significantly amplify inflammation by triggering the transcription factor NF-κB (Schenten & Medzhitov, 2011)(Ramji & Davies, 2015), which regulates the pro-inflammatory cytokines and chemokines that recruit immune cells, such as macrophages and T-cells, to the tunica intima, where they contribute to fatty streak formation (Silvis et al., 2021).

NF-κB also stimulates the expression of adhesion molecules, including ICAM-1 and VCAM-1, on the endothelial cell surface, facilitating the adhesion and infiltration of monocytes, neutrophils, and NK cells in the tunica intima. NF-kB can additionally promote the proliferation of Vascular Smooth Muscle Cells (VSMC), which results in the formation of the fibrous cap, stabilizing the atherosclerotic plaque. An *in-vivo* study by Kanters et al. assessed the development of atherosclerotic lesions in pro-atherogenic LDLr-/- mice with a non-functional NF-kB-1 subunit compared to LDLr-/- mice (Kanters et al., 2003). The group found that the deficient NF-kB-1 mice had considerably reduced lesion size, suggesting a critical role for NF-kB in atherogenesis (Tedgui & Mallat, 2006)(Kanters et al., 2003).

Like NF-kB, Jun N-terminal Kinase (JNK) is a pro-atherogenic transcription factor indirectly stimulated by the NLRP3 inflammasome through IL-1β and IL-18-mediated activation of TNF-α (Tedgui & Mallat, 2006). JNK regulates numerous pro-inflammatory genes, such as TNF-α, IL-2, IL-6, E-selectin, ICAM-1, VCAM-1, MCP-1, and MMPs -1, -9, -12. Moreover, JNK can induce cell apoptosis of endothelial cells, which can contribute to ECM degradation and expose the subendothelial layer to physical stress and circulating lipoproteins. Macrophages in atherosclerotic

plaques express two isoforms of JNK, JNK1 and JNK2, which may exhibit distinct effects on cell viability and atherosclerosis. A study conducted in 2004 by Ricci et al. demonstrated that atherosclerotic lesions were notably reduced in ApoE-/- mice deficient in JNK-2 compared to control ApoE-/- mice; however, this effect was not reported in JNK-1 deficient ApoE-/- mice (Ricci et al., 2004). Similarly, a study conducted in 2016 by Babaev et al., using LDLr−/− mice deficient in JNK-1 and LDLr−/− mice deficient in JNK-2, reported that JNK-1 deficiency inhibited macrophage apoptosis and resulted in larger atherosclerotic lesions. These findings suggest a multifactorial role of JNKs in atherosclerosis (Babaev et al., 2016).

JAK/STAT is another signalling pathway activated by cytokines, interleukins, interferons, and Granulocyte-Macrophage Colony-Stimulating Factor (GM-CSF) during the innate immune response. A wide variety of JAK/STAT members exert both protective and pro-atherogenic effects *in-vivo*. STAT4 and STAT6 are critical in immunoregulation by promoting Th1 and Th2 T-cell differentiation. Th1 T-cells are thought to mediate pro-atherogenic effects, while Th2 T-cells are atheroprotective. Interestingly, studies on patients showing early signs of atherosclerosis have reported that using statins, which lowers cholesterol levels, can have additional positive effects by reducing Th1-mediated inflammation by inhibiting STAT4 activation (Tedgui & Mallat, 2006). Additionally, studies of STAT3 deletion in macrophages and neutrophils in mice reported enhanced chronic inflammation due to the inhibition of IL-10 and subsequent amplification of the Th1 response (Tedgui & Mallat, 2006). These findings suggest a potential protective role of STAT3 by promoting anti-inflammatory reactions in macrophages and neutrophils during atherogenesis.

Besides their effects on intracellular signalling, cytokine studies have reported numerous complementary pro-atherogenic effects. Cytokines can activate, recruit, and retain other immune cells, promoting accumulation within the plaque (Fatkhullina et al., 2016). Active cytokines IL-1β and IL-18 amplify their expression in a feedback loop, encourage ECM degradation, and recruit phagocytic immune cells. While TNF-α, IL-1, IL-6, IL-10, and TGF-β significantly affect DC maturation and have been shown to promote lipoprotein uptake by DCs and their conversion into foam cells (Fatkhullina et al., 2016). TGF-β has a multifactorial role in atherosclerosis as a cytokine and intracellular signalling pathway. As a cytokine, TGF-β binds to its receptors on the cell surface, which activates the TGF-β signalling cascade that controls various processes, such as cell growth, proliferation, differentiation, and apoptosis.

1.3.6 Role of T-cells in late stage atherogenesis

Ribonucleic Acid (RNA) sequencing studies have reported the presence of T-cells in all stages of atherosclerosis progression (Roy et al., 2022). It is widely reported that regulatory T-cells such as FOXP3+ and IL-10+ type 1 regulatory T-cells are predominant prior to atherosclerosis initiation. However, during atherogenesis, T-cell differentiation favours the production of pro-inflammatory CD4+ effector T-cells. CD4+ effector T-cells further differentiate into a subtype of helper T cells, Th1, Th2, and Th17 (Figure 1.9)(Witztum & Lichtman, 2014)(Tse et al., 2013). In atherosclerotic plaques, Th1 cells are the primary type of CD4+ T-cells (Roy et al., 2022); Th1 cells secrete IFN-γ, which plays a significant role in the progression of atherosclerosis by promoting the infiltration of monocytes, monocyte differentiation to macrophages, formation of foam cells, accumulation of lipids, and destabilization of plaques (Miteva et al., 2018).

A study conducted in 2004 by Buono et al. assessed the role of Th1 formation in atherosclerosis by using LDLr−/− mice fed a high-fat diet with a deficiency in T-bet. This transcription factor controls the differentiation of Th1. The group found that the LDLr−/− mice with T-bet deficiency exhibited a notable reduction in atherosclerotic lesions and plaque formation compared to the LDLr−/− control. Additionally, they reported that a deficiency of T-bet resulted in a shift toward Th2 differentiation (Buono et al., 2005). Th2 cells were linked to producing atheroprotective EO6 IgM antibodies that are specific to oxidized lipoproteins and prevent macrophage uptake of ox-LDL (Buono et al., 2005). Other studies have also reported a protective role of Th2 cells in atherosclerosis. Th2 cells are found at lower concentrations in atherosclerotic plaques and have been linked to the production of IL-4, an atheroprotective cytokine that inhibits Th1 differentiation and subsequent IFN-γ production (Miteva et al., 2018). Th17 cells similarly produce IL-17, inhibiting IFN-γ expression and slowing atherogenesis. However, Il-17 also has pro-atherogenic effects by stimulating the production of pro-inflammatory cytokines, thus suggesting a more complex role of Th17 in atherosclerosis.

Furthermore, Treg cells are immunomodulatory cells that exhibit atheroprotective effects by reducing the intensity of the immune response (Figure 1.9)(Witztum & Lichtman, 2014)(Miteva et al., 2018). A study conducted in 2006 by Ait-Oufella et al. found that Treg cell depletion in LDLr −/− mice resulted in a twofold increase in lesion size after a 20-week high-fat diet compared to LDLr −/− controls (Ait-Oufella et al., 2006).

Additionally, a study published in 2020 reported a vital role of Treg cells in atherosclerotic plaque regression by transplanting the aortic arch of a pro-atherogenic ApoE-/- mouse into a healthy mouse and ApoE-/- mouse. The group reported a three-fold increase of Tregs in the healthy mouse model compared to the pro-atherogenic model (Sharma et al., 2020).

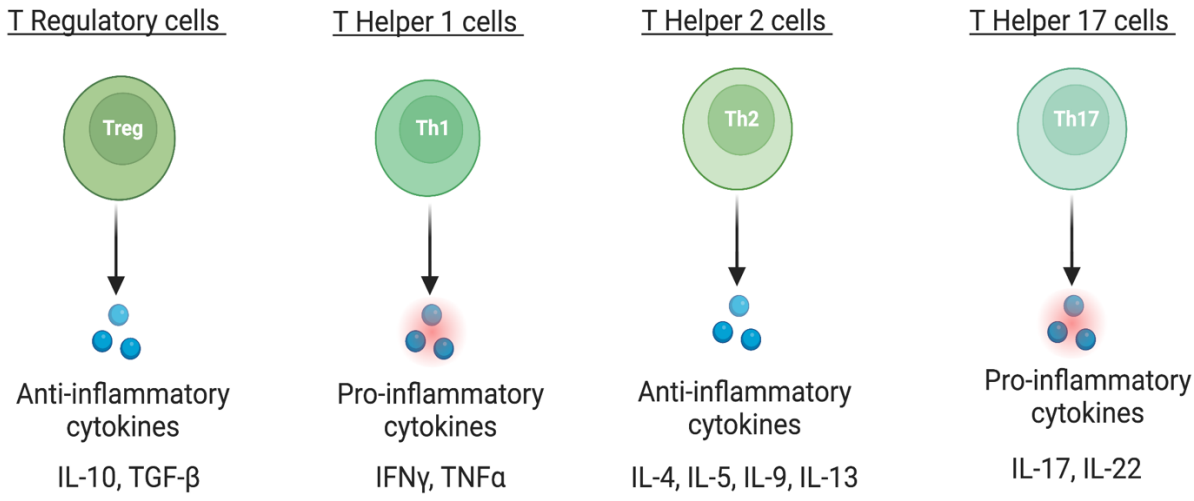

Figure 1.9 Simplified representation of the primary T-cell subtypes in atherosclerosis. Specifically, T regulatory, T helper 1, T helper 2, and T helper 17 cells. The figure illustrates the cytokines produced by each subset and their overall pro or anti-inflammatory effects in atherosclerosis. Created with BioRender.

1.3.7 Role of B-cells in late stage atherogenesis

B-cells play a vital role in the humoral immune response in atherosclerosis. Once atherosclerosis progresses, the adaptive immune response of B- and T-cells becomes the primary regulation system of the immune system. Antibody-producing plasma cells recognize and bind lipoprotein-immune complexes and are a significant determinant of an immune response's dissolution (contraction) stage (Sage et al., 2019). Overexpression or underexpression of B-cell populations can cause defects in antibody responses and immune checkpoints, promoting atherosclerosis (Sage et al., 2019). B-cells differentiate into two subtypes, B1 and B2 (Tsiantoulas et al., 2015). B1 cells then differentiate into B1a cells with atheroprotective effects by producing antibodies against ox-LDL, which prevents ox-LDL retention and macrophage phagocytosis (Sage & Mallat, 2014)(Tsiantoulas et al., 2015). A study conducted using a model of accelerated atherosclerosis

via splenectomy in Apoe-/- mice discovered a 50% reduction of B1a cells (Tsiantoulas et al., 2015). However, the role of B1b cells in atherosclerosis is less conclusive (Tsiantoulas et al., 2015). Like B1a cells, B1b cells produce anti-ox-LDL antibodies; however, this is only a minor atheroprotective effect as B1a produce the majority of natural antibodies (Sage et al., 2019)(Ma et al., 2021).

B2 cells circulate in the bloodstream and are predominately pro-atherogenic by producing pro-inflammatory cytokines and promoting T-cell activation (Mohmmad-Rezaei et al., 2021). B2 cells can also promote the differentiation of pro-atherogenic CD4+ T-cells (Sage et al., 2019). Studies of B2 cell deficiency reported a positive relationship between levels of B2 cells and Th1 cells; following B2 reduction, levels of IFN-γ were reduced (Sage et al., 2019). Additionally, a 2010 study of B2 cell inhibition in ApoE-/- mice found significant reductions in the rate of atherosclerosis and development (Kyaw et al., 2010). Moreover, B2 plasmablasts are found in large concentrations in the tunica adventitia of the arterial wall near the growing atherosclerotic plaque (Sage & Mallat, 2014). These findings suggest an essential role of B2 cells as pro-atherogenic mediators in the development of atherosclerosis.

1.4 Main classes of monoclonal antibody (mAb) therapies

Growing evidence supports the need for new specialized immunotherapies in the modulation of atherosclerosis. Immunotherapies, specifically monoclonal antibodies, have the unique potential to target the underlying mechanisms of atherosclerosis to prevent and slow its progression effectively. In developed countries, lipid-lowering and anti-inflammatory cytokine therapies are the first-line treatment in atherosclerosis management. However, new monoclonal antibodies targeting the arterial wall are becoming increasingly popular. These therapies target various immune response components and lipid metabolism and have shown promise in pre-clinical and clinical studies (Figure 1.10).

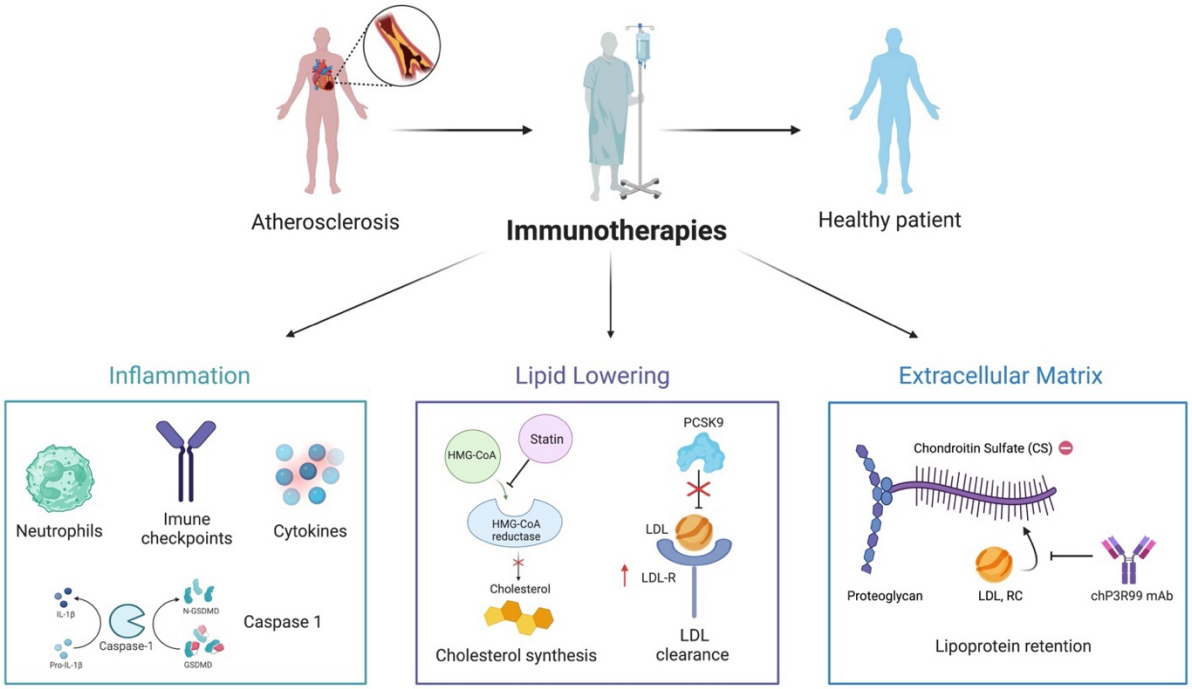

Figure 1.10 Model of the main immunotherapies for atherosclerosis treatment. Ranging from targeting inflammation to circulating lipoproteins and ECM proteins. Created with BioRender.

1.4.1 Anti-inflammatory therapies and mAbs

The CANTOS trial was a large-scale clinical trial that described the use of canakinumab, a mAb inhibitor of the pro-inflammatory cytokine IL-1β. Canakinumab reduces Il-1β signalling by directly binding to IL-1β, thereby preventing Il-1β mediated inflammation and consequently slowing atherosclerotic plaque growth. (Ridker et al., 2017). The CANTOS trial used a comprehensive randomized, blinded, placebo-controlled study design to follow 10,061 patients across 39 nations with previous reports of myocardial infarction and increased levels of High-Sensitivity C-Reactive Protein (hsCRP) from 2011 to 2017 (Ridker et al., 2017)(Pedro-Botet et al., 2020). The study found that over 3.7 years, the placebo group experienced 4.50 events per 100 person-years, while the 300 mg canakinumab treatment group experienced 3.90 events per 100 person-years (Ridker et al., 2017). Thus, 300 mg canakinumab administration reduced recurrent cardiovascular events by 0.60 per 100 person-years compared to the placebo cohort (Ridker et al., 2017). Interestingly, however, the canakinumab treatment group reported higher neutropenia cases

when compared to the placebo group. Similarly, the canakinumab group also exhibited higher rates of infection or sepsis-related deaths relative to the placebo group. Specifically, the canakinumab group experienced an incidence rate of 0.31 sepsis and infection-related death events per 100 person-years versus 0.18 events per 100 person-years for the placebo group. (Ridker et al., 2017). Additionally, thrombocytopenia was more frequent among those receiving canakinumab than the placebo group, but there were no notable differences in the incidence of hemorrhages (Ridker et al., 2017). Commercial approval for canakinumab and other notable IL-1β therapies, such as gevokizumab and mavrilimumab, has yet to be approved. TNF-α inhibitors, on the other hand, notably infliximab and certolizumab, have been commercially approved by the Federal Drug Agency (FDA) (Tousoulis et al., 2016). Preliminary studies using these anti-TNF-α therapies found reduced monocyte and neutrophil activity and improved endothelial and arterial wall function (Tousoulis et al., 2016). Additionally, various anti-inflammatory cytokine therapies inhibit the NLRP3 inflammasome, indirectly inhibiting IL-1β and TNF-α activity. A notable example is the synthetic NLRP3 inhibitor, MCC950, described by Coll et al. in 2015. (Coll et al., 2015). MCC950 works by binding to the NLRP3 protein, thereby preventing inflammasome assembly. This interaction suppresses IL-1β activation by inhibiting caspase-1 and caspase-11 pathways (Netea & Joosten, 2015). A 2021 study by Zeng et al. described the use of MCC950 in atherosclerotic models through ApoE-/- mice (Zeng et al., 2021). Following MCC950 administration, the group found evidence of decreases in atherosclerotic plaque size, macrophage levels, and pro-inflammatory cytokines, specifically IL-1β and IL-18 (83). Another prominent NLR3P inflammasome inhibitor, the ketone metabolite β-hydroxybutyrate (BHB), prevents potassium (K+) efflux, inhibiting ASC oligomerization, which is necessary for caspase-1 activation. A 2015 investigation reported that BHB use in mice with NLRP3-mediated disorders significantly reduced pro-inflammatory cytokines, specifically interleukins (Youm et al., 2015). However, anti-inflammatory cytokine therapies are not the only forms of anti-inflammatory therapies for atherosclerosis and CVD management. Similar to the CANTOS trial, the Low-Dose Colchicine (LoDoCo) trial was a first-of-its-kind prospective, observer-blinded clinical trial involving 532 participants diagnosed with coronary disease randomized to either a low-dose colchicine of 0.5 mg per day or non-colchicine group with a minimum two-year follow-up (Nidorf et al., 2013). However, unlike the CANTOS trial, which used a selective inhibitor of Il-1β, canakinumab, colchicine has broad-scale anti-inflammatory properties, most notably inhibiting

neutrophil function (Nidorf et al., 2020). Of the LoDoCo participants, 93% were taking aspirin and clopidogrel, and 95% were taking statins. 282 participants were assigned to the colchicine group, while 250 were assigned to the non-colchicine group (Nidorf et al., 2013). Overall, the colchicine group had 10.7% fewer combined occurrences of acute coronary syndrome, out-of-hospital cardiac arrest, or non-cardioembolic ischemic stroke (primary outcome) compared to the no-colchicine group (Nidorf et al., 2013). Fifteen of the 282 participants in the colchicine group experienced a primary outcome (5.3%) compared to forty of the 250 patients in the non-colchicine group (16%) (Nidorf et al., 2013). Although, as this was an open-labelled and moderate-scale trial, these results required validation in larger cohorts (Nidorf et al., 2020).

Following the LoDoCo trial, the Colchicine Cardiovascular Outcomes Trial (COLCOT) was conducted as a large-scale, randomized, parallel-arm, double-blind clinical trial involving a total of 4,745 participants with an average follow-up period of 1.88 years (22.6 months) (Tardif et al., 2019). The COLCOT trial recruited patients who had experienced a myocardial infarction within the last 30 days. Of the 4,745 participants, 2,366 received 0.5 mg of colchicine daily, while 2,379 received a placebo. They assessed incidences of cardiovascular-related deaths, instances of resuscitated cardiac arrest, myocardial infarction strokes, and severe angina that ultimately required hospitalization (Tardif et al., 2019). Overall, the colchicine group experienced 1.6% less of these cardiovascular outcomes than the placebo group. Of the 2,366 participants in the colchicine group, 5.5% experienced a cardiovascular outcome compared to the 7.1% in the placebo group (Tardif et al., 2019). Importantly, the results from the LoDoCo and COLCOT studies comprehensively established the applicability of low-dose colchicine as a CVD treatment. Conversely, Immune Checkpoint Inhibitors (ICI) are common mAbs used as pro-inflammatory therapies. As expanded on in section 1.2, immune checkpoints act as regulators of the immune response through T-cell inhibition and activation. However, despite the success of ICI mAbs in cancer treatment, studies have found a significant positive link between ICI therapies and atherosclerosis (Yousif et al., 2022). Interestingly, while cancer and atherosclerosis share similarities in their inflammatory-dependent pathophysiology, ICI mAbs, specifically CTLA-4– and PD-1–PD-L1 blocking antibodies, have been shown to increase cardiovascular events associated with atherosclerosis (Abreu et al. 2022). Although, a 2013 study that used to abatacept to increase CTLA-4 signalling downstream in ApoE 3-Leiden (E3L) mice found a reduction in the severity of atherosclerosis through a dramatic 78.1% decrease in arterial thickening (Ewing et al.,

2013), thus offering a different avenue for ICI therapy in atherosclerosis treatment. Nonetheless, it is critical to recognize that these anti-inflammatory therapies have negligible effects on circulating lipoproteins, a significant risk factor for atherosclerosis.

1.4.2 Lipid-lowering therapies and introduction to the use of mAbs

Statin therapy has served as the pinnacle of lipid-lowering treatments in Western medicine for over four decades. Statins function by inhibiting the enzyme β-Hydroxy β-methylglutaryl-CoA (HMG-CoA) Reductase in the cholesterol biosynthesis pathway, thereby inducing the synthesis of LDLr, which can then capture and reduce levels of circulating LDL (McFarland, 2014). A plethora of research on statin application has demonstrated its success in LDL reduction. A 2010 meta-analysis including 26 randomized controlled trials with 169,138 participants revealed that a 39 mg/dL reduction in LDL resulted in a 22% decline in Major Adverse Cardiovascular Events (MACE) over half a decade, independent of initial LDL levels and a 10% reduction in all-cause mortality across diverse clinical cohorts (Cholesterol Treatment Trialists' (CTT) Collaboration, 2010). Despite these significant findings, on-treatment events continue to occur in statin-treated patients (Libby, 2005).

Similarly, Proprotein Convertase Subtilisin/Kexin type 9 (PCSK9) inhibitors, which are lipid clearance agents that inhibit PCSK9-mediated degradation of LDLr, have been linked to reductions in circulating LDL, reduced myocardial infarction risk and overall decreases in mortality in some populations (Kim et al., 2022)(Farnier, 2014). Prominent PCSK9 inhibitors include mAbs such as evolocumab, bococizumab, and alirocumab (Rosenson et al., 2018). Administration of solely evolocumab resulted in a 53% reduction in plasma LDL levels (Kim et al., 2022), with similar outcomes reported for bococizumab and alirocumab. Furthermore, PCSK9 inhibitors, when administered with statins, have shown a pronounced reduction in LDL levels relative to only statin therapy. The Global Assessment of Plaque Regression with a PCSK9 Antibody as Measured by Intravascular Ultrasound (GLAGOV) and Evaluation of Cardiovascular Outcomes After an Acute Coronary Syndrome During Treatment With Alirocumab (ODYSSEY) trials were large-scale randomized, double-blind clinical control studies, that assessed the efficacy of evolocumab and alirocumab (with statins) in managing CV events (Rosenson et al., 2018)(Kim et al., 2022). The GLAGOV trial reported that evolocumab therapy mediated plaque regression, and the combined regimen of evolocumab and statins induced regression of the proliferating atheroma (Rosenson et

al., 2018). In the ODYSSEY trial, 80-88% of patients underwent statin treatment. The ODYSSEY trial found that combining alirocumab and statins reduced MACEs by 1.6 percent (9.5% for alirocumab vs 11.1% for placebo) and all-cause mortality by 0.6% (3.5% for alirocumab vs 4.1% for placebo) compared to the placebo + statin treatment (Rosenson et al., 2018).

A distinct randomized control trial by Pradhan et al. evaluated the combined regimen of bococizumab and statin therapy, involving 9,738 patients, and assessed on-treatment LDL levels 14 weeks post-intervention. The group reported a 60.5% reduction in LDL (Pradhan et al., 2018). However, they also acknowledged a significant correlation between patients with high hsCRP levels (>3 mg/L) and CV events. Moreover, even 14 weeks post-treatment, patients experienced residual risk associated with chronic inflammation (Pradhan et al., 2018). Pradhan et al. thus concluded that while PCSK9 and statin therapy reduce LDL levels and some CV events, they have minimal effects on inflammation. (Pradhan et al., 2018). Overall, lipid-lowering therapies, similar to anti-inflammatory therapies, are insufficient to mitigate CVD risk among all populations, illustrating the need for preventative immunotherapies targeting the arterial extracellular matrix.

1.5 Novel mAb immunotherapy; the chP3R99 mAb

Due to an evolving understanding of the underlying mechanisms involved in atherogenesis, mAbs for atherosclerosis have recently been shifting away from targeting LDL and inflammatory cytokines to targeting arterial wall components. Per the response-to-retention hypothesis, mAbs engineered to target ECM proteins of the tunica intima could provide an exciting opportunity for the prevention of lipoprotein retention and subsequent atherosclerotic plaque development. By addressing the ECM, mAbs would target the retention of lipoproteins and the consequent immune responses, inflammation, oxidative stress, and other processes involved in plaque formation. Currently, these mAbs are in early clinical and pre-clinical stages, with none having undergone regulatory approval. Further research, including large-scale trials, is needed to evaluate their safety, efficacy, and potential as therapeutic options for atherosclerosis. However, many have shown promising results in reducing atherosclerotic development, notably the proteoglycan targeting chP3R99 mAb (Soto et al., 2012)(Liu et al., 2022).

1.5.1 History, development, and production of the chP3R99 mAb

The chP3R99, developed by the Centre for Molecular Immunology (CIM) in Havana, Cuba, in 2012, was engineered as a novel therapy capable of targeting atherosclerosis initiation at the level of the arterial ECM (Soto et al., 2012). The chP3R99 mAb was created as a mutant form of the P3 monoclonal antibody. The P3 antibody described in a 1995 article by Vázquez et al. is a murine mAb with specificity to ganglioside molecules with N-glycolylated variants of sialic acid residues on the end of their carbohydrate chains (Vázquez et al., 1995). P3 binding to gangliosides occurs through an electric dipole interaction created by the charges of the sialic acid residues (Vázquez et al., 1995). Interestingly, the group also found that P3 mAb binds to sulfated glycolipids, suggesting that P3 binding requires a negative charge (Vázquez et al., 1995). The P3 was then modified to create the chP3, which combined murine and human immunoglobulins, specifically human IgG1. The prefix 'ch' describes the chimeric nature of the chP3 coming from both human and murine origins. Further site-specific single mutations of arginine residues at the Heavy Chain Complementarity Determining Regions 1 and 3 (HCDR1 and 3) wholly abrogated antigen binding, thus indicating that these regions were crucial for the specificity of the mAb (Lopez-Requena et al., 2007). Subsequently, a chP3 mutant with a higher affinity for negatively charged sulfated glycolipids and antigens was designed. This chP3 mutant, termed chP3R99, was engineered by replacing the glutamic acid residue with arginine at the 99th position of the immunoglobulin Heavy Chain Variable Region 3 (HCDR3, Kabat numbering) (Fernández-Marrero et al., 2011). These findings confirmed that HCDR3 is critical in mediating the P3's specific antigen and sulfate recognition qualities (Lopez-Requena et al., 2007). The chP3R99 is produced using the supernatant of murine myeloma (NS0) transfection cell cultures that express either the chimeric P3R99 or the humanized R3 antibodies (Mateo et al., 1997). Stable clones expressing chP3R99 were generated by the transfection of NS0 cells (Figure 1.11) by electroporation with the pAH4604 vector for chimeric heavy chain expression (Coloma et al., 1992) and the pMOS-blue vector for cloning and sequencing of antibody variable regions (Fernández-Marrero et al., 2011). Notably, the Fcγ receptor and complement-binding region of the chP3R99 mAb was refined to impair undesired induction of inflammatory responses (i.e. chP3R99-LALA) (Soto et al., 2012). Furthermore, the chP3R99's specificity and lack of binding to the Fcγ receptor prevent the occurrence of an inflammatory immune response (Figure 1.12).

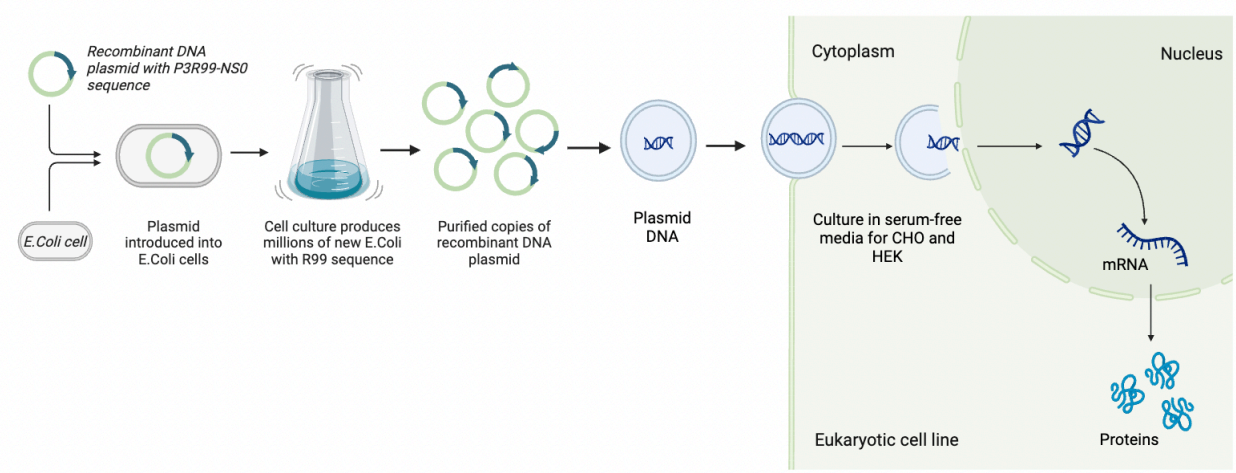

Figure 1.11 Deoxyribonucleic Acid (DNA) transfection production protocol for chP3R99 using a murine myeloma (NS0) cell line. Created with BioRender.

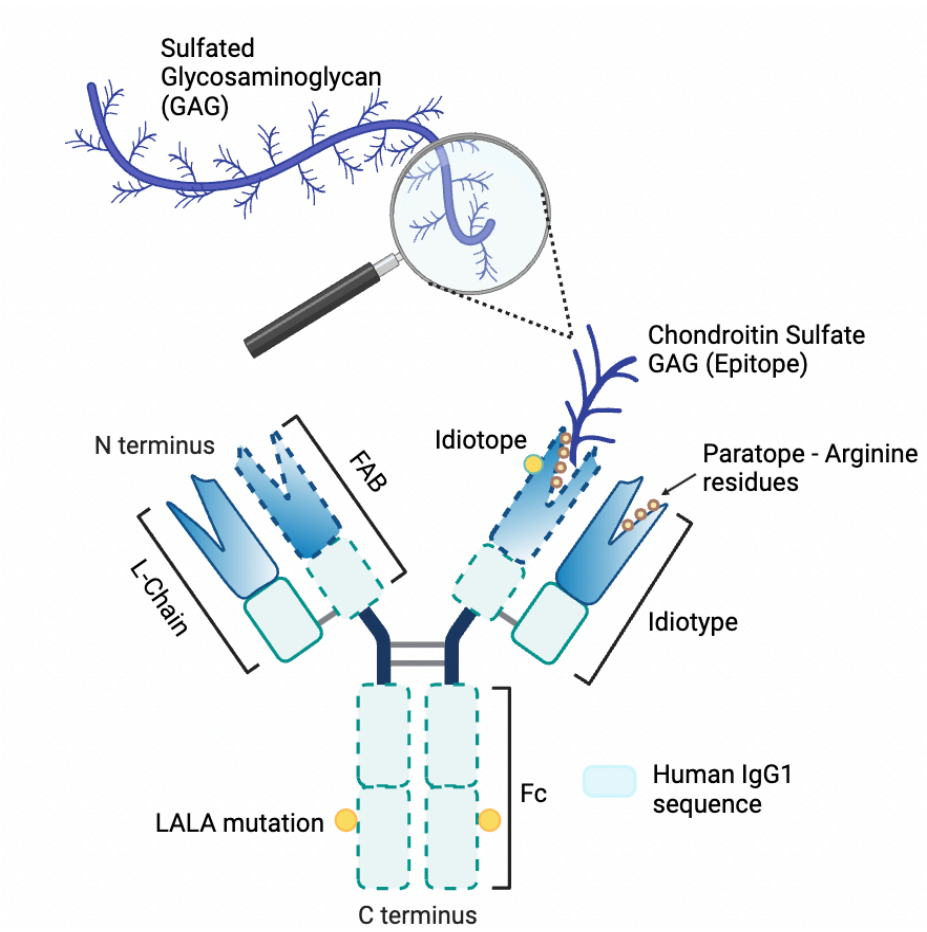

Figure 1.12 Summary of the main features and overall structure of the chP3R99. The chP3R99 is composed of murine idiotype (variable regions) and human IgG1 constant regions. The antigen recognition site, paratope, of chP3R99 contains arginine residues involved in the binding of chondroitin sulfate glycosaminoglycans and subsequent competitive inhibition of lipoprotein binding. The figure was redrawn and adapted from https://doi.org/10.1101/2023.08.30.555546. Created with BioRender.

1.5.2 Non-immunogenic effects of the chP3R99 mAb

As per the response to the retention hypothesis, the retention of lipoproteins by ECM components is the initiating factor of atherogenesis (Williams & Tabas, 1995). Evidence supports the notion that GAG branches found on proteoglycans, specifically sulfated GAGs, are responsible for lipoprotein binding and retention through ionic interactions. The negatively charged chondroitin sulfate is the prominent type of sulfated GAG found to form strong electrostatic bonds with basic (positively charged) amino acid residues on apolipoprotein B containing lipoproteins such as LDL and RC. Histological analysis of tissues with atherosclerotic remodelling has shown elevated levels of proteoglycans rich in chondroitin sulfate GAGs, specifically biglycan, decorin, and versican, compared to healthy controls (Tannock & King, 2008). A 2012 study by Soto et al. characterized the reactivity of chP3R99 to various GAG branches, including chondroitin sulfate, via Enzyme-linked Immunosorbent Assays (ELISAs). The group reported that chP3R99 exhibited a higher binding affinity to GAGs, especially sulfated GAGs, than the original chP3 antibody. Notably, chP3R99 exhibited preferential binding to chondroitin sulfate compared to other sulfated GAGs (Soto et al., 2012) (Table 1.1). As a result, the team evaluated the efficacy of chP3R99 in blocking the binding of LDL to chondroitin sulfate. Their results indicated that chP3R99 inhibited approximately ~70% of LDL binding to chondroitin sulfate and reduced ~80% of LDL oxidation *in-vitro* (Soto et al., 2012). Additionally, when chP3R99 mAb was delivered intravenously in rats, it preferentially accumulated within the arterial wall. Consequently, there was a significant decrease in LDL retention and oxidation within the arterial wall 24 hours after LDL introduction. Similarly, a 2023 pre-print study found that the chP3R99 inhibited the binding of LDL and remnant lipoproteins to chondroitin sulfate and the extracellular matrix at a similar cholesterol reduction proportion *in-vitro* (Soto et al., 2023).

Moreover, this study also assessed chP3R99 in obese insulin-resistant JCR:LA-cp rats as a model of accelerated atherosclerosis (Soto et al., 2023). Carotids taken from JCR:LA-cp rats treated with chP3R99 were perfused with fluorescently labelled LDL and remnant lipoproteins (RM) through the vasculature *ex-vivo*. ChP3R99-treated rat carotids demonstrated a notable reduction in LDL and RM carotid retention (Soto et al., 2023)(Table 1.1).

Furthermore, single-dose administrations of chP3R99 found that chP3R99 preferentially accumulates in areas prone to atherosclerotic remodelling, such as the aortic arch (Brito et al., 2012)(Delgado-Roche et al., 2013). This observation was further confirmed by two separate investigations, which employed radiolabeled technetium-99m (99mTc) chP3R99 (Soto et al., 2014) and Fluorescein Isothiocyanate (FITC) labelled chP3R99 (Brito et al., 2012). These studies demonstrated that the chP3R99 accumulates specifically in atherosclerotic lesions following intravenous antibody injection in rabbits (Soto et al., 2014) and mice (Brito et al., 2012), respectively.

1.5.3 Immunogenic effect of chP3R99 antibodies

In addition to chP3R99's ability to bind to pro-atherogenic GAGs, it has a long-term immunogenic effect through the induction of an anti-idiotypic cascade. This immunogenic quality was preserved from the original P3 murine antibody (Vázquez et al., 1995). Importantly, both CD4+ and CD8+ T-cell epitopes were identified at the HCDR motifs of the murine P3 idiotype, preserved within the chP3R99 mAb, conferring a high immunogenicity. chP3R99's unique idiotype stimulates the host immune system to produce antibodies of similar structure and function to the chP3R99, thus providing long-term protection like a vaccine (Soto et al., 2012)(Brito et al., 2012)(Urbain et al., 1977)(Behn, 2007). Specifically, chP3R99, termed Ab1 (antibody 1), stimulates the host to produce anti-idiotype secondary antibodies known as Ab2. A significant portion of these Ab2 antibodies resemble the antigen (Ab2β), chondroitin sulfate, and thus bind to Ab1 (Brito et al., 2012). The production of Ab2 antibodies then promotes anti-anti-idiotype antibodies known as Ab3, which are structurally and functionally similar to Ab1 (chP3R99) (Brito et al., 2012). These Ab3 antibodies, like the chP3R99, specifically recognize and bind chondroitin sulfate GAGs, thus preventing lipoprotein retention and subsequent plaque formation (Brito et al., 2012)(Soto et al., 2023)(Figure 1.13).

Moreover, a 2017 study in ApoE knockout mice discovered a dose-dependence of chP3R99

efficacy (Sarduy et al., 2017). They reported that a 4-fold increase in the chP3R99 dose reduced aortic lesion development significantly compared to the lower dose (1x) (Table 1.1). Significant increases in the dose of chP3R99 administered result in increased concentrations of circulating Ab2 and Ab3 antibodies (Sarduy et al., 2017)(Table 1.1). Although the humoral and cellular mechanisms of chP3R99 idiotype immunogenicity are not fully understood, it has been consistently observed that the detection of Ab2 precedes the Ab3 response in serum. This observation suggests that the induction of Ab2 antibodies is required to activate an Ab3 antibody production (Soto et al., 2023).

However, studies have found that after four injections of chP3R99, the Ab2 and Ab3 antibody levels reach a plateau, suggesting that the immunogenicity of chP3R99 peaks following four injections (Sarduy et al., 2017).

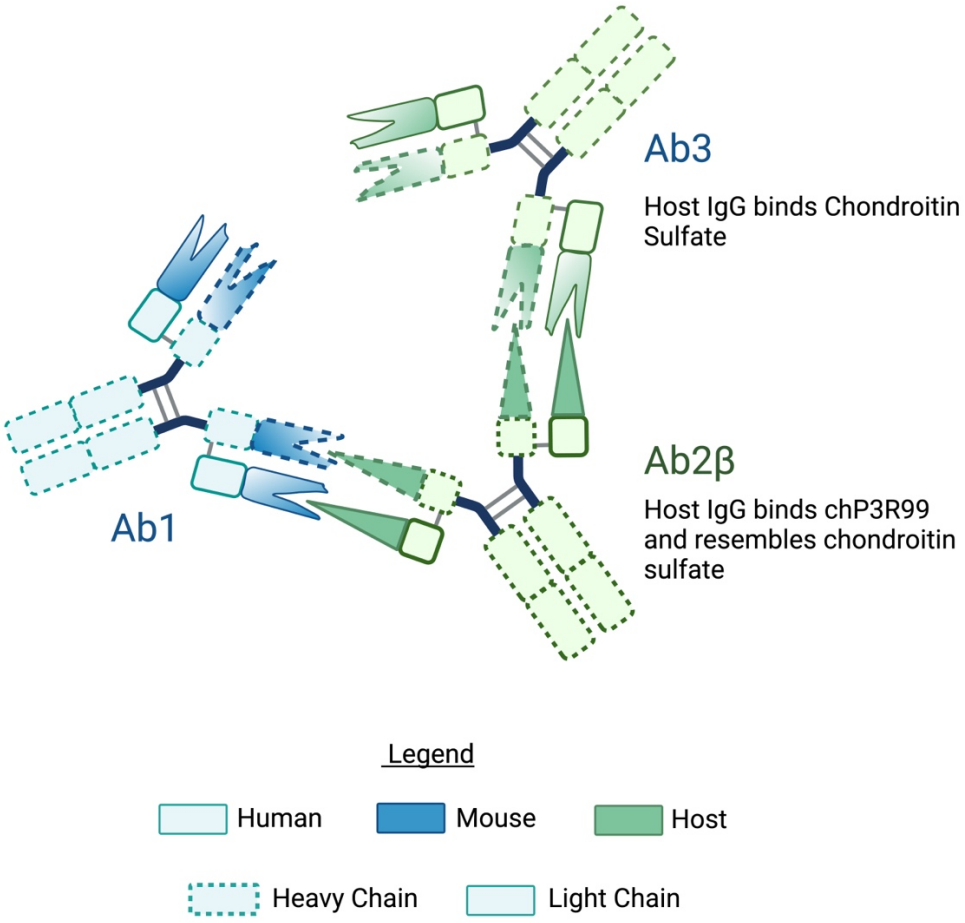

Figure 1.13 Illustration of the idiotypic cascade induced by the host as a result of chP3R99 (Ab1) injection. Ab1 stimulates the host immune system to produce anti-idiotypic antibodies (Ab2) and anti-anti-idiotypic antibodies (Ab3). Ab3 maintains the Ab1 idiotype and thus binds chondroitin sulfate with high specificity. The figure was redrawn and adapted from https://doi.org/10.1101/2023.08.30.555546. Created with BioRender.

1.5.4 Therapeutic effects of the chP3R99 mAb

A study using New Zealand white rabbits given an 8-day regimen of lipofundin to induce atherosclerosis found that chP3R99-treated rabbits experienced a 22-fold reduction in the intima-to-media ratio compared to control-treated rabbits (Soto et al., 2012). This occurrence was attributed to the induction of host-derived Ab3 anti-chondroitin sulfate antibodies.

Further studies using ApoE-/- mice similarly reported that Ab3 antibodies minimized the size and development of atherosclerotic lesions (Brito et al., 2012)(Sarduy et al., 2017). Additionally, Ab3 antibody induction in ApoE-/- mice fed a high-fat, high-cholesterol diet was linked to a 40-43% reduction in aortic lesion size (Brito et al., 2012) following 5 to 6 doses of chP3R99. Furthermore, a separate study that similarly used ApoE-/- mice fed a high-fat, high-cholesterol diet for 11 weeks to induce atherosclerosis found that chP3R99 administration not only completely halted lesion progression but also induced lesion regression in some mice with advanced cases of atherosclerosis (Brito et al. 2017). These results suggest that the anti-atherosclerotic effects of chP3R99 are mediated by the induction of Ab3 antibodies that target chondroitin sulfate, although the mechanism for Ab3 antibody production is not well described. Additionally, this anti-atherogenic effect of chP3R99 has been shown to be independent of sex. Six administrations of chP3R99 at 50ug/dose to both male and female ApoE-/- mice fed a high-fat, high-cholesterol diet for 20 weeks significantly arrested the progression of atherosclerotic lesions (Sarduy et al., 2017) (Table 1.1).

Moreover, the chP3R99 has the potential to serve as a diagnostic tool due to its unique ability to accumulate specifically in areas of atherosclerotic remodelling. Immunohistochemistry analysis of aortic segments of rabbits given lipofundin revealed an increased proportion of chondroitin sulfate in aortic and carotid lesions, resulting in higher chP3R99 reactivity to these areas (Soto et al., 2014). Consequently, when assessing chP3R99 accumulation in carotid lesions using a radiolabelled 99mTc-chP3R99 mAb, they reported a 4-times increase in chP3R99 in this area compared to healthy vessels (Soto et al., 2014).

Furthermore, recent data from a 2023 pre-print article demonstrated that the chP3R99 does not negatively impact lipid, glucose metabolism, or inflammation pathways in a rodent model of insulin resistance and susceptibility to vascular remodelling (Soto et al., 2023).

Pre-clinical results have also highlighted chP3R99's potential in minimizing lipid peroxidation, preventing the production of ROS (Soto et al., 2012)(Delgado-Roche et al., 2015) and reducing inflammation (Delgado-Roche et al., 2015)(Brito et al., 2017) which are all significant risk factors for atherosclerosis. Specifically, using Real-Time Polymerase Chain Reaction (RT-PCR) in mice, it was reported that chP3R99 reduced mRNAs of inflammatory cytokines IL-1β and TNF-α compared to PBS-treated control mice. Additionally, chP3R99 regulated the activation of NF-kB as observed through immunohistochemistry analysis in chP3R99-treated ApoE-/- mice. Simultaneously, chP3R99 also decreased aortic oxidative stress and the infiltration of CD4+ macrophages into the arterial wall and increased the IL-10/iNOS ratio. These results demonstrate the broad effects and diverse applications of the chP3R99 in managing atherosclerosis at distinct phases of disease progression and onset (Delgado-Roche et al., 2015).

Furthermore, preliminary data suggests that chP3R99 has an increased specificity for sulfated chondroitin sulfate proteoglycans. While chondroitin sulfate GAGs are expressed in various tissues, chondroitin sulfate GAGs produced by VSMC exhibit distinct characteristics, such as elongation and higher sulfation (Soto et al., 2014). Additionally, the chP3R99 displays a preference for aortic tissues, thereby reducing the risk of non-vascular proteoglycan GAG binding.

Table 1.1. Summary of key chP3R99 studies.

Authors	Year	Title	Study Design	Results
chP3R99 recognition to chondroitin sulfate				
Yosdel Soto , Emilio Acosta , Livan Delgado , Arlenis Pérez , Viviana Falcón , María A. Bécquer , Ángela Fraga , Víctor Brito , Irene Álvarez , Tania Griñán , Yuniel Fernández-Marrero , Alejandro López-Requena , Miriam Noa , Eduardo Fernández , and Ana María Vázquez	2012	Antiatherosclerotic Effect of an Antibody That Binds to Extracellular Matrix Glycosaminoglycans	**(Figure 1.0)** ELISA plates were coated with a variety of glycosaminoglycans (GAGs) of differing degrees of sulfation. Specifically, heparin, heparan sulfate, chondroitin sulfate, dermatan sulfate, hyaluronic acid each at 10 µg/mL. chP3R99, chP3, chP3S98 were then added and detected using an alkaline phosphatase-conjugated goat anti-human secondary antibody.	The chP3R99 had a higher reactivity to all the glycosaminoglycans compared to chP3 and chP3S98. However, the chP3R99 had the highest binding affinity to chondroitin sulfate (approximately 1.5x higher than the other GAGs), additionally the difference between the chP3R99 and chP3 and chP3S98.
chP3R99 idiotypic cascade and dose dependence				
Roger Sarduy, Victor Brito, Adriana Castillo, Yosdel Soto, Tania Griñán, Sylvie Marleau, Ana María Vázquez	2017	Dose-Dependent Induction of an Idiotypic Cascade by Anti-Glycosaminoglycan Monoclonal Antibody in apoE$^{-/-}$ Mice: Association with Atheroprotection	**(Figure 4.0)** 2 sets of ELISA plates were prepared. The first was coated with hR3 and chP3R99 to assess Ab2 antibody induction , and the second was coated with ch1E10 Ab2 mAb to assess Ab3 antibody induction. Sera from ApoE-/- mice sera (1:1000) at 50 and 200µg doses were then added and antibodies were detected via a peroxidase-conjugated goat anti-mouse IgG.	For Ab2 and Ab3 ELISAs the 200µg dose resulted in higher antibody production compared to the 50µg dose. For Ab2 ELISAs there was immunodominance of the chP3R99 idiotype relative to the hR3. Both Ab2 and AB3 ELISAs detected significant levels of sera-derived antibodies at the 4th dose relative to the pre-immunization sera.
chP3R99's effect on arterial lipoprotein deposition				
Yosdel Soto, Arletty Hernández, Roger Sarduy, Victor Brito, Sylvie Marleau, Donna F. Vine, Ana M. Vázquez, Spencer D. Proctor	2023	Novel chP3R99 mAb reduces subendothelial retention of atherogenic lipoproteins in Insulin-Resistant rats: Acute treatment versus long-term protection as an idiotypic vaccine for atherosclerosis	**(Figure 4.0)** Healthy and obese insulin resistant (IR) JCR:LA-cp rats received 6 weekly injections of chP3R99 or hR3 at 200µg. Following termination, IR rats underwent ex-vivo carotid perfusion of fluorescently labelled Cy3-LDL and Cy5-Remnant lipoproteins (RM) at 150µg/ml each.	IR rats treated with chP3R99 experienced a marked reduction in LDL and RM in the carotids. Additionally there was a reduction of 30% in ApoB100 levels and a 40% reduction in ApoB48 in the artery wall of IR rats treated with chP3R99 at the final dose.
chP3R99's effect on atherosclerosis development				
Roger Sarduy, Victor Brito, Adriana Castillo, Yosdel Soto, Tania Griñán, Sylvie Marleau, Ana María Vázquez	2017	Dose-Dependent Induction of an Idiotypic Cascade by Anti-Glycosaminoglycan Monoclonal Antibody in apoE$^{-/-}$ Mice: Association with Atheroprotection	**(Figure 2.0)** 12-week-old ApoE -/- mice (male and female) fed a high-fat-high-cholesterol diet from 6 weeks old to 20 weeks old and given 6 injections of chP3R99 or hR3 at 50 µg/dose (weeks 12-20). Following termination intact aortas underwent oil-red-O staining.	In male mice chP3R99 administration reduced aortic lesion size and development by 31%, while in female mice lesion size was reduced by 38% ($p<0.05$) relative to the control hR3.

1.6 Therapeutic effect of the chP3R99 in non-atherogenic and pre-clinical animal models

1.6.1 Insulin-resistant animal models and the chP3R99

Beyond its efficacy in pre-clinical animal atherogenic models, chP3R99 has exhibited therapeutic potential in models simulating metabolic dysfunction (Soto et al., 2023). Insulin-resistance, characteristic of Type 2 Diabetes mellitus (T2D), frequently coexists with vascular remodelling. Atherosclerosis remains the main cause of death in T2D patients (Razani et al., 2008). The hallmarks of insulin resistance include several multifactorial effects that can accelerate the progression of atherosclerosis (Beverly and Budoff, 2020)(Nigro et al., 2006)(Syed Ikmal et al., 2013)(Bornfeldt & Tabas, 2011). Firstly, insulin resistance causes oxidative stress, which promotes endothelial dysfunction. Endothelial dysfunction leads to increased permeability of the arterial wall and a reduction in nitric oxide bioavailability—a protective factor against atherosclerosis due to its vasodilation and antioxidation effects. This combination of endothelial dysregulation creates an environment which promotes atherogenesis (Syed Ikmal et al., 2013)(Ormazabal et al., 2018).

Furthermore, dyslipidemia, associated with insulin resistance and dysregulations in lipid metabolism, results in elevated levels of atherogenic lipoproteins, specifically high LDL and RC and low levels of HDL (Di Pino & DeFronzo, 2018). These lipoproteins aggravate the infiltration of lipids into the inner arterial wall, ultimately promoting the formation of atherosclerotic plaques. Moreover, insulin resistance causes chronic low-grade inflammation characterized by elevated pro-inflammatory cytokines and chemokines (Bloomgarden, 2005). This inflammatory state encourages the recruitment of immune cells into the arterial intima (Beverly & Budoff, 2020), enabling the formation of foam cells and the development of atherosclerotic plaques. Importantly, inflammation promotes atherogenesis and disrupts insulin signalling pathways, creating a feedback loop that encourages insulin resistance and atherosclerosis (Beverly & Budoff, 2020).

Additionally, vascular remodelling, a hallmark of insulin resistance, is partially coordinated by alterations in the organization of arterial proteoglycans (Olsson et al., 2001). Elevated levels of TGF-β, often reported in insulin-resistant patients, promote the production and release of proteoglycans rich in chondroitin sulfate and dermatan sulfate by arterial smooth muscle cells. This increase in proteoglycan levels increases lipoprotein retention within the arterial wall as per the response-to-retention hypothesis of atherosclerosis.

1.6.2 Characterization of the JCR:LA-cp rat model

The JCR:LA-cp rat model, established in 1978 by Dr. James C. Russell, was bred to express an autosomal recessive corpulent (cp) trait from a premature stop codon found within the extracellular domain of the leptin receptor, as described by Diane et al. in 2016 (Richardson et al., 1998)(Diane et al., 2016). Rats containing a single copy of the cp trait, termed heterozygous, tended to experience leanness and 'normal physiology.' In contrast, those with two copies (homozygous, cp/cp) spontaneously tended to experience pronounced obesity (Figure 1.14) (Diane et al., 2016)(Russell et al., 1998)(Russell et al., 1998). Additionally, these homozygous rats had a phenotype of insulin resistance and the early onset of cardiovascular disease (Vine et al., 2006)(Russell & Proctor, 2006)(Brindley & Russell, 2002).

The pathogenesis of atherogenesis in these rodent models is multifactorial. Elevated levels of circulating lipoproteins, attributed to metabolic dysfunction, promote infiltration of LDL and RC within the tunica intima (Diane et al., 2016)(Richardson et al., 1998)(Russell et al.,1998)(Russell et al., 1998), which triggers atherogenesis. Furthermore, the non-metabolic effects of insulin resistance, in part due to obesity in JCR:LA-cp rats, result in increased blood pressure and oxidative stress, which in turn cause endothelial damage and dysfunction. Increased ECM permeability further promotes the infiltration of lipoproteins and immune mediators into the inner arterial wall (Syed Ikmal et al., 2013)(Ormazabal et al., 2018).

Moreover, the inflammatory effects associated with metabolic dysfunction in JCR:LA-cp rats result in elevated levels of inflammatory cytokines, such as IL-1β, which promotes macrophage formation from monocytes and infiltration of the arterial wall. Macrophages can then phagocytose lipoproteins and form foam cells, the basis of atherosclerotic plaques. Furthermore, investigations conducted on JCR:LA-cp rats provided evidence of a robust age-dependent increase in aortic biglycan protein core content, which was positively linked with the aggravation of hyperinsulinemia. The increased expression of aortic biglycans is of particular interest, as it is implicated in the initiation of atherogenesis (Mangat et al., 2012) as per the response-to-retention hypothesis of atherosclerosis. Additionally, it is important to note that previous research has proven that this increase in the biglycan protein core is a result of various factors, including elevated levels of free fatty acids, angiotensin II, and TGF-β (Diane et al., 2016), all of which are

independently associated with the promotion of atherogenesis, as demonstrated by the work of Diane et al. in 2016 (Figure 1.14).

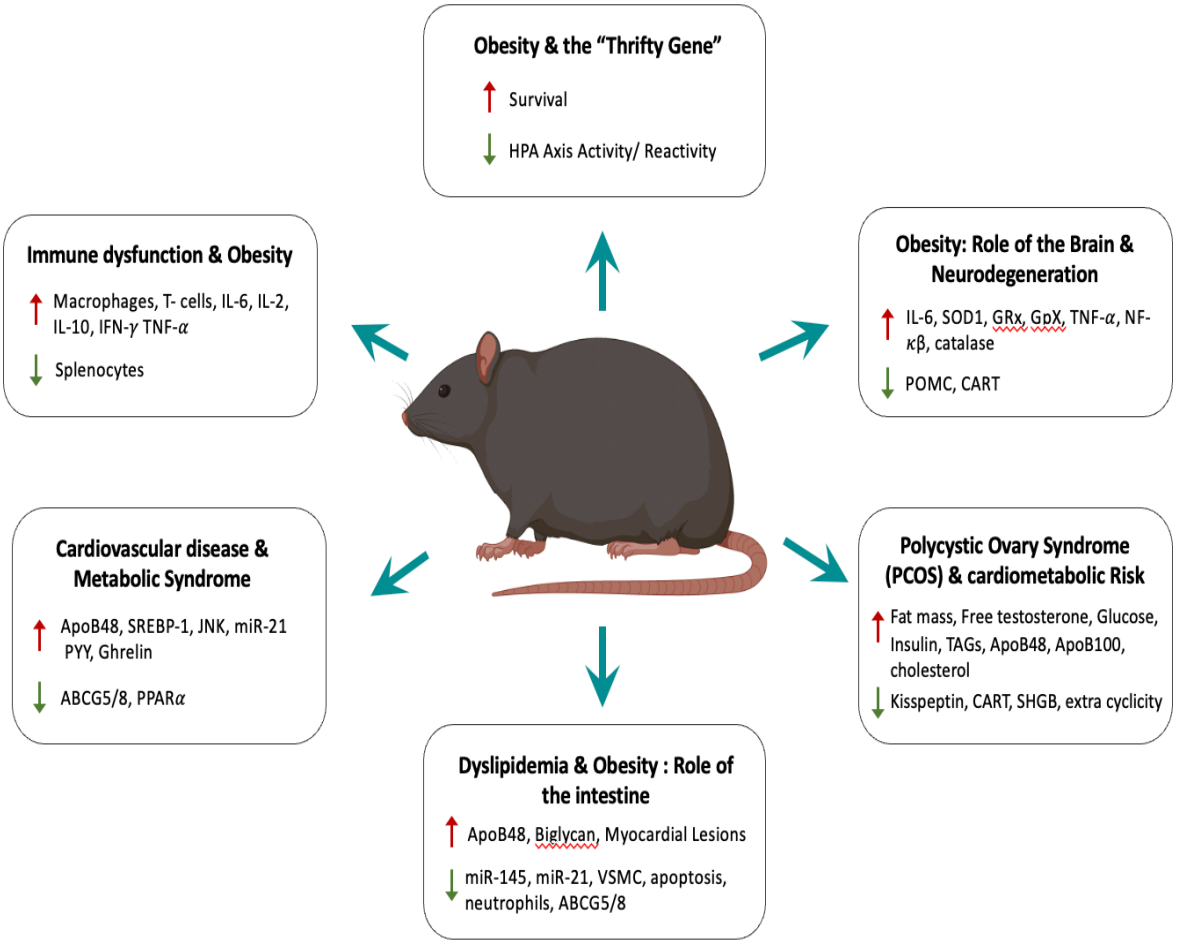

Figure 1.14 Summary of the main physiological features of the JCR:LA-cp rat with the autosomal recessive corpulent (cp) trait. The rat depicted is homozygous for the cp trait (cp/cp) and spontaneously develops the features shown. The figure was redrawn and adapted from https://doi.org/10.3389/fnut.2016.00044. Created with BioRender.

1.6.3 Swine models for cardiovascular research

There has been a growing interest in using large animal models in translational research in recent years. The primary objective driving this interest is the need to bridge the existing gap between

studies conducted on small animals, namely rodents and the development of therapies designed for human use (Schüttler et al., 2022).

Swine models, in particular, are considered invaluable for cardiovascular research due to their similar physiology to humans (Zaragoza et al., 2010)(Tsang et al., 2016)(Getz & Reardon, 2012). Their anatomical, hemodynamic, and electrophysiological characteristics closely mirror that of humans. These similarities allow pigs to serve as a unique, comprehensive model for studies focusing on cardiovascular health and disease (Zaragoza et al., 2010)(Tsang et al., 2016). Pigs have heart sizes and structures, blood flow patterns, gastrointestinal systems, and overall anatomy similar to humans (Schüttler et al., 2022)(Walters & Prather, 2013). Their large size also facilitates surgical procedures and the implantation of cutting-edge medical devices. Moreover, they share similar responses to these intervention therapies. Furthermore, pigs' dietary habits, lipid metabolism, and susceptibility to atherosclerosis closely resemble those of humans, as described by Gisterå et al. (Gisterå et al., 2022). This resemblance allows pigs to serve as ideal pre-clinical animal models for studies on the effects of chP3R99 prior to advancing to large-scale clinical trials. Additionally, the increased blood content of pigs relative to rodents, i.e., rats, facilitates the process of sera collection and allows for a greater number of repetitions and more extensive assays, which can enhance the accuracy and the scope of immunogenicity studies. Additionally, in immunomodulatory research, pigs are necessary as they can launch immune responses similar to those of humans, including, but not limited to, antibody production, cytokine release, and immune cell activation (Pabst, 2020). This similarity in immune responses further increases their potential as a model for studies on the immunogenicity of chP3R99.

Lastly, the longer lifespan of pigs, compared to rodents, is an additional significant advantage for long-term research endeavours and for observing the longevity of the immunogenicity of chP3R99 over time.

CHAPTER 2: RATIONALE, OBJECTIVES, AND HYPOTHESES

2.1 Thesis rationale and background

2.1.1 Inefficiency of NS0 production of chP3R99

Despite the promising features of the chP3R99, there have been challenges in advancing to large-scale clinical trials due to production limitations (Li et al. 2010)(Andersen & Reilly 2004). Given that immunotherapies often require multiple administrations over long periods, there is a need to produce large quantities consistently (Li et al., 2010)(Andersen & Reilly, 2004)(Dhara et al., 2018). This requires a production system adaptable to scaling, low cost, and high productivity to meet commercial requirements (Li et al., 2010)(Dhara et al., 2018). The original chP3R99 mAb is produced via DNA transfection using an NS0 cell line, chosen for its reliability in mAb production (Li et al., 2010)(Dhara et al., 2018). However, the NS0 cell line-derived chP3R99-producing clone has consistently resulted in low productivity, thus challenging adaptability for upscaling. Additionally, the chP3R99 (referred to as NS0-P3R99 from here on) uses a production system dependent on Fetal Bovine Serum (FBS), which can compound challenges related to its batch-to-batch variability and possible contamination sources due to its animal origins (Chelladurai et al., 2021)(van der Valk, 2010). The introduction of potential contaminants like fungi, bacteria, viruses, mycoplasma, and prions could cause adverse effects in patients and threaten the safety of the antibody (Brunner et al., 2010)(van der Valk et al., 2010)(Rodrigues et al., 2013)(Butler, 2015). Moreover, immunoglobulins can differ across batches of FBS, introducing variation across different lots of NS0-P3R99. Furthermore, we know that exogenous antibodies can interfere with detecting and measuring antibodies produced by the NS0 cells. Similarly, the proteins present in FBS can complicate the purification of the end product. Lastly, FBS is expensive and purchasing several batches for the production of large quantities of NS0-P3R99 is exceptionally costly. Consequently, many regulatory agencies that monitor pharmaceutical production favour the adoption of serum-free media (Brunner et al., 2010)(van der Valk et al., 2010)(Rodrigues et al., 2013). This alternative provides increased control over cell culture conditions while minimizing the variability, thereby creating a more dependable environment for the production of recombinant antibodies.

2.1.2 Introduction to P3R99 variants

In order to solve the production challenges related to the NS0-P3R99, new variants of higher scalability and reliability for clinical trials were evaluated from two well-characterized cell-lines: the Chinese Hamster Ovary (CHO-K1) and Human Embryonic Kidney 293 (HEK293). The P3R99 variants termed CHO-P3R99 and HEK-P3R99 have several advantages over the original NS0-P3R99 (Figure 2.1). CHO cells, which account for over 60% of sanctioned biotherapeutics, are commonly used for their high productivity, resistance to varying conditions, ability to synthesize intricate proteins with human-compatible glycosylation, and adaptability to suspension and serum-free cultures, ensuring scalability and consistent inter-batch products (Li et al., 2010)(Dhara et al., 2018)(Dumont et al., 2015). While HEK cells are recognized for their elevated productivity and transfection rates, minimal reactivity due to their human Post-Translational Modifications (PTM), and adaptability to suspension and serum-free cultures, thus enabling large-scale synthesis (Li et al., 2010)(Schofield, 2023)(Dumont et al., 2015).

Preliminary data from the CIM regarding the *in-vitro* binding of chondroitin sulfate of the HEK-P3R99 and CHO-P3R99s variants demonstrated a comparable dose-dependent recognition to chondroitin sulfate as the NS0-P3R99. This suggests that the variants preserved the primary function of the original NS0-P3R99 (Figure 2.2).

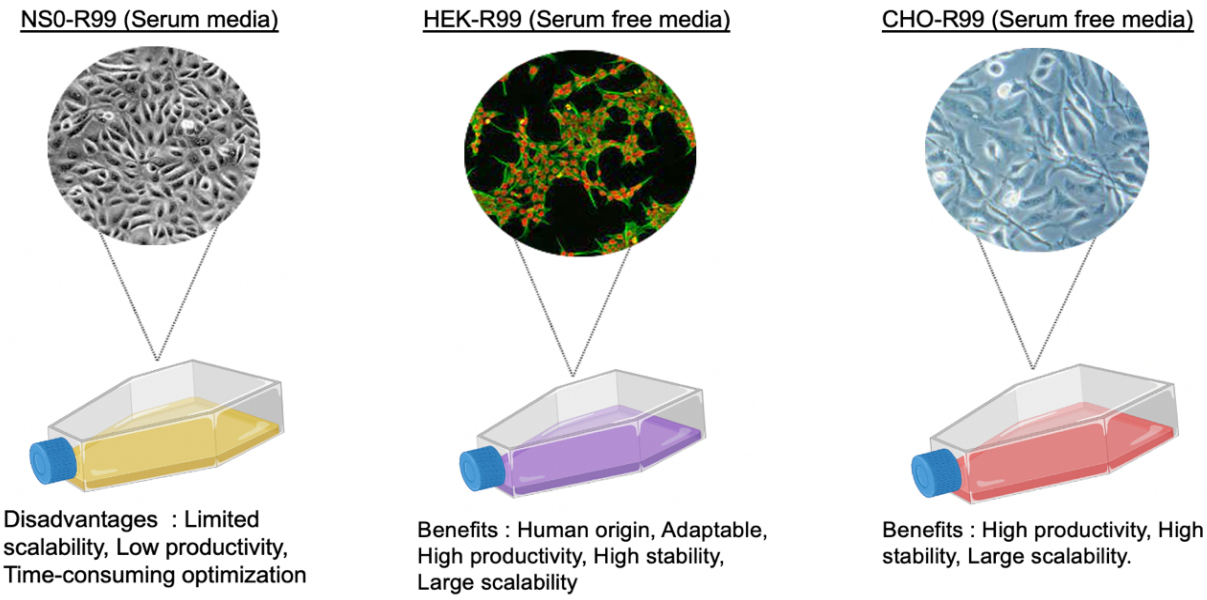

Figure 2.1 Summary and comparison of the P3R99 variants. Included are the main benefits (or disadvantages) associated with the cell lines used for production. Created with BioRender.

2.1.3 Production of P3R99 variants

The P3R99 variants were produced by our partners at CIM, using a lentiviral transduction approach to express the chP3R99-LALA mAb in CHO-K1 and HEK293 cells. Initially, the genes were integrated, encoding the light and heavy chains of the P3R99 into a pL6WBlast lentiviral vector. Subsequently, the resulting clones in both CHO-K1 and HEK293 cell lines were verified to exhibit high productivity, exceeding 100 μg/mL.

Additionally, all variant clones of P3R99 displayed a consistent recognition pattern for GAGs and its anti-idiotypic mAb, as confirmed through Enzyme-Linked Immunosorbent Assay (ELISA) analysis. Moreover, using size exclusion High-Performance Liquid Chromatography (HPLC) and Sodium Dodecyl-Sulfate Polyacrylamide Gel Electrophoresis (SDS-PAGE), the CIM demonstrated that the size of these batches consistently measured at approximately 150kDa, in line with human IgG specifications. Notably, there were minimal levels of aggregation and degradation, with purity exceeding 99%. Dynamic Light Scattering (DLS) analysis revealed a consistent mean particle size among all chP3R99 variants, ranging from 12.5 to 14.4nm. Circular dichroism spectroscopy indicated a similar secondary structure across all P3R99 variants, predominantly enriched in β-sheets (~42%) and β-turns (11.6-12.3%). Cation exchange chromatography further affirmed a high abundance of basic amino acids exposed on the surface of chP3R99, with a theoretical isoelectric point range of 8.5-9.5, consistent with the idiotype's arginine-rich nature.

2.1.4 P3R99 recognition to chondroitin sulfate preliminary data

Despite adopting a similar production technique and ensuring the P3R99 variants retain the overall structure and amino acid sequence of the NS0-P3R99, the glycosylation profile of the antibody is influenced by the host cell and culture medium used for production, thus potentially exhibiting alterations which can have overall implications on the stability, immunogenicity, potency, and function of the variants (Goh & Ng, 2017). The CHO-K1 and HEK-293 cell lines exhibited similar glycosylation profiles, characterized by a predominance of the G0F variant (60-70%). Conversely,

the NS0 profile exhibited a higher prevalence of G1F and G2F variants, featuring terminal galactose and a substantial degree of sialylation (15-23%).

While the new P3R99 variants displayed slight differences in glycosylation patterns compared to the parental NS0-P3R99, these modifications did not appear to compromise their recognition properties, as shown by *in-vitro* preliminary results from ELISA plates coated with chondroitin sulfate (Figure 2.2).

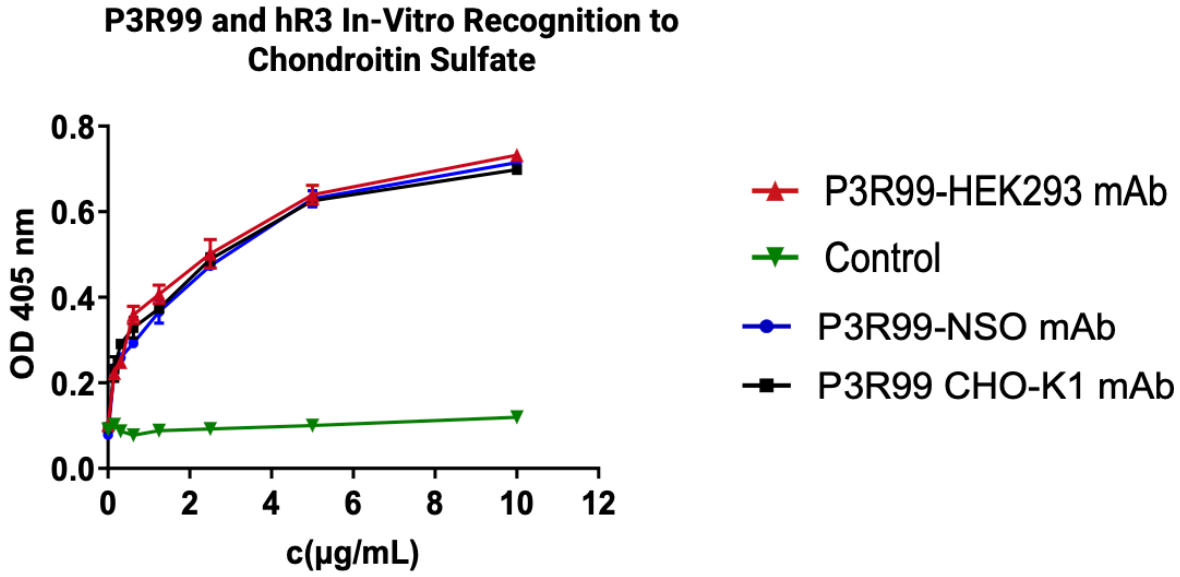

Figure 2.2 P3R99 variants *in-vitro* recognition to chondroitin sulfate via ELISA. Plates were coated with 100 µL of 10 µg/mL of shark cartilage chondroitin sulfate (REF C4384 Sigma Aldrich) and incubated at 25°C (room temperature) overnight. Plates were washed and subsequently incubated with different concentrations of the P3R99 variants and a negative isotype control hR3 mAb (0.15-10 µg/mL), followed by an alkaline phosphatase-conjugated anti-human IgG secondary antibody and visualized with TMB substrate.

2.2 Rationale

While the foundational structure and recognition of chondroitin sulfate of the NS0-P3R99 were maintained by the CHO-P3R99 and HEK-P3R99 variants, variations in the pattern of post-translational modifications could influence the P3R99's function, affecting their safety, efficacy, and immunogenicity, requiring testing.

Consequently, the primary goal of this thesis was to validate the immunogenicity of these variants, specifically through the induction of anti-idiotypic Ab2 and anti-anti-idiotypic Ab3 antibodies in physiologically distinct pre-clinical animal models.

Additionally, we were interested in comparing the strength of this response between the three P3R99 variants.

Moreover, we proposed to comprehensively evaluate the safety profile of the NS0-P3R99 variants in the context of cardiovascular health and lipid and carbohydrate metabolism. Due to the critical role of chondroitin sulfate and other sulfated GAGs in cellular integrity, cell communication, motility, and metabolism (Wang et al., 2022)(Staprans & Felts, 1985), it is necessary to continue to ascertain whether P3R99 binding to chondroitin sulfate affects these biological processes.

Thus, an additional sub-objective of this thesis is to determine whether the P3R99 variants have any adverse effects on cardiovascular function in a model susceptible to lipid and vascular remodelling. This outcome aims to complete a safety assessment of the P3R99 regarding cardiovascular function to address the concern of potential harm.

To complement these assessments we also planned to assess whether the variants could potentially interfere with lipid and carbohydrate metabolism downstream due to their high binding affinity for sulfated proteoglycan GAGs. As such, we aimed to assess the potential effect of the P3R99 variants on lipoprotein and, carbohydrate metabolism.

Rather than determining whether these variants improve these metabolic pathways, we were foremost interested in whether we could identify any off-target or adverse effects in a lipid and vascular susceptible model.

2.3 General hypotheses

Based on the rationale described above, we proposed several hypotheses with corresponding objectives, which are outlined below. Additionally, from here on, chP3R99 variants will be referred to as NS0-P3R99, HEK-P3R99, and CHO-P3R99 for all experimental chapters. Similarly, heterozygous JCR:LA-cp rats will be referred to as ‘lean JCR:LA-cp rats,’ while homozygous (cp/cp) JCR:LA-cp rats will be referred to as ‘obese insulin-resistant JCR:LA-cp rats’ for all experimental chapters.

First hypothesis: Immunogenicity of P3R99 variants

We hypothesize that the three variants would maintain their general immunogenic function *in-vivo* by producing Ab2 and Ab3 antibodies.

Second hypothesis: Comparison of the immunogenicity of the P3R99 variants

We hypothesize that the HEK-P3R99 and CHO-P3R99 variants would have a comparable immunogenic strength (magnitude of Ab2 and Ab3 antibody induction) as the original NS0-P3R99.

Third hypothesis: Immunogenicity of P3R99 variants in small animal models

We hypothesize that the HEK-P3R99, CHO-P3R99, and NS0-P3R99 will all induce Ab2 and Ab3 antibodies regardless of physiological state using distinct small animal models (healthy rodent model and a matched model of immune dysfunction with susceptibility to vascular and lipid remodelling).

Fourth hypothesis: Immunogenicity of P3R99 variants in a large animal model

We hypothesize that the HEK-P3R99, CHO-P3R99, and NS0-P3R99 will all induce Ab2 and Ab3 antibodies in a complex large animal model with comparable physiology to humans.

2.4 Chapter objectives, experiments, and expected outcomes

Specific Objectives from Chapter 3

In order to address aspects of hypotheses 1-3, we proposed the following objectives and study designs which are described in Chapter 3 of this thesis (Table 2.1):

3.1 Measure the induction of anti-idiotypic Ab2 and anti-anti-idiotypic Ab3 antibody production *in-vivo* following a minimum of 6 weekly injections of each respective treatment group in healthy young (3 months of age) lean JCR:LA-cp rats.

3.2 Complete a kinetics assessment of the Ab2 antibody induction at various time points (week 0, 2, 3, 4, 6).

3.3 Complete a kinetics assessment of the Ab3 antibody induction at various time points (week 0, 2, 3, 4).

Specific Objectives from Chapter 4:

In order to address additional aspects of hypotheses 1-3, we proposed the following objectives and study design which are described in Chapter 4 of this thesis (Table 2.1):

4.1 Measure the induction of anti-idiotypic Ab2 and anti-anti-idiotypic Ab3 antibody production *in-vivo* following a minimum of 6 injections of each respective treatment group in a model of immune dysfunction (9 months of age) obese insulin-resistant JCR:LA-cp rats fed a high-fat, high-fructose chow diet for 12 weeks.

4.2 Complete a kinetics assessment of the Ab2 antibody induction at critical points (week 0, week 4, week 6)

4.3 Test the potential of a kinetic profile for the Ab3 response.

Additional objectives and planned assessments of Chapter 4:

Due to the implication of chondroitin sulfate in various biological processes, we plan to conduct an assessment of the CHO-P3R99 and HEK-P3R99 variants' effects on cardiovascular function and lipid and carbohydrate metabolism (Table 2.1).

To do so, we designed two additional sub-objectives:

4.4 Using echocardiography, evaluate whether the lipid and vascular susceptible obese insulin-resistant JCR:LA-cp rats immunized with the three P3R99 variants alter markers of vascular health and function compared to the control hR3.

4.5 Assess whether the P3R99 variants alter the metabolism of plasma lipids, glucose, and insulin in the obese insulin-resistant JCR:LA-cp rodents at the final dose compared to the hR3 control-treated rats.

Specific Objectives for Chapter 5:

In order to address the final aspects of hypotheses 1, 2, and 4 we proposed the following objective and study design which are described in Chapter 5 (Table 2.1):

5.1 Measure the induction of anti-idiotypic Ab2 and anti-anti-idiotypic Ab3 antibody production *in-vivo* following a minimum of 5 weekly injections of each respective treatment group in a 3-week-old lean, healthy white-landrace piglet model.

Table 2.1

Summary of chapters 3, 4 and 5 study designs and planned assessments. Study design and assessments for healthy lean heterozygous JCR:LA-cp rats (chapter 3), obese insulin-resistant homozygous JCR:LA-cp rats (chapter 4), and healthy white-landrace piglets (chapter 5).

Study design				Planned Assessments		
Animal model	**Duration**	**Blood draws**	**Doses**	**Ab2, Kinetics**	**Ab3, Kinetics**	**Additional**
Male Heterozygous Lean JCR:LA-cp Rats - 3 months old - Standard chow diet	6 weeks.	5 blood draws at weeks 0,2,3,4,and 6	Two injections of 250uL of 400ug/mL. Total 200mg	Ab2 assessment planned (minimum at final dose) Kinetics planned.	Ab3 assessment planned (minimum at W0 and after the fourth or final dose) Kinetics planned.	(1) Weight gain over time.
Male Homozygous Obese Insulin-Resistant JCR:LA-cp Rats - 9 months old - High-Fat High-fructose diet (composed of 2% cholesterol, 20% lard, 15% fructose)	12 weeks total. 4-week diet, then 6 doses over 8 weeks with diet	5 blood draws at weeks 4,7,8,10,and 12	Two injections of 250uL of 400ug/mL. Total 200mg	Ab2 assessment planned (minimum at final dose) Kinetics planned.	Ab3 assessment planned (minimum at W0 and after the fourth (W8) or final dose (W12)) Kinetics not planned.	(1) Weight gain over time. (2) Lipoprotein and glucose metabolism. (3) Heart function and weight.
Male White-Landrace Piglets - 3 weeks old - Pre-grower and standard chow diet	5 Weeks.	4 blood draws at weeks 0,3,4, and 5	One injection of 3mL of 0.33mg/mL. Total 1mg	Ab2 assessment planned (minimum at final dose) Kinetics not planned.	Ab3 assessment planned (minimum at W0 and after the fourth or final dose) Kinetics not planned.	(1) Weight gain over time.

2.5 Thesis format

CHAPTER 3: Pilot immunogenicity study in healthy lean JCR:LA-cp rodents. Characterizes the immunogenicity (function and strength) of the P3R99 variants in lean JCR:LA-cp rats as a pilot study to develop a more comprehensive study in the lipid and vascular susceptible obese insulin-resistant JCR:LA-cp rats. Chapter 3 addresses hypotheses 1-3 and objectives 3.1-3.3. Results from Chapter 3 sought to validate the primary immunogenic effects of the P3R99 variants compared to the hR3 negative control and NS0-P3R99 in a healthy small animal model. These results additionally characterize the immunogenicity of the variants over time through kinetics assessment.

CHAPTER 4: Immunogenicity study and assessment of P3R99 non-canonical effects in obese insulin-resistant JCR:LA-cp rodents. Our study in the obese insulin-resistant JCR:LA-cp rats evaluated the immunogenicity of the P3R99 and possible non-canonical effects of the P3R99s related to regulating lipid and glucose metabolism. This was done by comparing the lipid, glucose, and insulin levels of the obese insulin-resistant JCR:LA-cp rodents who received the control hR3 and those who received P3R99 injections. Additionally, we assessed the effects of the P3R99 variants on cardiovascular function in the obese insulin-resistant JCR:LA-cp rodents using echocardiogram assessment. Chapter 4 addresses hypotheses 1-3 and objectives 4.1-4.5. Results from Chapter 4 sought to confirm the primary immunogenic effects of P3R99 variants compared to the hR3 negative control and NS0-P3R99 in a model of immune dysfunction with susceptibility to lipid and vascular remodelling. Additionally, these results confirm the lack of adverse effects related to P3R99 administration in regard to cardiovascular function and lipid and carbohydrate metabolism.

CHAPTER 5: Immunogenicity study of P3R99 variants in a healthy large animal model: white-landrace piglets. Describes the immunogenicity of the P3R99 variants in a healthy large animal model. Chapter 5 addresses hypotheses 1, 2 and 4 and only objective 5.1. Findings from Chapter 5 characterize the immunogenicity of the P3R99 variants compared to the NS0-P3R99 in an animal model with cardiovascular physiology closely related to humans. Results from Chapter 5 were inconsistent in regard to the strength of HEK-P3R99 in terms of an Ab2 response but

suggest that the P3R99 variants continue to maintain the immunogenicity of the original NS0-P3R99 in large animals and the capacity to induce comparable levels of Ab3.

CHAPTER 6: General Discussion. Summarizes the major findings of the studies in chapters 3, 4 and 5 and describes the practical implications of the results. Additionally, this chapter discusses possible limitations, sources of error and future directions for studies on the P3R99 variants.

2.6 Animal ethics requirement

JCR:LA-cp rodents were part of a closed outbred colony maintained at the Li Ka Shing Centre for Health Research Innovation at the University of Alberta, Canada. White-landrace piglets were acquired from the Swine Research and Technology Center (SRTC) (South Campus) by the Department of Agriculture, Food and Nutritional Science, University of Alberta, Canada.

All protocols adhered strictly to the guidelines set forth by the Canada Council on Animal Care (CCAC) and were approved by the University of Alberta's Animal Ethics Committee.

Rodents were made available from breeding heterozygous JCR:LA-cp rats for lean controls and homozygous JCR:LA-cp rats for obese insulin-resistant models on site on the U of A HSLAS. Genotyping was then done to confirm the rodents as heterozygous or homozygous. Access to water, food, temperature regulation, and hygiene conditions were maintained by a trained animal technician. Rodents were kept in cages of two to reduce stress and aggression related to social isolation.

Additionally, we maintained the principle of the "3Rs", Replacement, Reduction, and Refinement, that guide ethical research involving animals. By giving the rodents the minimum dose of 6 weekly injections for lean rats and 6 injections for obese insulin-resistant rats, we minimized exposure to potential sources of distress or harm caused by the research process. All rodent surgeries, blood draws, and termination were performed by our animal technician.

Swine resulted from crossbreeding between a duroc boar and large white-landrace sows. Living conditions were maintained by the SRTC staff, following guidelines of animal ethics and care. Animals were weaned and, at 3 weeks of age, were separated into groups of 5 to ensure proper socialization and minimize stress and isolation during subsequent experimental procedures. Piglets that exhibited signs of distress, low birth weight or anxiety were deliberately excluded from the study to alleviate any additional stress. All animal surgeries and blood draws were performed by

experienced veterinarians and skilled personnel at the SRTC. Piglets were given the minimum dose of 5 weekly injections of the respective treatment. Additionally, SRTC staff maintained daily records to monitor the piglets' health, food intake, weight, and overall well-being.

CHAPTER 3: PILOT IMMUNOGENICITY STUDY OF P3R99 VARIANTS IN HEALTHY LEAN JCR:LA-CP RODENTS

Gala Araujo [1,2], Kun Wang [1,2], Yosdel Soto [2,4], Spencer Proctor [2,3]*

[1] Division of Human Nutrition, Department of Agricultural, Food and Nutritional Science. [2] Metabolic and Cardiovascular Diseases Laboratory, Department of Agricultural, Food and Nutritional Science, and/or 3 Division of Animal Science, Department of Agricultural, Food and Nutritional Science, University of Alberta, Edmonton, Alberta, Canada. [3] Division of Immunobiology, Centre of Molecular Immunology, Havana 11600, Cuba; yosdel@cim.sld.cu

* Correspondence: proctor@ualberta.ca

3.1 Introduction

Atherosclerosis involves gradually accumulating cholesterol and fat-rich fibrous plaques on the innermost arterial membrane wall known as the tunica intima (see previous Figure 1.4 of Chapter 1). One significant feature of atherosclerosis is the presence of low-grade chronic inflammation, which serves as a protective reaction to the infiltration of arterial lipoproteins (Bäck et al., 2019). The response-to-retention hypothesis of atherosclerosis suggests that atherogenesis is triggered by lipoproteins such as Low-density lipoprotein (LDL) and Remnant Cholesterol (RC) binding within proteoglycan glycosaminoglycan (GAG) branches in the tunica intima (Williams & Tabas, 1995)(Fogelstrand & Borén, 2012)(Tannock & King, 2008)(Gisterå & Hansson, 2017). Lipoprotein binding triggers structural modifications that encourage lipid accumulation and subsequent plaque formation (Yurdagul et al., 2016). However, despite the prevalence of atherosclerosis, there are few preventative therapies.

The Center for Molecular Immunology (CIM) in Havana, Cuba, recently developed a ground-breaking atheroprotective therapy, NS0-P3R99 (chP3R99) mAb, which is capable of directly targeting the initiation of atherosclerosis. The NS0-P3R99 is a human-murine chimeric monoclonal antibody (mAb) capable of recognizing and binding proatherogenic GAGs, specifically Chondroitin Sulfate GAGs (CS) found on arterial proteoglycans and preferentially accumulating in regions in vascular remodelling (Soto et al., 2014)(Soto et al., 2012)(Brito et al., 2017)(Sarduy et al., 2017)(Delgado-Roche et al., 2015). Results from various animal models have validated the NS0-P3R99's capacity to competitively inhibit arterial lipid binding, arrest lipid

oxidation, and ultimately prevent and slow the development of atherosclerosis (Soto et al., 2014)(Soto et al., 2012)(Brito et al., 2017)(Sarduy et al., 2017)(Delgado-Roche et al., 2015).

Moreover, in addition to its effect on lipid retention, the NS0-P3R99 has a unique dose-dependent immunogenic function due to its ability to induce an idiotypic antibody cascade (Sarduy et al., 2017). Four doses of NS0-P3R99 (also known as Ab1) is sufficient to mount an immune response due to its unique idiotype, which prompts the host's immune system to produce Ab1-like antibodies (known as Ab3) that share the NS0-P3R99's structure and function, thus providing long-term protection like a vaccine (Brito et al., 2017)(Sarduy et al., 2017)(Urbain et al., 1977). This idiotypic cascade occurs through the generation of second-generation anti-idiotype antibodies (Ab2), which resemble chondroitin sulfate and, in turn, bind to Ab1 (Sarduy et al., 2017). Ab2 production, as a result, triggers the production of third-generation anti-anti-idiotype antibodies (Ab3) that share the Ab1 idiotype and thus can bind chondroitin sulfate with high specificity (Brito et al., 2012). As evidenced by studies conducted on New Zealand white rabbits and ApoE-/- mice given low doses of NS0-P3R99, the induction of anti-chondroitin sulfate Ab3 antibodies mediates the atheroprotective effect of the NS0-P3R99 antibody (Brito et al., 2012)(Soto et al., 2012).

However, due to production limitations, the NS0-P3R99 has encountered challenges in advancing to large-scale clinical trials (Li et al., 2010). The original NS0-P3R99 clone was produced via DNA transfection using a murine myeloma cell line (NS0). However, the NS0 clone has consistently resulted in low P3R99 productivity, thus challenging adaptability for upscaling. To address these challenges, The CIM developed two new P3R99 variants of higher production efficiency and adaptability to scale-up use, the hamster-derived CHO(K1)-P3R99 and human-derived HEK(293)-P3R99. While the foundational structure of the original NS0-P3R99 was maintained, potential changes in the pattern of Post-Translational Modifications (PTMs), specifically glycosylation, may occur due to the use of distinct cell lines (Goh & Ng, 2018). These variations in PTMs can potentially influence the variants' immunogenicity, thereby affecting the function of the P3R99.

Thus, our study aimed to validate these variants' overall immunogenicity and immunogenic strength, specifically in the context of inducing Ab2 and Ab3 antibodies in a healthy pre-validated small animal model. As such, we designed an immunogenicity study using the lean JCR:LA-cp rat model. The JCR:LA-cp rats were chosen due to previous experience using this model to assess the immunogenicity of the NS0-P3R99 (Soto et al., 2023). Moreover, we were interested in first

assessing the immunogenicity of the variants under standard conditions without the influence of physiological dysfunction. This study design served as a comprehensive pilot study to later assess the variants in a physiologically compromised small animal model and large animal model.

Our investigation was designed to determine whether HEK-P3R99 and CHO-P3R99 maintained the overall immunogenic function of the NS0-P3R99, compared to a negative isotype control hR3, which shares the non-idiotypic structure of the P3R99. We hypothesized that the P3R99 variants would maintain the immunogenic function and strength of the original NS0-P3R99. Additionally, we planned to complete a kinetic profile of the idiotypic cascade induced by the variants.

Immunogenicity was defined by a significant Ab2 and Ab3 antibody response. Specifically, Ab2 antibody induction was considered significant when the immune response toward P3R99's idiotype was dominant compared to the non-idiotypic regions (represented by the anti-isotypic response). Ab3 antibody production was considered significant when there was a minimal two-fold increase in recognition of chondroitin sulfate from the pre-immune state to the final dose.

Results from this chapter confirmed the maintained immunogenicity and immunogenic strength of the NS0-P3R99 in the HEK and CHO P3R99 variants in the lean JCR:LA-cp rats.

3.2 Methods

3.2.1 Animal housing and treatment protocol

Rodents were raised from the established colony maintained in the Metabolic and Cardiovascular Disease (MCVD) Laboratory in the Department of Agriculture, Food and Nutritional Science at the University of Alberta, Edmonton, Alberta, Canada., (Vine et al., 2006)(Russell & Proctor, 2006). Rodents were part of an outbred closed colony housed in the Li Ka Shing Centre for Health Research Innovation in standard conditions, received water and food ad libitum, and were cared for by trained MCVD staff. Heterozygous rats were bred for lean controls, while homozygous rats were bred for obese insulin-resistant rats. Rodents were maintained in cages of two with sufficient environmental enrichment to provide stimulation. All study protocols were approved by the University of Alberta Animal Care and Use Committee (ACUC) and the Protocol Livestock Committee in accordance with the Canadian Council of Animal Care (CCAC) regulations for the use of experimental animals (Rat Protocol AUP00004174).

3.2.2 Monoclonal antibody preparation

NS0-P3R99, humanized R3 (hR3), HEK-P3R99 and CHO-P3R99 mAbs were all generated at the Center for Molecular Immunology (Havana, Cuba). NS0-P3R99 is the original P3R99 mAb generated in an NS0 murine myeloma cell line used as a positive control (Fernández-Marrero et al., 2011). Humanized R3 (hR3) is an anti-human epidermal growth factor receptor mAb generated from the NS0 cell line and used as the negative isotype control (Brito et al.,2012)(Mateo et al.,1997). HR3 does not share the idiotype of the P3R99 but does share a similar overall human IgG1 structure (non-idiotypic regions). HEK-P3R99 and CHO-P3R99 are variants of NS0-P3R99 mAb, produced in the Human Embryonic Kidney 293 cell line (HEK) and Chinese Hamster Ovary cell line (CHO), respectively. The mAbs were purified using protein-A affinity chromatography (Pharmacia, Uppsala, Sweden) from supernatants of their respective antibody-producing clones cell cultures (NS0, HEK, CHO) expressing the P3R99 variants or hR3 antibodies (Brito et al., 2012)(Soto et al., 2012). The mAbs were analyzed under reducing conditions using Sodium Dodecyl Sulfate Polyacrylamide Gel Electrophoresis (SDS-PAGE) (Brito et al., 2012)(Soto et al., 2012). As outlined in previous studies, an Enzyme-Linked Immunosorbent Assay (ELISA) confirmed the production and specificity of the purified antibodies and the Optical Density (OD) set at 280nm was used to estimate the protein concentration (Brito et al., 2012)(Soto et al., 2012).

3.2.3 Study design lean JCR:LA-cp rats

Twenty 3-month-old, lean, male JCR:LA-cp rats were fed a chow diet prior to and during immunizations (Figure 3.1, Table 3.1). Rodents received six subcutaneous (s.c.) immunizations at a concentration of 400 μg/mL of either NS0-P3R99 (positive control), HEK-P3R99 (variant), CHO-P3R99 (variant) or hR3 (negative control) (n=5 animals per group) at weekly intervals (1 injection/week) over six weeks. Immunizations were given as two 250 μL injections of 400 μg/mL in both the right and left flanks. The total dose was 100 μg per shank (200 μg total). Rodents were weighed semi-regularly to monitor food intake. They had venous blood (sera and plasma) (150 μL) drawn at the start of the study prior to the first antibody immunization (Pre-immune, PI) and a minimum of 7 days after the second, third, fourth, and sixth immunizations. Due to ethical requirements, rats only underwent five blood draws to minimize distress. Plasma was collected in purple top BD Vacutainer® Plasma Preparation Tubes (PPT™) containing Ethylenediaminetetraacetic Acid (EDTA) to prevent coagulation, and sera was collected in red top

BD Vacutainer® Blood Collection Tubes. Following 6 injections at ~4 months of age, rodents were individually placed in an isoflurane inhalation chamber, ensuring a gradual and safe induction by starting with 0.5% isoflurane and adjusting as needed. The remaining rodent cages kept in the room were covered with an opaque tarp to reduce stress caused by the termination. Our animal technician assessed the level of anesthesia by pedal reflex (firm toe pinch) to ensure the rodents did not demonstrate pain recognition. Once the rodent was unconscious, we transitioned them to a nose cone and bain circuit setup while maintaining anesthesia at 2% and monitoring vital signs. Rodents were cleaned with 70% ethyl alcohol (EtOH), and various tissues were collected, including the right kidney, liver, gastrocnemius muscle fragment, aorta, heart, and blood by cardiac puncture (Table 3.2).

Table 3.1 Ingredients of chow diet used for lean JCR:LA-cp rats. PicoLab® Rodent Diet 20. REF #5053.

Chemical Composition	Quantity
Proteins	**21.0%**
Arginine, %	1.29
Cystine %	0.36
Glycine %	0.98
Histidine %	0.53
Isoleucine %	0.87
Leucine %	1.58
Lysine %	1.18
Methionine %	0.62
Phenylalanine %	0.92
Tyrosine %	0.61
Threonine %	0.79
Tryptophan %	0.24
Valine %	0.97
Serine %	1.00
Aspartic Acid %	2.23
Glutamic Acid %	4.26
Alanine %	1.20
Proline %	1.32
Taurine %	0.03
Fats	**11.3%**
Cholesterol, ppm	135
Linoleic Acid, %	2.32
Linolenic Acid, %	0.28
Arachidonic Acid, %	0.02
Omega-3 Fatty Acids, %	0.42
Total Saturated Fatty Acids,	0.77
Total Monounsaturated Fatty Acids	1.00
Fiber (Crude) %	**4.4**
Neutral Detergent Fiber3, %	15.5
Acid Detergent Fiber4, %	5.6
Minerals	
Ash, %	**6.0**

Calcium, %	0.81
Phosphorus, %	0.61
Phosphorus (non-phytate), %.	0.33
Potassium, %	1.07
Magnesium, %	0.21
Sulfur, %	0.31
Sodium, %	0.30
Chloride, %	0.53
Fluorine, ppm	9.2
Iron, ppm	184
Zinc, ppm	79
Manganese, ppm	82
Copper, ppm	13
Cobalt, ppm	0.72
Iodine, ppm	0.97
Chromium (added), ppm	0.01
Selenium, ppm	0.37

Vitamins	**ppm**
Carotene, ppm	1.5
Vitamin K, ppm	3.3
Thiamin, ppm	16
Riboflavin, ppm	8.1
Niacin, ppm	84
Pantothenic Acid, ppm	17
Choline, ppm	1575
Folic Acid, ppm	3.0
Pyridoxine, ppm	9.6
Biotin, ppm	0.30
B12, mcg/kg	51
Vitamin A, IU/gm	15
Vitamin D3 (added), IU/gm	2.3
Vitamin E, IU/kg	99
Ascorbic Acid, mg/gm	0.00

Calories provided by:

Protein, %	24.495
Fat (ether extract), %	13.122
Carbohydrates, %	62.382

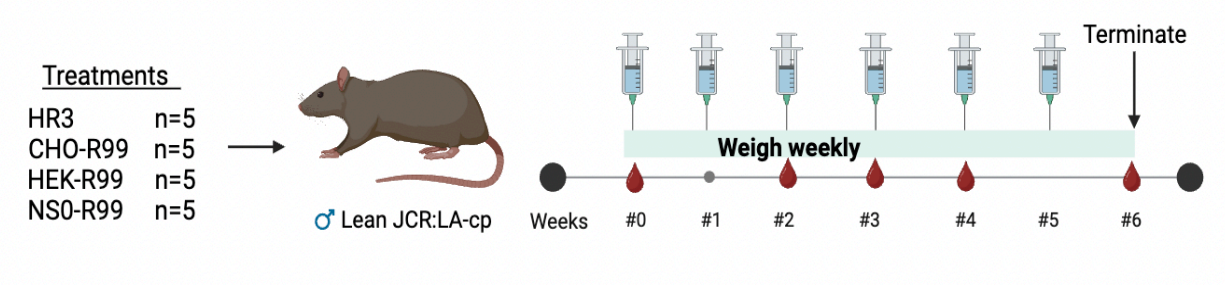

Figure 3.1 Study design for the male lean JCR:LA-cp rats. The lean rats received 6 weekly doses of two injections of 250 µL of 400 µg/mL (total 200 µg). Blood draws were done at weeks 0,2,3,4, and 6. Week 0 represents the pre-immune sera (before the first injection) while weeks 2,3,4, and 6 represent doses 2,3,4, and 6. n=5 for all treatment groups. Created with BioRender.

Table 3.2 Study design and planned assessments for the male lean JCR:LA-cp rats.

Study design				**Planned Assessments**		
Animal model	**Duration**	**Blood draws**	**Doses**	**Ab2, Kinetics**	**Ab3, Kinetics**	**Additional**
Male Heterozygous Lean JCR:LA-cp Rats - 3 months old - Standard chow diet	6 weeks.	5 blood draws at weeks 0,2,3,4,and 6	Two injections of 250uL of 400ug/mL. Total 200mg	Ab2 assessment planned (minimum at final dose) Kinetics planned.	Ab3 assessment planned (minimum at W0 and after the fourth or final dose) Kinetics planned.	(1) Weight gain over time.

3.2.4 Plasma and sera preparation

Sera and plasma samples were centrifuged at 7000 rpm (radius 8.4 cm) for 10 minutes at 4°C; the supernatant (~150 µL) was then collected via micropipette and stored in 0.6 mL Eppendorf tubes at -80°C for immunogenicity testing via ELISA. The remaining pellet and pipette tips were discarded in biohazard bins. Due to ethical considerations, rodents only underwent five blood draws at weeks 0,2,3,4 and 6.

3.2.5 Sample collection and processing

Tissue samples collected were flushed with ice-cold sterile PBS (Phosphate Buffered Saline, pH 7.4) and minced into small portions, except for the heart, which was kept whole. Tissues were

packaged in labelled tin foil and snap-frozen in liquid nitrogen before being stored in a -80°C freezer.

3.2.6 Enzyme-Linked Immunosorbent Assay (ELISA) for Ab2 recognition

Pre-Immune (PI), dose 2, dose 3, dose 4 and final dose sera (dose six) were assessed for recognition of the P3R99 idiotype and a matched isotype control (hR3) using a modified solid-phase indirect ELISA to detect the presence of induced Ab2 (anti-P3R99) antibodies as evidence of a host immune reaction to injection with P3R99 variants (CHO-P3R99, NS0-P3R99, and HEK-P3R99) (Figure 3.2)(Soto et al., 2012)(Brito et al., 2017)(Sarduy et al., 2017)(Delgado-Roche et al., 2015). ELISA details and modifications have been documented and validated in previous NS0-P3R99 studies (Brito et al., 2017). Briefly, 96-well Corning polystyrene ELISA plates (Sigma Aldrich REF3506, Darmstadt, Germany) were coated half (rows 1-6) with 100 µL of 10 µg/mL of the idiotype (FAB region) of the P3R99 and half (rows 7-12) with 100 µL of 10 µg/mL of a negative isotype control (the humanized murine hR3 mAb) and incubated at 4°C overnight. Plates were washed with 300 µL of 1X PBS per well (Table 3.3) 3-5 times to remove any remaining coating in the wells. Then, 200 µL of 1% Bovine Serum Albumin (BSA) (or skim milk) - 1X PBS (Sigma Aldrich REF 9048-46-8) was added to block non-specific binding sites and incubated at 37°C for one hour. Following blocking, rodent sera from the P3R99 variants and hR3 injection groups were prepared in 1% BSA (or skim milk) - 1X PBS and diluted. 100 µL of diluted sera from all treatment groups and 100uL of 1% BSA (or skim milk) - 1X PBS (blank) were added to the coated ELISA plates and then incubated at 37°C for 1 hour and 30 minutes. Plates were washed with 0.1% BSA (or skim milk) – 0.02% tween-20 – 1X PBS (BIORAD REF: 1610781) with 300 µL per well 3-5 times to remove sera. Plates were then incubated at 37°C for an additional hour after 100 µL of peroxidase-conjugated goat anti-rat IgG polyclonal secondary antibody (Jackson ImmunoResearch Laboratories Peroxidase AffiniPure™ Goat Anti-Rat IgG (H+L) REF 112-035-003) was added at varying concentrations (typically 1/5000 dilution prepared in 0.1% BSA (or skim milk) – 0.02% tween-20 – 1X PBS) to determine sera reactivity to the IgG fractions. The reaction was visualized with 100uL of room-temperature 1-Step Ultra TMB Liquid Substrate for ELISA (Thermofisher REF 34028). TMB caused an enzymatic colour change proportional to the plate's bound Ab2 (anti-P3R99) antibodies. Once an adequate colour change was reached, 50uL of 10% sulfuric acid was added to stop the reaction. The plates were then read by

spectrophotometer at 490nm. The magnitude of sera reactivity to the plated P3R99 represents the amount of anti-idiotypic Ab2 (anti-P3R99) antibodies that were induced in response to the immunizations (P3R99 variants and hR3), while the sera reactivity to the isotype control represents the production of non-idiotypic antibodies (Brito et al., 2017). Assays were performed in triplicate to ensure accuracy and consistency. ELISA results were expressed as Optical Density (OD) values (at 490nm).

Table 3.3. 10X Phosphate Buffered Saline (PBS) recipe for Ab2 ELISAs (prepared in 1000mL).

	MW	Grams (per 1000 mL)
NaCl 20m M	58.44g/mol	80.0g
KCl	74.55g/mol	2.0g
KH_2PO_4	136.09g/mol	2.4g
Na_2HPO_4 $2H_2O$	177.99g/mol	17.8g

- Adjust pH to 7.4 with 5M NaOH. Store at -4°C until use.

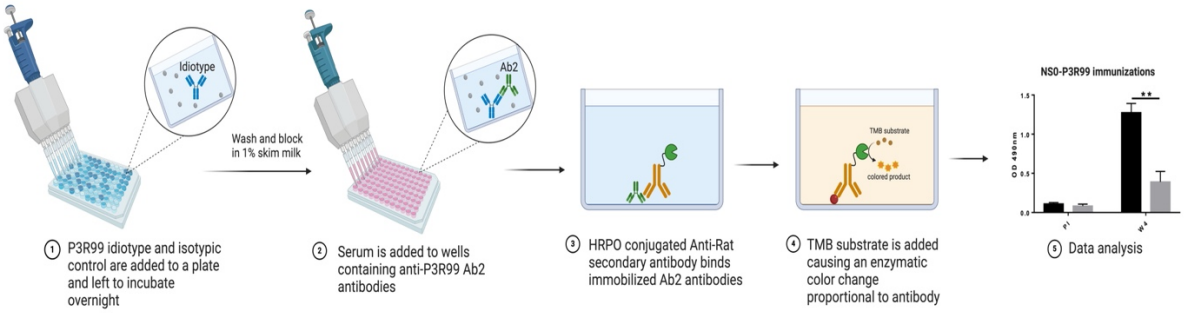

Figure 3.2 General Enzyme-Linked Immunosorbent Assay (ELISA) protocol for Ab2 antibody recognition and assessment. Created with BioRender.

3.2.7 Enzyme-Linked Immunosorbent Assay (ELISA) for Ab3 recognition

Pre-immune (PI) and final dose sera (sixth dose) were assessed for recognition of chondroitin sulfate and compared against the original NS0-P3R99 and the matched isotype control hR3 using

a modified solid-phase indirect ELISA. This Ab3 ELISA was used to detect the presence of induced Ab3 (anti-chondroitin sulfate) antibodies as evidence of a host immune reaction to the injection with P3R99 variants (CHO-P3R99, NS0-P3R99, and HEK-P3R99) (Figure 3.3) (Soto et al., 2012)(Brito et al., 2017)(Sarduy et al., 2017)(Delgado-Roche et al., 2015). Briefly, 96-well Corning polystyrene ELISA plates were coated with 100 μL of 10 μg/mL of shark cartilage chondroitin sulfate (Sigma Aldrich REF C4384) and incubated at 25°C (room-temperature) overnight. Plates were then washed with 300 μL per well of 1X HBS (Table 3.4) 3-5 times to remove any remaining chondroitin sulfate in the wells. Then, 200 μL of 1% BSA (or skim milk) - 1X HBS (Sigma Aldrich REF 9048-46-8) was added to block non-specific binding sites and incubated at 25°C for one hour. Following blocking rodent sera from the P3R99 variants and hR3 injection groups were prepared in sample buffer (Table 3.5) and diluted. 100uL of diluted sera from all treatment groups and 100uL of sample buffer (blank) were added to the chondroitin sulfate-coated ELISA plates and then incubated at 25°C for 1 hour and 30 minutes. Plates were washed with 0.02% tween-20 – 1X HBS with 300 μL per well 3-5 times to remove sera. Plates were then incubated at 25°C for an additional hour after 100 μL of species-specific peroxidase-conjugated goat anti-rat IgG polyclonal secondary antibody was added at varying concentrations (typically 1/5000 dilution prepared in 0.02% tween-20 – 1X HBS) to determine sera reactivity to the IgG fractions.

The reaction was visualized with 100 μL of room-temperature 1-Step Ultra TMB Liquid Substrate for ELISA. TMB caused an enzymatic colour change proportional to the bound Ab3 (anti-chondroitin sulfate) antibodies on the plate. Once an adequate colour change was reached, 50 μL of 10% sulfuric acid was added to stop the reaction. The plates were then read by spectrophotometer at 490nm. The magnitude of sera reactivity to the plated chondroitin sulfate is used as an indirect measure of the anti-anti-idiotypic Ab3 (anti-chondroitin sulfate) antibodies that were induced in response to the immunizations (P3R99 variants and hR3). Assays were performed in triplicate to ensure accuracy and consistency. ELISA results were expressed as Optical Density (OD) values (at 490nm) (Brito et al., 2012).

Table 3.4 Hepes Buffer Saline (HBS) recipe for Ab3 ELISAs.

	MW	Conc.	Grams (500 mL)	Grams (1000 mL)	Grams (1500 mL)	Grams (2000 mL)
Hepes	238.3g/mol	20mM	2.383g	4.766g	7.149g	9.532g
NaCl	58.44g/mol	150mM	4.383g	8.766g	13.149g	17.532g

- Adjust pH to 7.4 with 5M NaOH. Store at -4°C until use.

Table 3.5 Sample buffer recipe for Ab3 ELISAs (prepared in 200 ml).

	MW	Grams (200 mL)
Hepes 10mM	238.3g/mol	0.48g
NaCl 20m M	58.44g/mol	0.234g
$CaCl_2.2H_2O$ 2mM	147.02g/mol	0.059g
$MgCl_2.6H_2O$ 2mM	203.03g/mol	0.0813g

- Adjust pH to 7.4 with 5M NaOH. Store at -4°C until use.

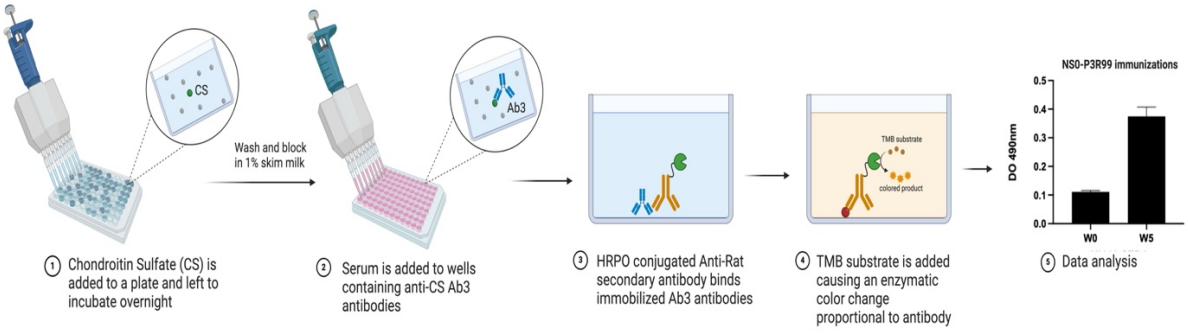

Figure 3.3 General Enzyme-Linked Immunosorbent Assay (ELISA) protocol for Ab3 antibody recognition and assessment. Created with BioRender.

3.2.8 Data and statistical analysis

Significance of the Ab2 response was characterized by dominance of the anti-idiotypic response (black bars) compared to the anti-isotypic response (gray bars).

Significance of the Ab3 response was characterized by a minimum two-fold induction of anti-chondroitin sulfate Ab3 antibodies from the pre-immune state (before immunizations) to the final (or peak) dose.

Statistical analyses were performed with the GraphPad Prism software (GraphPad Software Inc., San Diego, CA, USA). All data is presented as mean ± SEM (Standard Error of the Mean). The distribution of means was assessed via the D'Agostino and Pearson test, Anderson-Darling test, Shapiro-Wilk test, and Kolmogorov-Smirnoff test. If the distribution was normal, then parametric tests were used; if the distribution was lognormal, then non-parametric tests were used. For parametric results comparing one group to another, a parametric T-test was used. For non-parametric results, a Mann-Whitney T-test was used. One-way ANOVA with Tukey's test for multiple comparisons was used for parametric results comparing more than two groups. Kruskal-Wallis with Dunn post hoc for multiple comparisons was used for non-parametric results comparing more than two groups. Values at $P<0.05$ were considered statistically significant.

3.3 Results

3.3.1 Lean JCR:LA-cp rat weight over time

All lean rats fed the standard chow diet exhibited normal weight gain regardless of the treatment group. No significant differences were found in the rats' weight gain pattern or final body weight among the four treatment groups from W0 to W6. (Figure 3.3.1)

A. Lean JCR:LA-cp rat weight over time.

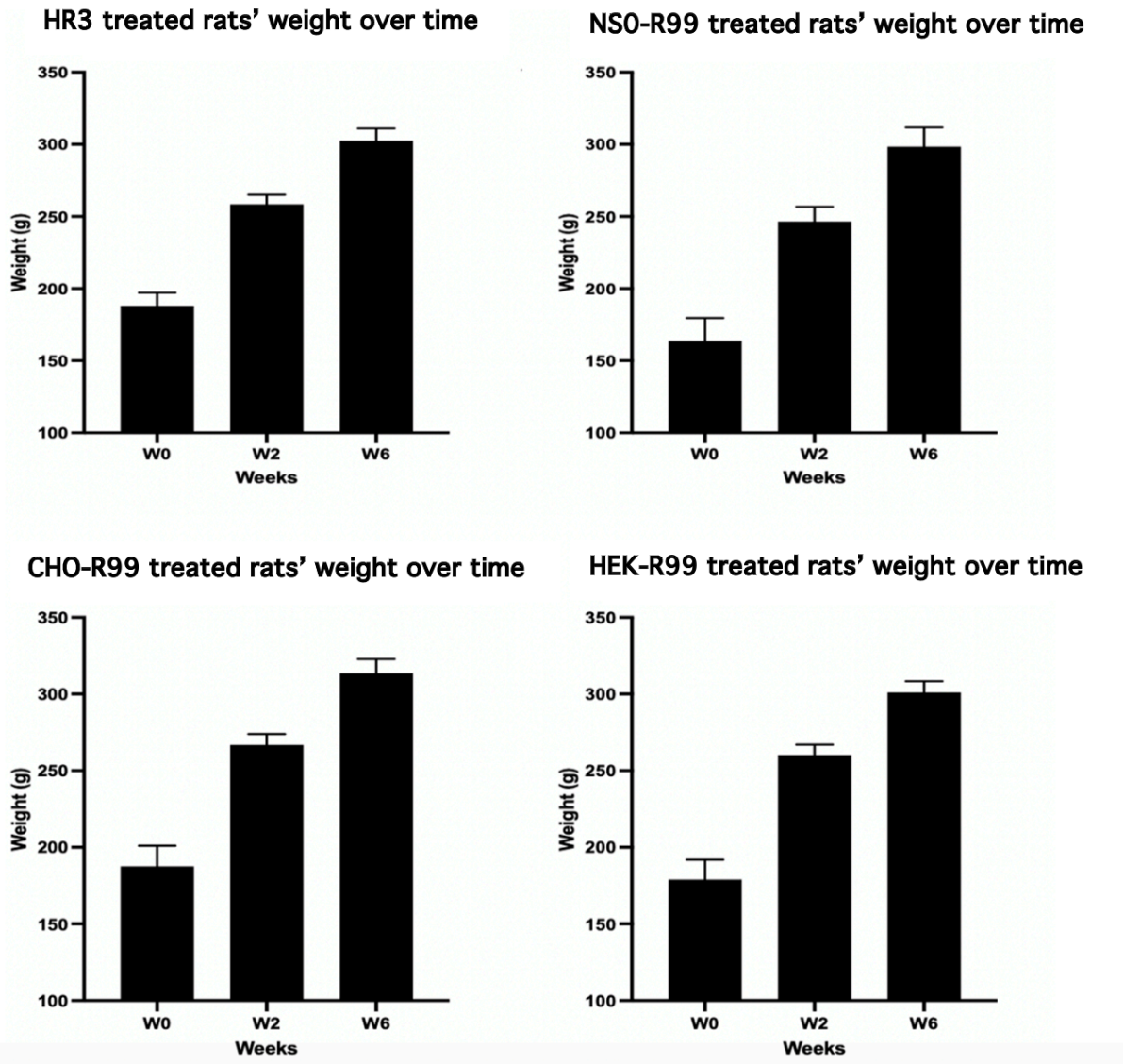

B. Comparison of lean JCR:LA-cp rat weight gain during immunizations.

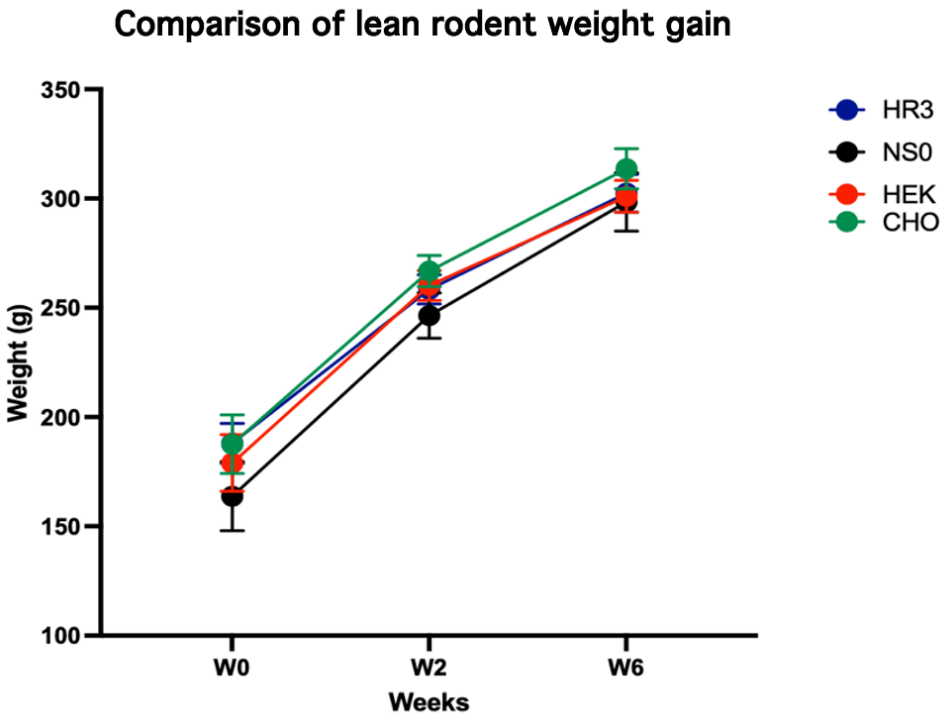

Figure 3.3.1 (A) Weight for the lean JCR:LA-cp rats in the four immunization groups. (B) Comparison of rodent weight represented as kinetics from W0 to W6. n=5 for all groups. Results were analyzed via One-way ANOVA, P>0.05 (not significant). All values are presented as mean ± SEM.

3.3.2 Ab2 response of lean JCR:LA-cp rats immunized with P3R99 variants and a negative isotype control hR3

Sera taken from lean JCR:LA-cp rats immunized with the three P3R99 variants exhibited a significant increase in the recognition for the idiotypic region of P3R99 from W0 to W6. As expected, the control hR3 treated rats did not induce significant levels of anti-idiotypic antibodies at any point in time (Figure 3.3.2A).

Additionally, there were significant differences in the induction of anti-idiotypic antibodies compared to anti-isotypic (non-idiotypic) antibodies for the three P3R99 variants.

No significant differences were found among the P3R99 variants anti-idiotypic response at the final (sixth) dose (Figure 3.3.2B)

A. Ab2 response in lean JCR:LA-cp rats immunized with P3R99 variants from weeks 0-6.

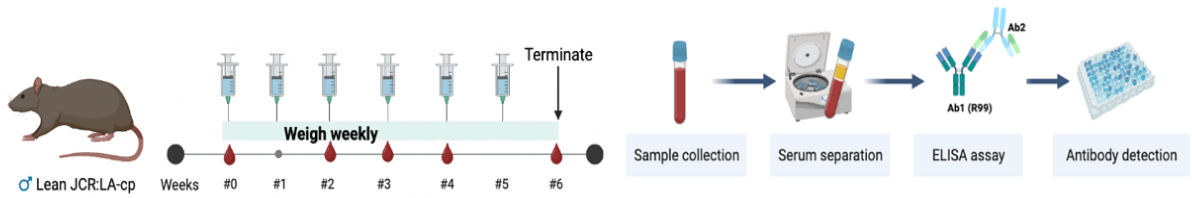

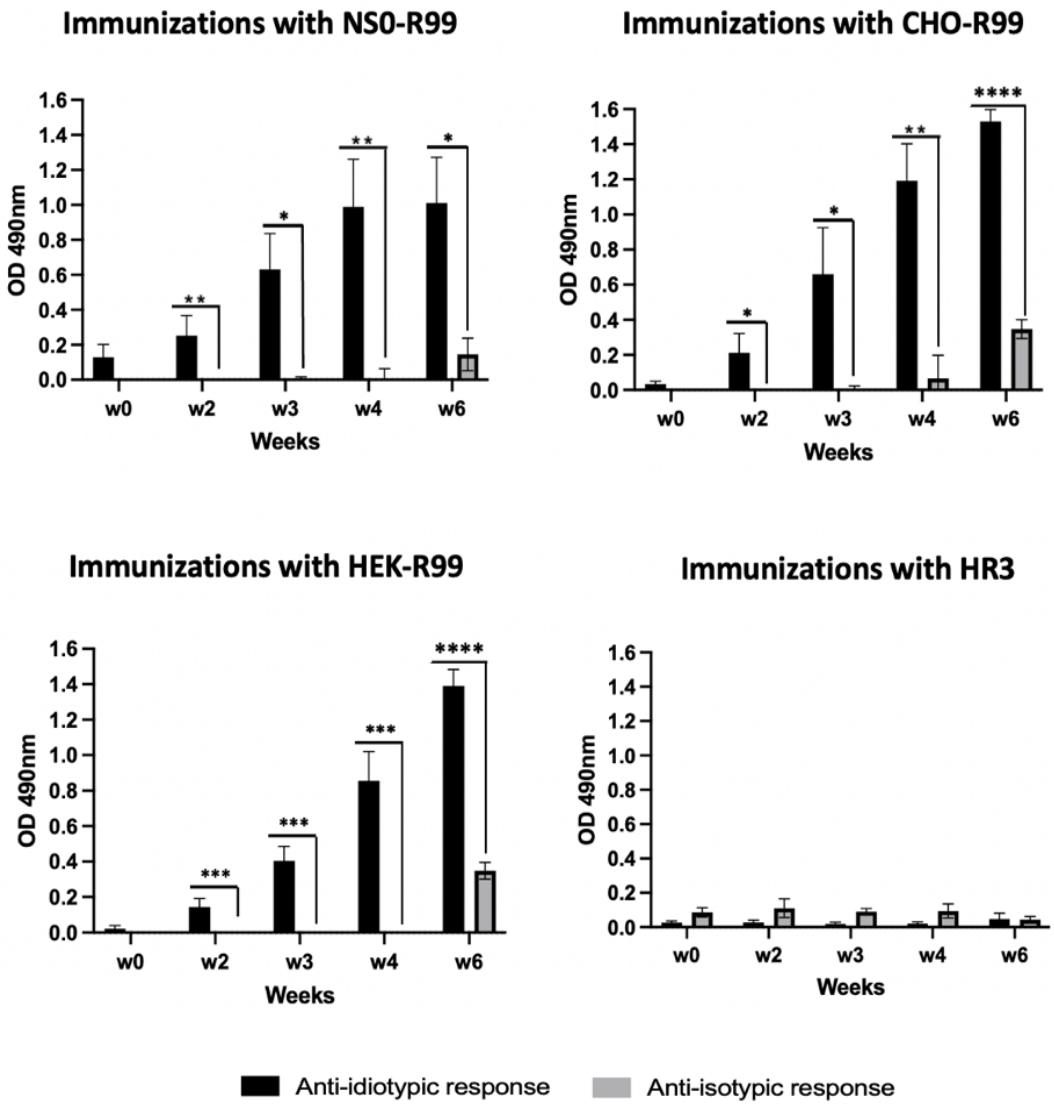

B. Kinetics and comparison of the anti-idiotypic response induced by P3R99 variants in lean JCR:LA-cp rats.

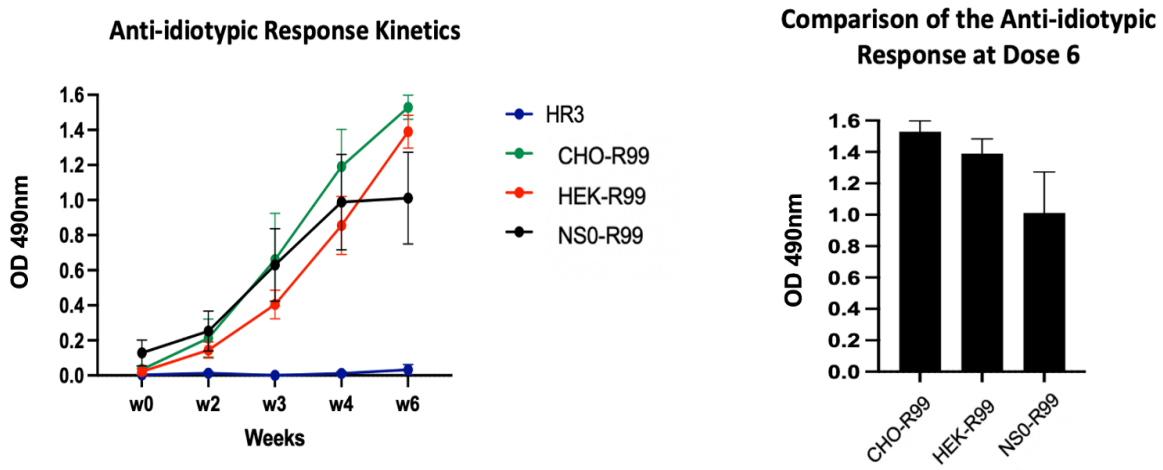

Figure 3.3.2 (A) Enzyme-Linked Immunosorbent Assay (ELISA) results of Ab2 antibody induction at a sera dilution of 1/5000. Represented as the response against the idiotype of P3R99 (anti-idiotypic response) vs the response against the non-idiotype regions of P3R99 (anti-isotypic response). (B) Comparison of solely the anti-idiotypic response of the P3R99 variants represented over time as kinetics and at the sixth dose. n=5 for all groups. Results were analyzed via parametric T-test (Figure 3.3.2 A) and One-way ANOVA (figure 3.3.2 B, (not significant)) * = $P<0.05$, ** = $P<0.01$, *** = $P<0.001$, **** = $P< 0.0001$. All values are presented as mean ± SEM.

3.3.3 Ab3 response of lean JCR:LA-cp rats immunized with P3R99 variants or a negative isotype control hR3

Sera taken from lean JCR:LA-cp rats immunized with the P3R99 variants exhibited a minimum two-fold increase in recognition of chondroitin sulfate from W0 to W4 (Figure 3.3.3A), while the hR3 treated rats did not.

No significant differences were found in the induction of an anti-chondroitin sulfate response at the fourth dose among the three P3R99 treatment groups (Figure 3.3.3B).

A. Ab3 Response in lean JCR:LA-cp rats immunized with P3R99 variants from weeks 0-4.

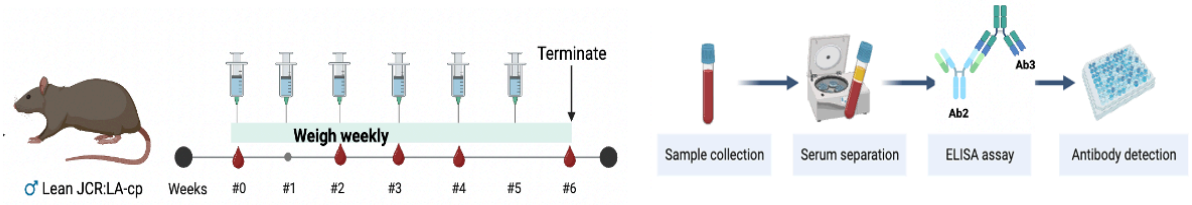

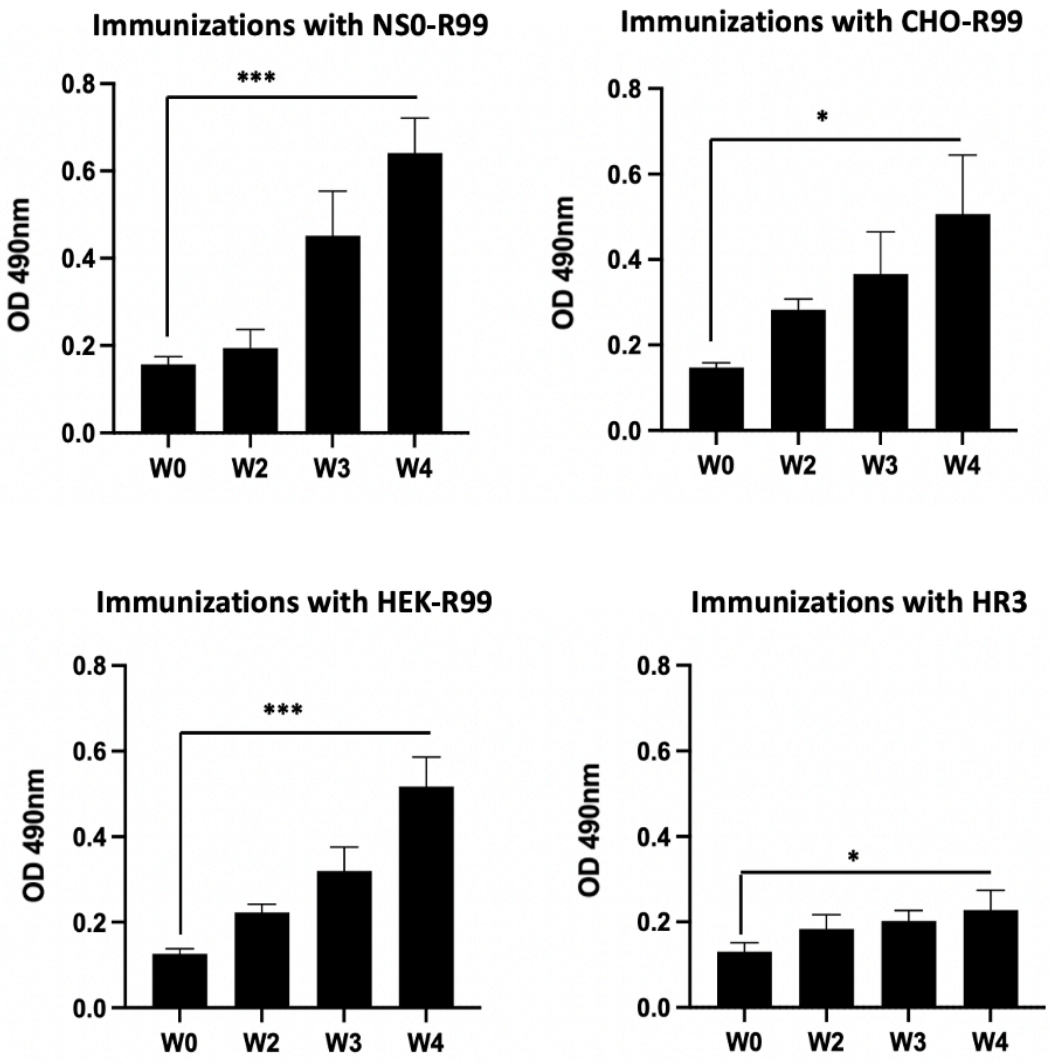

B. Kinetics and comparison of the anti-chondroitin sulfate response induced by P3R99 variants in lean JCR:LA-cp rats.

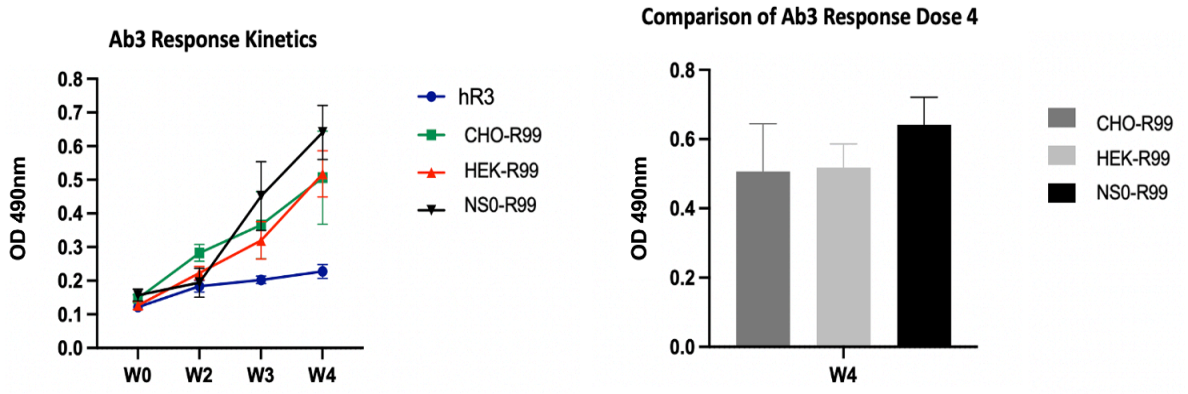

Figure 3.3.3 (A) Enzyme-linked immunosorbent Assay (ELISA) results of Ab3 antibody induction at a sera dilution of 1/400. Represented as the response against chondroitin sulfate from weeks 0-4. (B) Comparison of solely the Ab3 response of the P3R99 variants represented over time as kinetics and at the fourth dose. n=5 for all groups. Results were analyzed via Mann Whitney non-parametric T-test (Figure 3.3.3 A) and One-way ANOVA (figure 3.3.3 B, (not significant)). * = P<0.05, ** = P<0.01, *** = P<0.001, **** = P< 0.0001. All values are presented as mean ± SEM.

3.4 Discussion

Inefficiencies with the production of the original NS0-P3R99 mAb via a murine myeloma cell line (NS0) led to the development of two new untested P3R99 variants produced from two more productive cell lines: Chinese Hamster Ovary (CHO) and Human Embryonic Kidney (HEK) (Dhara et al., 2018)(Goh & Ng, 2015). Despite the maintenance of the NS0-P3R99 structure postproduction, the P3R99 variants, HEK-P3R99 and CHO-P3R99, needed validation of their immunogenic capability.

Maintenance of immunogenicity is critical for the anti-atherogenic effect of the P3R99 (Sarduy et al., 2017)(Brito et al., 2017)(Soto et al., 2012). This was the first study to assess the immunogenicity of the P3R99 variants using ELISAs.

In this study, we examined the immunogenicity of lean 3-month-old JCR:LA-cp rats immunized with three P3R99 variants: NS0-P3R99, HEK-P3R99, and CHO-P3R99. The findings from this

study presented strong evidence that the HEK-P3R99 and CHO-P3R99 variants maintained the immunogenicity of the original NS0-P3R99. Additionally, we found that the CHO-P3R99 and HEK-P3R99 had a similar strength (magnitude of Ab2 and Ab3 antibody induction) as the original NS0-P3R99, confirming our hypotheses.

3.4.1 P3R99 variant administration did not impact weight gain of lean JCR:LA-cp rats

Lean JCR:LA-CP rodents given P3R99 had weight gain like the hR3 control rats (Figure 3.3.1). These results suggest that P3R99 administration did not affect rodent weight over time.

3.4.2 CHO, HEK, and NS0-P3R99 variants met the requirement of Ab2 immunogenicity in a healthy small animal model: lean JCR:LA-cp rats

The established metric for assessing Ab2 antibody induction is through the presence of idiotypic dominance. Although the idiotype only accounts for 25% of the P3R99 structure, and the entire structure of the P3R99 is immunogenic, the majority of Ab2 antibodies are anti-idiotypic (Brito et al., 2010)(Soto et al., 2012). This occurrence is due to the higher affinity and specificity of Ab2 antibodies to the idiotype of the P3R99 compared to the non-idiotypic regions of the P3R99. However, as the Ab2 antibodies are able to recognize the whole molecule of the P3R99, a minority can bind the non-idiotypic regions of the P3R99. To detect the induction of Ab2 antibodies capable of binding the non-idiotypic regions of the P3R99, we use a negative isotype control. This control does not share the idiotype of the P3R99 but does share a similar overall structure and thus shares the non-idiotypic regions.

A 2017 study involving ApoE-/- mice immunized with 200 μg of NS0-P3R99, or control hR3 assessed the dominance of the P3R99 idiotype by comparing the anti-idiotypic response to the anti-isotypic response (Sarduy et al., 2017). They reported significant differences in the induction of anti-idiotypic Ab2 antibodies compared to the anti-isotypic response following the third and fourth doses in the NS0-P3R99 treated mice. This observation was not conserved for the hR3 treated mice, confirming the immunogenicity of the P3R99 in regard to Ab2 antibody induction.

Results from this 2017 murine experiment are quite comparable to our findings in the lean JCR:LA-cp rats (Figure 3.3.2A). The lean JCR:LA-cp rats were chosen due to previous experience with this model and our interest in assessing the P3R99 variants under normal physiological conditions. The lean JCR:LA-cp rats tend towards leanness and a state of well-being. The rats were also at 3 months of age in order to minimize old-age-related effects on health and the immune

system. Similar to the 2017 study in ApoE-/- mice, we found that the induction of Ab2 antibodies by the non-idiotype regions of the P3R99 (anti-isotypic response, gray bars) was significantly lower than the Ab2 antibodies induced by the idiotype of P3R99 (anti-idiotypic response, black bars). Dominance of the idiotypic response was specifically present for all the P3R99s variants at weeks 2,3,4, and 6 (doses 2,3,4, and 6)(Figure 3.3.2A).

Moreover, we also observed a slight increase in the anti-isotypic response at week 6 following the sixth dose. This result was expected as the non-idiotypic region of the P3R99 is immunogenic and thus should demonstrate a minimal response with increased administration of P3R99. These results confirm the maintenance of the immunogenicity of both the idiotype and non-idiotype regions of the NS0-P3R99 in the HEK-P3R99 and CHO-P3R99 variants.

Lastly, when comparing the magnitude of the induction of anti-idiotypic antibodies at the final (6^{th} dose) by the P3R99 variants via One-Way ANOVA, we found no significant differences, confirming that the CHO-P3R99 and HEK-P3R99 are similarly immunogenic as the NS0-P3R99 in the lean JCR:LA-cp rats (Figure 3.3.2 B).

3.4.3 CHO, HEK, and NS0-P3R99 variants met the requirement of Ab3 immunogenicity in a healthy small animal model: lean JCR:LA-cp rats

For Ab3 antibody production, we classify a response as significant (immunogenic) when there is a minimum 2-fold increase in anti-chondroitin sulfate Ab3 antibodies present in the sera from the pre-immunization state (W0) to the fourth (peak) or final dose. This metric has been consistently used for previous studies of the immunogenicity of the NS0-P3R99 (Sarduy et al., 2017). Four doses can be used to assess Ab3 induction, as previous studies have shown that following four immunizations, the P3R99 reaches its peak immunogenicity (Sarduy et al., 2017)(Soto et al., 2023). Following four doses, the generation of Ab2 and Ab3 antibodies reaches a plateau and stabilizes. Further administration of P3R99 at this point does not increase antibody induction. Due to a slight decrease in recognition of chondroitin sulfate (production of Ab3 antibodies) at week 6, our Ab3 results only include up to week 4.

However, when comparing week 0 (0^{th} dose) to week 4 (4^{th} dose), the requirement of a minimum two-fold increase in the induction of Ab3 antibodies was indeed met by the three P3R99 variants (Figure 3.3.3A). This observation was not maintained for the hR3 control-treated rats. In fact, the

P3R99 treated rats underwent a ~3x increase in Ab3 antibody induction from the 0^{th} to the 4^{th} dose, thus meeting the criteria of immunogenicity.

Furthermore, comparing the induction of Ab3 antibodies at the fourth dose by the three P3R99 variants via One-way ANOVA revealed no significant differences, suggesting that the CHO-P399 and HEK-P3R99 variants are similarly immunogenic as the NS0-P3R99 in lean JCR:LA-cp rats (Figure 3.3.3B).

3.4.4 Assessment of the kinetics of the Ab2 and Ab3 response of the CHO, HEK, and NS0-P3R99 variants in lean JCR:LA-cp rats

Significant levels of anti-idiotypic Ab2 antibodies are typically detected one week prior to Ab3 antibodies (Sarduy et al., 2017). This occurrence is due to the reliance of Ab3 antibody induction on Ab2 antibody induction (Sarduy et al., 2017). As a result, Ab2 antibodies consistently precede Ab3 antibodies. However, this process is not well described in exisiting literature.

In our study, when assessing the anti-idiotypic Ab2 response of the P3R99 variants over time as kinetics (Figure 3.3.2B), we begin to see a significant induction of anti-idiotypic antibodies at week 2 following the second dose of their respective treatment. Similarly, when assessing the Ab3 antibody response of the P3R99 variants over time as kinetics (Figure 3.3.3B), we begin to see Ab3 induction at week 3 following the third dose. Thus, our results align with previous NS0-P3R99 studies.

These results are critical as they highlight the temporal relationship between Ab2 and Ab3 antibodies and provide insights into the kinetics of the immune response as a result of administrations of P3R99. By assessing the timing of Ab2 and Ab3 antibody production, we can develop a better understanding of how the immune system responds to the P3R99 and the possible timing of key immune events like antigen recognition.

Additionally, these results are promising as they may also indicate that other features of the NS0-P3R99 have been maintained in the HEK-P3R99 and CHO-P3R99 due to their dependence on the immunogenicity of the P3R99 idiotype; however, this will need further testing to confirm.

3.5 Conclusions

To summarize, the results presented in this chapter confirmed our two principal hypotheses:

1). The HEK-P3R99 and CHO-P3R99 variants maintained the immunogenic ability of the original NS0-P3R99 in healthy lean JCR:LA-cp rats, as per the induction of Ab2 and Ab3 antibodies.
2). The HEK-P3R99 and CHO-P3R99 variants had a similar immunogenic strength as the NS0-P3R99, as per the magnitude of Ab2 and Ab3 antibody induction.
However, it is critical to additionally assess the immunogenicity of the P3R99 variants under different physiological states. Results in small animal models may not be fully applicable to humans and should be confirmed in a large animal model with cardiovascular physiology similar to humans. Moreover, assessing the P3R99s in a model of immune dysfunction with susceptibility to lipid and vascular remodelling can provide necessary insight into possible limitations of the variants and provide a more accurate representation of the P3R99 in an intended patient population.

CHAPTER 4: IMMUNOGENICITY STUDY AND ASSESSMENT OF P3R99 VARIANTS NON-CANONICAL EFFECTS IN OBESE INSULIN-RESISTANT JCR:LA-CP RODENTS

Gala Araujo [1,2], Agata Martin-Ozimek [1,2], Kun Wang [1,2], Yosdel Soto [2,4], Spencer Proctor [2,3]*

[1] Division of Human Nutrition, Department of Agricultural, Food and Nutritional Science.
[2] Metabolic and Cardiovascular Diseases Laboratory, Department of Agricultural, Food and Nutritional Science, and/or 3 Division of Animal Science, Department of Agricultural, Food and Nutritional Science, University of Alberta, Edmonton, Alberta, Canada.
[3] Division of Immunobiology, Centre of Molecular Immunology, Havana 11600, Cuba; yosdel@cim.sld.cu
* Correspondence: proctor@ualberta.ca

4.1 Introduction

In Chapter 3, we characterized the immunogenicity of the P3R99 variants in a healthy small animal model using the lean JCR:LA-cp rats. However, it is necessary to also assess these variants in a model that is applicable to atherosclerosis.

Obesity, characterized as the excess accumulation of body fat, is increasing drastically in the western world (Lim et al., 2023)(Reaven, 2011). Excess levels of adipose tissues are strongly linked to Type 2 Diabetes (T2D) onset, hypertension, dyslipidemia, and cardiovascular dysfunction (Reaven, 2011). Insulin resistance, a key feature of T2D, involves an impaired cellular response to the hormone insulin. As a result, blood sugar levels remain elevated for prolonged periods of time, which, like obesity, can promote inflammation, oxidative damage, endothelial damage, dyslipidemia, and weight gain (McFarlane et al., 2001). Due to similarities in their underlying pathophysiology, both obesity and insulin resistance are major comorbidities of atherosclerosis. Atherosclerosis is estimated to account for 80% of all deaths in diabetic patients (Aronson et al., 2002).

Thus, assessing the immunogenicity of the P3R99 variants in a model of obesity and insulin resistance may be a more clinically relevant model and provide applicable results for human studies. As such, we used our immunogenicity study in the lean JCR:LA-cp rats as a pilot study to develop a protocol for assessment in 9-month-old obese insulin-resistant JCR:LA-cp rats. The JCR:LA-cp rats were chosen in part due to previous experience using this model to assess the

immunogenicity of the NS0-P3R99 (Soto et al., 2023). Additionally, the obese insulin-resistant JCR:LA-cp model is characterized by chronic inflammation and immune dysfunction, including increased pro-inflammatory cytokines (Il-6, Il-2, TNF-α, IFN-γ) and over-stimulation of macrophages and T-cells (Diane et al., 2016). This physiological state could provide critical insights into possible limitations of the P3R99's ability to induce an idiotypic cascade through host immune system stimulation.

Thus, our investigation in this chapter was designed to determine whether the HEK-P3R99 and CHO-P3R99 maintained the overall immunogenicity of the NS0-P3R99, compared to a negative isotype control hR3 (which shares the non-idiotypic structure of the P3R99) in a model of immune dysfunction. We hypothesized that the P3R99 variants would maintain the immunogenic function and strength of the original NS0-P3R99. We maintained the same criteria for assessing the significance of Ab2 and Ab3 antibody induction (immunogenicity) that was used in the lean JCR:LA-cp rats.

Additionally, we were interested in assessing possible non-canonical effects of the P3R99 related to its recognition and binding of chondroitin sulfate Glycosaminoglycans (GAGs). In order to do so, we assessed lipid and carbohydrate metabolism in the obese insulin-resistant JCR:LA-cp rats treated with the P3R99s compared to the control hR3 treated rats. Furthermore, we assessed the cardiovascular function of the obese insulin-resistant rats in the P3R99 and hR3 treatment groups to determine possible adverse effects.

Results from this chapter confirm the immunogenicity of the P3R99 variants and validate the lack of non-canonical adverse effects related to P3R99 chondroitin sulfate recognition using the obese insulin-resistant JCR:LA-cp rats.

4.2 Methods

4.2.1 Animal housing and treatment protocol

Refer to section 3.2.1 of chapter 3.

4.2.2 Monoclonal antibody preparation

Refer to section 3.2.2 of chapter 3.

4.2.3 Study design obese insulin-resistant JCR:LA-cp rats

Twenty middle-aged (9-month-old), obese insulin-resistant male JCR:LA-cp rats were fed a high-fat, high-fructose chow diet for 4 weeks prior to the start of immunizations and for 8 weeks during immunizations (Figure 4.1, Table 4.1). The diet was composed of 15% fructose, 2% cholesterol, and 20% lard to induce insulin resistance. Rodents received a total of six subcutaneous (s.c.) immunizations of 400 μg/ml of either NS0-P3R99 mAb (positive control), HEK-P3R99 mAb (variant), CHO-P3R99 mAb (variant) or hR3 mAb (negative control) (n=5 animals per group) at weekly intervals for the first 4 injections (1 injection per week), followed by two biweekly 'booster' injections (1 injection per 2 weeks) over a total of 8 weeks. Immunizations were given as two 250 μL injections of 400 μg/mL in both the right and left shanks. Total dose was 200 μg (100 μg per flank).

Rodents were weighed weekly to monitor food intake and had venous blood (sera and plasma) (150 μL) drawn at the start of the study prior to the first immunization (PI) and 7 days after the third, fourth, fifth and sixth immunizations. Plasma was collected in purple top BD Vacutainer® Plasma Preparation Tubes (PPT™) containing Ethylenediaminetetraacetic Acid (EDTA) to prevent coagulation, and sera was collected in red top BD Vacutainer® Blood Collection Tubes. Following the six injections at ~12 months of age, rodents were individually placed in an isoflurane inhalation chamber, ensuring a gradual and safe induction by starting with 0.5% isoflurane and adjusting as needed based on the animal's response. The remaining rodent cages kept in the room were covered with an opaque tarp to reduce stress caused by the termination. Our animal technician assessed the level of anesthesia by pedal reflex (firm toe pinch) to ensure the rodents did not demonstrate pain recognition. Once the rodent was unconscious, we transitioned them to a nose cone and bain circuit setup while maintaining anesthesia at 2% and monitoring vital signs. Rodents were then cleaned with ethanol, and various tissues were collected, including the right kidney, liver, gastrocnemius muscle fragment, aorta, heart, and a blood draw by cardiac puncture (Table 4.2).

Table 4.1 Ingredients of the high-fat, high-fructose diet (refer to chow diet for lean rats - supplemented with fat and fructose) used for the obese insulin-resistant JCR:LA-cp rats.

	Grams (per 1Kg)	Percent
Chow	630g	63%
Lard	200g	20%
Cholesterol	20g	2%
Fructose	150g	15%

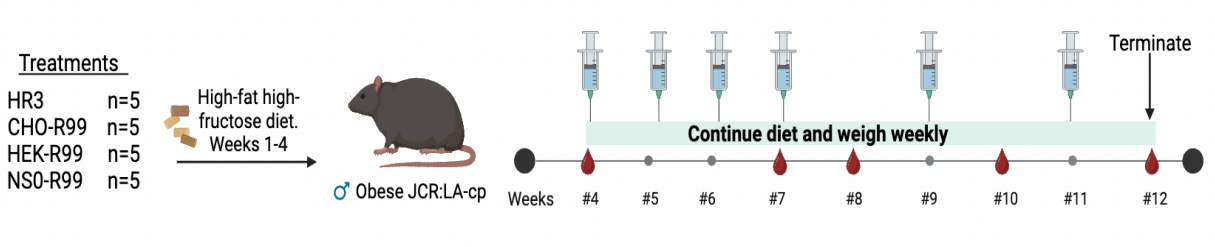

Figure 4.1 Study design for the male obese insulin-resistant JCR:LA-cp rats. The rats received 4 weekly and then 2 biweekly booster doses of two injections of 250 µL at 400 µg/mL (total 200 µg). Blood draws were done at weeks 4,7,8,10, and 12. Week 4 represents the pre-immune sera (before the first injection), while weeks 7,8,10 and 12 represent doses 3,4,5 and 6. n=5 for all treatment groups. Created with BioRender.

Table 4.2 Study design and planned assessments for the male obese insulin-resistant JCR:LA-cp rats.

Study design				**Planned Assessments**		
Animal model	**Duration**	**Blood draws**	**Doses**	**Ab2, Kinetics**	**Ab3, Kinetics**	**Additional**
Male Homozygous Obese Insulin-Resistant JCR:LA-cp Rats - 9 months old - High-Fat High-fructose diet (composed of 2% cholesterol, 20% lard, 15% fructose)	12 weeks total. 4-week diet, then 6 doses over 8 weeks with diet	5 blood draws at weeks 4,7,8,10,and 12	Two injections of 250uL of 400ug/mL. Total 200mg	Ab2 assessment planned (minimum at final dose) Kinetics planned.	Ab3 assessment planned (minimum at W0 and after the fourth (W8) or final dose (W12)) Kinetics not planned.	(1) Weight gain over time. (2) Lipoprotein and glucose metabolism. (3) Heart function.

4.2.4 Plasma and sera preparation

Refer to section 3.2.4 of chapter 3. Due to ethical considerations, rodents only underwent five blood draws at weeks 4,7,8,10 and 12.

4.2.5 Sample collection and processing

Tissue samples collected were flushed with ice-cold sterile PBS (Phosphate Buffered Saline, pH 7.4) and minced into small portions, except for the heart, which was kept whole. Tissues were packaged in labelled tin foil and snap-frozen in liquid nitrogen before being stored in a -80°C freezer.

4.2.6 Enzyme-Linked Immunosorbent Assay (ELISA) for Ab2 recognition

Refer to section 3.2.6 of chapter 3.

4.2.7 Enzyme-Linked Immunosorbent Assay (ELISA) for Ab3 recognition

Refer to section 3.2.7 of chapter 3.

4.2.8 Biochemical analysis (carbohydrate and lipid metabolism)

Plasma samples from the final immunization (dose six) were assessed in triplicate (25uL per well) using 96-well Maxisorp polystyrene plates (Nunc, Thermo Fisher Scientific, Mississauga, ON, Canada, REF: 243656). Lipid and glucose concentrations were assessed at dilution factors of 1/10 or 1/5, respectively, using commercially available colorimetric kits purchased from Wako Pure Chemical Industries Ltd. (Tokyo, Japan). FUJIFILM Wako kits assessed glucose (REF: 997-03001), Triglycerides (TG) (REF: 992-02892), Total Cholesterol (TC) (REF: 999-02601), and High-Density Lipoprotein (HDL) (REF: 993-72691). Insulin from final injection plasma samples (no dilution, 25 µL per well) was measured via rat-specific ELISA kits purchased from Mercodia, USA (REF: 10-1250-01). The Homeostatic Model Assessment for Insulin Resistance (HOMA-IR) was used to evaluate the insulin resistance of obese rats in the 4 treatment groups.

The following formula was used to calculate the HOMA-IR score:

Equation 4.1 Calculation of Homeostatic Model Assessment for Insulin Resistance (HOMA-IR) score.

$$\text{HOMA-IR} = (\text{Fasting Insulin } (\mu\text{U/mL}) \times \text{Fasting Glucose (mmol/L)}) / 22.5$$

Conversion Formulas: mg/dl × 0.0555 = mmol

Conversion Formulas: mmol/l × 18.018 = mg/dl.

4.2.9 Echocardiogram protocol

The Echocardiogram (ECHO) was completed by trained staff, and the protocol was adapted from SOP G-4' Ultrasound (ECHO) for Small Animal Imaging' found on the Alberta Research Information Services (ARISE) online system. First, the rodent was removed from its cage, noting essential information such as weight, date of birth, sex, strain, and the reason for the ECHO. Subsequently, the rodent was anesthetized using an isoflurane inhalation chamber, ensuring a gradual and safe induction by starting with 0.5% isoflurane and adjusting as needed based on the animal's response. Once the animal was unconscious, we transitioned them to a nose cone and bain circuit setup while maintaining anesthesia at 2% and monitoring vital signs. Throughout the procedure, the depth of anesthesia was assessed via pedal reflex and physiological parameters such as heart rate, respiration, and coloration. The rat was prepared for ultrasound imaging by applying eye lubricating gel, securing the paws to contact pads, and ensuring good conductance for ECHO monitoring.

Depilatory cream was used for hair removal, ensuring a short exposure time to prevent skin burns. A rectal probe is carefully inserted and secured, maintaining the animal's body temperature at 37°C with a heat lamp. Pre-warmed ultrasound gel was applied to the area of interest. The imaging process involved attaching the scan head, positioning the rat, adjusting the scan head, and handling the table for optimal image quality. All images and physiological data were recorded and saved in an Excel file.

Once the echocardiogram was completed, the scan head was disassembled, the ultrasound gel was cleaned from the animal, and the temperature probe and tape were carefully removed. Anesthesia was gradually discontinued, and the animal was monitored until it regained its reflexes. Lastly, the scan heads and ECHO platform were disinfected with Protex disinfectant, and other equipment and surfaces were cleaned with a diluted Virkon solution.

4.2.10 Data and statistical analysis

Refer to Section 3.2.8 of Chapter 3.

4.3 Results

4.3.1 Obese insulin-resistant JCR:LA-cp rat weight over time.

All obese insulin-resistant rats fed the high-fat, high-fructose chow diet exhibited increased weight gain regardless of the treatment group. No significant differences were found in the weight gain pattern or final body weight among the 4 treatment groups from W0 to W12 (Figure 4.3.1).

A. Obese insulin-resistant JCR:LA-cp rat weight over time.

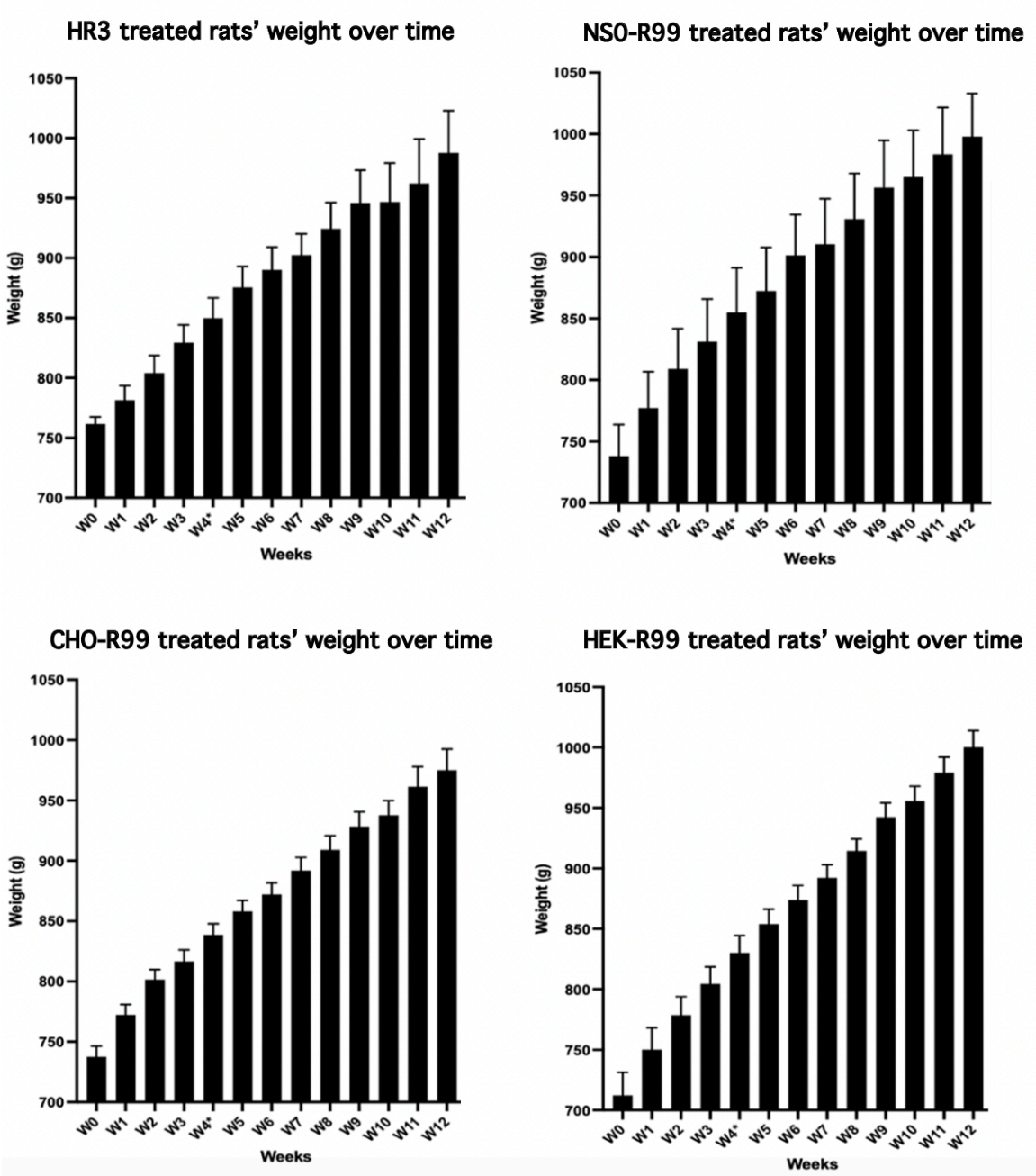

B. Comparison of obese insulin-resistant JCR:LA-cp rat weight gain during immunizations.

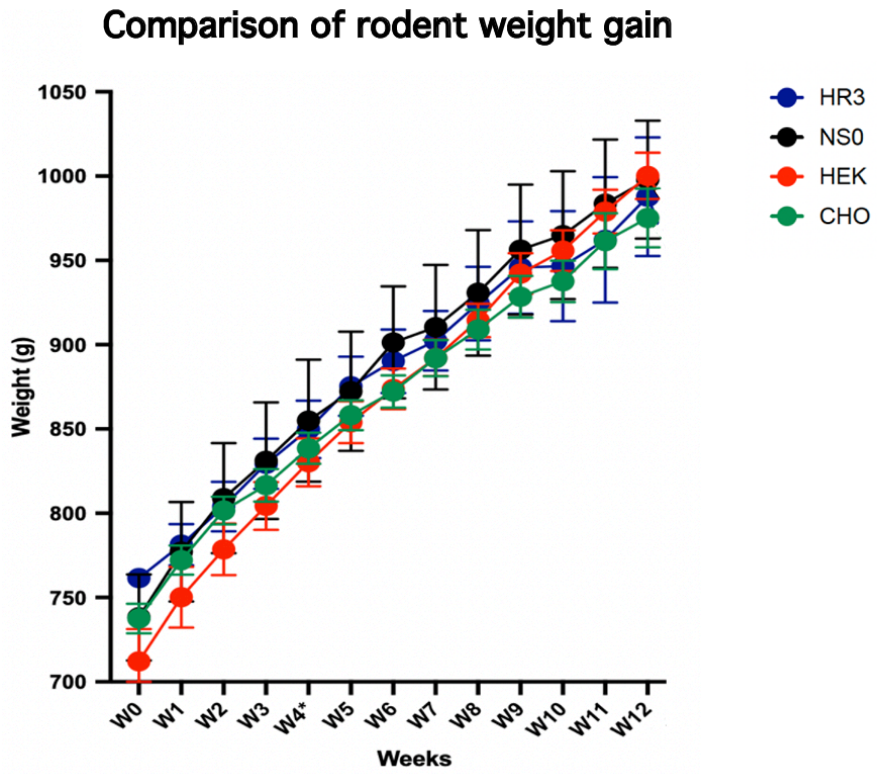

Figure 4.3.1 (A) Weight for obese insulin-resistant JCR:LA-cp rats in the 4 immunization groups. n=5 for all groups. In weeks 0-4, the rats solely received the high-fat, high-fructose diet. Week 4* represents when immunizations started. (B) Comparison of rodent weight represented as kinetics from W0 to W12. n=5 for all groups. Results were analyzed via One-way ANOVA, P>0.05 (not significant). All values are presented as mean ± SEM.

4.3.2 JCR:LA-cp rat heart final weight

All treatment groups exhibited significant differences in the final weight of the hearts of the obese insulin-resistant rats fed a high-fat, high-fructose diet and historical lean age-matched control JCR:LA-cp rats fed a standard chow diet (Figure 4.3.2).

However, there were no significant differences between the final heart weight between the P3R99 treated and control hR3 treated obese insulin-resistant JCR:LA-cp rats.

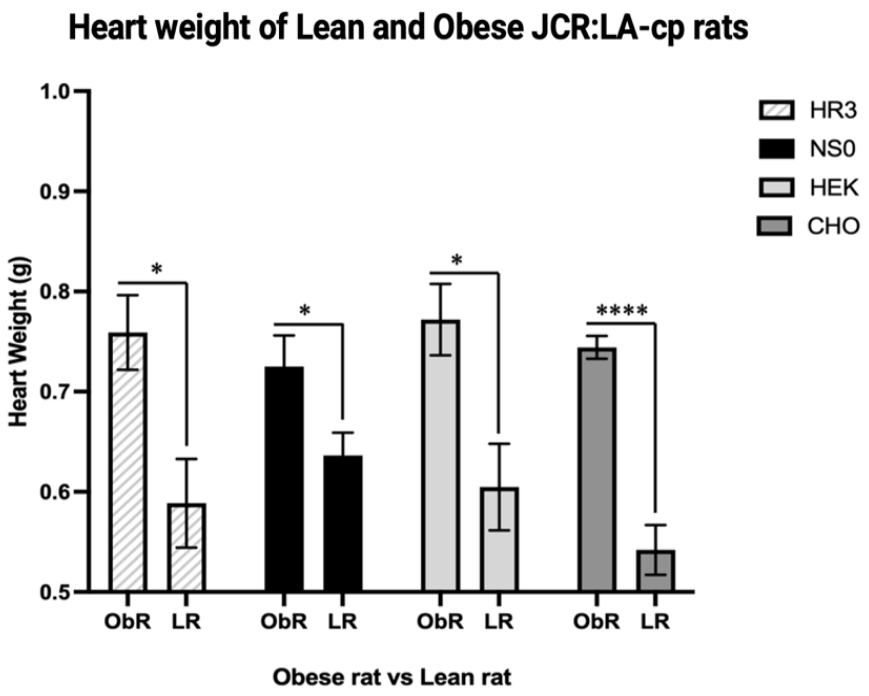

Figure 4.3.2 Final heart weight for age-matched lean and obese insulin-resistant JCR:LA-cp rats in all treatment groups. Comparison of the final mass of the heart (week 12 for obese insulin-resistant rats, week 4 for lean rats). n=5 for all groups. Results were analyzed via parametric T-test and one-way ANOVA. * = P<0.05, ** = P<0.01, *** = P<0.001, **** = P< 0.0001. All values are presented as mean ± SEM.

4.3.3 Ab2 response of obese insulin-resistant JCR:LA-cp rats immunized with P3R99 variants and a negative isotype control hR3

Sera taken from obese insulin-resistant JCR:LA-cp rats immunized with the P3R99 variants exhibited a significant increase in the recognition of the idiotypic region of the P3R99 from the first to the last dose (week 4 to week 12) (Figure 4.3.3A). As expected, the control hR3 treated rats did not present significant levels of anti-idiotypic antibodies at any point in time. Additionally, there were significant differences in the induction of anti-idiotypic antibodies (black bar) vs the anti-isotypic antibodies (gray bar) for the three P3R99 treatment groups.

No significant differences were found in the magnitude of the anti-idiotypic response at the final (sixth) dose among the three P3R99 treatment groups (Figure 4.3.3B).

A. Ab2 Response in obese insulin-resistant JCR:LA-cp rats immunized with P3R99 variants at doses 0, 4 and 6.

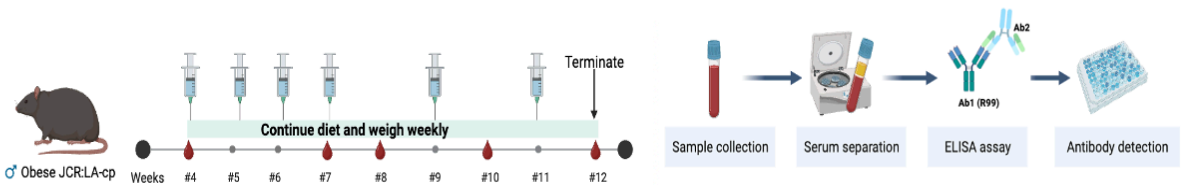

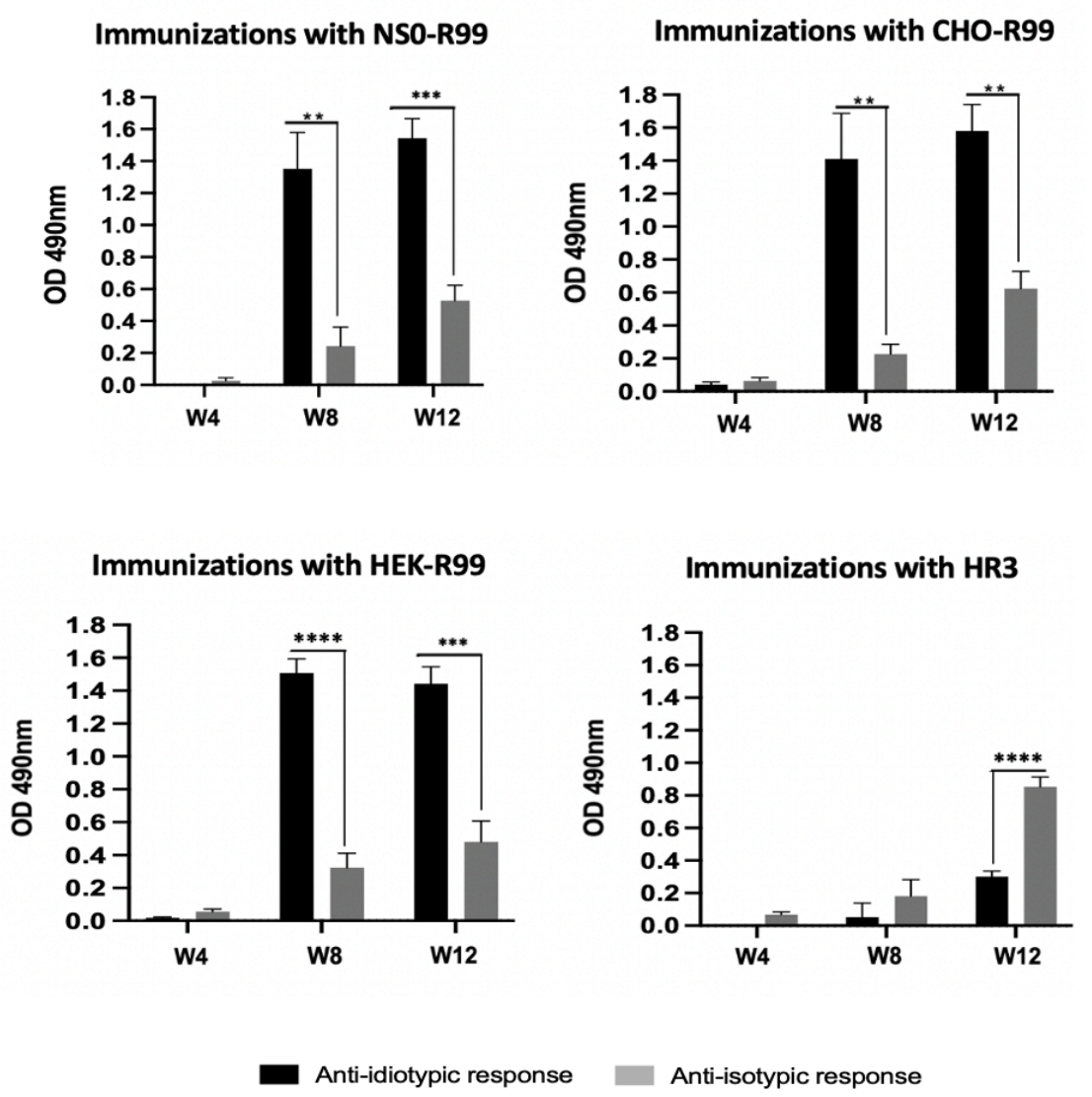

B. Comparison of the anti-idiotypic response induced by P3R99 variants in obese insulin-resistant JCR:LA-cp rats.

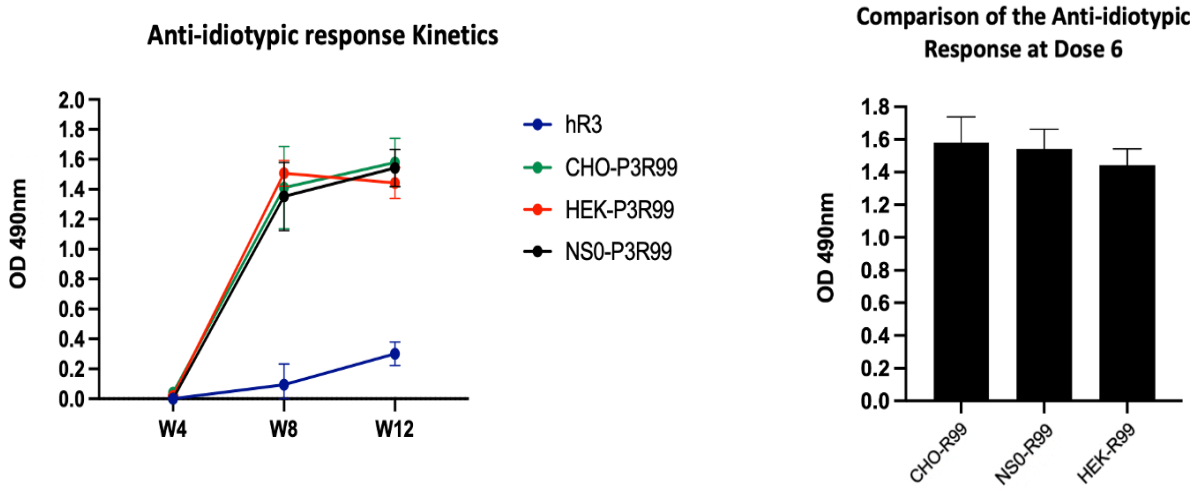

Figure 4.3.3 (A) Enzyme-Linked Immunosorbent Assay (ELISA) results of Ab2 antibody induction at a sera dilution of 1/800. Represented as the response against the idiotype of P3R99 (anti-idiotypic response) vs the response against the non-idiotype regions of P3R99 (anti-isotypic response). (B) Comparison of solely the anti-idiotypic response of the P3R99 variants at the sixth dose. n=5 for all groups. Results were analyzed via parametric T-test (figure 4.3.3A) and One-way ANOVA (figure 4.3.3B, (not significant)). * = P<0.05, ** = P<0.01, *** = P<0.001, **** = P< 0.0001. All values are presented as mean ± SEM.

4.3.4 Ab3 response of obese insulin-resistant JCR:LA-cp rats immunized with P3R99 variants and a negative isotype control hR3

Sera taken from obese insulin-resistant JCR:LA-cp rats immunized with the CHO-P3R99 and NS0-P3R99 variants exhibited a minimum two-fold increase in the recognition of chondroitin sulfate from W4 to W12 (Dose 0, Dose 6) (Figure 4.3.4A), while the hR3 and HEK-P3R99 treated rats did not.

No significant differences were found in the magnitude of the anti-chondroitin sulfate response at the sixth dose among the three P3R99 treatment groups (Figure 4.3.4B).

A. Ab3 Response in obese insulin-resistant JCR:LA-cp rats immunized with P3R99 variants at doses 0 and 6.

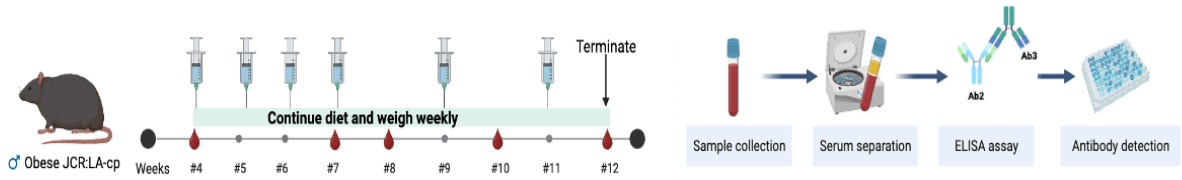

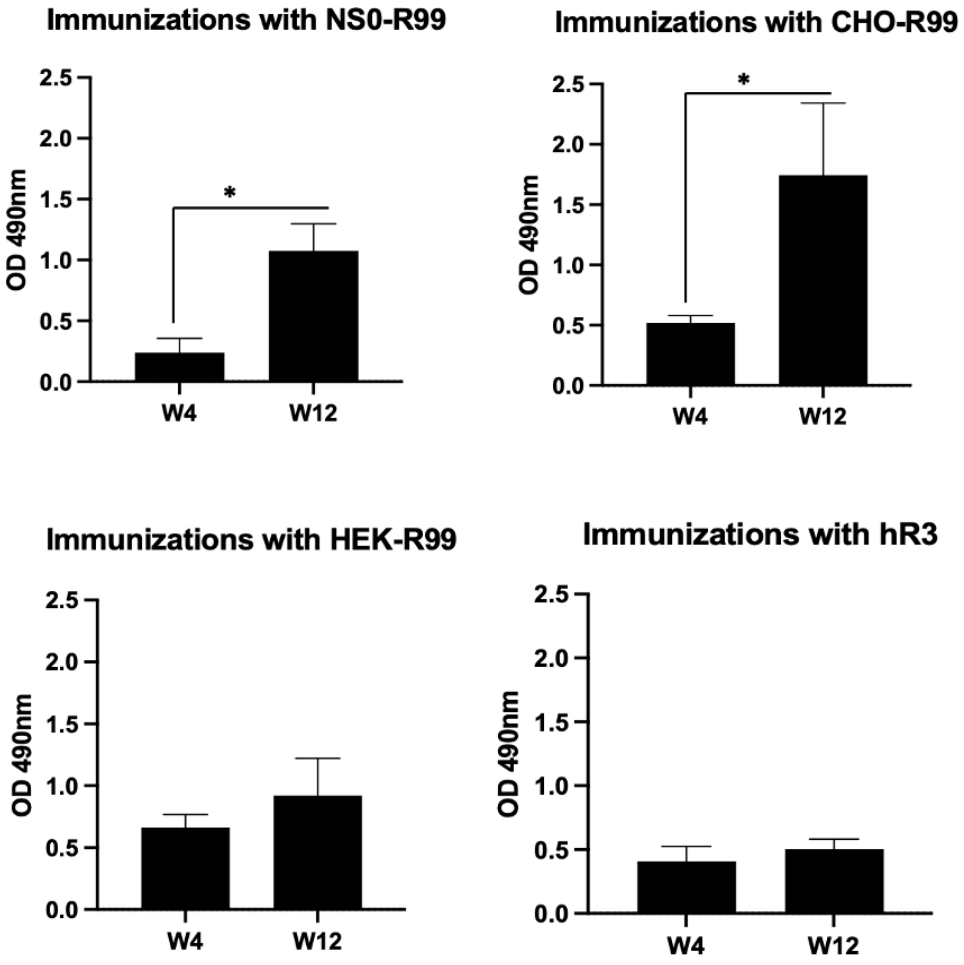

B. Comparison of the Ab3 response induced by P3R99 variants in obese insulin-resistant JCR:LA-cp rats at dose 6.

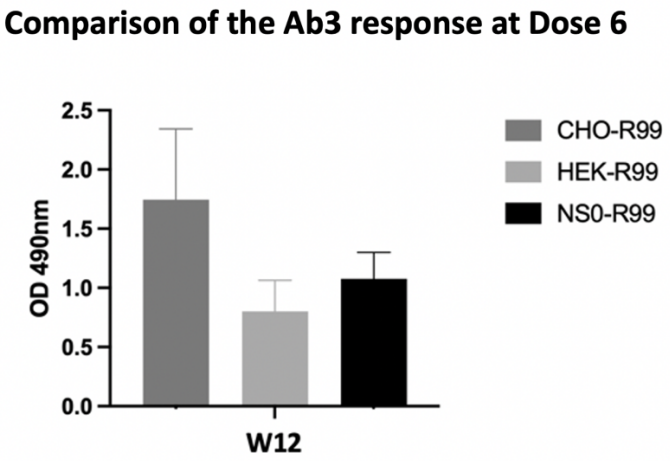

Figure 4.3.4 (A) Enzyme-Linked Immunosorbent Assay (ELISA) results of Ab3 antibody induction at a sera dilution of 1/200. Represented as the response against chondroitin sulfate at weeks 4 and 12 (doses 0 and 6, respectively). (B) Comparison of solely the Ab3 response of the P3R99 variants at the sixth dose. n=5 for all groups. Results were analyzed via Parametric T-test (Figure 4.3.4A) and One-way ANOVA (figure 4.3.4B, (not significant)), $P<0.05$. All values are presented as mean ± SEM.

4.3.5 Fasting plasma fat content of obese insulin-resistant JCR:LA-cp rats immunized with P3R99 variants and a negative isotype control hR3

Obese insulin-resistant rats fed the high-fat, high-fructose chow diet immunized with the three P3R99 variants had similar fasting plasma concentrations of Total Cholesterol (TC), High-Density Lipoprotein (HDL), and Triglycerides (TG) compared to hR3 treated rats.

There were no significant differences in the fasting plasma lipid concentrations between P3R99 immunization groups (or hR3) (Figure 4.3.5).

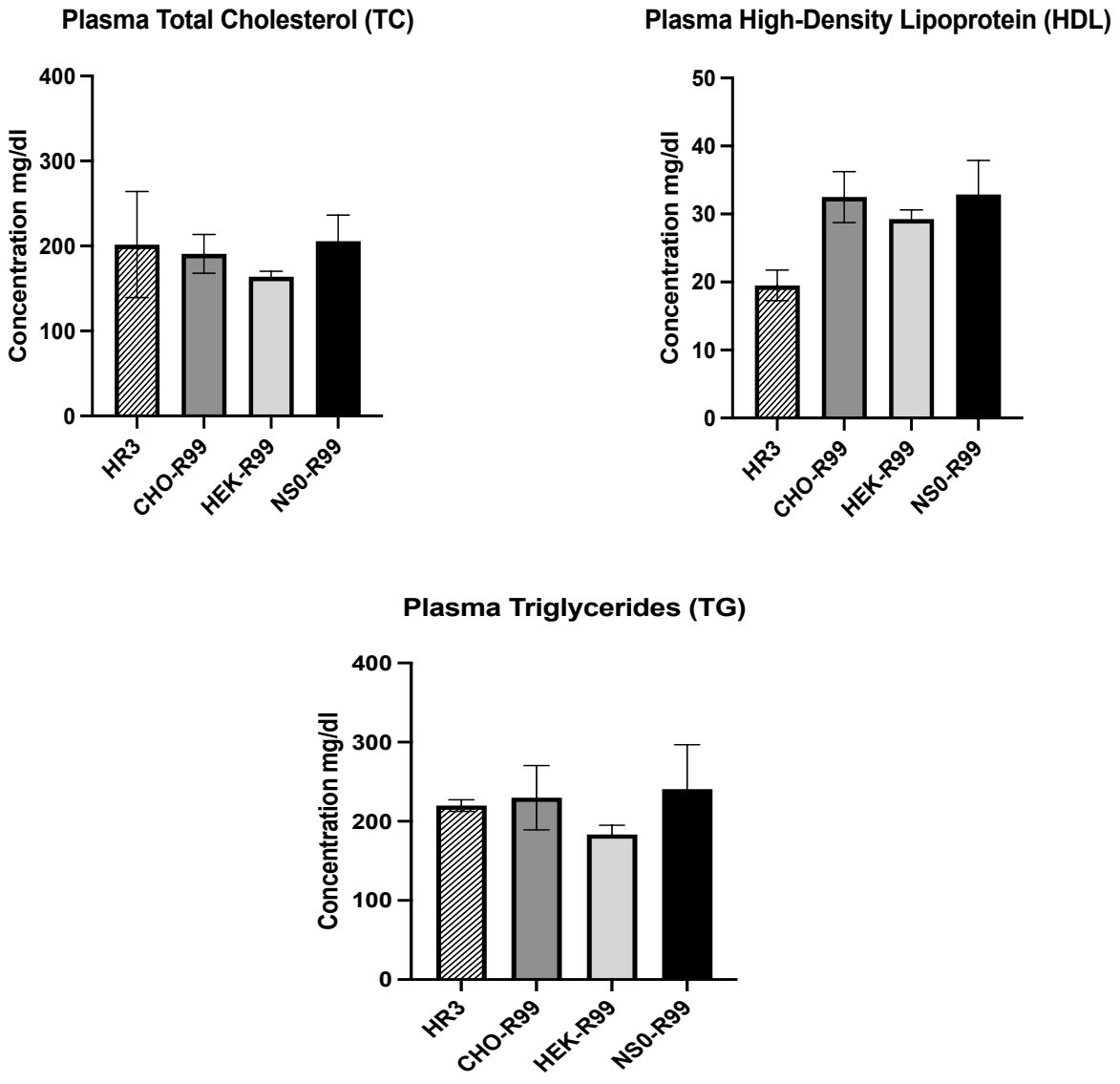

Figure 4.3.5 Comparison of fasting plasma fat content of obese insulin-resistant rats in the four treatment groups at week 12. Encompassing Total Cholesterol (TC), High-Density Lipoprotein (HDL), and Triglycerides (TGs). n=5 for all groups. Results were analyzed via One-way ANOVA, $P>0.05$ (not significant). All values are presented as mean ± SEM.

4.3.6 Fasting insulin, glucose content, and HOMA-IR score of obese insulin-resistant JCR:LA-cp rats immunized with P3R99 variants and a negative isotype control hR3

Obese insulin-resistant rats fed the high-fat, high-fructose chow diet immunized with HEK-P3R99, NS0-P3R99, and CHO-P3R99 had comparable fasting plasma concentrations of glucose and insulin compared to the hR3 control-treated rats.

There were no significant differences in the fasting plasma concentrations of insulin, glucose, or HOMA-IR score between immunization groups (Figure 4.3.6)(Table 4.3).

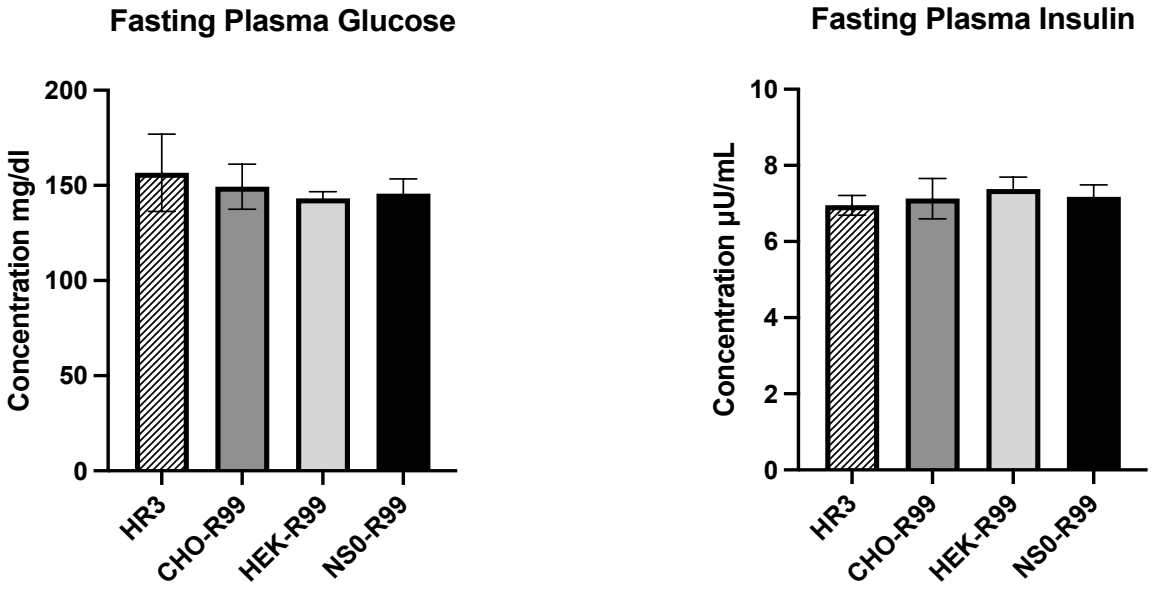

Figure 4.3.6 Comparison of the fasting plasma content of glucose and insulin of the obese insulin-resistant rats in the four treatment groups at week 12. n=5 for all groups. Results were analyzed via parametric T-test and one-way ANOVA, P>0.05 (not significant). All values are presented as mean ± SEM.

Table 4.3 HOMA-IR of P3R99 and hR3 treated obese insulin-resistant JCR:LA-cp rats.

As per Equation 4.1: Calculation of Homeostatic Model Assessment for Insulin Resistance (HOMA-IR) score.

HOMA-IR = (Fasting Insulin (µU/mL) × Fasting Glucose (mmol/L)) / 22.5

Conversion Formulas: mg/dl × 0.0555 = mmol/L

	Fasting Insulin Mean (μU/mL)	Fasting Glucose Mean (mmol/L)	HOMA-IR score
hR3	6.95 μU/mL	156.64 mg/dl x 0.055= 8.62 mmol/L	2.66
CHO-R99	7.13 μU/mL	149.35 mg/dl x 0.055= 8.21 mmol/L	2.60
HEK-R99	7.38 μU/mL	143.14 mg/dl x 0.055= 7.87 mmol/L	2.58
NS0-R99	7.17 μU/mL	145.74 mg/dl x 0.055= 8.02 mmol/L	2.56

4.3.7 Echocardiogram parameters of obese insulin-resistant JCR:LA-cp rats immunized with P3R99 variants and a negative isotype control hR3

Obese insulin-resistant rats fed a high-fat, high-fructose chow diet exhibited similar echocardiographic parameters among the P3R99 treatment groups and the control hR3 treatment group.

No significant differences were found in any echocardiogram values between treatment groups (Figure 4.3.7).

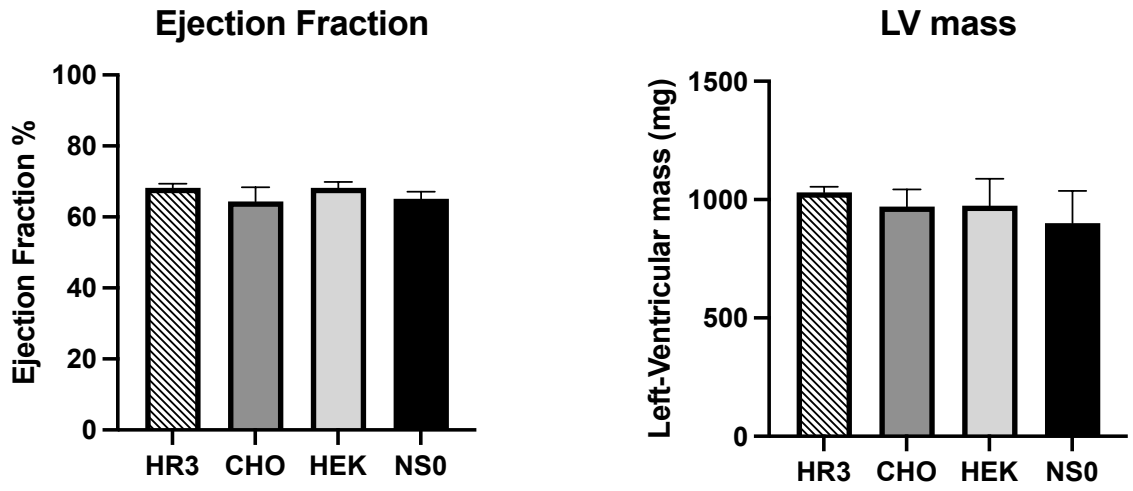

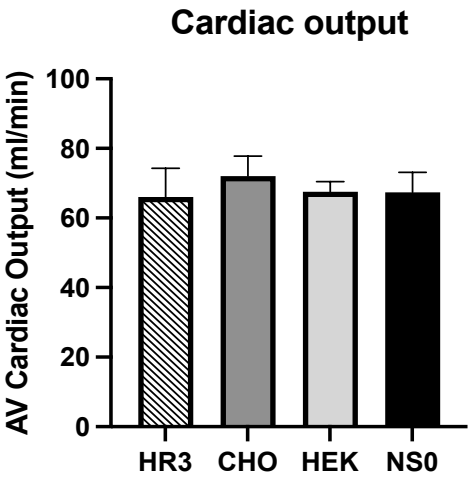
Cardiac output
AV Cardiac Output (ml/min)
100
80
60
40
20
0
HR3
CHO
HEK
NS0

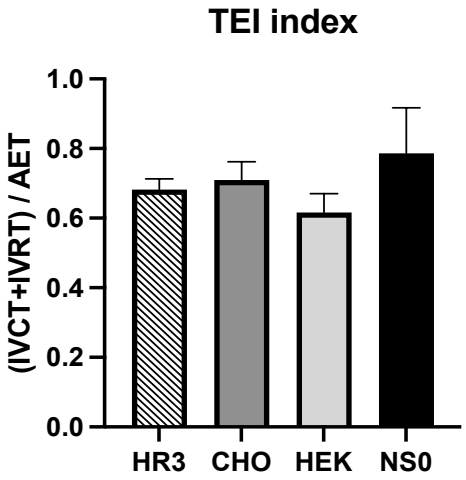
TEI index
(IVCT+IVRT) / AET
1.0
0.8
0.6
0.4
0.2
0.0
HR3
CHO
HEK
NS0

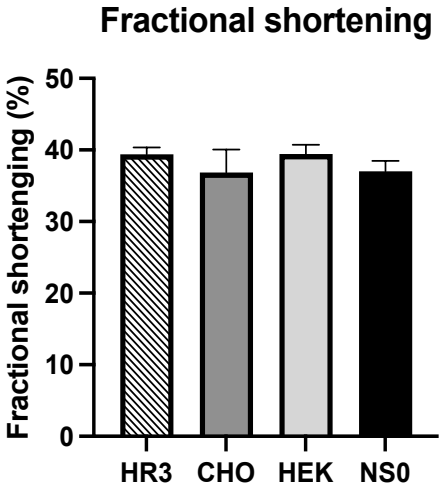
Fractional shortening
Fractional shortenging (%)
50
40
30
20
10
0
HR3
CHO
HEK
NS0

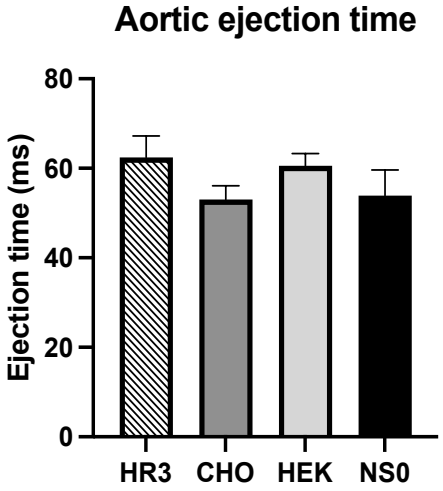
Aortic ejection time
Ejection time (ms)
80
60
40
20
0
HR3
CHO
HEK
NS0

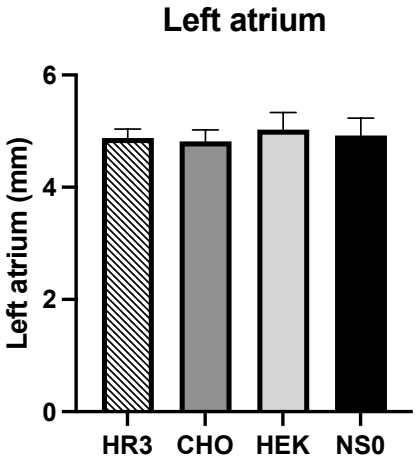
Left atrium
Left atrium (mm)
6
4
2
0
HR3
CHO
HEK
NS0

Figure 4.3.7 Obese insulin-resistant JCR:LA-cp rats echocardiogram parameters prior to termination (week 12). Encompassing: Ejection fraction, Left-Ventricular mass (LV mass), Atrioventricular cardiac output, TEI index (represented as the sum of Isovolumic Contraction Time (IVCT) and Isovolumic Relaxation Time (IVRT) divided by Aortic Ejection Time (AET)), E'/A' ratio (represented by the ratio of the peak velocity blood flow from left ventricular relaxation in early diastole (the E wave) to peak velocity flow in late diastole caused by atrial contraction (the A wave)), Stroke Volume, Fractional shortening, Ejection time, and Left atrium size. n=5 for all groups. Results were analyzed via One-way ANOVA $P>0.05$ (not significant). All values are presented as mean ± SEM.

4.4 Discussion

In this study, we examined the immunogenicity, lipid and carbohydrate metabolism, and cardiovascular function of obese insulin-resistant JCR:LA-cp rats immunized with the three P3R99 production variants, NS0-P3R99, HEK-P3R99, and CHO-P3R99. The findings from this study confirm that the CHO-P3R99 variant (and suggest that the HEK-P3R99 variant) maintains the immunogenic function of the original NS0-P3R99.

Additionally, we found that the P3R99 variants had neutral effects on cardiovascular function and lipid and carbohydrate metabolism, suggesting a lack of adverse effects related to P3R99 administration. This chapter addressed hypotheses 1-3 of Chapter 2.

4.4.1 P3R99 variant administration did not impact weight gain of obese insulin-resistant JCR:LA-cp rats

Obese insulin-resistant JCR:LA-cp rodents given P3R99 had similar weight gain as the hR3 control rats over time (Figure 4.3.1 A, B). These results suggest that P3R99 administration did not affect rodent weight over time.

However, obese insulin-resistant rat hearts were significantly larger than age-matched lean rat hearts (results from a previous study) fed a standard chow diet, indicative of hypertrophy and left-ventricular remodelling (Figure 4.3.2).

4.4.2 CHO, HEK, and NS0-P3R99 variants met the requirement of Ab2 immunogenicity in a model of immune dysfunction with susceptibility to lipid and vascular remodelling: obese insulin-resistant JCR:LA-cp rats

Using our results in the lean JCR:LA-cp rats as a pilot study, we then chose to assess the immunogenicity of the P3R99 variants in a more complex, physiologically compromised animal model. The homozygous JCR:LA-cp rats were chosen due to their pathophysiology of insulin resistance and obesity. Insulin resistance and obesity are top comorbidities of atherosclerosis, and they exhibit many similarities in their pathogenesis, notably dyslipidemia, hypertension, inflammation, and oxidative stress (Beverly & Budoff, 2020)(Nigro et al., 2006)(Syed Ikmal et al., 2013). Moreover, the obese insulin-resistant JCR: LA-cp model is characterized by chronic inflammation and immune dysfunction, including increased pro-inflammatory cytokines (Il-6, Il-2, TNF-α, IFN-γ) and over-stimulation of macrophages and T-cells (Diane et al., 2016). This impaired regulation of the immune system could potentially affect the P3R99's ability to induce an idiotypic cascade through the host's immune system. Thus, this model serves as an important assessment tool to determine possible limitations of the P3R99's immunogenicity. Moreover, we also used an older 9-month-old model, compared to the 3-month-old lean rats, as they would experience middle-age-related effects on health and immune function.

As mentioned in Chapter 3, section 3.4.2, Ab2 antibody induction is considered significant (immunogenic) when there is marked dominance of the anti-idiotypic response relative to the anti-isotypic response (Sarduy et al., 2017). Obese insulin-resistant JCR:LA-cp rats treated with the three P3R99 variants at both the fourth and sixth dose (weeks 8 and 12, respectively) exhibited this idiotypic dominance, thus meeting the requirements of significance of Ab2 antibody induction (Figure 4.3.3A). Moreover, this occurrence was not observed for the control hR3 group.

Furthermore, we also observed a slight increase in the anti-isotypic response at weeks 8 and 12; similarly, the hR3 group demonstrated heightened anti-isotypic responses without an increase in the anti-idiotypic (P3R99 idiotype) response at week 12. This result is consistent with previous NS0-P3R99 immunogenicity studies, as the non-idiotypic region of the P3R99 is immunogenic and is expected to exhibit a slight increase with increased administration of P3R99 (Sarduy et al., 2017).

Lastly, we found no significant differences when comparing the strength of the anti-idiotypic response at week 12 after the sixth dose between the P3R99 variants via One-Way ANOVA

(Figure 4.3.3B). These results were consistent in both lean and obese insulin-resistant rodent models independent of physiological state, suggesting that despite differences in the pathophysiology of the rats, the P3R99s were equally immunogenic.

4.4.3 CHO, HEK, and NS0-P3R99 variants met the requirement of Ab3 immunogenicity in a model of immune dysfunction with susceptibility to lipid and vascular remodelling: obese insulin-resistant JCR:LA-cp rats

As per section 3.4.3 of Chapter 3, Ab3 antibody induction is considered significant (immunogenic) when there is a minimum two-fold increase in recognition of chondroitin sulfate (induction of Ab3 anti-chondroitin sulfate antibodies) from before the first injection (week 4) to the final dose (week 12).

However, in contrast to our results in the lean JCR:LA-cp rats, only CHO-P3R99 and NS0-P3R99 treated obese insulin-resistant JCR:LA-cp rats met this requirement from the pre-immune state (week 4) to the sixth dose (week 12) (Figure 4.3.4A), while the HEK-P3R99 and hR3 treated rats did not. Despite the significant induction of anti-idiotypic antibodies in the HEK-P3R99 treated rats (Figure 4.3.3A), we were unable to detect a significant 2-fold increase in Ab3 antibodies in the rodents' sera at weeks 8 or 12 (following the 4^{th} or 6^{th} dose). As mentioned in section 3.4.4 of Chapter 3, Ab2 antibody induction is necessary for Ab3 induction and consistently precedes Ab3 induction, although this process is not well understood. As such, our results, which demonstrate a strong Ab2 response and a lack of an Ab3 response in the HEK-P3R99 treated rats, are intriguing. However, results from an unpublished study in rabbits immunized with the original NS0-P3R99 reported similar findings and successfully attributed this occurrence to the Ab3 antibodies accumulating in areas of atherosclerotic remodelling. While the group was unable to detect Ab3 antibodies in the rabbits' sera, upon assessing aortic homogenates via immunohistochemistry, they found a significant accumulation of Ab3 antibodies. This is due to the unique feature of the P3R99 to preferentially bind to areas prone to atherosclerosis, such as the aortic arch (Brito et al., 2012)(Delgado-Roche et al., 2013)(Soto et al., 2014).

An additional possibility is that these Ab3 antibodies are bound to the Ab2 produced by the immune system. As Ab2 antibody production by the immune system is typically stronger than Ab3 production, it is possible that an excessive Ab2 response results in the free Ab2 binding to Ab3 forming immune complexes. This antibody-antibody (protein-protein) interaction has a stronger

binding affinity than the antibody-carbohydrate interaction (Haji-Ghassemi et al., 2015) of the Ab3 binding to chondroitin sulfate (Figure 4.4.1). However, as this result was only present in the HEK-P3R99 treatment group, the immunogenicity of the variants in the obese insulin-resistant JCR:LA-cp rat model requires further testing to make definitive conclusions. Additionally, the variants will require validation using other animal models, particularly those with a similar physiological makeup to humans, as well as models of cardiovascular disease.

Lastly, when comparing the induction of Ab3 antibodies at the sixth dose by the three P3R99 variants via One-way ANOVA, we found no significant differences (Figure 4.3.4B). These results suggest that the CHO-P3R99 and HEK-P3R99 variants are similarly immunogenic as the NS0-P3R99 in the obese insulin-resistant JCR:LA-cp rats, despite the HEK-P3R99 not meeting the criteria for Ab3 immunogenicity.

Figure 4.4.1 Illustration of the primary factors that influence the levels and detection of Ab3 antibodies in sera. Ab3 antibodies have a higher binding affinity to Ab2 antibodies than to chondroitin sulfate due to Ab2-Ab3 acting as an antibody-antibody bond compared to Ab3-chondroitin sulfate acting as an antibody-carbohydrate bond. Additionally, the P3R99 has the ability to preferentially accumulate in areas of atherosclerotic remodelling, such as aortic and carotid lesions. Created with BioRender.

4.4.4 P3R99 variants had neutral effects on lipid and carbohydrate metabolism in obese insulin-resistant JCR:LA-cp rats. HOMA-IR confirmed the presence of insulin resistance regardless of treatment group

Glycosaminoglycans (GAGs), including chondroitin sulfate, are a complex group of linear polysaccharides covalently attached to proteoglycans that play critical roles in various biological processes (Wang et al., 2022). GAGs are involved in cell communication, immune responses, cellular integrity, nervous system development, cell adhesion, motility, tissue homeostasis, and lipid metabolism, among other key roles (Wang et al., 2022)(Staprans & Felts, 1985). Hepatic clearance of triglyceride-rich lipoprotein remnants has been well-documented to rely on the transmembrane heparan sulfate proteoglycan syndecan 1. Similarly, chondroitin sulfate GAGs have been shown to interact with Insulin-like Growth Factor Binding Proteins (IGFBPs), including IGFBP-3 (Fowlkes & Serra, 1996) and IGFBP-5 (Arai et al., 1994), which mediate the bioavailability and activity of Insulin-like Growth Factor (IGF). Moreover, chondroitin sulfate has also been reported to bind to Lipoprotein Lipase (LPL), the enzyme involved in the hydrolysis of triglycerides from circulating lipoproteins (Bengtsson et al., 1980).

As demonstrated in Figure 2.1 of Chapter 2, the P3R99 variants, like the original NS0-P3R99, can recognize and bind chondroitin sulfate with high specificity. However, due to the implication of chondroitin sulfate and other sulfated GAGs in carbohydrate and lipid metabolism, this raises important questions about the potential adverse effects of the P3R99 variants.

Nonetheless, a previous study in 2017 by Brito et al. demonstrated the neutral effect of NS0-P3R99 on lipid metabolism using ApoE-/- mice fed a high-fat, high-cholesterol diet until 19 weeks of age. A biochemical assessment of plasma cholesterol confirmed that P3R99 administration did not alter lipid metabolism (Brito et al., 2017).

As a result, our study was interested in determining whether the P3R99 variants maintained this negligible effect on lipid and carbohydrate metabolism of the original NS0-P3R99 in the obese insulin-resistant JCR:LA-cp rats. Using commercially available kits, we found that the three P3R99 variants had neutral effects on overall lipid and carbohydrate metabolism in the obese insulin-resistant JCR:LA-cp rats fed a high-fat, high-fructose chow diet for 12 weeks. Comparing the results obtained from biochemical assays measuring plasma concentrations of major lipid markers, HDL, TG, and TC, we found no significant differences between the values for the three P3R99 variants and the hR3 control-treated rats (Figure 4.3.5).

This trend was maintained for glucose and insulin concentrations (Figure 4.3.6). Additionally, there were no significant differences in the plasma lipid and glucose concentrations between the P3R99 treated rats, confirming that the CHO-P3R99 and HEK-P3R99 have similar effects on lipid and carbohydrate metabolism as the NS0-P3R99. These results serve as a key safety assessment of the P3R99 variants.

Additionally, the Homeostasis Model Assessment Of Insulin Resistance (HOMA-IR) of the three P3R99-treated rats and hR3 control-treated rats confirmed that the obese insulin-resistant JCR:LA-cp rats had moderate insulin resistance following the 12-week high-fat, high-fructose chow diet. HOMA-IR is a widely used assessment tool for insulin sensitivity developed in 1985 by Matthews et al. (Son et al., 2022)(Matthews et al., 1985). A HOMA-IR score of >1 is optimal for insulin sensitivity, >1.9 indicates early insulin resistance, >2.5 indicates moderate insulin resistance, and >2.9 indicates severe insulin resistance (Gutch et al., 2015). As per Table 4.3.6, all of the obese insulin-resistant JCR:LA-cp, regardless of treatment group rats, had a score of >2.5, indicating moderate insulin resistance.

4.4.5 P3R99 variants had neutral effects on cardiovascular function in obese insulin-resistant JCR:LA-cp rats

As mentioned in section 4.4.4, GAGs are diverse polysaccharides that are implicated in various cellular and biological processes. A major feature of GAGs is their role in wound healing through the regulation of the organization, structure, and integrity of the Extracellular Matrix (ECM) (Yang et al., 2023). GAGs are also major constituents in aortic heart valves due to their structural roles (Krishnamurthy & Grande-Allen, 2018). Chondroitin sulfate GAGs specifically are critical components of connective tissue present throughout the body. Histology reports of the heart have revealed the significant composition of cardiomyocytes and connective tissue (Arackal & Alsayouri 2023). Dysregulation of chondroitin sulfate metabolism or ECM composition could have significant implications on cardiovascular function.

Due to the ability of the P3R99 variants to bind chondroitin sulfate (Figure 2.1 of Chapter 2), the effect on cardiovascular function needed to be assessed in a model with susceptibility to vascular remodelling. The obese insulin-resistant JCR:LA-cp rats have been shown to act as a model of spontaneous Left Ventricular (LV) dysfunction. As a result, we conducted an Echocardiogram (ECHO) of the P3R99-treated and hR3-control-treated obese insulin-resistant JCR:LA-cp rats after

the sixth dose to determine possible adverse effects related to vascular function. ECHO results of the obese insulin-resistant JCR:LA-cp rats treated with the three P3R99 variants had similar cardiovascular outcomes as the hR3 treated rats. Among the cardiovascular parameters measured, no significant differences existed between the hR3 treated rats, and P3R99 treated rats, suggesting that P3R99 administration did not adversely affect cardiovascular function (Figure 4.3.7). Additionally, from these results, we can concur that the obese insulin-resistant JCR:LA-cp rats did not experience significant cardiac hypertrophy or cardiac dysfunction despite their pathology of obesity and insulin resistance. Values were in the normal range for major cardiovascular outcomes, including ejection fraction (normal range 53-73%), fractional shortening (normal range 26-45%), and cardiac output (normal range 48-131ml/min) (Lang et al., 2015)(ASE guidelines, 2018)(Tissot et al., 2018)(Bezank, 1958)(Darbandi et al., 2014).

In contrast to humans, rodents are generally resistant to atherosclerosis (Zhao et al., 2020) due to differences in lipid metabolism and overall physiology (Ritskes-Hoitinga & Beynen, 1988). As such, a crucial next step could include assessing the cardiovascular outcomes associated with P3R99 administration in a model more suited for atherosclerosis and CVD onset.

However, ECHO results confirmed the presence of spontaneous LV dysfunction. A TEI index of >0.45 indicates the presence of LV dysfunction (Tao et al., 2008); all obese insulin-resistant JCR:LA-cp rats had a reported TEI index of ~0.6.

Additionally, LV dysfunction was confirmed by their increased overall heart weight compared to lean age-matched controls (Figure 4.3.2).

These results provided a pivotal safety assessment of the P3R99 variants, confirming that the CHO-P3R99 and HEK-P3R99s, like the original NS0-P3R99, do not adversely affect lipid or glucose metabolism or cardiovascular function.

4.5 Conclusions

To summarize, the results presented in this chapter suggest that the CHO-P3R99 variant maintains the immunogenicity of the NS0-P3R99 in the obese insulin-resistant JCR:LA-cp rats. Furthermore, both HEK-P3R99 and CHO-P3R99 variants exhibited immunogenic strength similar to the NS0-P3R99 in terms of Ab2 and Ab3 induction magnitude.

However, results in HEK-P3R99 treated obese insulin-resistant JCR:LA-cp rats were inconsistent due to issues with the Ab3 antibody response, thus requiring further testing in models of immune

dysfunction and cardiovascular disease. Moreover, the P3R99 variants did not alter lipid metabolism, carbohydrate metabolism, or cardiovascular function in the obese insulin-resistant JCR:LA-cp rats.

Finally, while we were able to confirm the presence of left ventricular dysfunction and insulin resistance in the rats regardless of their treatment group, we did not observe any changes from P3R99 treatment.

CHAPTER 5: IMMUNOGENICITY STUDY OF P3R99 VARIANTS IN A HEALTHY LARGE ANIMAL MODEL: WHITE-LANDRACE PIGLETS

Gala Araujo [1,2], Agata Martin-Ozimek [1,2], Kun Wang [1,2], Yosdel Soto [2,4] , Spencer Proctor [2,3]*

[1] Division of Human Nutrition, Department of Agricultural, Food and Nutritional Science.
[2] Metabolic and Cardiovascular Diseases Laboratory, Department of Agricultural, Food and Nutritional Science, and/or 3 Division of Animal Science, Department of Agricultural, Food and Nutritional Science, University of Alberta, Edmonton, Alberta, Canada.
[3] Division of Immunobiology, Centre of Molecular Immunology, Havana 11600, Cuba; yosdel@cim.sld.cu
* Correspondence: proctor@ualberta.ca

5.1 Introduction

Findings from this thesis have provided evidence of the maintained immunogenic function of the NS0-P3R99 in the HEK-P3R99 and CHO-P3R99 variants using rodent pre-clinical animal models. The use of animal models in Atherosclerotic Cardiovascular Disease (ASCVD) research has significantly advanced the field and substantially contributed to breakthroughs in translational endeavours (Schüttler et al., 2022 (Zaragoza et al., 2010)(Getz & Reardon, 2012). Although there is no standard animal model of atherosclerosis, swine are fundamental assets in ASCVD research due to their extensive history as pre-clinical models of atherosclerosis (Zaragoza et al., 2010). Pigs are considered a more relevant and translational model for pre-clinical studies due to their physiological similarities to humans (Tsang et al., 2016). Specifically, similarities in their cardiovascular anatomy, metabolism and signalling pathways, immune systems, and hemodynamics (Tsang et al., 2016)(Walters & Prather, 2013). While small animal models like rodents are extensively used in translational research and have provided valuable insights regarding the pathophysiology of atherosclerosis, they have some inherent limitations. Rodents do not naturally develop atherosclerosis (Zhao et al., 2020) and typically require expensive specialized transgenic or knockout models (Zaragoza et al., 2010). Moreover, their short life span can severely challenge studies interested in assessing the long-term effects of a specific therapy. Additionally, studies related to immunotherapies, like the P3R99 mAb, can encounter issues related to the vast differences in the immune responses and lipid metabolism of rodents in

comparison to humans. As such, when progressing to the clinical stage of therapeutic development, the use of pigs as pre-clinical models is invaluable.

Therefore, in order to ensure the safe and effective use of the P3R99 variants in humans, it is necessary to re-evaluate the variants using a larger and more complex animal such as swine. Using our rodent results from Chapters 3 and 4 as preliminary data, we aim to confirm these results in a swine model. Thus, the objective of this study is to assess the immunogenicity of the P3R99 variants and determine if they maintained the immunogenic strength of the NS0-P3R99 in white-landrace piglets. By using piglets, we hope to bridge the gap between our results in small animal models and future clinical trials, as well as provide insight into the limitations and strengths of the variants in complex species similar to humans. This approach ensures the safety and efficacy of the variants prior to advancing to human trials.

To achieve this goal, we designed an immunogenicity study for the white-landrace piglets similar to our lean JCR:LA-cp rats. However, we administered only 5 weekly doses of 3 mL at 1 mg of each respective antibody (0.33nmg/mL), compared to 6 doses of 200 μg for both the obese insulin-resistant and lean JCR:LA-cp rats (400 μg/mL).

We hypothesized that the P3R99 variants would maintain the immunogenic function and strength of the original NS0-P3R99 in the white-landrace piglets. We maintained the same criteria for assessing the immunogenicity of Ab2 and Ab3 antibody induction that was used in the lean and obese insulin-resistant JCR:LA-cp rats.

Results from this chapter confirmed the maintained immunogenicity and immunogenic strength of the NS0-P3R99 in the CHO and HEK-P3R99 variants using a large animal model.

5.2 Methods

5.2.1 Animal housing and treatment protocol

Pigs were attained from the bio-secure Swine Research and Technology Center (SRTC) at the University of Alberta in Edmonton, Alberta, Canada. All piglets were produced by breeding a duroc boar and a large white-landrace sow. SRTC staff provided and were responsible for the maintenance of proper living conditions, specifically water, food, temperature, hygiene, and medical care. Animals were kept in pens of 5 depending on their treatment group. Additionally, each of the five piglets came from distinct sows to minimize littermates within the same treatment group and increase genetic variation. Prior to immunizations, one piglet suddenly died and was

removed and replaced from the study. All procedures adhered to the guidelines provided by the Canada Council on Animal Care (CCAC) and were approved by the University of Alberta's Animal Ethics Committee (pig protocol: AUP002321).

5.2.2 Monoclonal antibody preparation

Refer to Chapter 3, section 3.2.1.

5.2.3 Study design lean white-landrace piglets

Twenty young (3-week-old), lean, male white-landrace piglets were fed a standard pre-grower chow diet after weaning until they reached 15 kg (Table 5.1). They were then switched to a normal hog chow diet. Piglets received five subcutaneous (s.c.) immunizations of 0.33 mg/mL of either NS0-P3R99 mAb (positive control), HEK-P3R99 mAb (variant), CHO-P3R99 mAb (variant) or hR3 mAb (negative control) (n=5 animals per group) at weekly intervals (1 injection per week) over a five-week period (Figure 5.1). Immunizations were given as one injection of 3mL at a concentration of 0.33 mg/mL (total dose was 1 mg). Piglets were weighed weekly by SRTC staff to monitor food intake and had venous blood (sera and plasma) (~3 mL) drawn at the start of the study prior to the first antibody immunization (Pre-immune, PI) and 7 days after the third, fourth, and fifth immunizations. Plasma was collected in purple top BD Vacutainer® Plasma Preparation Tubes (PPT™) containing Ethylenediaminetetraacetic Acid (EDTA) to prevent coagulation, and sera was collected in red top BD Vacutainer® Blood Collection Tubes. Following 5 injections at 2 months of age, piglets were terminated via a captive bolt pistol. Following termination, piglets were cleaned with 70% ethyl alcohol (EtOH), and various tissues were collected, including the right kidney, liver, spleen, muscle, cartilage, aorta, and heart (Table 5.2).

Table 5.1 Ingredients of pre-grow chow diet used for piglets. University of Alberta hog pre-grow non-medicated pellets REF #52852.

Chemical Composition	**Quantity**
Wheat ground, %	35.838
Wheat Mill Run, %	15.0
Distillers Corn %	15.0
Soybean Meal %	12.40
Peas Ground %	7.50
Canola Meal %	5.50
Extrapro %	3.50
Limestone, glass %	1.922
Fat %	1.80
L-Lysine %	0.440
Salt %	0.390
UF FORT%	0.250
Threonine-L %	0.150
MHA %	0.115
Water %	0.080
Copper Sulfate %	0.040
Choline %	0.040
Superzyme %	0.020
Ethoxyquin %	0.015
Nutrients	
Dry Matter, %	89.484
Crude Fat, %	5.440
Crude Fibre, %	5.406
Crude Protein, %	21.496
Lysine, %	1.299
Avail Lysin, %	1.079
Methionine, %	0.428
Methionine & Cystine, %	0.840
Tryptophan, %	0.251
Avail Tryptophan, %	0.186
Calcium, %	0.940
Phosphate Total, %	0.657

Avail Phosphate, %	0.357
Sodium, %	0.199
Chlorine, %	0.37
Salt, %	0.494
Manganese Total, %	80.397 MG
Zinc Total, %	181.60 MG
Iron Total, %	232.95 MG
Copper Total, %	124.9 MG
Selenium, %	0.314 MG
Vitamin A, %	8.000 KIU
Vitamin D, %	1.250 KIU
Vitamin E, %	0.053 KIU
Choline Total, %	2,047.09 MG
Folic Acid, %	1.383 MG
Biotin, %	0.416 MG
Manganese Added,	40.032 MG
Zinc Added,	130.00 MG
Iron Added,	150.12 MG
Copper Added,	115.00 MG
Thiamin Added,	1.250 MG
Riboflavin Added,	6.663 MG
Niacin Added,	37.500 MG
Pyridoxine Added,	1.663 MG
Pantothenate Added,	20.850 MG
Choline Added,	243.00 MG
Vitamin B12 Added,	0.025 MG
Folic Acid Added,	0.0625 MG
Biotin Added,	0.125 MG

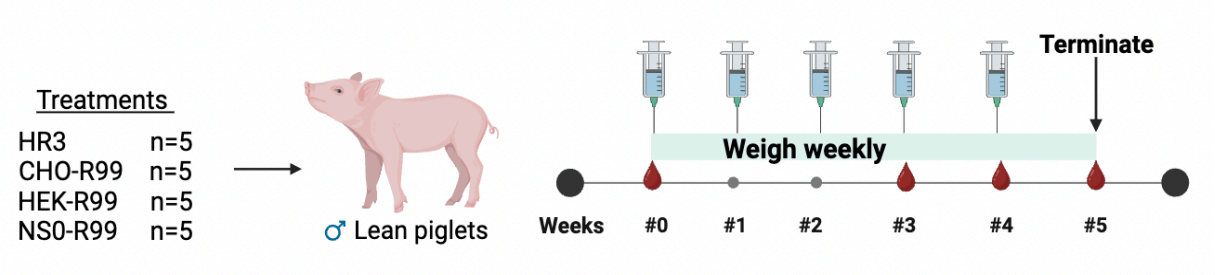

Figure 5.1 Study design for the male white-landrace piglets. The piglets received 5 weekly doses of one injection of 3 mL of 0.33 mg/mL (total 1 mg). Blood draws were done at weeks 0,3,4 and 5. Week 0 represents the pre-immune sera (before the first injection), while weeks 3,4 and 5 represent doses 3,4 and 5. n=5 for all treatment groups. Created with BioRender.

Table 5.2 Study design and planned assessments for the male white-landrace piglets.

Study design				**Planned Assessments**		
Animal model	**Duration**	**Blood draws**	**Doses**	**Ab2, Kinetics**	**Ab3, Kinetics**	**Additional**
Male White-Landrace Piglets - 3 weeks old - Pre-grower and standard chow diet	5 Weeks.	4 blood draws at weeks 0,3,4, and 5	One injection of 3mL of 0.33mg/mL. Total 1mg	Ab2 assessment planned (minimum at final dose) Kinetics not planned.	Ab3 assessment planned (minimum at W0 and after the fourth or final dose) Kinetics not planned.	(1) Weight gain over time.

5.2.4 Plasma and sera preparation

Sera and plasma samples were centrifuged at 7000 rpm (radius 17.8 cm) for 10 minutes at 4°C; the supernatant (~1 mL) was then collected via micropipette and stored in 1.5 mL Eppendorf tubes at -80°C for immunogenicity testing via ELISA. The remaining pellet and pipette tips were discarded in biohazard bins. Due to ethical considerations, piglets only underwent four blood draws at weeks 0,3,4, and 5.

5.2.5 Sample collection and processing

Tissue samples collected were flushed with ice-cold sterile PBS (phosphate buffered saline, pH 7.4) and minced into small portions, except for the heart, which was kept whole. Tissues were

packaged in labelled tin foil and snap-frozen in liquid nitrogen before being stored in a -80℃ freezer.

5.2.6 Enzyme-Linked Immunosorbent Assay (ELISA) for Ab2 recognition

Methods were the same as discussed in Chapter 3, section 3.2.6. However, pre-immune sera and final dose (fifth injection) sera were assessed for the pigs. Moreover, sera was pre-adsorbed with a negative isotype control to minimize cross-reactivity (see discussion). Briefly, the sera was incubated for one hour and 30 minutes at 25℃ with a negative isotype control at half the concentration of the sera (double the sera dilution factor). Following pre-adsorption sera was then added to the ELISA plate, and the protocol continued as per section 3.2.6.

Additionally, we used a pre-adsorbed goat anti-porcine IgG (H+L) secondary antibody conjugated to HRP (Novus Biologicals REF: NB750). This pre-adsorbed antibody was selected to minimize cross-reactivity with the human IgG.

5.2.7 Enzyme-Linked Immunosorbent Assay (ELISA) for Ab3 recognition

Methods were the same as discussed in Chapter 3, section 3.2.7. However, pre-immune sera and final dose (fifth injection) sera were assessed for the pigs.

Additionally, we used a pre-adsorbed goat anti-porcine IgG (H+L) secondary antibody conjugated to HRP (Novus Biologicals REF: NB750).

5.2.8 Data and statistical analysis

Refer to Section 3.2.8 of Chapter 3.

5.3 Results

5.3.1 White-landrace piglet weight gain

All piglets exhibited normal weight gain regardless of the treatment group. No significant differences were found in the weight gain pattern or final body weight of the pigs among the 4 treatment groups from Weaning (Wn) to W5 (Figure 5.3.1).

A. Piglet weight over time during immunizations.

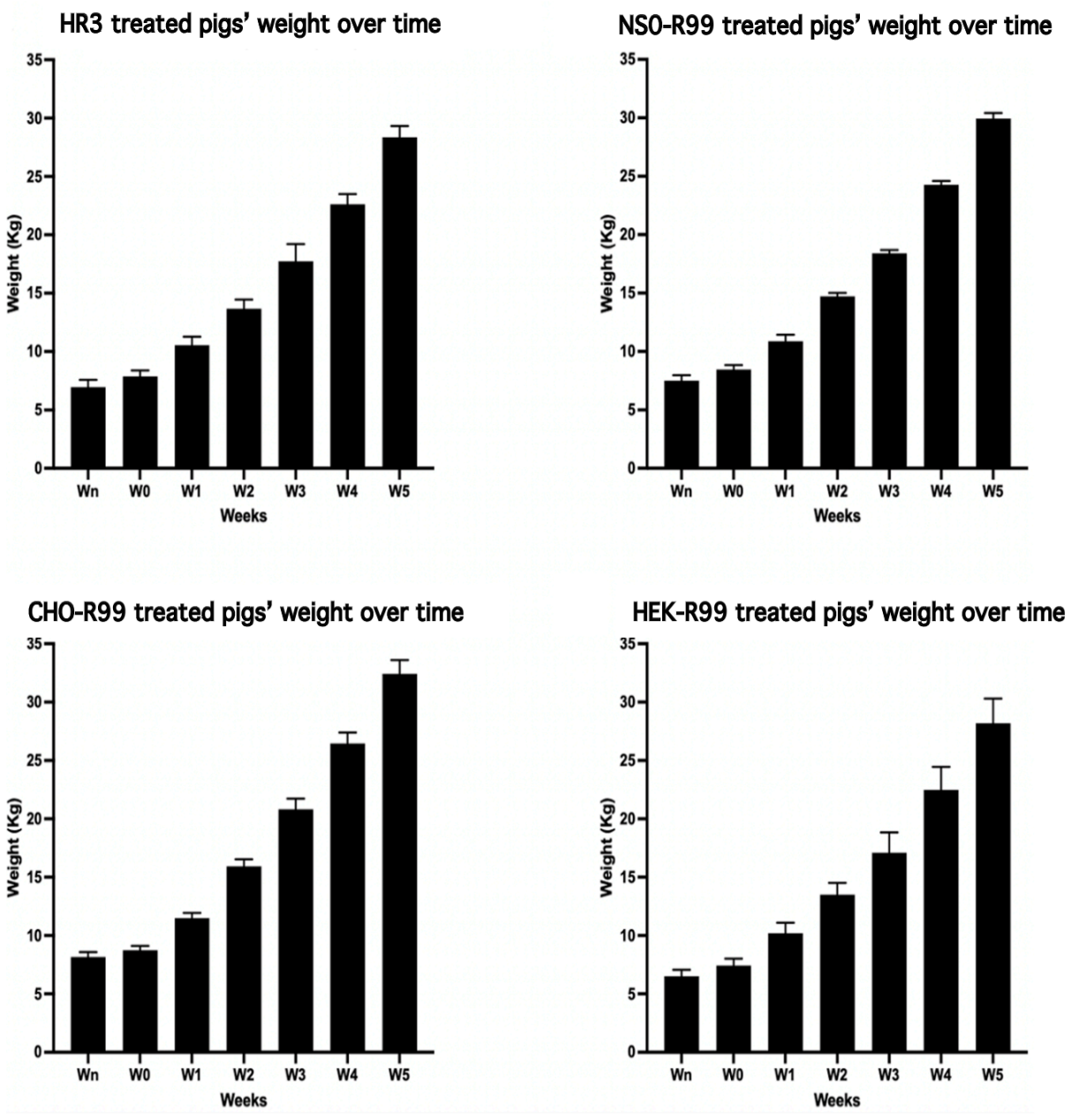

B. Comparison of piglet weight gain during immunizations.

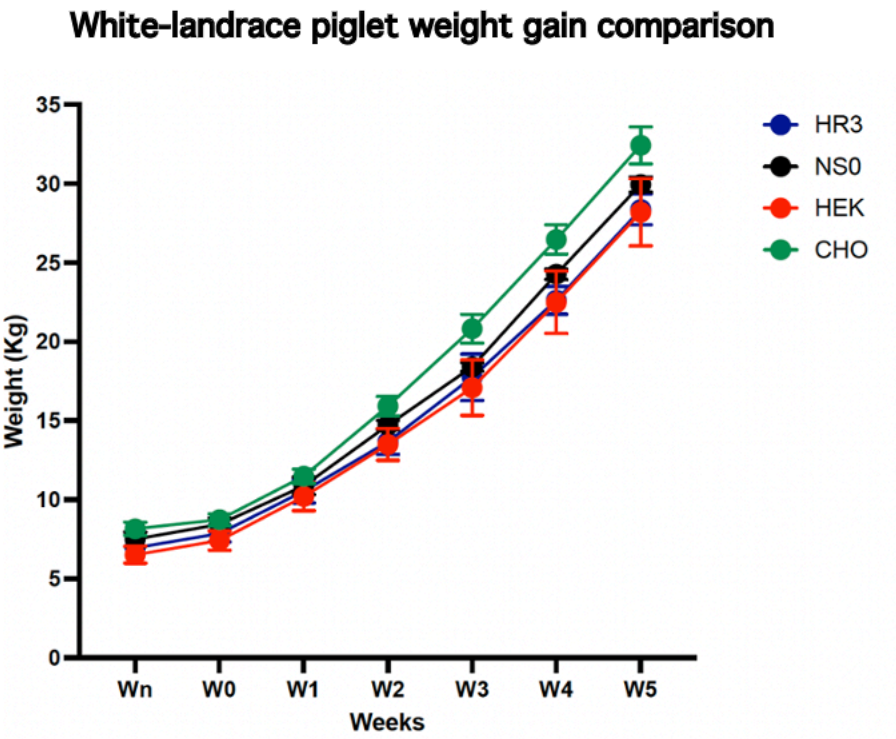

Figure 5.3.1 (A) Weight of the white-landrace piglets in the four treatment groups. n=5 for all groups. Weeks (weaning) - week 5. (B) Comparison of piglet weight represented as kinetics from weaning to W5. n=5 for all groups. Analyzed via One-way ANOVA, P>0.05 (not significant). All values are presented as mean ± SEM.

5.3.2 Ab2 response of white-landrace piglets immunized with P3R99 variants and a negative isotype control hR3

Sera taken from piglets immunized with the three P3R99 variants exhibited a significant increase in the recognition for the idiotypic region of P3R99 from W0 to W5.

As expected, the control hR3 treated piglets did not induce significant levels of anti-idiotypic (P3R99 idiotype) antibodies at any point in time. (Figure 5.3.2A).

Additionally, there were significant differences in the induction of anti-idiotypic antibodies relative to anti-isotypic antibodies for the three P3R99 treatment groups.

Lastly, differences were found in the induction of an anti-idiotypic response at the final (fifth) dose between the HEK-P3R99 and NS0-P3R99 (Figure 5.3.2B).

A. Ab2 response in white-landrace piglets immunized with the P3R99 variants at the fifth dose (week 5).

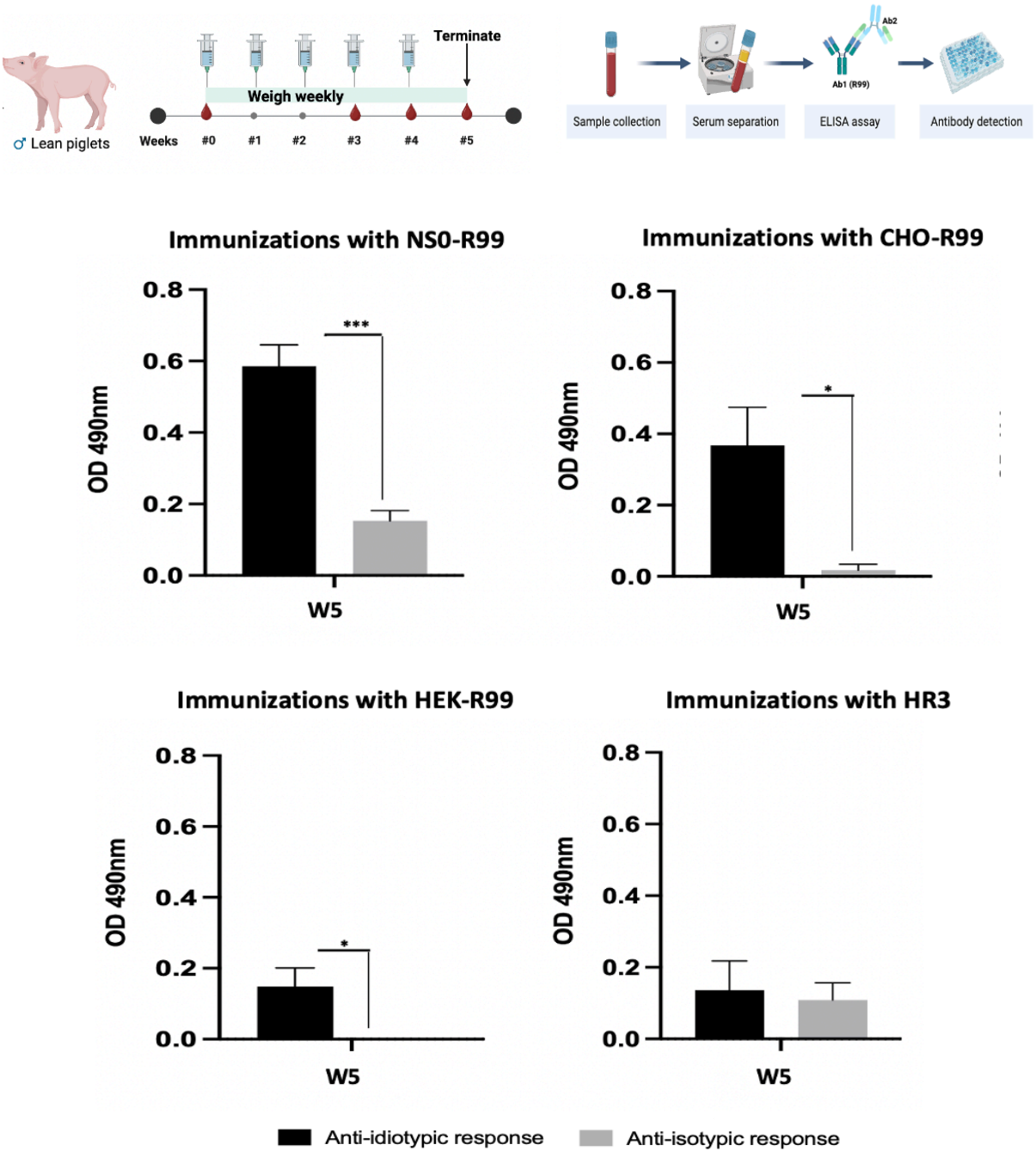

B. Comparison of the anti-idiotypic response induced by the P3R99 variants in white-landrace piglets.

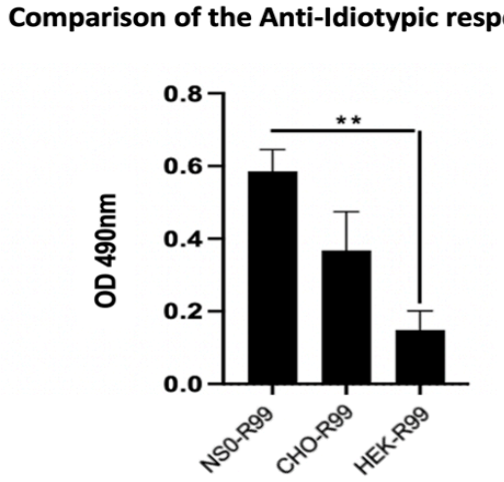

Figure 5.3.2 (A) Enzyme-Linked Immunosorbent Assay (ELISA) results of Ab2 antibody induction at a sera dilution of 1/1000. Represented as the response against the idiotype of P3R99 (anti-idiotypic response) vs the response against the non-idiotype regions of P3R99 (anti-isotypic response). (B) Comparison of solely the anti-idiotypic response of the P3R99 variants at the fifth dose (week 5). n=5 for all groups. Analyzed via parametric T-test (Figure 5.3.2A) and One-way ANOVA (figure 5.3.2B, (not significant)). * = P<0.05, ** = P<0.01, *** = P<0.001, **** = P< 0.0001. All values are presented as mean ± SEM.

5.3.3 Ab3 response of white-landrace piglets immunized with P3R99 variants and a negative isotype control hR3

Sera taken from piglets immunized with the P3R99 variants exhibited a minimum two-fold increase in the recognition of chondroitin sulfate from before the first immunization (pre-immune) to the fifth dose, while the hR3 treated piglets did not (Figure 5.3.3A).

No significant differences were found in the induction of anti-chondroitin sulfate antibodies at the final (fifth) dose among the three P3R99 treatment groups (Figure 5.3.3B).

A. Ab3 response in white-landrace piglets immunized with the P3R99 variants before the first immunization and after the fifth dose.

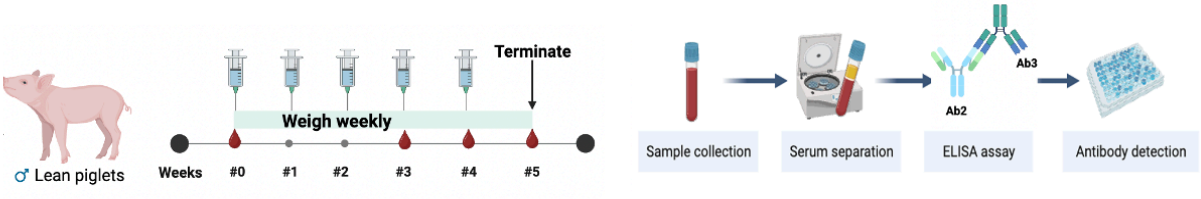

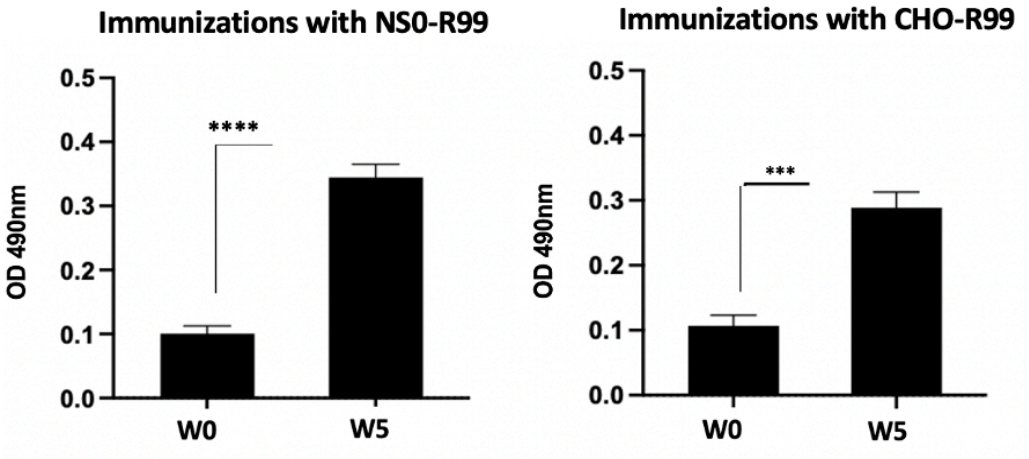

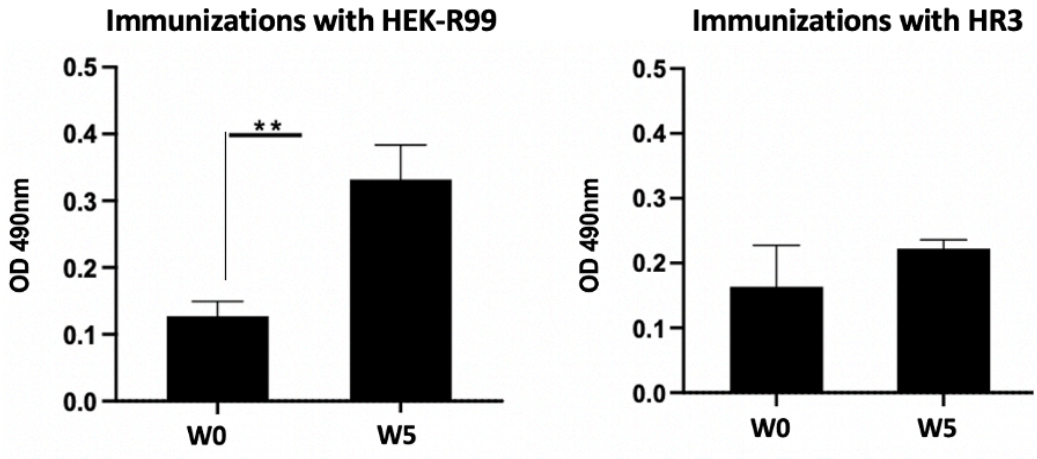

B. Comparison of the Ab3 response induced by the P3R99 variants in white-landrace piglets at the fifth dose.

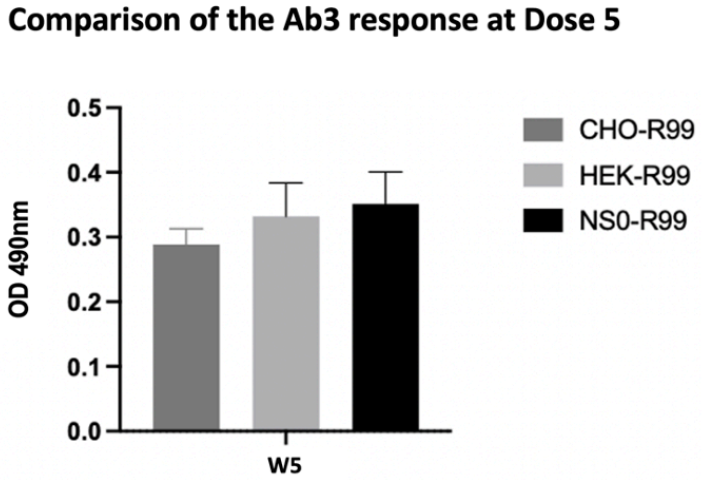

Figure 5.3.3 (A) Enzyme-Linked Immunosorbent Assay (ELISA) results of Ab3 antibody induction at a sera dilution of 1/500. Represented as the response against chondroitin sulfate before the first immunization (week 0) and at the fifth dose (week 5). (B) Comparison of solely the Ab3 response of the P3R99 variants at the fifth dose (W5). n=5 for all groups. Analyzed via parametric T-test (Figure 5.3.3A) and One-way ANOVA (figure 5.3.3B, (not significant)). * = $P<0.05$, ** = $P<0.01$, *** = $P<0.001$, **** = $P< 0.0001$. All values are presented as mean ± SEM.

5.4 Discussion

In this study, we examined the immunogenicity of the P3R99 production variants (NS0-P3R99, HEK-P3R99, and CHO-P3R99) vs a negative isotype control hR3 in healthy young white-landrace piglets. From our findings, we can conclude that the P3R99 variants maintained the immunogenicity of the original NS0-P3R99 in piglets.

However, when comparing the immunogenic strength of the variants relative to the NS0-P3R99, we found significant differences in the production of anti-idiotypic (Ab2) antibodies between the HEK-P3R99 and NS0-P3R99. Interestingly, this pattern was not observed for the induction of anti-anti-idiotypic (Ab3) antibodies.

5.4.1 P3R99 variant administration did not impact weight gain of white-landrace piglets

Similar to our results from Chapters 3 and 4, piglets that received P3R99 had weight gain similar to the hR3 control-treated piglets. The final weight of the piglets was similar regardless of the treatment group. From these results, we can conclude that the P3R99 variants did not affect the weight of the piglets.

5.4.2 CHO, HEK, and NS0-P3R99 variants met the requirement of Ab2 immunogenicity in a healthy large animal model: 3-week-old white-landrace piglets

In Chapters 3 and 4, we confirmed the immunogenicity of the HEK-P3R99 and CHO-P3R99 compared to the NS0-P3R99 using small animal models of different physiological states. However, we needed to additionally assess the immunogenicity of the variants in a larger and more complex animal model prior to advancing to human trials. Using a young, healthy piglet model, we detected significant levels of anti-idiotypic antibodies (Ab2) by all three P3R99 variants at the final (fifth) dose (Figure 5.3.2A).

As mentioned in Chapter 3, section 3.4.2, we assess the significance of an Ab2 response through the presence of dominance of the idiotype relative to the non-idiotype regions of the P3R99. Typically, the majority of Ab2 antibodies produced are anti-idiotypic, while a minority are anti-isotypic, which represents the non-idiotype regions. In the piglets at the fifth dose, as expected, we detected dominance of the idiotype via statistically significant differences between the anti-idiotypic response and anti-isotypic response.

However, unlike our rodent results, for the piglets, we chose to share the Ab2 results at just the final dose (W5) due to issues with our pre-immune response (see Figure 5.4.1)(Figure 5.3.2A). It is important to note that the piglets exhibited a high sera reactivity across all groups, including the negative isotype control hR3, prior to the start of immunizations (pre-immune, W0) and took longer to respond to treatment than the rats. As a result, for these ELISAs it was necessary to pre-adsorb both the pre-immune and post-immune sera with a negative isotype control antibody to minimize this unspecific reactivity. Pre-adsorption reduced this response (OD at 490nm) by a factor of approximately 2-5x at week five for the piglets. A low reactivity of the pre-immune sera is necessary to accurately reflect the induction of Ab2 antibodies produced in response to the immunizations. Additionally, this is critical due to our relatively small sample size of each treatment group (n=5). Our results from Chapters 3 and 4 show a low, ideal pre-immune sera

response (Figure 3.3.2, 4.3.3) that is consistent with past P3R99 studies (Brito et al., 2012)(Soto et al., 2012)(Soto et al., 2014)(Delgado-Roche et al., 2015). A low serum reactivity in the pre-immunization state allows for the accurate detection of differences in the induction of antibodies at various time points. Oversaturation of the pre-immune sera response can lead to an underestimation of antibody induction due to an overestimated baseline response. This may also cause the response to appear slower.

Interestingly, this over-saturation of the pre-immune response was also present for the hR3 treatment group, which is inconsistent with previous P3R99 studies and results. This suggests that the piglets may have naturally higher levels of anti-P3R99 Ab2 antibodies. Due to their young age and state of well-being, their immune systems may be over-active and naturally produce higher levels of endogenous anti-P3R99 antibodies prior to immunizations. Additionally, this could be attributed to over-saturation of the binding sites with the sera due to an inadequate dilution factor during the ELISA, contamination of the signal with other non-antibody components present in the sera, the presence of non-specific binding proteins, or potential cross-reactivity of the IgG goat anti-pig secondary antibody with the human IgG component of the P3R99 (Hosseini et al., 2018). As a result, we were only able to assess the induction of Ab2 antibodies at the fifth dose, as represented in the results (figure 5.3.2A). However, these results were positive and indeed confirm our hypothesis that the CHO-P3R99 and HEK-P3R99 variants maintain the immunogenic function of the NS0-P3R99 after a minimum of five doses.

Moreover, when comparing the magnitude of anti-idiotypic (Ab2) antibodies present at the fifth dose for the three P3R99 variants via One-Way ANOVA, we found no significant differences between CHO-P3R99 and NS0-P3R99 or CHO-P3R99 and HEK-P3R99. However, we did find differences between HEK-P3R99 and NS0-P3R99 (Figure 5.3.2B). However, this could be attributed to the pre-adsorption of the pre-immune and post-immune sera necessary to reduce unspecific cross-reactivity with the human antibodies.

As a result, in order to make definitive conclusions regarding the immunogenicity of the HEK-P3R99, we need to examine the Ab3 response as well as the Ab2 response. As the Ab3 is considered a final product in this idiotypic cascade, it can provide comprehensive insights into the immunogenicity of the HEK-P3R99 relative to the NS0-P3R99.

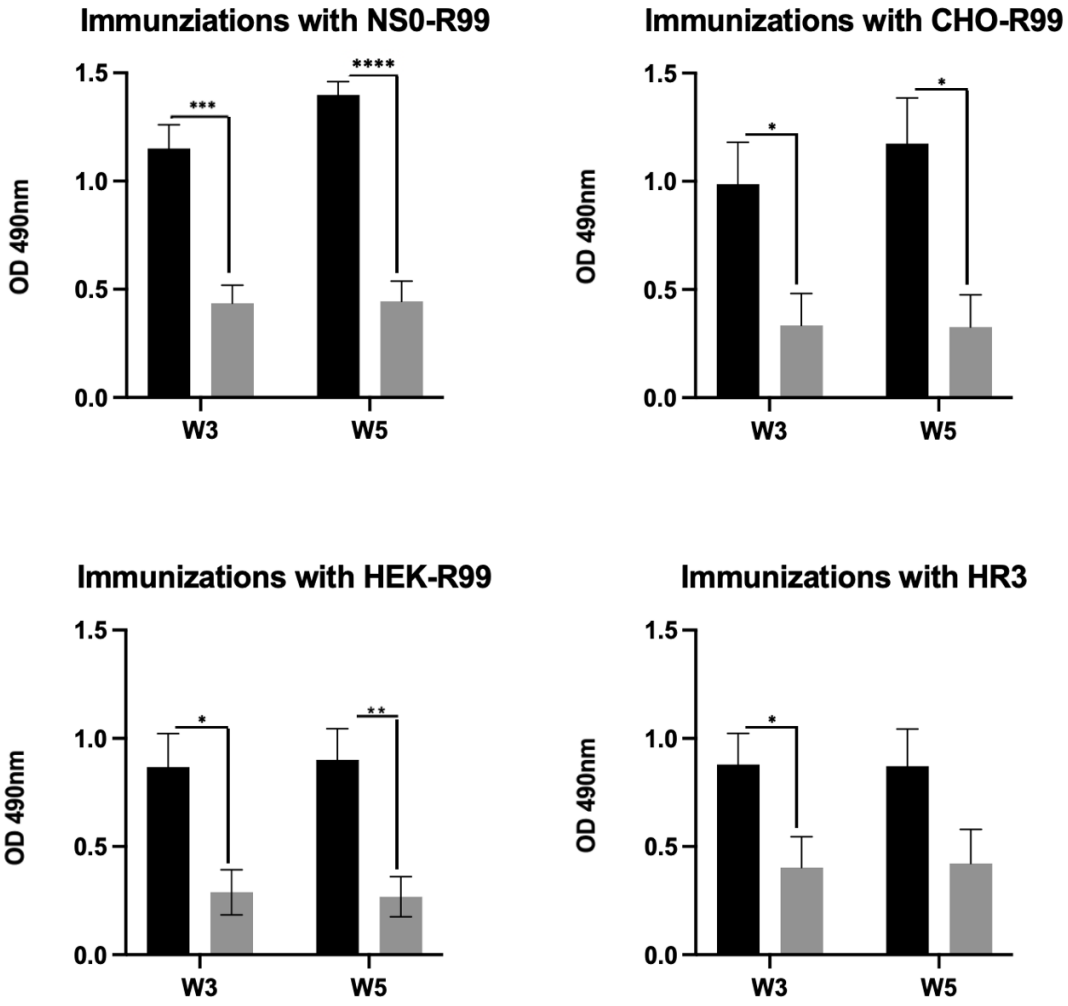

Figure 5.4.1 Enzyme-Linked Immunosorbent Assay (ELISA) results of Ab2 antibody induction at a sera dilution of 1/800. Historical results from an ELISA conducted without sera pre-adsorption (November 23, 2022). Represented as the response against the idiotype of P3R99 (anti-idiotypic response) vs the response against the non-idiotype regions of P3R99 (anti-isotypic response). Analyzed via parametric T-test * = $P<0.05$, ** = $P<0.01$, *** = $P<0.001$, **** = $P< 0.0001$. All values are presented as mean ± SEM.

5.4.3 CHO, HEK, and NS0-P3R99 variants met the requirement of Ab3 immunogenicity in a healthy large animal model: 3-week-old white-landrace piglets

As per section 3.4.3 of Chapter 3, Ab3 antibody induction is considered significant when there was a minimum two-fold increase in the production of anti-chondroitin sulfate (Ab3) antibodies from the pre-immune state to the final dose (Sarduy et al., 2017).

For the piglets, when comparing the pre-immune (W0) state to the fifth dose (W5) of P3R99 treated piglets, this requirement of a two-fold increase was met.

In fact, we can see an induction of approximately 2.5-fold from W0 to W5. Thus, in the piglets, we can conclude that the induction of Ab3 antibodies for the three P3R99 variants met the criteria of immunogenicity. As expected, the hR3 control did not induce significant anti-chondroitin sulfate antibodies.

Moreover, when comparing the magnitude of Ab3 antibody induction at the fifth dose for the P3R99 variants, we found no significant differences, suggesting that the CHO-P3R99 and HEK-P3R99 variants had similar immunogenicity as the original NS0-P3R99. Interestingly, as discussed in section 5.4.2, the HEK-P3R99 had a lower induction of anti-idiotypic antibodies compared to the NS0-P3R99. However, this relationship did not correspond to Ab3 antibody induction. As mentioned in Chapter 3, section 3.4.3, and Chapter 4, section 4.4.3, while Ab2 antibody induction is necessary to produce Ab3 antibodies (Sarduy et al., 2017), this relationship is not linear. Higher production of Ab2 antibodies does not consistently correlate with a higher production of Ab3 antibodies due to the potential of Ab2 antibodies to form immune complexes with Ab3. As such, despite the differences in the induction of Ab2 antibodies between HEK-P3R99 and NS0-P3R99, this occurrence was not maintained for Ab3 antibody production in the white-landrace piglets. Thus, the results strongly suggest that the P3R99 variants maintained the overall immunogenicity and strength of the original NS0-P3R99 in piglets in terms of Ab3 and Ab2 antibody induction. However, due to issues related to the piglet's over-reactivity to P3R99, leading to high detection of Ab2 antibodies in the pre-immune state these results require further testing.

5.5 Conclusions

In conclusion, our ELISA results in 3-week-old lean white-landrace piglets suggest that the HEK-P3R99 and CHO-P3R99 variants maintain the immunogenicity of the NS0-P3R99. Furthermore, the CHO-P3R99 and HEK-P3R99 variants exhibited immunogenic strength similar to the NS0-P3R99 in regard to Ab3 antibody induction. However, due to challenges in our detection of Ab2 antibody induction in the inter-immunization weeks (weeks 0-4) related to an over-active sera response prior to immunizations these results require further validation.

CHAPTER 6: GENERAL DISCUSSION AND CONCLUSIONS

6.1 Summary of results

The results of this thesis focus on the novel mAb production variants CHO-P3R99 and HEK-P3R99, specifically assessing their immunogenicity compared to the original NS0-P3R99. Chapters 3, 4 and 5 used distinct animal models to assess the immunogenicity of the variants under different physiological states. Additionally, chapter 4 included a comprehensive safety evaluation of the P3R99 variants in regard to lipid metabolism, carbohydrate metabolism (glucose and insulin metabolism), and cardiovascular function.

Chapter 3

We hypothesized that the CHO-P3R99 and HEK-P3R99 variants maintained the overall immunogenicity and strength of the NS0-P3R99 in a 3-month-old lean JCR:LA-cp rat model. Our results confirmed that administration of CHO-P3R99, HEK-P3R99, and NS0-P3R99 induced an idiotypic cascade in the lean JCR:LA-cp rats, evidenced through the detection of Ab2 and Ab3 host-derived antibodies. These results were validated through the use of a negative isotype control, hR3, which did not induce significant levels of either Ab2 or Ab3 antibodies. Additionally, when comparing the levels of Ab2 and Ab3 antibodies induced by the HEK-P3R99, CHO-P3R99, and NS0-P3R99, we found no significant differences, thus providing strong evidence that the variants maintained the immunogenic strength of the original NS0-P3R99 in the lean JCR:LA-cp rats.

Chapter 4

Due to positive results in our lean JCR:LA-cp rodent pilot study, we then choose to complete a more comprehensive evaluation of the immunogenicity, metabolic effects, and cardiovascular outcomes of the P3R99 variants compared to the control hR3 in a lipid and vascular remodelling susceptible animal model of 9-month-old obese insulin-resistant JCR:LA-cp rats. For this study, we hypothesized that the CHO-P3R99 and HEK-P3R99 variants would have similar effects as the NS0-P3R99 in terms of immunogenicity, as well as neutral effects on lipid and carbohydrate metabolism and cardiovascular function. Our findings from the obese insulin-resistant JCR:LA-cp rat study demonstrated that the CHO-P3R99, HEK-P3R99, and NS0-P3R99 were immunogenic through successful induction of Ab2 antibodies in a physiologically compromised animal model. These results were critical as they validated the variants' ability to stimulate the immune system

in a model of chronic inflammation and immune dysfunction. Moreover, the variants had a similar immunogenic strength (magnitude of Ab2 and Ab3 antibody induction) as the original NS0-P3R99. However, when assessing the induction of Ab3 antibodies, the HEK-P3R99 was unable to meet the criteria for immunogenicity in the obese insulin-resistant JCR:LA-cp rats. This could possibly be due to Ab3 accumulation in areas of atherosclerotic remodelling or Ab3 forming immune complexes with the Ab2 antibodies present in the sera.

Furthermore, we found that the P3R99 variants did not influence lipid or carbohydrate metabolism. P3R99-treated rats had comparable concentrations of fasting plasma lipids, glucose, and insulin as the hR3 treated rats, confirming our hypothesis that the P3R99 variants do not exert non-canonical metabolic effects related to their chondroitin sulfate binding affinity. Additionally, HOMA-IR analysis confirmed the presence of moderate insulin resistance in all rats regardless of treatment group. Similarly, the P3R99 variants were demonstrated to have neutral effects on cardiovascular function in the obese insulin-resistant JCR:LA-cp rats through echocardiogram assessment of the P3R99 treated rats compared to the hR3 treated rats. Echocardiogram results also confirmed the pathology of spontaneous left ventricular dysfunction in the obese insulin-resistant JCR:LA-cp rats regardless of their treatment group.

Chapter 5

Based on the outcomes of Chapters 3 and 4 we were able to consider testing the capacity of the P3R99 variants in a large animal model (white-landrace swine) with similar cardiovascular physiology, anatomy, and lipid metabolism as humans. We hypothesized that the CHO-P3R99 and HEK-P3R99 variants were immunogenic and had immunogenic capabilities similar to the original NS0-P3R99 in the 3-week-old white-landrace piglets. Our data confirmed our hypothesis that the three variants were immunogenic through the significant induction of Ab2 and Ab3 antibodies, while the control hR3 was non-immunogenic. However, when comparing the strength of the Ab2 response of the three P3R99 variants, we found statistically significant differences between the HEK-P3R99 and NS0-P3R99, which were not seen when comparing the strength of Ab3 antibody induction between the two. Although, this can be attributed to the pre-adsorption of the sera with an isotypic control antibody to minimize cross-reactivity. Thus, at this time, we can confirm that the CHO-P3R99 maintained the immunogenic strength of the NS0-P3R99 in the white-landrace piglets, while the results from the HEK-P3R99 immunizations suggest that the HEK-P3R99 variant had a similar immunogenic strength as the NS0-P3R99.

Table 6.1

Thesis chapter results and assessment summary. Study design, planned assessments, and final results for healthy lean heterozygous JCR:LA-cp rats, obese insulin-resistant homozygous JCR:LA-cp rats, and healthy white-landrace piglets' studies.

Study design				Planned Assessments			Results
Animal model	**Duration**	**Blood draws**	**Doses**	**Ab2, Kinetics**	**Ab3, Kinetics**	**Additional**	**Results obtained**
Male Heterozygous Lean JCR:LA-cp Rats - 3 months old - Standard chow diet	6 weeks.	5 blood draws at weeks 0,2,3,4,and 6	Two injections of 250uL of 400ug/mL. Total 200mg	Ab2 assessment planned (minimum at final dose) Kinetics planned.	Ab3 assessment planned (minimum at W0 and after the fourth or final dose) Kinetics planned.	(1) Weight gain over time.	(1) Ab2 antibody induction. Ab2 kinetics at 5 time points. (2) Ab3 antibody induction at W0 to W4. Ab3 kinetics at 4 time points. (3) Weight gain at 3 time points.
Male Homozygous Obese Insulin-Resistant JCR:LA-cp Rats - 9 months old - High-Fat High-fructose diet (composed of 2% cholesterol, 20% lard, 15% fructose)	12 weeks total. 4-week diet, then 6 doses over 8 weeks with diet	5 blood draws at weeks 4,7,8,10,and 12	Two injections of 250uL of 400ug/mL. Total 200mg	Ab2 assessment planned (minimum at final dose) Kinetics planned.	Ab3 assessment planned (minimum at W0 and after the fourth (W8) or final dose (W12)) Kinetics not planned.	(1) Weight gain over time. (2) Lipoprotein and glucose metabolism. (3) Heart function and weight.	(1) Ab2 antibody induction. Ab2 kinetics at 3 time points. (2) Ab3 antibody induction at W4 to W12. (3) Weight gain at 14 time points. (4) Fasting HDL, TG, TC, glucose, and insulin plasma levels. HOMA-IR score. (5) Various cardiovascular function outcomes and heart weight.
Male White-Landrace Piglets - 3 weeks old - Pre-grower and standard chow diet	5 Weeks.	4 blood draws at weeks 0,3,4, and 5	One injection of 3mL of 0.33mg/mL. Total 1mg	Ab2 assessment planned (minimum at final dose) Kinetics not planned.	Ab3 assessment planned (minimum at W0 and after the fourth or final dose) Kinetics not planned.	(1) Weight gain over time.	(1) Ab2 antibody induction at W5 only. (2) Ab3 antibody induction at W0 to W5. (3) Weight gain at 7 time points.

6.2 Discussion of findings

6.2.1 The use of in-vitro methods to assess immunogenicity

A direct solid-phase Enzyme-Linked Immunosorbent Assay (ELISA) was conducted to validate the immune response generated by P3R99 and hR3 by assessing the presence and magnitude of anti-idiotypic (Ab2) and anti-anti-idiotypic (Ab3) antibodies produced (Sarduy et al., 2017)(Brito et al., 2017). The solid phase direct ELISA was chosen due to its validation in previous NS0-P3R99 studies, high degree of accuracy in antibody detection and ease of use (Brito et al., 2012)(Soto et al., 2012)(Soto et al., 2014).

Immunochemical assays, like ELISAs, are often used to assess the characterization and specificity of antibody-antigen interactions. However, there are several techniques available, and while the gold standard is the ELISA, there are some limitations. The high sensitivity of the ELISA can detect nonspecific binding, thus over-estimating anti-isotypic and anti-idiotypic interactions (Alhajj & Farhana, 2023)(Fernández-Quintero et al.,2023). Additionally, the accuracy of the ELISA can be impacted by interference factors, including insufficient dilution and the presence of contaminants, especially when using biological samples such as sera, which, if not properly addressed, can lead to over-reactivity and inaccurate readings of antibodies bound to the plate (Hosseini et al., 2018). These factors may have, in part, influenced our results in the white-landrace swine. As mentioned in section 5.4.2 of chapter 5, the pre-immune sera of the swine displayed high levels of anti-idiotypic Ab2 antibodies prior to immunizations with the P3R99s. These results are inconsistent with published NS0-P3R99 studies in various small animal models, which consistently demonstrated minimal Ab2 response in the pre-immune sera (Sarduy et al., 2017)(Brito et al., 2017).

Moreover, as there were no existing protocols for assessing the immunogenicity of the P3R99 variants in piglets, many different facets of the procedure were modified and adjusted, such as sera dilution factor, sera incubation time, secondary antibody concentration, pre-adsorption of sera, and TMB incubation time. However, our standardization was not able to sufficiently reduce the high pre-immune response of the white-landrace piglets. Which, as discussed in Chapter 5, could indicate oversaturation of the binding sites, contamination of the signal with non-antibody components of the sera, endogenous antibodies in the sera, presence of non-specific binding proteins, or cross-reactivity of the secondary antibody (Hosseini et al., 2018).

These factors could additionally have contributed to the inconsistencies with the HEK-P3R99 results in the white-landrace piglets among the Ab2 and Ab3 responses. As per Figure 5.3.2B and Figure 5.3.3B of Chapter 5, the anti-idiotypic Ab2 response of HEK-P3R99 was significantly lower than NS0-P3R99. However, this trend was not maintained for the Ab3 response. This could also be due to the high sensitivity of the ELISA and the use of Fetal Bovine Serum (FBS) for only NS0-P3R99 production. The presence of FBS in NS0-P3R99 could potentially lead to an overestimation of the NS0-P3R99 anti-idiotypic Ab2 response compared to the HEK-P3R99, which is not produced with FBS. This can occur due to the endogenous antibodies and proteins of FBS, which can lead to non-specific binding and cross-reactivity, resulting in a higher background signal (Kim et al., 2015). Thus, challenging the accuracy and consistency of these results.

6.2.2 The possible effect of dose-per-kilogram on the immunogenicity of the P3R99 variants in different animal models

Administration of a 200 μg dose (400 μg/mL) of P3R99 and hR3 in small animals was pre-validated and proven sufficient to generate a detectable immune response. Previous studies with ApoE-/- mice receiving 200 μg of NS0-R99 and hR3 demonstrated significant anti-idiotypic Ab2 and anti-anti-idiotypic Ab3 responses (Sarduy et al., 2017)(Delgado-Roche et al., 2015). However, as previously mentioned, our study was the first to assess the effects of the P3R99 variants in distinct animal models, specifically in a large animal model of white-landrace piglets. As per Figure 3.1 of Chapter 5, the final weight of the piglets was approximately 30 kg. The dose-per-kilogram for the piglets can be calculated through the following equations:

Equation 6.1 Calculation of dose-per-kilogram.

Total Dose = Concentration (mg/mL) x Volume (mL)
Total Dose For Piglets= 0.33 mg/mL x 3 mL = 1 mg
Dose per Kilogram = Total Dose (mg) / Animal Weight (kg)
Dose per Kilogram = 1 mg / 30 kg = 0.033 mg/kg

The final dose-per-kilogram for the piglets was 0.033 mg/kg. As per figures 3.1 and 3.2 of Chapter 4, the final weight of the lean JCR:LA-cp rats and obese insulin-resistant JCR:LA-cp rats were approximately 300 grams and 975 grams, respectively. Using the layout of equation one, the lean

rats which received 500 μL of a 400 μg/mL dose had a final dose-per-kilogram of 0.67 mg/kg. The obese insulin-resistant rats which similarly received 500 μL of a 400 μg/mL dose had a final dose-per-kilogram of 0.21 mg/kg. This difference in the dose-per-kilogram of our various animal models can have significant implications for our results and explain some of the discrepancies we observed (Pan et al., 2016).

A higher dose per kilogram could result in a stronger immune response as it could potentially saturate the immune system, allowing for the immune response to reach its maximum capacity. Moreover, in the context of mAbs, body weight has been shown to be a predictor of antibody clearance and is a critical consideration factor in the field of pharmacokinetics (Mould et al., 2010)(Bai et al., 2012). As discussed in the 2017 article by Sarduy et al., the P3R99 has significant dose-dependent effects, which determine the ability of the P3R99 to launch an immune response and ultimately prevent atherogenesis. When they increased the dose of NS0-P3R99 by a factor of four (4x) in ApoE-/- mice, they discovered that the higher dose reduced aortic lesion development significantly compared to the lower dose (1x) (Sarduy et al., 2017). Moreover, the dose-dependent effect of P3R99 reaches a peak following four administrations, suggesting that this effect has a minimum threshold of exposure needed to stimulate a response. Thus, due to this strong dose-dependent effect of the P3R99, it's possible that the difference in dose-per-kilogram of the lean JCR:LA-cp rats (0.67 mg/kg) compared to the obese insulin-resistant JCR:LA-cp rats (0.21 mg/kg) and white-landrace piglets (0.033 mg/kg) in part accounts for the differences in their induction of Ab2 and Ab3. The lean JCR:LA-cp rats had the highest dose-per-kilogram and exhibited ideal results in regard to the induction of anti-idiotypic Ab2 and anti-anti-idiotypic Ab3 antibodies compared to the other two animal models. Specifically, the lean JCR:LA-cp rats did not experience issues regarding the HEK-P3R99 induction of Ab3 antibodies that we observed in the obese insulin-resistant JCR:LA-cp rats. Nor did the lean rats have issues of high-pre-immune sera reactivity or inconsistencies of the HEK-P3R99 Ab2 and Ab3 response that were found for the white-landrace piglets.

6.2.3 The use of different animal models and the effect on their immune responses

All animal models were male in order to mitigate the influence of estrous cycles and reduce variability related to differences in hormones (Klein & Flanagan, 2016). The reproductive features and hormonally complexity of female animals can have major implications on the function of the

immune system, specifically antibody production and immunomodulation. Sex hormones such as estrogen and progesterone strongly influence immune regulation (Klein & Flanagan, 2016) and cardiovascular outcomes. Sex differences additionally occur in both the innate and adaptive immune systems and can influence the susceptibility to immune dysfunction and monoclonal antibody treatment outcomes (Klein & Flanagan, 2016)(Wilkinson et al., 2022). Female animal models are also more prone to adverse effects when undergoing antibody-based interventions (Fischinger et al., 2018).

Moreover, we choose to assess the effect of P3R99 administration specifically in the JCR:LA-cp rat models due to previous use of this animal model for P3R99 studies (Soto et al., 2023). The lean JCR:LA-cp rat model was chosen to determine the effect of the CHO-P3R99 and HEK-P3R99 under normal physiological conditions without the influences of old age and diet, which are major determinants of atherosclerosis onset and outcomes. Conversely, the obese insulin-resistant rats were chosen to assess the influence of P3R99 administration in a model of physiological dysfunction, specifically of immune dysfunction. As this study was interested in the immunogenic effects of the P3R99, we wanted to know how and if a state of immune dysfunction would limit the ability of the P3R99 to stimulate an immune response. We were also interested in the adaptability of the P3R99 variants under this state of immune dysfunction compared to 'normal' physiology.

Additionally, as obesity and insulin resistance are low-grade chronic inflammatory disorders like atherosclerosis, the obese insulin-resistant JCR:LA-cp rats were a relevant model for the inflammatory features of atherosclerosis. As discussed in detail in the introduction of Chapter 5 and section 1.6.3 of Chapter 1, the white-landrace piglet model was chosen due to its inherent similarities to human pathophysiology, anatomy, metabolism, and immune responses (Tsang et al., 2016). Using this large animal model under normal physiological conditions can provide insight into how a human immune system may respond to P3R99 treatment. As such, the use of these distinct animal models with varying immune systems and immunomodulation can explain some of the differences between our results. It's in part due to their immune systems' varying complexities and differing states of health that we observed differences in their anti-idiotypic Ab2 and anti-anti-idiotypic Ab3 responses to the P3R99. It is also possible the antibody itself could have been recognized differently by the species-specific immune systems due to its chimeric mouse/human makeup (Malm et al., 2020)(Liu et al., 2022). The healthy lean JCR:LA-cp rat

immune system, for example, could have had a higher reactivity to the mouse IgG, thus inducing a larger number of anti-idiotypic antibodies in response, while this reaction could have been less strong in the white-landrace piglets. This is especially relevant as the piglets likely had a higher baseline of endogenous antibodies capable of non-specific and low binding affinity interactions as per their elevated pre-immune sera response.

6.3 Limitations and future directions

As described in this discussion, some limitations of our immunogenicity studies included the use of the ELISA assays, differences in dose-per-kilogram among the animals' models, and variability of the immune systems of the animal models.

Additionally, another limitation was the lack of accounting for sex differences. As discussed in section 6.2.3, female and male animal species have strong sex-dependent differences in their immune responses (Klein & Flanagan, 2016)(Wilkinson et al., 2022), which were not addressed in this study. Using both male and female species while introducing a higher level of variability can provide necessary insight into how the P3R99 variants function under the influence of reproduction and hormonal fluctuations.

Moreover, having a relatively small sample size (n=5) also limits our ability to make definitive conclusions, as having one outlier can significantly skew our data. Our sample size also limited the statistical analyses we were able to undertake.

Lastly, as mentioned in Chapter 4 Section 4.4.5, the obese insulin-resistant JCR:LA-cp rats, while having a similar underlying pathophysiology to atherosclerosis, were not the ideal model for assessing atherosclerosis due to inherent differences in the physiology and metabolism of rats compared to large mammals like humans. Thus, we were unable to determine if P3R99 administration ameliorated atherosclerosis. Although, we did find that the P3R99 administration did not negatively affect cardiovascular function.

Moving forward, this immunogenicity study could be reassessed using common models of atherosclerosis, such as ApoE-/- mice or rabbits given lipofundin. Additionally, we could use both male and female animals to account for any sex-related differences.

Moreover, in order to reduce the level of variability present in our study, future studies could use a consistent dose-per-kilogram among similar animal models and increase the sample size of each P3R99 variant.

Furthermore, based on previous studies of NS0-P3R99, future experiments could include an immunohistochemistry assay to assess variant accumulation in areas of atherosclerosis, which, as discussed, is a major feature of the P3R99.

Longer-term studies could also be carried out to assess the vaccine-like ability of the variants to induce longer-term atheroprotective effects seen in the original NS0-P3R99 and to determine the appropriate dosing of the variants (Brito et al., 2012)(Sarduy et al., 2017).

6.4 Conclusions

There is a gap in cardiovascular therapies that can target disease initiation and address residual risk. The NS0-P3R99, a human murine, chimeric atheroprotective monoclonal antibody capable of binding proatherogenic proteoglycan glycosaminoglycans and inducing an idiotypic cascade through the host immune system, has been shown in previous studies to inhibit lipid retention and reduce atherosclerosis.

Production issues with its NS0 cell line led to the creation of two new, more productive variants, CHO-P3R99 and HEK-P3R99, that were assessed for immunogenic capability.

The results from this thesis suggest that the variants have immunogenic effects similar to the NS0-P3R99 in distinct animal models. These results are promising as the idiotypic cascade induced by the P3R99 mediates the antiatherosclerotic effects (Brito et al., 2012)(Soto et al., 2012)(Sarduy et al., 2017), suggesting that the variants may also retain other novel features of the NS0-P3R99.

These results provide critical next steps for the development of the P3R99, aiding the future adaption of the P3R99 for scale-up use in large animal models and large-scale clinical trials.

BIBLIOGRAPHY

1. Abdul-Rahman T, Bukhari SMA, Herrera EC, Awuah WA, Lawrence J, de Andrade H, Patel N, Shah R, Shaikh R, Capriles CAA, Ulusan S, Ahmad S, Corriero AC, Mares AC, Goel A, Hajra A, Bandyopadhyay D, Gupta R. Lipid Lowering Therapy: An Era Beyond Statins. Curr Probl Cardiol. 2022 Dec;47(12):101342. doi: 10.1016/j.cpcardiol.2022.101342. Epub 2022 Jul 31. PMID: 35918009.

2. Aguib Y, Al Suwaidi J. The Copenhagen City Heart Study (Østerbroundersøgelsen). Glob Cardiol Sci Pract. 2015 Oct 9;2015(3):33. doi: 10.5339/gcsp.2015.33. PMID: 26779513; PMCID: PMC4625209.

3. Ait-Oufella H, Salomon BL, Potteaux S, Robertson AK, Gourdy P, Zoll J, Merval R, Esposito B, Cohen JL, Fisson S, Flavell RA, Hansson GK, Klatzmann D, Tedgui A, Mallat Z. Natural regulatory T cells control the development of atherosclerosis in mice. Nat Med. 2006 Feb;12(2):178-80. doi: 10.1038/nm1343. Epub 2006 Feb 5. PMID: 16462800.

4. Ait-Oufella H, Libby P, Tedgui A. Antibody-based immunotherapy targeting cytokines and atherothrombotic cardiovascular diseases. Arch Cardiovasc Dis. 2020 Jan;113(1):5-8. doi: 10.1016/j.acvd.2019.11.001. Epub 2020 Jan 6. PMID: 31917124.

5. Akyea RK, Kai J, Qureshi N, Iyen B, Weng SF. Sub-optimal cholesterol response to initiation of statins and future risk of cardiovascular disease. Heart. 2019 Jul;105(13):975-981. doi: 10.1136/heartjnl-2018-314253. Epub 2019 Apr 15. PMID: 30988003; PMCID: PMC6582718.

6. Alberts B, Johnson A, Lewis J, et al. Molecular Biology of the Cell. 4th edition. New York: Garland Science; 2002. Innate Immunity. https://www.ncbi.nlm.nih.gov/books/NBK26846/.

7. Alhajj M, Zubair M, Farhana A. Enzyme Linked Immunosorbent Assay. [Updated 2023 Apr 23]. In: StatPearls [Internet]. Treasure Island (FL): StatPearls Publishing; 2024 Jan. https://www.ncbi.nlm.nih.gov/books/NBK555922/.

8. Anaya JM, Shoenfeld Y, Rojas-Villarraga A, et al., editors. Autoimmunity: From Bench to Bedside [Internet]. Bogota (Colombia): El Rosario University Press; 2013 Jul 18. Available from: https://www.ncbi.nlm.nih.gov/books/NBK459447/.

9. Andersen DC, Reilly DE. Production technologies for monoclonal antibodies and their fragments. Curr Opin Biotechnol. 2004 Oct;15(5):456-62. doi: 10.1016/j.copbio.2004.08.002. PMID: 15464378.

10. Andersson J, Libby P, Hansson GK. Adaptive immunity and atherosclerosis. Clin Immunol. 2010 Jan;134(1):33-46. doi: 10.1016/j.clim.2009.07.002. Epub 2009 Jul 26. PMID: 19635683.

11. Arackal A, Alsayouri K. Histology, Heart. 2023 Jan 2. In: StatPearls [Internet]. Treasure Island (FL): StatPearls Publishing; 2024 Jan. PMID: 31424727.

12. Arai T, Arai A, Busby WH Jr, Clemmons DR. Glycosaminoglycans inhibit degradation of insulin-like growth factor-binding protein-5. Endocrinology. 1994 Dec;135(6):2358-63. doi: 10.1210/endo.135.6.7527332. PMID: 7527332.

13. Aronson D, Rayfield EJ. How hyperglycemia promotes atherosclerosis: molecular mechanisms. Cardiovasc Diabetol. 2002 Apr 8;1:1. doi: 10.1186/1475-2840-1-1. PMID: 12119059; PMCID: PMC116615.

14. "ASE's First Guideline Summary Available Online." The American Society of echocardiography recommendations for cardiac chamber quantification in adults: a quick reference guide from the ASE workflow and lab management task force, July 2018, Available from: www.asecho.org/ases-first-guideline-summary-available-online/.

15. Atherosclerotic Cardiovascular Disease Risk Markers. ARUP Consult®. Updated January 2024, Available from: https://arupconsult.com/content/cardiovascular-disease-traditional-risk-markers.

16. Atheroscleosis-Treatment. National Heart Lung and Blood Institute, U.S [Internet]. Department of Health and Human Services, Mar. 2022. Available from: www.nhlbi.nih.gov/health/atherosclerosis/treatment.

17. Babaev VR, Yeung M, Erbay E, Ding L, Zhang Y, May JM, Fazio S, Hotamisligil GS, Linton MF. Jnk1 Deficiency in Hematopoietic Cells Suppresses Macrophage Apoptosis and Increases Atherosclerosis in Low-Density Lipoprotein Receptor Null Mice. Arterioscler Thromb Vasc Biol. 2016 Jun;36(6):1122-31. doi: 10.1161/ATVBAHA.116.307580. Epub 2016 Apr 21. PMID: 27102962; PMCID: PMC4882236.

18. Bäck M, Yurdagul A Jr, Tabas I, Öörni K, Kovanen PT. Inflammation and its resolution in atherosclerosis: mediators and therapeutic opportunities. Nat Rev Cardiol. 2019 Jul;16(7):389-406. doi: 10.1038/s41569-019-0169-2. PMID: 30846875; PMCID: PMC6727648.

19. Badimon L, Padró T, Vilahur G. Atherosclerosis, platelets and thrombosis in acute ischaemic heart disease. Eur Heart J Acute Cardiovasc Care. 2012 Apr;1(1):60-74. doi: 10.1177/2048872612441582. PMID: 24062891; PMCID: PMC3760546.

20. Bai S, Jorga K, Xin Y, Jin D, Zheng Y, Damico-Beyer LA, Gupta M, Tang M, Allison DE, Lu D, Zhang Y, Joshi A, Dresser MJ. A guide to rational dosing of monoclonal antibodies. Clin Pharmacokinet. 2012 Feb 1;51(2):119-35. doi: 10.2165/11596370-000000000-00000. PMID: 22257150.

21. Baldrighi M, Mallat Z, Li X. NLRP3 inflammasome pathways in atherosclerosis. Atherosclerosis. 2017 Dec;267:127-138. doi: 10.1016/j.atherosclerosis.2017.10.027. Epub 2017 Oct 22. PMID: 29126031.

22. Banday AH, Abdalla M. Immune Checkpoint Inhibitors: Recent Clinical Advances and Future Prospects. Curr Med Chem. 2023;30(28):3215-3237. doi: 10.2174/0929867329666220819115849. PMID: 35986535.

23. Barrett TJ. Macrophages in Atherosclerosis Regression. Arterioscler Thromb Vasc Biol. 2020 Jan;40(1):20-33. doi: 10.1161/ATVBAHA.119.312802. Epub 2019 Nov 14. PMID: 31722535; PMCID: PMC6946104.

24. Behn U. Idiotypic networks: toward a renaissance? Immunol Rev. 2007 Apr;216:142-52. doi: 10.1111/j.1600-065X.2006.00496.x. PMID: 17367340.

25. Bengtsson G, Olivecrona T, Höök M, Riesenfeld J, Lindahl U. Interaction of lipoprotein lipase with native and modified heparin-like polysaccharides. Biochem J. 1980 Sep 1;189(3):625-33. doi: 10.1042/bj1890625. PMID: 6452123; PMCID: PMC1162043.

26. Bermúdez V, Rojas-Quintero J, Velasco M. The quest for immunotherapy in atherosclerosis: CANTOS study, interleukin-1β and vascular inflammation. J Thorac Dis. 2018 Jan;10(1):64-69. doi: 10.21037/jtd.2017.12.47. PMID: 29600023; PMCID: PMC5863198.

27. Beutler B. Innate immunity: an overview. Mol Immunol. 2004 Feb;40(12):845-59. doi: 10.1016/j.molimm.2003.10.005. PMID: 14698223.

28. Beverly JK, Budoff MJ. Atherosclerosis: Pathophysiology of insulin resistance, hyperglycemia, hyperlipidemia, and inflammation. J Diabetes. 2020 Feb;12(2):102-104. doi: 10.1111/1753-0407.12970. Epub 2019 Aug 14. PMID: 31411812.

29. BEZNAK M. Cardiac output in rats during the development of cardiac hypertrophy. Circ Res. 1958 Mar;6(2):207-12. doi: 10.1161/01.res.6.2.207. PMID: 13511677.

30. Bloomgarden ZT. Inflammation, atherosclerosis, and aspects of insulin action. Diabetes Care. 2005 Sep;28(9):2312-9. doi: 10.2337/diacare.28.9.2312. PMID: 16123510.

31. Bobryshev YV, Ivanova EA, Chistiakov DA, Nikiforov NG, Orekhov AN. Macrophages and Their Role in Atherosclerosis: Pathophysiology and Transcriptome Analysis. Biomed Res Int. 2016;2016:9582430. doi: 10.1155/2016/9582430. Epub 2016 Jul 17. PMID: 27493969; PMCID: PMC4967433.

32. Bonaccorsi I, De Pasquale C, Campana S, Barberi C, Cavaliere R, Benedetto F, Ferlazzo G. Natural killer cells in the innate immunity network of atherosclerosis. Immunol Lett. 2015 Nov;168(1):51-7. doi: 10.1016/j.imlet.2015.09.006. Epub 2015 Sep 15. PMID: 26384623.

33. Bonilla FA, Oettgen HC. Adaptive immunity. J Allergy Clin Immunol. 2010 Feb;125(2 Suppl 2):S33-40. doi: 10.1016/j.jaci.2009.09.017. Epub 2010 Jan 12. PMID: 20061006.

34. Bornfeldt KE, Tabas I. Insulin resistance, hyperglycemia, and atherosclerosis. Cell Metab. 2011 Nov 2;14(5):575-85. doi: 10.1016/j.cmet.2011.07.015. PMID: 22055501; PMCID: PMC3217209.

35. Brindley DN, Russell JC. Animal models of insulin resistance and cardiovascular disease: some therapeutic approaches using JCR:LA-cp rat. Diabetes Obes Metab. 2002 Jan;4(1):1-10. doi: 10.1046/j.1463-1326.2002.00164.x. PMID: 11890162.

36. Brito V, Mellal K, Portelance SG, Pérez A, Soto Y, deBlois D, Ong H, Marleau S, Vázquez AM. Induction of anti-anti-idiotype antibodies against sulfated glycosaminoglycans reduces atherosclerosis in apolipoprotein E-deficient mice. Arterioscler Thromb Vasc Biol. 2012 Dec;32(12):2847-54. doi: 10.1161/ATVBAHA.112.300444. Epub 2012 Oct 18. PMID: 23087361.

37. Brito V, Mellal K, Zoccal KF, Soto Y, Ménard L, Sarduy R, Faccioli LH, Ong H, Vázquez AM, Marleau S. Atheroregressive Potential of the Treatment with a Chimeric Monoclonal Antibody against Sulfated Glycosaminoglycans on Pre-existing Lesions in Apolipoprotein E-Deficient Mice. Front Pharmacol. 2017 Nov 1;8:782. doi: 10.3389/fphar.2017.00782. PMID: 29163168; PMCID: PMC5672559.

38. Brunner D, Frank J, Appl H, Schöffl H, Pfaller W, Gstraunthaler G. Serum-free cell culture: the serum-free media interactive online database. ALTEX. 2010;27(1):53-62. doi: 10.14573/altex.2010.1.53. PMID: 20390239.

39. Buono C, Binder CJ, Stavrakis G, Witztum JL, Glimcher LH, Lichtman AH. T-bet deficiency reduces atherosclerosis and alters plaque antigen-specific immune responses. Proc Natl Acad Sci U S A. 2005 Feb 1;102(5):1596-601. doi: 10.1073/pnas.0409015102. Epub 2005 Jan 21. PMID: 15665085; PMCID: PMC547865.

40. Butler, M. (2015). Serum and Protein Free Media. In: Al-Rubeai, M. (eds) Animal Cell Culture. Cell Engineering, vol 9. Springer, https://doi.org/10.1007/978-3-319-10320-4_8.

41. Cai X, Zhan H, Ye Y, Yang J, Zhang M, Li J, Zhuang Y. Current Progress and Future Perspectives of Immune Checkpoint in Cancer and Infectious Diseases. Front Genet. 2021 Nov 30;12:785153. doi: 10.3389/fgene.2021.785153. PMID: 34917131; PMCID: PMC8670224.

42. Canada PHA of. Heart disease in Canada: Highlights from the Canadian Chronic Disease Surveillance System, 2017. Published August 22, 2017 [Internet]. Available from: https://www.canada.ca/en/public-health/services/publications/diseases-conditions/heart-disease-canada-fact-sheet.html.

43. Chahine J, Alvey H. Left Ventricular Failure. [Updated 2023 Jun 26]. In: StatPearls [Internet]. Treasure Island (FL): StatPearls Publishing; 2024 Jan-. Available from: https://www.ncbi.nlm.nih.gov/books/NBK537098/.

44. Chen L, Flies DB. Molecular mechanisms of T cell co-stimulation and co-inhibition. Nat Rev Immunol. 2013 Apr;13(4):227-42. doi: 10.1038/nri3405. Epub 2013 Mar 8. Erratum in: Nat Rev Immunol. 2013 Jul;13(7):542. PMID: 23470321; PMCID: PMC3786574.

45. Cholesterol Treatment Trialists' (CTT) Collaboration; Baigent C, Blackwell L, Emberson J, Holland LE, Reith C, Bhala N, Peto R, Barnes EH, Keech A, Simes J, Collins R. Efficacy and safety of more intensive lowering of LDL cholesterol: a meta-analysis of data from 170,000 participants in 26 randomised trials. Lancet. 2010 Nov 13;376(9753):1670-81. doi: 10.1016/S0140-6736(10)61350-5. Epub 2010 Nov 8. PMID: 21067804; PMCID: PMC2988224.

46. Cianflone K, Paglialunga S, Roy C. Intestinally derived lipids: metabolic regulation and consequences--an overview. Atheroscler Suppl. 2008 Sep;9(2):63-8. doi: 10.1016/j.atherosclerosissup.2008.05.014. Epub 2008 Aug 6. PMID: 18693144.

47. Coll RC, Robertson AA, Chae JJ, Higgins SC, Muñoz-Planillo R, Inserra MC, Vetter I, Dungan LS, Monks BG, Stutz A, Croker DE, Butler MS, Haneklaus M, Sutton CE, Núñez G, Latz E, Kastner DL, Mills KH, Masters SL, Schroder K, Cooper MA, O'Neill LA. A small-molecule inhibitor of the NLRP3 inflammasome for the treatment of inflammatory diseases. Nat Med. 2015 Mar;21(3):248-55. doi: 10.1038/nm.3806. Epub 2015 Feb 16. PMID: 25686105; PMCID: PMC4392179.

48. Coloma MJ, Hastings A, Wims LA, Morrison SL. Novel vectors for the expression of antibody molecules using variable regions generated by polymerase chain reaction. J Immunol Methods. 1992 Jul 31;152(1):89-104. doi: 10.1016/0022-1759(92)90092-8. PMID: 1640112.

49. Darbandi Azar A, Tavakoli F, Moladoust H, Zare A, Sadeghpour A. Echocardiographic evaluation of cardiac function in ischemic rats: value of m-mode echocardiography. Res Cardiovasc Med. 2014 Nov 1;3(4):e22941. doi: 10.5812/cardiovascmed.22941. PMID: 25785251; PMCID: PMC4347793.

50. Das R, Ganapathy S, Mahabeleshwar GH, Drumm C, Febbraio M, Jain MK, Plow EF. Macrophage gene expression and foam cell formation are regulated by plasminogen. Circulation. 2013 Mar 19;127(11):1209-18, e1-16. doi: 10.1161/CIRCULATIONAHA.112.001214. Epub 2013 Feb 11. Erratum in: Circulation. 2014 Feb 4;129(5):e326. PMID: 23401155; PMCID: PMC3638243.

51. Dash S, Xiao C, Morgantini C, Lewis GF. New Insights into the Regulation of Chylomicron Production. Annu Rev Nutr. 2015;35:265-94. doi: 10.1146/annurev-nutr-071714-034338. Epub 2015 May 13. PMID: 25974693.

53. Delgado-Roche L, Brito V, Acosta E, Pérez A, Fernández JR, Hernández-Matos Y, Griñán T, Soto Y, León OS, Marleau S, Vázquez AM. Arresting progressive atherosclerosis by immunization with an anti-glycosaminoglycan monoclonal antibody in apolipoprotein E-deficient mice. Free Radic Biol Med. 2015 Dec;89:557-66. doi: 10.1016/j.freeradbiomed.2015.08.027. Epub 2015 Oct 8. PMID: 26454078.

54. Delgado-Roche L, Acosta E, Soto Y, Hernández-Matos Y, Olivera A, Fernández-Sánchez E, Vázquez AM. The treatment with an anti-glycosaminoglycan antibody reduces aortic oxidative stress in a rabbit model of atherosclerosis. Free Radic Res. 2013 Apr;47(4):309-15. doi: 10.3109/10715762.2013.772995. Epub 2013 Mar 5. PMID: 23409997.

55. Delves PJ, Roitt IM. The immune system. First of two parts. N Engl J Med. 2000 Jul 6;343(1):37-49. doi: 10.1056/NEJM200007063430107. PMID: 10882768.

56. Delves PJ, Roitt IM. The immune system. Second of two parts. N Engl J Med. 2000 Jul 13;343(2):108-17. doi: 10.1056/NEJM200007133430207. PMID: 10891520.

57. Dempsey PW, Vaidya SA, Cheng G. The art of war: Innate and adaptive immune responses. Cell Mol Life Sci. 2003 Dec;60(12):2604-21. doi: 10.1007/s00018-003-3180-y. PMID: 14685686.

58. Diane A, Pierce WD, Kelly SE, Sokolik S, Borthwick F, Jacome-Sosa M, Mangat R, Pradillo JM, Allan SM, Ruth MR, Field CJ, Hutcheson R, Rocic P, Russell JC, Vine DF, Proctor SD. Mechanisms of Comorbidities Associated With the Metabolic Syndrome: Insights from the JCR:LA-cp Corpulent Rat Strain. Front Nutr. 2016 Oct 10;3:44. doi: 10.3389/fnut.2016.00044. PMID: 27777929; PMCID: PMC5056323.

59. Di Pino A, DeFronzo RA. Insulin Resistance and Atherosclerosis: Implications for Insulin-Sensitizing Agents. Endocr Rev. 2019 Dec 1;40(6):1447-1467. doi: 10.1210/er.2018-00141. PMID: 31050706; PMCID: PMC7445419.

60. Dhara VG, Naik HM, Majewska NI, Betenbaugh MJ. Recombinant Antibody Production in CHO and NS0 Cells: Differences and Similarities. BioDrugs. 2018 Dec;32(6):571-584. doi: 10.1007/s40259-018-0319-9. PMID: 30499081.

61. Doran AC, Meller N, McNamara CA. Role of smooth muscle cells in the initiation and early progression of atherosclerosis. Arterioscler Thromb Vasc Biol. 2008 May;28(5):812-9. doi: 10.1161/ATVBAHA.107.159327. Epub 2008 Feb 14. PMID: 18276911; PMCID: PMC2734458.

62. Dumont J, Euwart D, Mei B, Estes S, Kshirsagar R. Human cell lines for biopharmaceutical manufacturing: history, status, and future perspectives. Crit Rev Biotechnol. 2016 Dec;36(6):1110-1122. doi: 10.3109/07388551.2015.1084266. Epub 2015 Sep 18. PMID: 26383226; PMCID: PMC5152558.

63. Eisenberg S, Levy RI. Lipoprotein metabolism. Adv Lipid Res. 1975;13:1-89. PMID: 174409.

64. Ewing MM, Karper JC, Abdul S, de Jong RC, Peters HA, de Vries MR, Redeker A, Kuiper J, Toes RE, Arens R, Jukema JW, Quax PH. T-cell co-stimulation by CD28-CD80/86 and its negative regulator CTLA-4 strongly influence accelerated atherosclerosis development. Int J Cardiol. 2013 Oct 3;168(3):1965-74. doi: 10.1016/j.ijcard.2012.12.085. Epub 2013 Jan 23. PMID: 23351788.

65. Farnier M. PCSK9: From discovery to therapeutic applications. Arch Cardiovasc Dis. 2014 Jan;107(1):58-66. doi: 10.1016/j.acvd.2013.10.007. Epub 2013 Dec 27. PMID: 24373748.

66. Fatkhullina AR, Peshkova IO, Koltsova EK. The Role of Cytokines in the Development of Atherosclerosis. Biochemistry (Mosc). 2016 Nov;81(11):1358-1370. doi: 10.1134/S0006297916110134. PMID: 27914461; PMCID: PMC5471837.

67. Feingold KR. Introduction to Lipids and Lipoproteins. 2024 Jan 14. In: Feingold KR, Anawalt B, Blackman MR, Boyce A, Chrousos G, Corpas E, de Herder WW, Dhatariya K, Dungan K, Hofland J, Kalra S, Kaltsas G, Kapoor N, Koch C, Kopp P, Korbonits M, Kovacs CS, Kuohung W, Laferrère B, Levy M, McGee EA, McLachlan R, New M, Purnell J, Sahay R, Shah AS, Singer F, Sperling MA, Stratakis CA, Trence DL, Wilson DP, editors. Endotext [Internet]. South Dartmouth (MA): MDText.com, Inc.; 2000–. PMID: 26247089.

68. Fernández-Marrero Y, Hernández T, Roque-Navarro L, Talavera A, Moreno E, Griñán T, Vázquez AM, de Acosta CM, Pérez R, López-Requena A. Switching on cytotoxicity by a single mutation at the heavy chain variable region of an anti-ganglioside antibody. Mol Immunol. 2011 Apr;48(8):1059-67. doi: 10.1016/j.molimm.2011.01.008. PMID: 21306777.

69. Fernández-Marrero Y, Roque-Navarro L, Hernández T, Dorvignit D, Molina-Pérez M, González A, Sosa K, López-Requena A, Pérez R, de Acosta CM. A cytotoxic humanized anti-ganglioside antibody produced in a murine cell line defective of N-glycolylated-glycoconjugates. Immunobiology. 2011 Dec;216(12):1239-47. doi: 10.1016/j.imbio.2011.07.004. Epub 2011 Jul 7. PMID: 21802167.

70. Fernández-Quintero ML, Ljungars A, Waibl F, Greiff V, Andersen JT, Gjølberg TT, Jenkins TP, Voldborg BG, Grav LM, Kumar S, Georges G, Kettenberger H, Liedl KR, Tessier PM, McCafferty J, Laustsen AH. Assessing developability early in the discovery process for novel biologics. MAbs. 2023 Jan-Dec;15(1):2171248. doi: 10.1080/19420862.2023.2171248. PMID: 36823021; PMCID: PMC9980699.

71. Fischinger S, Boudreau CM, Butler AL, Streeck H, Alter G. Sex differences in vaccine-induced humoral immunity. Semin Immunopathol. 2019 Mar;41(2):239-249. doi: 10.1007/s00281-018-0726-5. Epub 2018 Dec 13. PMID: 30547182; PMCID: PMC6373179.

72. Fogelstrand P, Borén J. Retention of atherogenic lipoproteins in the artery wall and its role in atherogenesis. Nutr Metab Cardiovasc Dis. 2012 Jan;22(1):1-7. doi: 10.1016/j.numecd.2011.09.007. PMID: 22176921.

73. Fowlkes JL, Serra DM. Characterization of glycosaminoglycan-binding domains present in insulin-like growth factor-binding protein-3. J Biol Chem. 1996 Jun 21;271(25):14676-9. doi: 10.1074/jbc.271.25.14676. PMID: 8663298.

74. Galkina E, Ley K. Immune and inflammatory mechanisms of atherosclerosis (*). Annu Rev Immunol. 2009;27:165-97. doi: 10.1146/annurev.immunol.021908.132620. PMID: 19302038; PMCID: PMC2734407.

75. Getz GS, Reardon CA. Animal models of atherosclerosis. Arterioscler Thromb Vasc Biol. 2012 May;32(5):1104-15. doi: 10.1161/ATVBAHA.111.237693. Epub 2012 Mar 1. PMID: 22383700; PMCID: PMC3331926.

76. Gisterå A, Hansson GK. The immunology of atherosclerosis. Nat Rev Nephrol. 2017 Jun;13(6):368-380. doi: 10.1038/nrneph.2017.51. Epub 2017 Apr 10. PMID: 28392564.

77. Gisterå A, Ketelhuth DFJ, Malin SG, Hansson GK. Animal Models of Atherosclerosis-Supportive Notes and Tricks of the Trade. Circ Res. 2022 Jun 10;130(12):1869-1887. doi: 10.1161/CIRCRESAHA.122.320263. Epub 2022 Jun 9. PMID: 35679358.

78. Goh JB, Ng SK. Impact of host cell line choice on glycan profile. Crit Rev Biotechnol. 2018 Sep;38(6):851-867. doi: 10.1080/07388551.2017.1416577. Epub 2017 Dec 20. PMID: 29262720.

79. Gupta KK, Ali S, Sanghera RS. Pharmacological Options in Atherosclerosis: A Review of the Existing Evidence. Cardiol Ther. 2019 Jun;8(1):5-20. doi: 10.1007/s40119-018-0123-0. Epub 2018 Dec 12. PMID: 30543029; PMCID: PMC6525235.

80. Gutch M, Kumar S, Razi SM, Gupta KK, Gupta A. Assessment of insulin sensitivity/resistance. Indian J Endocrinol Metab. 2015 Jan-Feb;19(1):160-4. doi: 10.4103/2230-8210.146874. PMID: 25593845; PMCID: PMC4287763.

81. Haji-Ghassemi O, Blackler RJ, Martin Young N, Evans SV. Antibody recognition of carbohydrate epitopes†. Glycobiology. 2015 Sep;25(9):920-52. doi: 10.1093/glycob/cwv037. Epub 2015 Jun 1. PMID: 26033938.

82. Hansson GK. Immune mechanisms in atherosclerosis. Arterioscler Thromb Vasc Biol. 2001 Dec;21(12):1876-90. doi: 10.1161/hq1201.100220. PMID: 11742859.

83. Hansson GK, Libby P, Schönbeck U, Yan ZQ. Innate and adaptive immunity in the pathogenesis of atherosclerosis. Circ Res. 2002 Aug 23;91(4):281-91. doi: 10.1161/01.res.0000029784.15893.10. PMID: 12193460.

84. Hennekens CH. Increasing burden of cardiovascular disease: current knowledge and future directions for research on risk factors. Circulation. 1998 Mar 24;97(11):1095-102. doi: 10.1161/01.cir.97.11.1095. Erratum in: Circulation 1998 May 19;97(19):1995. PMID: 9531257.

85. Herrington W, Lacey B, Sherliker P, Armitage J, Lewington S. Epidemiology of Atherosclerosis and the Potential to Reduce the Global Burden of Atherothrombotic Disease. Circ Res. 2016 Feb 19;118(4):535-46. doi: 10.1161/CIRCRESAHA.115.307611. PMID: 26892956.

86. Herrington W, Lacey B, Sherliker P, Armitage J, Lewington S. Epidemiology of Atherosclerosis and the Potential to Reduce the Global Burden of Atherothrombotic Disease. Circ Res. 2016 (B) Feb 19;118(4):535-46. doi: 10.1161/CIRCRESAHA.115.307611. PMID: 26892956.

87. Hetherington I, Totary-Jain H. Anti-atherosclerotic therapies: Milestones, challenges, and emerging innovations. Mol Ther. 2022 Oct 5;30(10):3106-3117. doi: 10.1016/j.ymthe.2022.08.024. Epub 2022 Sep 5. PMID: 36065464; PMCID: PMC9552812.

88. Hosseini, Samira & Vazquez-Villegas, Patricia & Rito-Palomares, Marco & Martinez-Chapa, Sergio O. (2018). Evaluation of the Detection Results Obtained from ELISA. doi: 10.1007/978-981-10-6766-2_4.

89. Ilhan F, Kalkanli ST. Atherosclerosis and the role of immune cells. World J Clin Cases. 2015 Apr 16;3(4):345-52. doi: 10.12998/wjcc.v3.i4.345. PMID: 25879006; PMCID: PMC4391004.

91. Insull W Jr. The pathology of atherosclerosis: plaque development and plaque responses to medical treatment. Am J Med. 2009 Jan;122(1 Suppl):S3-S14. doi: 10.1016/j.amjmed.2008.10.013. PMID: 19110086.

92. Institute of Medicine (US) Committee on Preventing the Global Epidemic of Cardiovascular Disease: Meeting the Challenges in Developing Countries; Fuster V, Kelly BB, editors. Promoting Cardiovascular Health in the Developing World: A Critical Challenge to Achieve Global Health. Washington (DC): National Academies Press (US); 2010. 2, Epidemiology of Cardiovascular Disease. Available from: https://www.ncbi.nlm.nih.gov/books/NBK45688/

93. Isles HM, Herman KD, Robertson AL, Loynes CA, Prince LR, Elks PM, Renshaw SA. The CXCL12/CXCR4 Signaling Axis Retains Neutrophils at Inflammatory Sites in Zebrafish. Front Immunol. 2019 Jul 31;10:1784. doi: 10.3389/fimmu.2019.01784. PMID: 31417560; PMCID: PMC6684839.

94. Iwasaki A, Medzhitov R. Control of adaptive immunity by the innate immune system. Nat Immunol. 2015 Apr;16(4):343-53. doi: 10.1038/ni.3123. PMID: 25789684; PMCID: PMC4507498.

95. Janeway CA Jr, Travers P, Walport M, et al. Immunobiology: The Immune System in Health and Disease. 5th edition. New York: Garland Science; 2001. Principles of innate and adaptive immunity. Available from: https://www.ncbi.nlm.nih.gov/books/NBK27090/.

96. Ji E, Lee S. Antibody-Based Therapeutics for Atherosclerosis and Cardiovascular Diseases. Int J Mol Sci. 2021 May 28;22(11):5770. doi: 10.3390/ijms22115770. PMID: 34071276; PMCID: PMC8199089.

97. Kanters E, Pasparakis M, Gijbels MJ, Vergouwe MN, Partouns-Hendriks I, Fijneman RJ, Clausen BE, Förster I, Kockx MM, Rajewsky K, Kraal G, Hofker MH, de Winther MP. Inhibition of NF-kappaB activation in macrophages increases atherosclerosis in LDL receptor-deficient mice. J Clin Invest. 2003 Oct;112(8):1176-85. doi: 10.1172/JCI18580. PMID: 14561702; PMCID: PMC213488.

98. Karasawa T, Takahashi M. Role of NLRP3 Inflammasomes in Atherosclerosis. J Atheroscler Thromb. 2017 May 1;24(5):443-451. doi: 10.5551/jat.RV17001. Epub 2017 Mar 4. PMID: 28260724; PMCID: PMC5429158.

99. Khalil MF, Wagner WD, Goldberg IJ. Molecular interactions leading to lipoprotein retention and the initiation of atherosclerosis. Arterioscler Thromb Vasc Biol. 2004 Dec;24(12):2211-8. doi: 10.1161/01.ATV.0000147163.54024.70. Epub 2004 Oct 7. PMID: 15472124.

100. Kim HJ, Park JS, Kwon SR. Development of a stringent ELISA protocol to evaluate anti-viral hemorrhagic septicemia virus-specific antibodies in olive flounder Paralichthys olivaceus with improved specificity. J Microbiol. 2015 Jul;53(7):481-5. doi: 10.1007/s12275-015-5101-9. Epub 2015 Jun 27. PMID: 26115998.

101. Kim K, Ginsberg HN, Choi SH. New, Novel Lipid-Lowering Agents for Reducing Cardiovascular Risk: Beyond Statins. Diabetes Metab J. 2022 Jul;46(4):517-532. doi: 10.4093/dmj.2022.0198. Epub 2022 Jul 27. Erratum in: Diabetes Metab J. 2022 Sep;46(5):817-818. PMID: 35929170; PMCID: PMC9353557.

102. Klein SL, Flanagan KL. Sex differences in immune responses. Nat Rev Immunol. 2016 Oct;16(10):626-38. doi: 10.1038/nri.2016.90. Epub 2016 Aug 22. PMID: 27546235.

103. Krishnamurthy, Varun & Grande-Allen, Kathryn. (2018). The Role of Proteoglycans and Glycosaminoglycans in Heart Valve Biomechanics. doi: 10.1007/978-3-030-01993-8_3.

104. Kyaw T, Tay C, Khan A, Dumouchel V, Cao A, To K, Kehry M, Dunn R, Agrotis A, Tipping P, Bobik A, Toh BH. Conventional B2 B cell depletion ameliorates whereas its adoptive transfer aggravates atherosclerosis. J Immunol. 2010 Oct 1;185(7):4410-9. doi: 10.4049/jimmunol.1000033. Epub 2010 Sep 3. PMID: 20817865.

105. Lang RM, Badano LP, Mor-Avi V, Afilalo J, Armstrong A, Ernande L, Flachskampf FA, Foster E, Goldstein SA, Kuznetsova T, Lancellotti P, Muraru D, Picard MH, Rietzschel ER, Rudski L, Spencer KT, Tsang W, Voigt JU. Recommendations for cardiac chamber quantification by echocardiography in adults: an update from the American Society of Echocardiography and the European Association of Cardiovascular Imaging. J Am Soc Echocardiogr. 2015 Jan;28(1):1-39.e14. doi: 10.1016/j.echo.2014.10.003. PMID: 25559473.

106. Langsted A, Nordestgaard BG. Nonfasting versus fasting lipid profile for cardiovascular risk prediction. Pathology. 2019 Feb;51(2):131-141. doi: 10.1016/j.pathol.2018.09.062. Epub 2018 Dec 3. PMID: 30522787.

107. Lau LL, Jiang J, Shen H. In vivo modulation of T cell responses and protective immunity by TCR antagonism during infection. J Immunol. 2005 Jun 15;174(12):7970-6. doi: 10.4049/jimmunol.174.12.7970. PMID: 15944303.

108. Lechner K, von Schacky C, McKenzie AL, Worm N, Nixdorff U, Lechner B, Kränkel N, Halle M, Krauss RM, Scherr J. Lifestyle factors and high-risk atherosclerosis: Pathways and mechanisms beyond traditional risk factors. Eur J Prev Cardiol. 2020 Mar;27(4):394-406. doi: 10.1177/2047487319869400. Epub 2019 Aug 13. PMID: 31408370; PMCID: PMC7065445.

109. Lent-Schochet D, Jialal I. Biochemistry, Lipoprotein Metabolism. [Updated 2023 Jan 16]. In: StatPearls [Internet]. Treasure Island (FL): StatPearls Publishing; 2024 Jan-. Available from: https://www.ncbi.nlm.nih.gov/books/NBK553193/

110. Lewis SJ. Prevention and treatment of atherosclerosis: a practitioner's guide for 2008. Am J Med. 2009 Jan;122(1 Suppl):S38-50. doi: 10.1016/j.amjmed.2008.10.016. PMID: 19110087.

111. Li F, Vijayasankaran N, Shen AY, Kiss R, Amanullah A. Cell culture processes for monoclonal antibody production. MAbs. 2010 Sep-Oct;2(5):466-79. doi: 10.4161/mabs.2.5.12720. Epub 2010 Sep 1. PMID: 20622510; PMCID: PMC2958569.

112. Libby P, Buring JE, Badimon L, Hansson GK, Deanfield J, Bittencourt MS, Tokgözoğlu L, Lewis EF. Atherosclerosis. Nat Rev Dis Primers. 2019 Aug 16;5(1):56. doi: 10.1038/s41572-019-0106-z. PMID: 31420554.

113. Libby P. The forgotten majority: unfinished business in cardiovascular risk reduction. J Am Coll Cardiol. 2005 Oct 4;46(7):1225-8. doi: 10.1016/j.jacc.2005.07.006. PMID: 16198835.

114. Lim Y, Boster J. Obesity and Comorbid Conditions. [Updated 2023 Aug 28]. In: StatPearls [Internet]. Treasure Island (FL): StatPearls Publishing; 2024 Jan-. Available from: https://www.ncbi.nlm.nih.gov/books/NBK574535/

115. Liu X, Su J, Zhou H, Zeng Z, Li Z, Xiao Z, Zhao M. Collagen VI antibody reduces atherosclerosis by activating monocyte/macrophage polarization in ApoE-/- mice. Int Immunopharmacol. 2022 Oct;111:109100. doi: 10.1016/j.intimp.2022.109100. Epub 2022 Aug 3. PMID: 35932614.

116. López-Requena A, De Acosta CM, Moreno E, González M, Puchades Y, Talavera A, Vispo NS, Vázquez AM, Pérez R. Gangliosides, Ab1 and Ab2 antibodies I. Towards a molecular dissection of an idiotype-anti-idiotype system. Mol Immunol. 2007 Jan;44(4):423-33. doi: 10.1016/j.molimm.2006.02.020. Epub 2006 Apr 3. PMID: 16581129.

117. Lundberg AM, Hansson GK. Innate immune signals in atherosclerosis. Clin Immunol. 2010 Jan;134(1):5-24. doi: 10.1016/j.clim.2009.07.016. Epub 2009 Sep 9. PMID: 19740706.

118. Ma SD, Mussbacher M, Galkina EV. Functional Role of B Cells in Atherosclerosis. Cells. 2021 Jan 29;10(2):270. doi: 10.3390/cells10020270. PMID: 33572939; PMCID: PMC7911276.

119. Makover ME, Shapiro MD, Toth PP. There is urgent need to treat atherosclerotic cardiovascular disease risk earlier, more intensively, and with greater precision: A review of current practice and recommendations for improved effectiveness. Am J Prev Cardiol. 2022 Aug 6;12:100371. doi: 10.1016/j.ajpc.2022.100371. PMID: 36124049; PMCID: PMC9482082.

120. Malm M, Saghaleyni R, Lundqvist M, Giudici M, Chotteau V, Field R, Varley PG, Hatton D, Grassi L, Svensson T, Nielsen J, Rockberg J. Evolution from adherent to suspension: systems biology of HEK293 cell line development. Sci Rep. 2020 Nov 4;10(1):18996. doi: 10.1038/s41598-020-76137-8. Erratum in: Sci Rep. 2021 Mar 2;11(1):5407. PMID: 33149219; PMCID: PMC7642379.

121. Mangat R, Warnakula S, Borthwick F, Hassanali Z, Uwiera RR, Russell JC, Cheeseman CI, Vine DF, Proctor SD. Arterial retention of remnant lipoproteins ex vivo is increased in insulin resistance because of increased arterial biglycan and production of cholesterol-rich atherogenic particles that can be improved by ezetimibe in the JCR:LA-cp rat. J Am Heart Assoc. 2012 Oct;1(5):e003434. doi: 10.1161/JAHA.112.003434. Epub 2012 Oct 25. PMID: 23316299; PMCID: PMC3541624.

122. Marques LR, Diniz TA, Antunes BM, Rossi FE, Caperuto EC, Lira FS, Gonçalves DC. Reverse Cholesterol Transport: Molecular Mechanisms and the Non-medical Approach to Enhance HDL Cholesterol. Front Physiol. 2018 May 15;9:526. doi: 10.3389/fphys.2018.00526. PMID: 29867567; PMCID: PMC5962737.

123. Marshall JS, Warrington R, Watson W, Kim HL. An introduction to immunology and immunopathology. Allergy Asthma Clin Immunol. 2018 Sep 12;14(Suppl 2):49. doi: 10.1186/s13223-018-0278-1. PMID: 30263032; PMCID: PMC6156898.

124. Mateo C, Moreno E, Amour K, Lombardero J, Harris W, Pérez R. Humanization of a mouse monoclonal antibody that blocks the epidermal growth factor receptor: recovery of antagonistic activity. Immunotechnology. 1997 Mar;3(1):71-81. doi: 10.1016/s1380-2933(97)00065-1. PMID: 9154469.

125. Matthews DR, Hosker JP, Rudenski AS, Naylor BA, Treacher DF, Turner RC. Homeostasis model assessment: insulin resistance and beta-cell function from fasting plasma glucose and insulin concentrations in man. Diabetologia. 1985 Jul;28(7):412-9. doi: 10.1007/BF00280883. PMID: 3899825.

126. McFarland AJ, Anoopkumar-Dukie S, Arora DS, Grant GD, McDermott CM, Perkins AV, Davey AK. Molecular mechanisms underlying the effects of statins in the central nervous system. Int J Mol Sci. 2014 Nov 10;15(11):20607-37. doi: 10.3390/ijms151120607. PMID: 25391045; PMCID: PMC4264186.

127. McFarlane SI, Banerji M, Sowers JR. Insulin resistance and cardiovascular disease. J Clin Endocrinol Metab. 2001 Feb;86(2):713-8. doi: 10.1210/jcem.86.2.7202. PMID: 11158035.

128. Minelli S, Minelli P, Montinari MR. Reflections on Atherosclerosis: Lesson from the Past and Future Research Directions. J Multidiscip Healthc. 2020 Jul 17;13:621-633. doi: 10.2147/JMDH.S254016. PMID: 32801729; PMCID: PMC7398886.

129. Miteva K, Madonna R, De Caterina R, Van Linthout S. Innate and adaptive immunity in atherosclerosis. Vascul Pharmacol. 2018 Apr 22:S1537-1891(17)30464-0. doi: 10.1016/j.vph.2018.04.006. Epub ahead of print. PMID: 29684642.

130. Mohammad-Rezaei, Mina & Arefnezhad, Reza & Ahmadi, Reza & Abdollahpour-Alitappeh, Meghdad & Mirzaei, Yousef & Arjmand, Mohammad Hassan & Ferns, Gordon & Ferns, A & Bashash, Davood & Bagheri, Nader. (2020). An overview of the innate and adaptive immune system in atherosclerosis. International Union of Biochemistry and Molecular Biology Life. 73. 10.1002/iub.2425.

131. Moore KJ, Sheedy FJ, Fisher EA. Macrophages in atherosclerosis: a dynamic balance. Nat Rev Immunol. 2013 Oct;13(10):709-21. doi: 10.1038/nri3520. Epub 2013 Sep 2. PMID: 23995626; PMCID: PMC4357520.

132. Mould DR, Green B. Pharmacokinetics and pharmacodynamics of monoclonal antibodies: concepts and lessons for drug development. BioDrugs. 2010 Feb 1;24(1):23-39. doi: 10.2165/11530560-000000000-00000. PMID: 20055530.

133. Nakashima Y, Wight TN, Sueishi K. Early atherosclerosis in humans: role of diffuse intimal thickening and extracellular matrix proteoglycans. Cardiovasc Res. 2008

Jul 1;79(1):14-23. doi: 10.1093/cvr/cvn099. Epub 2008 Apr 22. PMID: 18430750.

134. Netea MG, Joosten LA. Inflammasome inhibition: putting out the fire. Cell Metab. 2015 Apr 7;21(4):513-4. doi: 10.1016/j.cmet.2015.03.012. PMID: 25863243.

135. Nidorf SM, Fiolet ATL, Mosterd A, Eikelboom JW, Schut A, Opstal TSJ, The SHK, Xu XF, Ireland MA, Lenderink T, Latchem D, Hoogslag P, Jerzewski A, Nierop P, Whelan A, Hendriks R, Swart H, Schaap J, Kuijper AFM, van Hessen MWJ, Saklani P, Tan I, Thompson AG, Morton A, Judkins C, Bax WA, Dirksen M, Alings M, Hankey GJ, Budgeon CA, Tijssen JGP, Cornel JH, Thompson PL; LoDoCo2 Trial Investigators. Colchicine in Patients with Chronic Coronary Disease. N Engl J Med. 2020 Nov 5;383(19):1838-1847. doi: 10.1056/NEJMoa2021372. Epub 2020 Aug 31. PMID: 32865380.

136. Nidorf SM, Eikelboom JW, Budgeon CA, Thompson PL. Low-dose colchicine for secondary prevention of cardiovascular disease. J Am Coll Cardiol. 2013 Jan 29;61(4):404-410. doi: 10.1016/j.jacc.2012.10.027. Epub 2012 Dec 19. PMID: 23265346.

137. Nigro J, Osman N, Dart AM, Little PJ. Insulin resistance and atherosclerosis. Endocr Rev. 2006 May;27(3):242-59. doi: 10.1210/er.2005-0007. Epub 2006 Feb 21. PMID: 16492903.

138. Nordestgaard BG, Langsted A, Mora S, Kolovou G, Baum H, Bruckert E, Watts GF, Sypniewska G, Wiklund O, Borén J, Chapman MJ, Cobbaert C, Descamps OS, von Eckardstein A, Kamstrup PR, Pulkki K, Kronenberg F, Remaley AT, Rifai N, Ros E, Langlois M; European Atherosclerosis Society (EAS) and the European Federation of Clinical Chemistry and Laboratory Medicine (EFLM) joint consensus initiative. Fasting is not routinely required for determination of a lipid profile: clinical and laboratory implications including flagging at desirable concentration cut-points-a joint consensus statement from the European Atherosclerosis Society and European Federation of Clinical Chemistry and Laboratory Medicine. Eur Heart J. 2016 Jul 1;37(25):1944-58. doi: 10.1093/eurheartj/ehw152. Epub 2016 Apr 26. PMID: 27122601; PMCID: PMC4929379.

139. Olsson U, Egnell AC, Lee MR, Lundén GO, Lorentzon M, Salmivirta M, Bondjers G, Camejo G. Changes in matrix proteoglycans induced by insulin and fatty acids in hepatic cells may contribute to dyslipidemia of insulin resistance. Diabetes. 2001 Sep;50(9):2126-32. doi: 10.2337/diabetes.50.9.2126. PMID: 11522680.

140. Ormazabal V, Nair S, Elfeky O, Aguayo C, Salomon C, Zuñiga FA. Association between insulin resistance and the development of cardiovascular disease. Cardiovasc Diabetol. 2018 Aug 31;17(1):122. doi: 10.1186/s12933-018-0762-4. PMID: 30170598; PMCID: PMC6119242.

141. Pabst R. The pig as a model for immunology research. Cell Tissue Res. 2020 May;380(2):287-304. doi: 10.1007/s00441-020-03206-9. Epub 2020 Apr 30. PMID: 32356014; PMCID: PMC7223737.

142. Paigen B, Holmes PA, Novak EK, Swank RT. Analysis of atherosclerosis susceptibility in mice with genetic defects in platelet function. Arteriosclerosis. 1990 Jul-Aug;10(4):648-52. doi: 10.1161/01.atv.10.4.648. PMID: 2369371.

143. Palmas W, Ma S, Psaty B, Goff DC Jr, Darwin C, Barr RG. Antihypertensive medications and C-reactive protein in the multi-ethnic study of atherosclerosis. Am J Hypertens. 2007 Mar;20(3):233-41. doi: 10.1016/j.amjhyper.2006.08.006. PMID: 17324732.

144. Pan SD, Zhu LL, Chen M, Xia P, Zhou Q. Weight-based dosing in medication use: what should we know? Patient Prefer Adherence. 2016 Apr 12;10:549-60. doi: 10.2147/PPA.S103156. PMID: 27110105; PMCID: PMC4835122.

145. Paszkowiak JJ, Dardik A. Arterial wall shear stress: observations from the bench to the bedside. Vasc Endovascular Surg. 2003 Jan-Feb;37(1):47-57. doi: 10.1177/153857440303700107. PMID: 12577139.

146. Paulson KE, Zhu SN, Chen M, Nurmohamed S, Jongstra-Bilen J, Cybulsky MI. Resident intimal dendritic cells accumulate lipid and contribute to the initiation of atherosclerosis. Circ Res. 2010 Feb 5;106(2):383-90. doi: 10.1161/CIRCRESAHA.109.210781. Epub 2009 Nov 5. PMID: 19893012.

147. Pearson GJ, Thanassoulis G, Anderson TJ, Barry AR, Couture P, Dayan N, Francis GA, Genest J, Grégoire J, Grover SA, Gupta M, Hegele RA, Lau D, Leiter LA, Leung AA, Lonn E, Mancini GBJ, Manjoo P, McPherson R, Ngui D, Piché ME, Poirier P, Sievenpiper J, Stone J, Ward R, Wray W. 2021 Canadian Cardiovascular Society Guidelines for the Management of Dyslipidemia for the Prevention of Cardiovascular Disease in Adults. Can J Cardiol. 2021 Aug;37(8):1129-1150. doi: 10.1016/j.cjca.2021.03.016. Epub 2021 Mar 26. PMID: 33781847.

148. Pedro-Botet J, Climent E, Benaiges D. Atherosclerosis and inflammation. New therapeutic approaches. Med Clin (Barc). 2020 Sep 25;155(6):256-262. English, Spanish. doi: 10.1016/j.medcli.2020.04.024. Epub 2020 Jun 20. PMID: 32571617.

149. Pradhan AD, Aday AW, Rose LM, Ridker PM. Residual Inflammatory Risk on Treatment With PCSK9 Inhibition and Statin Therapy. Circulation. 2018 Jul 10;138(2):141-149. doi: 10.1161/CIRCULATIONAHA.118.034645. Epub 2018 May 1. PMID: 29716940; PMCID: PMC8108606.

150. Proctor SD, Mamo JC. Retention of fluorescent-labelled chylomicron remnants within the intima of the arterial wall--evidence that plaque cholesterol may be derived from post-prandial lipoproteins. Eur J Clin Invest. 1998 Jun;28(6):497-503. doi: 10.1046/j.1365-2362.1998.00317.x. PMID: 9693943.

151. Public Health Agency of Canada. Tracking heart disease and stroke in Canada, 2009, viii. Ottawa: Public Health Agency of Canada; 2009).

152. Rafieian-Kopaei M, Setorki M, Doudi M, Baradaran A, Nasri H. Atherosclerosis: process, indicators, risk factors and new hopes. Int J Prev Med. 2014 Aug;5(8):927-46. PMID: 25489440; PMCID: PMC4258672.

153. Ramji DP, Davies TS. Cytokines in atherosclerosis: Key players in all stages of disease and promising therapeutic targets. Cytokine Growth Factor Rev. 2015 Dec;26(6):673-85. doi: 10.1016/j.cytogfr.2015.04.003. Epub 2015 May 12. PMID: 26005197; PMCID: PMC4671520.

154. Razani B, Chakravarthy MV, Semenkovich CF. Insulin resistance and atherosclerosis. Endocrinol Metab Clin North Am. 2008 Sep;37(3):603-21, viii. doi: 10.1016/j.ecl.2008.05.001. PMID: 18775354; PMCID: PMC2639785.

155. Reaven GM. Insulin resistance: the link between obesity and cardiovascular disease. Med Clin North Am. 2011 Sep;95(5):875-92. doi: 10.1016/j.mcna.2011.06.002. PMID: 21855697.

156. Ricci R, Sumara G, Sumara I, Rozenberg I, Kurrer M, Akhmedov A, Hersberger M, Eriksson U, Eberli FR, Becher B, Borén J, Chen M, Cybulsky MI, Moore KJ, Freeman MW, Wagner EF, Matter CM, Lüscher TF. Requirement of JNK2 for scavenger receptor A-mediated foam cell formation in atherogenesis. Science. 2004 Nov 26;306(5701):1558-61. doi: 10.1126/science.1101909. PMID: 15567863.

157. Richardson M, Schmidt AM, Graham SE, Achen B, DeReske M, Russell JC. Vasculopathy and insulin resistance in the JCR:LA-cp rat. Atherosclerosis. 1998 May;138(1):135-46. doi: 10.1016/s0021-9150(98)00012-4. PMID: 9678779.

158. Ridker PM, Everett BM, Thuren T, MacFadyen JG, Chang WH, Ballantyne C, Fonseca F, Nicolau J, Koenig W, Anker SD, Kastelein JJP, Cornel JH, Pais P, Pella D, Genest J, Cifkova R, Lorenzatti A, Forster T, Kobalava Z, Vida-Simiti L, Flather M, Shimokawa H, Ogawa H, Dellborg M, Rossi PRF, Troquay RPT, Libby P, Glynn RJ; CANTOS Trial Group. Antiinflammatory Therapy with Canakinumab for Atherosclerotic Disease. N Engl J Med. 2017 Sep 21;377(12):1119-1131. doi: 10.1056/NEJMoa1707914. Epub 2017 Aug 27. PMID: 28845751.

159. Rikhi R, Shapiro MD. Newer and Emerging LDL-C Lowering Agents and Implications for ASCVD Residual Risk. J Clin Med. 2022 Aug 8;11(15):4611. doi: 10.3390/jcm11154611. PMID: 35956226; PMCID: PMC9369522.

160. Ritskes-Hoitinga J, Beynen AC. Atherosclerosis in the rat. Artery. 1988;16(1):25-50. PMID: 3061372.

161. Rodrigues ME, Costa AR, Henriques M, Cunnah P, Melton DW, Azeredo J, Oliveira R. Advances and drawbacks of the adaptation to serum-free culture of CHO-K1

cells for monoclonal antibody production. Appl Biochem Biotechnol. 2013 Feb;169(4):1279-91. doi: 10.1007/s12010-012-0068-z. Epub 2013 Jan 11. PMID: 23306891.

162. Rosenson RS, Hegele RA, Fazio S, Cannon CP. The Evolving Future of PCSK9 Inhibitors. J Am Coll Cardiol. 2018 Jul 17;72(3):314-329. doi: 10.1016/j.jacc.2018.04.054. Epub 2018 Jul 9. PMID: 30012326.

163. Roy P, Orecchioni M, Ley K. How the immune system shapes atherosclerosis: roles of innate and adaptive immunity. Nat Rev Immunol. 2022 Apr;22(4):251-265. doi: 10.1038/s41577-021-00584-1. Epub 2021 Aug 13. PMID: 34389841; PMCID: PMC10111155.

164. Roth GA, Mensah GA, Johnson CO, Addolorato G, Ammirati E, Baddour LM, Barengo NC, Beaton AZ, Benjamin EJ, Benziger CP, Bonny A, Brauer M, Brodmann M, Cahill TJ, Carapetis J, Catapano AL, Chugh SS, Cooper LT, Coresh J, Criqui M, DeCleene N, Eagle KA, Emmons-Bell S, Feigin VL, Fernández-Solà J, Fowkes G, Gakidou E, Grundy SM, He FJ, Howard G, Hu F, Inker L, Karthikeyan G, Kassebaum N, Koroshetz W, Lavie C, Lloyd-Jones D, Lu HS, Mirijello A, Temesgen AM, Mokdad A, Moran AE, Muntner P, Narula J, Neal B, Ntsekhe M, Moraes de Oliveira G, Otto C, Owolabi M, Pratt M, Rajagopalan S, Reitsma M, Ribeiro ALP, Rigotti N, Rodgers A, Sable C, Shakil S, Sliwa-Hahnle K, Stark B, Sundström J, Timpel P, Tleyjeh IM, Valgimigli M, Vos T, Whelton PK, Yacoub M, Zuhlke L, Murray C, Fuster V; GBD-NHLBI-JACC Global Burden of Cardiovascular Diseases Writing Group. Global Burden of Cardiovascular Diseases and Risk Factors, 1990-2019: Update From the GBD 2019 Study. J Am Coll Cardiol. 2020 Dec 22;76(25):2982-3021. doi: 10.1016/j.jacc.2020.11.010. Erratum in: J Am Coll Cardiol. 2021 Apr 20;77(15):1958-1959. PMID: 33309175; PMCID: PMC7755038.

165. Russell JC, Graham SE, Richardson M. Cardiovascular disease in the JCR:LA-cp rat. Mol Cell Biochem. 1998 Nov;188(1-2):113-26. PMID: 9823017.

166. Russell JC, Proctor SD. Small animal models of cardiovascular disease: tools for the study of the roles of metabolic syndrome, dyslipidemia, and atherosclerosis. Cardiovasc Pathol. 2006 Nov-Dec;15(6):318-30. doi: 10.1016/j.carpath.2006.09.001. PMID: 17113010.

167. Russell JC, Shillabeer G, Bar-Tana J, Lau DC, Richardson M, Wenzel LM, Graham SE, Dolphin PJ. Development of insulin resistance in the JCR:LA-cp rat: role of triacylglycerols and effects of MEDICA 16. Diabetes. 1998 May;47(5):770-8. doi: 10.2337/diabetes.47.5.770. PMID: 9588449.

168. Sage AP, Mallat Z. Multiple potential roles for B cells in atherosclerosis. Ann Med. 2014 Aug;46(5):297-303. doi: 10.3109/07853890.2014.900272. Epub 2014 May 9. PMID: 24813455.

169. Sage AP, Tsiantoulas D, Binder CJ, Mallat Z. The role of B cells in atherosclerosis. Nat Rev Cardiol. 2019 Mar;16(3):180-196. doi: 10.1038/s41569-018-0106-9. PMID: 30410107.

170. Sarduy R, Brito V, Castillo A, Soto Y, Griñán T, Marleau S, Vázquez AM. Dose-Dependent Induction of an Idiotypic Cascade by Anti-Glycosaminoglycan Monoclonal Antibody in apoE-/- Mice: Association with Atheroprotection. Front Immunol. 2017 Mar 3;8:232. doi: 10.3389/fimmu.2017.00232. PMID: 28316603; PMCID: PMC5334371.

171. Schenten D, Medzhitov R. The control of adaptive immune responses by the innate immune system. Adv Immunol. 2011;109:87-124. doi: 10.1016/B978-0-12-387664-5.00003-0. PMID: 21569913.

172. Schiller NK, Boisvert WA, Curtiss LK. Inflammation in atherosclerosis: lesion formation in LDL receptor-deficient mice with perforin and Lyst(beige) mutations. Arterioscler Thromb Vasc Biol. 2002 Aug 1;22(8):1341-6. doi: 10.1161/01.atv.0000024082.46387.38. PMID: 12171798.

173. Schoeler M, Caesar R. Dietary lipids, gut microbiota and lipid metabolism. Rev Endocr Metab Disord. 2019 Dec;20(4):461-472. doi: 10.1007/s11154-019-09512-0. PMID: 31707624; PMCID: PMC6938793

174. Schofield D. HEK293 cells versus CHO cells. Evitria [Internet]. Published January 13, 2022. Available from: https://www.evitria.com/journal/cho-cells/hek293-cells-vs-cho-cells/.

175. Schüttler D, Tomsits P, Bleyer C, Vlcek J, Pauly V, Hesse N, Sinner M, Merkus D, Hamers J, Kääb S, Clauss S. A practical guide to setting up pig models for cardiovascular catheterization, electrophysiological assessment and heart disease research. Lab Anim (NY). 2022 Feb;51(2):46-67. doi: 10.1038/s41684-021-00909-6. Epub 2022 Jan 27. PMID: 35087256.

176. Shah P, Bajaj S, Virk H, Bikkina M, Shamoon F. Rapid Progression of Coronary Atherosclerosis: A Review. Thrombosis. 2015;2015:634983. doi: 10.1155/2015/634983. Epub 2015 Dec 28. PMID: 26823982; PMCID: PMC4707354.

177. Shapiro MD, Fazio S. From Lipids to Inflammation: New Approaches to Reducing Atherosclerotic Risk. Circ Res. 2016 Feb 19;118(4):732-49. doi: 10.1161/CIRCRESAHA.115.306471. PMID: 26892970.

178. Sharma M, Schlegel MP, Afonso MS, Brown EJ, Rahman K, Weinstock A, Sansbury BE, Corr EM, van Solingen C, Koelwyn GJ, Shanley LC, Beckett L, Peled D, Lafaille JJ, Spite M, Loke P, Fisher EA, Moore KJ. Regulatory T Cells License Macrophage Pro-Resolving Functions During Atherosclerosis Regression. Circ Res. 2020 Jul 17;127(3):335-353. doi: 10.1161/CIRCRESAHA.119.316461. Epub 2020 Apr 27. PMID: 32336197; PMCID: PMC7367765.

179. Silvis MJM, Demkes EJ, Fiolet ATL, Dekker M, Bosch L, van Hout GPJ, Timmers L, de Kleijn DPV. Immunomodulation of the NLRP3 Inflammasome in Atherosclerosis, Coronary Artery Disease, and Acute Myocardial Infarction. J Cardiovasc Transl Res. 2021 Feb;14(1):23-34. doi: 10.1007/s12265-020-10049-w. Epub 2020 Jul 9. PMID: 32648087; PMCID: PMC7892681.

180. Sirtori CR. The pharmacology of statins. Pharmacol Res. 2014 Oct;88:3-11. doi: 10.1016/j.phrs.2014.03.002. Epub 2014 Mar 20. PMID: 24657242.

181. Skaggs BJ, Hahn BH, McMahon M. Accelerated atherosclerosis in patients with SLE--mechanisms and management. Nat Rev Rheumatol. 2012 Feb 14;8(4):214-23. doi: 10.1038/nrrheum.2012.14. PMID: 22331061; PMCID: PMC3765069.

182. Smith JD, Trogan E, Ginsberg M, Grigaux C, Tian J, Miyata M. Decreased atherosclerosis in mice deficient in both macrophage colony-stimulating factor (op) and apolipoprotein E. Proc Natl Acad Sci U S A. 1995 Aug 29;92(18):8264-8. doi: 10.1073/pnas.92.18.8264. PMID: 7667279; PMCID: PMC41137.

183. Soehnlein O. Multiple roles for neutrophils in atherosclerosis. Circ Res. 2012 Mar 16;110(6):875-88. doi: 10.1161/CIRCRESAHA.111.257535. PMID: 22427325.

184. Son DH, Ha HS, Park HM, Kim HY, Lee YJ. New markers in metabolic syndrome. Adv Clin Chem. 2022;110:37-71. doi: 10.1016/bs.acc.2022.06.002. Epub 2022 Jul 25. PMID: 36210076.

185. Song P, Fang Z, Wang H, Cai Y, Rahimi K, Zhu Y, Fowkes FGR, Fowkes FJI, Rudan I. Global and regional prevalence, burden, and risk factors for carotid atherosclerosis: a systematic review, meta-analysis, and modelling study. Lancet Glob Health. 2020 May;8(5):e721-e729. doi: 10.1016/S2214-109X(20)30117-0. PMID: 32353319.

186. Soto Y, Acosta E, Delgado L, Pérez A, Falcón V, Bécquer MA, Fraga Á, Brito V, Álvarez I, Griñán T, Fernández-Marrero Y, López-Requena A, Noa M, Fernández E, Vázquez AM. Antiatherosclerotic effect of an antibody that binds to extracellular matrix glycosaminoglycans. Arterioscler Thromb Vasc Biol. 2012 Mar;32(3):595-604. doi: 10.1161/ATVBAHA.111.238659. Epub 2012 Jan 19. PMID: 22267481.

187. Soto Y, Mesa N, Alfonso Y, Pérez A, Batlle F, Griñán T, Pino A, Viera J, Frómeta M, Brito V, Olivera A, Zayas F, Vázquez AM. Targeting arterial wall sulfated glycosaminoglycans in rabbit atherosclerosis with a mouse/human chimeric antibody. MAbs. 2014;6(5):1340-6. doi: 10.4161/mabs.29970. Epub 2014 Oct 30. PMID: 25517318; PMCID: PMC4622498.

188. Soto Y, Hernández A, Sarduy R, Brito V, Marleau S, Vine D, Vázquez A, Proctor S. Novel chP3R99 mAb reduces subendothelial retention of atherogenic lipoproteins in Insulin-Resistant rats: Acute treatment versus long-term protection as an idiotypic vaccine for atherosclerosis. Preprint 2023 Sept. doi: 10.1101/2023.08.30.555546.

189. Staprans I, Felts JM. Isolation and characterization of glycosaminoglycans in human plasma. J Clin Invest. 1985 Nov;76(5):1984-91. doi: 10.1172/JCI112198. PMID: 4056061; PMCID: PMC424260.

190. Subbiahanadar-Chelladurai K, Selvan Christyraj JD, Rajagopalan K, Yesudhason BV, Venkatachalam S, Mohan M, Chellathurai Vasantha N, Selvan Christyraj JRS. Alternative to FBS in animal cell culture - An overview and future perspective. Heliyon. 2021 Jul 28;7(8):e07686. doi: 10.1016/j.heliyon.2021.e07686. PMID: 34401573; PMCID: PMC8349753.

191. Subramanian M, Tabas I. Dendritic cells in atherosclerosis. Semin Immunopathol. 2014 Jan;36(1):93-102. doi: 10.1007/s00281-013-0400-x. Epub 2013 Nov 6. PMID: 24196454; PMCID: PMC3946524.

192. Syed Ikmal SI, Zaman Huri H, Vethakkan SR, Wan Ahmad WA. Potential biomarkers of insulin resistance and atherosclerosis in type 2 diabetes mellitus patients with coronary artery disease. Int J Endocrinol. 2013;2013:698567. doi: 10.1155/2013/698567. Epub 2013 Oct 24. PMID: 24282409; PMCID: PMC3824310.

193. Tall AR. An overview of reverse cholesterol transport. Eur Heart J. 1998 Feb;19 Suppl A:A31-5. PMID: 9519340.

194. Tannock LR, King VL. Proteoglycan mediated lipoprotein retention: a mechanism of diabetic atherosclerosis. Rev Endocr Metab Disord. 2008 Dec;9(4):289-300. doi: 10.1007/s11154-008-9078-0. Epub 2008 Jun 27. PMID: 18584330.

195. Tao K, Sakata R, Iguro Y, Ueno T, Ueno M, Tanaka Y, Otsuji Y, Tei C. Abnormal Tei index predicts poor left ventricular mass regression and survival after AVR in aortic stenosis patients. J Cardiol. 2009 Apr;53(2):240-7. doi: 10.1016/j.jjcc.2008.11.014. Epub 2009 Feb 11. PMID: 19304129.

196. Tedgui A, Mallat Z. Cytokines in atherosclerosis: pathogenic and regulatory pathways. Physiol Rev. 2006 Apr;86(2):515-81. doi: 10.1152/physrev.00024.2005. PMID: 16601268.

197. Tissot C, Singh Y, Sekarski N. Echocardiographic Evaluation of Ventricular Function-For the Neonatologist and Pediatric Intensivist. Front Pediatr. 2018 Apr 4;6:79. doi: 10.3389/fped.2018.00079. PMID: 29670871; PMCID: PMC5893826.

198. Todoroki K, Mizuno H, Sugiyama E, Toyo'oka T. Bioanalytical methods for therapeutic monoclonal antibodies and antibody-drug conjugates: A review of recent advances and future perspectives. J Pharm Biomed Anal. 2020 Feb 5;179:112991. doi: 10.1016/j.jpba.2019.112991. Epub 2019 Nov 14. PMID: 31761377.

199. Tousoulis D, Oikonomou E, Economou EK, Crea F, Kaski JC. Inflammatory cytokines in atherosclerosis: current therapeutic approaches. Eur Heart J. 2016 Jun 7;37(22):1723-32. doi: 10.1093/eurheartj/ehv759. Epub 2016 Feb 2. PMID: 26843277.

200. Tsang HG, Rashdan NA, Whitelaw CB, Corcoran BM, Summers KM, MacRae VE. Large animal models of cardiovascular disease. Cell Biochem Funct. 2016 Apr;34(3):113-32. doi: 10.1002/cbf.3173. Epub 2016 Feb 24. PMID: 26914991; PMCID: PMC4834612.

201. Tse K, Tse H, Sidney J, Sette A, Ley K. T cells in atherosclerosis. Int Immunol. 2013 Nov;25(11):615-22. doi: 10.1093/intimm/dxt043. PMID: 24154816; PMCID: PMC3806170.

202. Tsiantoulas D, Sage AP, Mallat Z, Binder CJ. Targeting B cells in atherosclerosis: closing the gap from bench to bedside. Arterioscler Thromb Vasc Biol. 2015 Feb;35(2):296-302. doi: 10.1161/ATVBAHA.114.303569. Epub 2014 Oct 30. PMID: 25359862.

203. Urbain J, Wikler M, Franssen JD, Collignon C. Idiotypic regulation of the immune system by the induction of antibodies against anti-idiotypic antibodies. Proc Natl Acad Sci U S A. 1977 Nov;74(11):5126-30. doi: 10.1073/pnas.74.11.5126. PMID: 303775; PMCID: PMC432113.

204. Van der Valk J, Brunner D, De Smet K, Fex Svenningsen A, Honegger P, Knudsen LE, Lindl T, Noraberg J, Price A, Scarino ML, Gstraunthaler G. Optimization of chemically defined cell culture media--replacing fetal bovine serum in mammalian in vitro methods. Toxicol In Vitro. 2010 Jun;24(4):1053-63. doi: 10.1016/j.tiv.2010.03.016. Epub 2010 Mar 31. PMID: 20362047.

205. Van Leeuwen M, Gijbels MJ, Duijvestijn A, Smook M, van de Gaar MJ, Heeringa P, de Winther MP, Tervaert JW. Accumulation of myeloperoxidase-positive neutrophils in atherosclerotic lesions in LDLR-/- mice. Arterioscler Thromb Vasc Biol. 2008 Jan;28(1):84-9. doi: 10.1161/ATVBAHA.107.154807. Epub 2007 Nov 8. PMID: 17991873.

206. Varbo A, Benn M, Tybjærg-Hansen A, Nordestgaard BG. Elevated remnant cholesterol causes both low-grade inflammation and ischemic heart disease, whereas elevated low-density lipoprotein cholesterol causes ischemic heart disease without inflammation. Circulation. 2013 Sep 17;128(12):1298-309. doi: 10.1161/CIRCULATIONAHA.113.003008. Epub 2013 Aug 7. PMID: 23926208.

207. Vázquez AM, Alfonso M, Lanne B, Karlsson KA, Carr A, Barroso O, Fernández LE, Rengifo E, Lanio ME, Alvarez C, et al. Generation of a murine monoclonal antibody specific for N-glycolylneuraminic acid-containing gangliosides that also recognizes sulfated glycolipids. Hybridoma. 1995 Dec;14(6):551-6. doi: 10.1089/hyb.1995.14.551. PMID: 8770642.

208. Vine DF, Takechi R, Russell JC, Proctor SD. Impaired postprandial apolipoprotein-B48 metabolism in the obese, insulin-resistant JCR:LA-cp rat: increased atherogenicity for the metabolic syndrome. Atherosclerosis. 2007 Feb;190(2):282-90. doi: 10.1016/j.atherosclerosis.2006.03.013. Epub 2006 Apr 19. PMID: 16624317.

209. Walters EM, Prather RS. Advancing swine models for human health and diseases. Mo Med. 2013 May-Jun;110(3):212-5. PMID: 23829105; PMCID: PMC6179855.

210. Wang Q, Chi L. The Alterations and Roles of Glycosaminoglycans in Human Diseases. Polymers (Basel). 2022 Nov 18;14(22):5014. doi: 10.3390/polym14225014. PMID: 36433141; PMCID: PMC9694910.

211. Weaver OR, Krysa JA, Ye M, Vena JE, Eurich DT, Proctor SD. Nonfasting remnant cholesterol and cardiovascular disease risk prediction in Albertans: a prospective cohort study. CMAJ Open. 2023 Jul 25;11(4):E645-E653. doi: 10.9778/cmajo.20210318. PMID: 37491049; PMCID: PMC10374248.

212. Weaver OR, Ye M, Vena JE, Eurich DT, Proctor SD. Non-fasting lipids and cardiovascular disease in those with and without diabetes in Alberta's Tomorrow Project: A prospective cohort study. Diabet Med. 2023 Sep;40(9):e15133. doi: 10.1111/dme.15133. Epub 2023 May 30. PMID: 37171453.

213. Wilkinson NM, Chen HC, Lechner MG, Su MA. Sex Differences in Immunity. Annu Rev Immunol. 2022 Apr 26;40:75-94. doi: 10.1146/annurev-immunol-101320-125133. Epub 2022 Jan 5. PMID: 34985929; PMCID: PMC9805670.

214. Williams KJ, Tabas I. The response-to-retention hypothesis of early atherogenesis. Arterioscler Thromb Vasc Biol. 1995 May;15(5):551-61. doi: 10.1161/01.atv.15.5.551. PMID: 7749869; PMCID: PMC2924812.

215. Witztum JL, Lichtman AH. The influence of innate and adaptive immune responses on atherosclerosis. Annu Rev Pathol. 2014;9:73-102. doi: 10.1146/annurev-pathol-020712-163936. Epub 2013 Aug 7. PMID: 23937439; PMCID: PMC3988528.

216. Wolf D, Ley K. Immunity and Inflammation in Atherosclerosis. Circ Res. 2019 Jan 18;124(2):315-327. doi: 10.1161/CIRCRESAHA.118.313591. PMID: 30653442; PMCID: PMC6342482.

217. Wong ND, Rosenblit PD, Greenfield RS. Advances in dyslipidemia management for prevention of atherosclerosis: PCSK9 monoclonal antibody therapy and beyond. Cardiovasc Diagn Ther. 2017 Apr;7(Suppl 1):S11-S20. doi: 10.21037/cdt.2017.03.02. PMID: 28529918; PMCID: PMC5418210.

218. World health statistics 2022: monitoring health for the SDGs, sustainable development goals. Available at: https://www.who.int/data/gho/publications/world-health-statistics.

219. Yang P, Lu Y, Gou W, Qin Y, Tan J, Luo G, Zhang Q. Glycosaminoglycans' Ability to Promote Wound Healing: From Native Living Macromolecules to Artificial Biomaterials. Adv Sci (Weinh). 2023 Dec 10:e2305918. doi: 10.1002/advs.202305918. Epub ahead of print. PMID: 38072674.

220. Yao Y, Xu XH, Jin L. Macrophage Polarization in Physiological and Pathological Pregnancy. Front Immunol. 2019 Apr 15;10:792. doi: 10.3389/fimmu.2019.00792. PMID: 31037072; PMCID: PMC6476302.

221. Youm YH, Nguyen KY, Grant RW, Goldberg EL, Bodogai M, Kim D, D'Agostino D, Planavsky N, Lupfer C, Kanneganti TD, Kang S, Horvath TL, Fahmy TM, Crawford PA, Biragyn A, Alnemri E, Dixit VD. The ketone metabolite β-hydroxybutyrate blocks NLRP3 inflammasome-mediated inflammatory disease. Nat Med. 2015 Mar;21(3):263-9. doi: 10.1038/nm.3804. Epub 2015 Feb 16. PMID: 25686106; PMCID: PMC4352123.

222. Yousif LI, Tanja AA, de Boer RA, Teske AJ, Meijers WC. The role of immune checkpoints in cardiovascular disease. Front Pharmacol. 2022 Oct 3;13:989431. doi: 10.3389/fphar.2022.989431. PMID: 36263134; PMCID: PMC9574006.

223. Yurdagul A Jr, Finney AC, Woolard MD, Orr AW. The arterial microenvironment: the where and why of atherosclerosis. Biochem J. 2016 May 15;473(10):1281-95. doi: 10.1042/BJ20150844. PMID: 27208212; PMCID: PMC5410666.

224. Zaragoza C, Gomez-Guerrero C, Martin-Ventura JL, Blanco-Colio L, Lavin B, Mallavia B, Tarin C, Mas S, Ortiz A, Egido J. Animal models of cardiovascular diseases. J Biomed Biotechnol. 2011;2011:497841. doi: 10.1155/2011/497841. Epub 2011 Feb 16. PMID: 21403831; PMCID: PMC3042667.

225. Zeng W, Wu D, Sun Y, Suo Y, Yu Q, Zeng M, Gao Q, Yu B, Jiang X, Wang Y. The selective NLRP3 inhibitor MCC950 hinders atherosclerosis development by attenuating inflammation and pyroptosis in macrophages. Sci Rep. 2021 Sep 29;11(1):19305. doi: 10.1038/s41598-021-98437-3. PMID: 34588488; PMCID: PMC8481539.

226. Zilversmit DB. Atherogenesis: a postprandial phenomenon. Circulation. 1979 Sep;60(3):473-85. doi: 10.1161/01.cir.60.3.473. PMID: 222498.

227. Zhang JM, An J. Cytokines, inflammation, and pain. Int Anesthesiol Clin. 2007 Spring;45(2):27-37. doi: 10.1097/AIA.0b013e318034194e. PMID: 17426506; PMCID: PMC2785020.

228. Zhao Y, Qu H, Wang Y, Xiao W, Zhang Y, Shi D. Small rodent models of atherosclerosis. Biomed Pharmacother. 2020 Sep;129:110426. doi: 10.1016/j.biopha.2020.110426. Epub 2020 Jun 20. PMID: 32574973.